Computational Actinide Chemistry: Structure, Bonding and Thermodynamics

COMPUTATIONAL ACTINIDE CHEMISTRY: STRUCTURE, BONDING AND THERMODYNAMICS

By Sophie KERVAZO,

A Thesis Submitted to the School of Graduate Studies in the Partial Fulfillment of the Requirements for the Degree Doctor of Philosophy

Université de Lille, McMaster University

Université de Lille, McMaster University
Doctor of Philosophy (2018)
Lille, France
Hamilton, Ontario (Department of Chemistry and Chemical Biology)

TITLE: Computational Actinide Chemistry:
Structure, Bonding and Thermodynamics
AUTHOR: Sophie KERVAZO (Université de Lille, McMaster University)
SUPERVISOR: Dr. Valérie VALLET, Dr. Paul AYERS, Dr. Florent RÉAL, André SEVERO PEREIRA GOMES
NUMBER OF PAGES: xxviii, 216

ABSTRACT

The main question of this thesis is: do we have today the tools to efficiently describe the structure, the bonding and the thermodynamics of actinide systems? This broad question is answered thanks to three studies. The first two are directly applied to the plastic industry and the nuclear plant safety. The last one, more fundamental, concerns the benchmarking of newly developed theoretical approach on f-element systems. First, actinides and transition metal arene-coordinated alkyl cations have been recently proven to be efficient catalysts for ethylene polymerizations. Interestingly, thorium, uranium and zirconium alkyl cations? catalytic activity depends on the solvent. To understand these behaviors and to confirm the tendency of these complexes to engage in unusual-arene coordination, relativistic DFT calculations combined with a characterization of the interaction thanks to the ETS-NOCV method are used. Second, in accident scenario along the reprocessing of spent nuclear fuel, plutonium can be released in various volatile forms (PuO_2, PuO_3 or $PuO_2(OH)_2$, ...). The exploration of these scenarios by the use of simulations requires, among the various parameters, the knowledge of the thermodynamic properties of the possibly formed elements. Our in-silico study focusses on the determination of the enthalpies of formation of the former two species for which experimental uncertainties remain, using multi-configurational relativistic wavefunction method. The last part of the thesis focusses on the benchmark of the B2-PLYP functional for f-element systems, which turns out quite accurate with respect to the experimental data and the gold-standard CCSD(T) method.

ABSTRACT

La question générale traitée dans cette thèse est de déterminer si, aujourd'hui, nous disposons d óutils théoriques efficaces pour d' écrire la structure, la liaison et les propriétés thermodynamiques de système comprenant un actinide. Cette large question va être abordée à láide de trois études différentes. Les deux premières sont directement liées à l?industrie plastique et à la sureté nucléaire. La dernière, plus fondamentale concerne une analyse comparative d?une approche théorique nouvellement développée sur des systèmes comprenant des éléments f. Tout dábord, les cations alkyles contenant un actinide (Th, U) ou un métal de transition (Zr) coordonné à un arène se sont révélés efficaces pour la catalyse de la synthèse du polyéthylène. étonnamment, les activités catalytiques des cations alkyles dépendent du solvant. Pour comprendre cela et confirmer la tendance quónt ces complexes à se lier à l?arène, une étude en DFT dans un contexte relativiste combinée à une caractérisation de liaison avec la méthode ETS-NOCV fut faite. La deuxième étude vise à étoffer les bases de données thermodynamiques qui servent à explorer numériquement les scénarios d?accidents. Notre étude in silico porte sur la détermination des enthalpies de formation des deux espèces pour lesquelles des incertitudes expérimentales subsistent (PuO_3 ou $PuO_2(OH)_2$, ...), en utilisant une méthode quantique multiconfigurationnelle et relativiste. La dernière partie de la théorie se concentre sur l?estimation de la précision de la fonctionnelle B2-PLYP pour les éléments f, qui sávère assez précise en comparaison aux données expérimentales et à la méthode de référence CCSD(T).

Acknowledgements

First, I want to thank the protractors Emmanuel Fromager and Nathalie Guihery the jury Dominique Guillaumont and Laurent Maron who take the time to read, listen and give me a feedback on my work. I would like to acknowledge David Emslie et Randy Dumont for getting up so early to attend my PhD defence. My directors also need to be thanked, the four of them is the perfect mixture and is the whole spectrum in their scientific knowledges, listening, advices and managing skills. In science, collaboration is a key to success and I was lucky enough to work with amazing searchers: Franǫis Virot, David Emslie, Stefan Knecht, Leon Freitag and Benjamin Helmich-Paris.

A french comedian Pierre Desproges in one of his chronicles of ordinary hatred said the humanity is divided in four categories: relations, friends, close friends and people you do not know. The the people I do not know, thank you for reading this lines. I hope it can help for your project or to fight insomnia.

Friends/ colleagues: during a PhD, the time spend with friends being inversely proportional to that spend with the colleagues so I thank you all for enlightening scientific conversions, nice beers or a nice scientific conversions with enlightening beers. Family (not describe by Desproges): I have the luck to have a great family, always there when needed or just to share a slice of pizza. Thank you for being here, it is also a pleasure to go home thanks to you all. Close friend: Desproges said that you can count them on the Baron Empain's hand or Django Reihart's for the most misanthrope of us. Nonetheless, you are still being here, thank you !

Desproges was then adding the woman he loved. I will just change the gender to thank to man who is here for me day after day. Finally I think Desproges forget another type of people: the mothers. I thank mine for always supporting me and being there.

REMERCIEMENTS

Premièrement, je voudrais remercier les rapporteurs Emmanuel Fromager et Nathalie Guihery et le jury Dominique Guillaumont et Laurent Maron qui ont pris le temps de lire et d´ écouter mon travail et pris celui de me donner un retour sur celui-ci. Je souhaite aussi remercier David Emslie et Randy Dumont qui ont dû se lever de bonne heure pour suivre ma soutenance de thèse. Je me dois aussi de remercier mes directeurs, à eux quatre, ils furent un parfait mélange, représentant un spectre total dans leurs connaissances scientifiques, leurs écoutes, leurs conseils et leurs façons d´ encadrer un thésard. Les collaborations sont importantes en sciences et j'ai eu la chance de travailler avec de formidables chercheurs merci à Françis Virot, David Emslie, Stefan Knecht, Leon Freitag et Benjamin Helmich-Paris. Pierre Desproges dans une de ses chroniques de la haine ordinaire disait que l´ humanité se divise en quatre grandes catégories les relations, les copains, les amis et les gens qu´ on ne connait pas. Les gens qu´ on ne connaît pas, merci de me lire en espérant que cela vous aide dans vos recherches ou dans la lutte contre l´ insomnie. Les copains/collègues, en thèse, le temps passé avec les uns étant directement inversement proportionnel à celui passé avec les autres, je vous remercie que ce soit pour une conversion scientifique éclairante, une sympathique petite bière ou pour une sympathique conversation scientifique autour d´ une bière éclairante. La famille (qui n´ était pas une catégorie de Desproges): avoir la chance d´ avoir une famille en arrière-plan toujours là, que ce soit pour les déménagements, faire des punchs ou manger une pizza en parlant de tout et de rien mais toujours dans la bonne humeur, c?est un réel luxe dont j?ai eu la chance d?héritée. Merci à chacun d?entre vous pour être qui vous êtes, car rentrer en Normandie est toujours un plaisir et me donne un nouveau souffle grâce à vous. Les amis, disait Desproges se comptent sur les doigts de la main du baron Empain voir de Django Reihart pour les plus misanthropes. Néanmoins, vous êtes encore présent aujourd´ hui, alors merci ! Desproges, aux quatre catégories y ajouté la femme que l´ on aime. Je passerai donc à la version masculine pour remercier celui qui me supporte au quotidien.Enfin, je pense que Desproges a oublié une catégorie très importante les mamans. Je remercie la mienne pour m´ avoir toujours soutenu, que ce soit par un coup de pied au cul (plus ou moins littéral) quand j´ en en avait besoin que par le petit Tupperware du dimanche soir qui en réduit la

mélancolie.

Contents

List of Figures

List of Tables

List of Abbreviations

AMFI	**A**verage **M**ean **F**ield **I**ntegrals
ANO	**A**tomic **N**atural **O**rbitals
ASTEC	**A**ccident **S**ource **T**erm **E**valuation **C**ode
BSSE	**B**asis **S**ets **S**uperpositon **E**rror
CASSCF	**C**omplete **Actif** **S**pace **S**elf **C**onsistent **F**ield
CASPT2	**C**omplete **Actif** **S**pace **P**erturbation **T**heory at the $\mathbf{2}^{nd}$ order
CBS	**C**omplete **B**asis **S**et
CC	**C**oupled **C**luster
CCSD(T)	**C**oupled **C**luster with **S**ingles and **D**ouble and **T**riple
CI	**C**onfiguration **I**nteraction
CPP	**C**ore **P**olarisation **P**otential
CSF	**C**onfiguration **S**tate **F**unction
DFT	**D**ensity **F**unctional **T**heory
DKH	**D**ouglas **K**roll **H**ess
DMRG	**D**ensity **M**atrix **R**enormalisation **G**roup
EA	**E**lectronic **A**finity
ECP	**E**ffective **C**ore **P**otential
EOM	**E**quation **O**f **M**otion
ETS	**E**xtended **T**ransition **S**tate
FCI	**F**ull **C**onfiguration **I**nteraction
FORA	**F**irst **O**rder **R**egular **A**pproximation
GGA	**G**eneralized **G**radient **A**pproximation
HF	**H**artree **F**ock
IP	**I**onisation **Potential**
IRSN	**I**nstitut **R**adioprotection et de **S**ureté **N**ucléaire
KS	**K**ohn **S**ham
GTO	**G**aussian **T**ype **O**rbitals
LCAO	**L**inear **C**ombimaison of **A**tomic **O**rbitals
LDA	**L**ocal **D**ensity **A**pproximation

MAD	**M**ean **A**verage **D**eviation
MO	**M**olecular **O**rbital
MP	**M**øller-**P**lesset
MP2	**M**øller-**P**lesset at the **2**nd order
NEVPT2	**N** -**E**lectron **V**alence state **P**erturbation **T**heory at the **2**nd order
NOCV	**N**atural **O**rital for **C**hemical **V**alence
PE	**P**oly**E**tylene
PT	**P**erturbation **T**heory
PUREX	**P**lutonium **U**ranium **R**edox **EX**traction
RASSI	**R**estricted **Actif S**pace **S**tate **I**nteraction
RECP	**R**elativistic **E**ffective **C**ore **P**otential
RHF	**R**estricted **H**artree **F**ock
SA	**S**tate **A**verage
SCF	**S**elf **C**onsistent **F**ield
SF	**S**pin **F**ree
SO	**S**pin **O**rbit
SOC	**S**pin **O**rbit **C**oupling
SR	**S**calar **R**elativistic
SS	**S**tate **S**pecific
STO	**S**later **T**ype **O**rbitals
TDDFT	**T**ime **D**ependent **D**ensity **F**unctional **T**heory
TPH	**T**tetra-**P**ropylene
UCCSD(T)	**U**nrestricted **C**oupled **C**luster with **S**ingle **D**ouble and (**T**riple)
UHF	**U**nrestricted **H**artree **F**ock
ZORA	**Z**eroth **O**rder **R**egular **A**pproximation
ZPE	**Z**ero **P**otential **E**nergy

Chapter 1

General Introduction

Actinides are located in the last row of the periodic table, with an atomic number of 89 to 103 and even if they are large atoms with limited natural availability, for some of them, their use are present in our daily life. The plastic piece holding this pages together and the electric power used to write them do not contain actinides but could be the result of the daily exploitation of actinides complexes.

As quantum chemist, the modelling actinides can be a challenge for two main reasons. The first is the inclusion of relativistic effects, the second is how to properly take into account the electronic correlation within the partially occupied 7s, 5f and 6d valence orbitals of actinides. The main question of this thesis is: do we have today the tools to efficiently describe the structure, the bonding and the thermodynamics of actinide systems ?

This broad question is answered thanks to three studies. The two first are directly applied to the plastic industry and the nuclear plant safety. The last one, more fundamental, concerns the benchmarking of double hybrid functional on f-element systems.

The first applied use of actinides we are interested in is the use of actinides complexes as catalyst for the ethylene polymerisation. As with many great discoveries in chemistry, and sciences in general, polyethylene (PE) was first synthesised in Germany by accident in 1898 by Hans von Pechmann. It has now an important position in our daily life since it is used in many plastic items such as plastic bags, bottles, etc...

The most widely used ethylene polymerisation catalysis process is the Ziegler-Natta that allows an ethylene coordination and 1,2 insertion [1] in arene solvent in industry [2] or alkane one in academic laboratory [3]. Many patents are filled as the industrial application of new and better catalysts for ethylene polymerisation could really be lucrative. The most interesting patent here was filled by Dow Chemical Company in 1987 in order to base, for the first time, the polymerisation of ethylene on actinides and more precisely on a mixture of bis(metallocene) precursor [$Cp^*_2AnX_2$] and [Cp^*AnX_3] (An = Th, U and X = Cl, Me, CH_2SiMe_3) with different activating agents.
With the goal of improving the polymerisation of polyethylene, Pr David Emslie and his former PhD student Nicholas R. Andreychuk at McMaster University worked on new compounds based on actinides as catalysts. They could obtain the arene-coordinated alkyl cations $[(XA_2)An(CH2SiMe_3)(arene)]^+$ with (An = Th, U; XA_2 = 4,5-bis(2,6-diisopropylanilido)-2,7-di-*tert*-butyl-9,9-dimethylxanthene); arene = benzene, toluene, bromobenzene or fluorobenzene) (Figure 1.1) and $[B(C_6F_5)_4]^-$ as counter ion and the close equivalent $[(XN_2)Zr(CH_2SiMe_3)(arene)]^+$ with the same arenes and (XN_2) being the 4,5-bis(2,4,6-triisopropylanilido)-2,7-di-*tert*-butyl-9,9-dimethylxanthene.

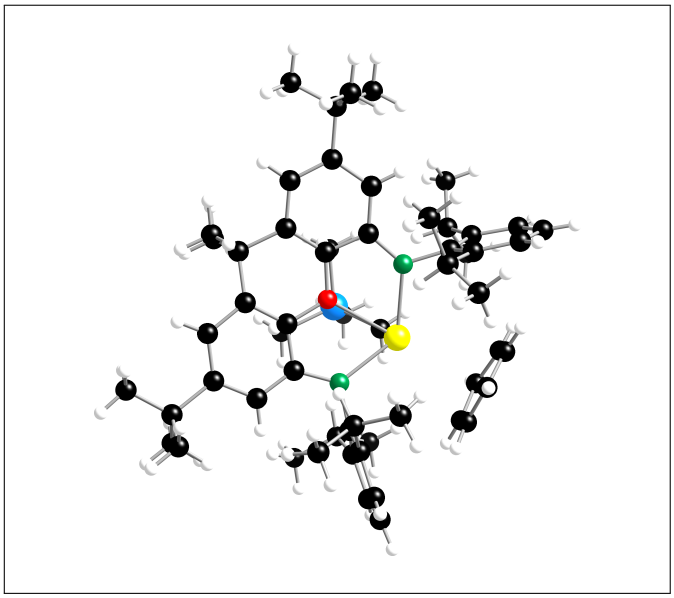

FIGURE 1.1: $(XA_2)U(CH2SiMe_3)(benzene)^+$

The activity of the catalyst does not only dependent on the arene but also of the metallic center. Our theoretical contribution, presented in Chapter 3 aims at understanding the mechanism of the catalysis by an in-depth study of the

bond between the arene and the transition metal Zr or an actinide (Th or U) center

As second study, we worked with the French Radioprotection and Nuclear Safety agency (IRSN). While in the past decades the climate change and the future nuclear plants are at the heart of political debate, it is important to recall that no matter the prospective political decisions, nuclear safety must be addressed now. One of the challenge of nuclear power plants is the recycling of the nuclear fuel. Wordwide the chosen recycling process is the PUREX (Plutonium Uranium Redox EXtraction) one. It uses a liquid-liquid extraction in order to separate the fission products from Plutonium and Uranium in order to reinject the former in the nuclear cycle. The problem with PUREX process is that the solvent tetra-propylene (TPH) could ignite itself and lead to a release, among numerous species, of gaseous plutonium in the atmosphere. This actually happened three times, twice at Savannah River (USA) in 1953 and 1975 and at Tomsk (Russia) in 1993. Even if the plutonium species only represents 0.9% of the fission products it is still responsible for 50% of the radio-toxicity after 100 years (see Figure 1.2).

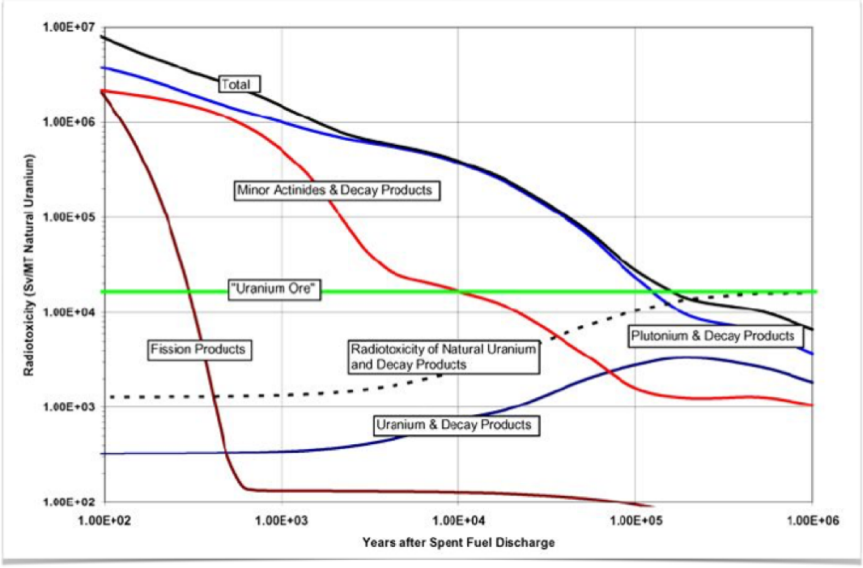

FIGURE 1.2: Radiotoxicity of spend nuclear fuel [4]

To perform nuclear safety analysis, the chemical behaviour of the Pu species need to be known. Experimental studies are complicated to pursue for safety reason. Since Pu can have multiple degrees of oxidation including (VI) it cannot be replaced by the less radioactive Th or Ce for the experiments. The

volatile species expected to be formed in the contact with oxygen are the dioxide PuO_2, trioxide PuO_3 and oxyhydroxide ($PuO_2(OH)_2$) of plutonium. Horeover, the experiments conducted in the past 30 years disagree on the formation of PuO_3 *i.e.* some analysis of experimental data proposed that PuO3 could be formed along the chemical processes, while others do not. Thus theoretical simulations of an accident is the best solution to answer this question. The ASTEC (Accident Source Term Evaluation Code) simulator code, developed by the IRSN, can simulate the accident condition of pression and temperature but precise thermodynamic data such as heat capacities, entropies and enthalpies of formation of the different species involved are needed as input parameters. This study will limit itself to the plutonium oxides PuO_2 and PuO_3 and the oxyhydroxide $PuO_2(OH)_2$. Those thermodynamic values can be obtained computationally thanks to a detailed knowledge of their electronic structure which implies to take into account thoroughly relativistic effects and electronic correlation. The challenging aspect of this work as detailed in Chapter 4, is the multiconfigurational character of the ground-state wave function.

The treatment of electronic correlation is still source of new developments in quantum chemistry. For the past 10 years, the DFT community tried to better account for electronic correlation in the functionals by proposing new approaches. One of them is the so-called double-hybrid method, which is based on the use of a hybrid functional combined with the MP2 correlated method. This family of functionals has proven its efficiency for a lot of system but so far it was never applied to f-elements. During this thesis, one double hybrid (B2-PLYP) was tested for f-elements systems and representative chemical reaction in Chapter 5

In this thesis the general methods of quantum chemistry are first presented in Chapter 2. These will be followed in Chapter 3 by the exploration of the bonding between alkyl cations and arenes to rationalise the catalytic process of polyethylen. A third part (Chapter 4) will be devoted to the determination of thermodynamic properties of plutonium oxides and oxyhydroxide. The last chapter (Chapter 5) will evaluate the performances of double hybrid functional B2-PLYP for the determination of thermodynamic properties of f-elements containing systems. We will close this manuscript with general conclusions and perspectives.

Chapter 2

Methods

2.1 Introduction to Quantum Chemistry

As discussed in the introduction, the experimental expertise is complementary to theoretical studies. In this chapter, I will define all the necessary tools to understand what is solved from a computational point of view and all the important concepts that were used during my PhD work. As we already mentioned, the context of this study implies accounting for relativistic effects due to the presence of actinides. However, for the sake of clarity, we will start with the presentation of quantum chemical mechanics notions in a non-relativistic framework before introducing the relativistic Dirac equation and the other flavors of relativistic approximate Hamiltonians. Last but not least the concept of basis sets will be presented.

2.1.1 Schrödinger equation

The time-dependent Schrödinger equation describes the physics of a molecular system with respect to time [5]:

$$\hat{H}\psi = i\hbar\frac{\partial\psi}{\partial t} \tag{2.1}$$

Where ψ(t) is the wave function of the state under consideration, in general the ground state (or an excited state), $\hat{H}$ the Hamiltonian operator, i the imaginary number and $\hbar$ the Planck contants divided by 2π. The first approximation is to consister the system as stationary at a moment t [6] and thus the equation becomes an eigenvalue equation, independent of time:

$$\hat{H}(\boldsymbol{r}, \boldsymbol{R})\psi(\boldsymbol{r}, \boldsymbol{R}) = E\psi(\boldsymbol{r}, \boldsymbol{R}) \tag{2.2}$$

with $\psi(\boldsymbol{r}, \boldsymbol{R})$ the wave function of the system made on our case of electrons at positions { $\boldsymbol{r}$ = r_1, ..., r_n} and nuclei at the positions {$\boldsymbol{R}$ = R_1, ..., R_N} and E being the total energy. $\hat{H}$ is written for a molecule, in atomic units as:

$$\hat{H} = -\sum_i \frac{1}{2} \bigtriangledown_i^2 - \sum_A \frac{1}{2M_A} \bigtriangledown_A^2 - \sum_{i,A} \frac{Z_A}{r_{iA}} + \frac{1}{2} \sum_{i \neq j} \frac{1}{r_{ij}} + \frac{1}{2} \sum_{A \neq B} \frac{Z_A Z_B}{R_{AB}} \tag{2.3}$$

i and j are indices running over the electrons while A and B indices are related to the nuclei. r_{ij} is the distance between the electron i and j , r_{iA} the one between an electron i and a nucleus A and R_{AB} is the distance between two nuclei. Finally, Z_A is the atomic number of nucleus A. The two-first terms of equation 2.3 represent the kinetic energies terms of the electrons and the nuclei, respectively. The last three terms are the standard Coulomb interaction potential terms for electron-nucleus, electron-electron and nucleus-nucleus interactions.

2.1.2 Born-Oppenheimer approximation

As a proton is heavier than an electron (mass ratio of 1 836) the velocity of the nucleus considered to be negligible. Thus, it is possible to decouple the Hamiltonian as a sum of the electronic Hamiltonian $\hat{H}^{el}$ and the nuclear one $\hat{H}^{nuc}$

$$\hat{H} = \hat{H}^{el} + \hat{H}^{nuc} \tag{2.4}$$

In the adiabatic approximation [7] or Born-Oppenheimer approximation, the wave function $\psi(\boldsymbol{r}, \boldsymbol{R})$ can be written as a product of the electronic contribution, ψ^{el}, and the nuclear one ψ^{nuc}:

$$\psi(\boldsymbol{r}, \boldsymbol{R}) = \psi^{el}_{\boldsymbol{R}}(\boldsymbol{r})\psi^{nuc}(\boldsymbol{R}) \tag{2.5}$$

The electronic Hamiltonian operator is define as:

$$\hat{H}^{el} = -\sum_i \frac{1}{2} \bigtriangledown_i^2 - \sum_{i,A} \frac{Z_A}{r_{iA}} + \frac{1}{2} \sum_{i \neq j} \frac{1}{r_{ij}} + \frac{1}{2} \sum_{A \neq B} \frac{Z_A Z_B}{R_{AB}} \tag{2.6}$$

It can be shown that the contribution of the nucleus-nucleus interaction term is just a constant in the total energy calculation. The eigenvectors are the electronic wave functions $\psi^{el}_{\boldsymbol{R}}(\boldsymbol{r})$ that depend parametrically on $\boldsymbol{R}$. Therefore, the electrons move on a potential energy surface (PES), $E^{el}_{\boldsymbol{R}}$, that can be obtained by solving the following:

$$\hat{H}^{el}\psi^{el}_{\boldsymbol{R}} = E^{el}_{\boldsymbol{R}}\psi^{el}_{\boldsymbol{R}} \tag{2.7}$$

The methods presented in the following pages have for purpose to solve this eigenvalue problem.

2.1.3 Constraints on the wave-function

The first hypothesis is to consider the electrons as independent particules. Thus the n-particule wave function can be written as the product of N one-particule orbitals ϕ (see Section 2.5.1).

$$\psi(r_1, r_2, ..., r_N) = \phi_1(r_1)...\phi_N(r_N) \tag{2.8}$$

A prerequisite for the form of the electronic wave function (now written as ψ), because it characterises fermion particules, is its anti-symmetric character with respect to the particle exchange:

$$\psi(i, j) = -\psi(j, i) \tag{2.9}$$

A a manifestation of the Pauli exclusion principle [8], which states that two fermions cannot occupied the same quantum state, *i.e.* they cannot have the same four quantum numbers (n, l, m and s).

A trial wave function that satisfies both criteria is the Slater determinant [9] composed of orthonormal spin orbitals.

$$\psi(r_1, r_2, ..., r_N) = \frac{1}{\sqrt{N!}} \begin{vmatrix} \phi_1(r_1) & \phi_2(r_1) & ... & \phi_N(r_1) \\ \phi_1(r_2) & \phi_2(r_2) & ... & \phi_N(r_2) \\ \vdots & \vdots & \ddots & \vdots \\ \phi_1(r_N) & \phi_2(r_N) & ... & \phi_N(r_N) \end{vmatrix} \tag{2.10}$$

with the spin orbitals in column and the electron coordinates in row. From now on, ψ will denote Slater determinants.
One can notice:

- The anti-symmetry of the wave-function is present since the exchange of two rows changes the sign of the determinant.
- The Pauli principle and the indiscernibility of the electrons remains. Indeed, having two electrons in the same state will give a determinant equals to zero since two columns will be equal.
- The normalisation constant is $\frac{1}{\sqrt{N!}}$.

2.2 Single-Reference Methods

In this section, the methods common to the three thesis projects using the single-reference approximation will be presented. The specific methods proper to each of them are introduced in the chapter in question.

2.2.1 Hartree-Fock method

In the context of Wave Function Theory, equation 2.10 can be solved thanks to different approximations. The Hartree-Fock approach [10] is the foundation of many other methods and more specifically the so-called *post* Hartree-Fock methods, presented later. It rests on the mean-field approximation which

assumes that a given electron is sujected to the average potential (which as discussed below, consists of a classical (electrostatic) and a non-classical (exchange) interaction) of the other electrons, rather than the individual electron-electron interactions. The Hartree-Fock wave function is determined by the variation principle by minimising the energy of the system:

$$E_{HF} = \frac{\langle \Phi | \, H^{el} \, | \Phi \rangle}{\langle \Phi | \Phi \rangle} \geq E \tag{2.11}$$

E_{HF} being the HF energy and E the exact total energy of the system. Since the N-electrons problem can be decomposed in N one-electron problems, the solution Φ can be described by a Slater determinant built from the orbitals ϕ_i. The variational conditions on the orbitals lead to a new effective one-electron operator, the Fock operator [6] $\hat{F}_i$.

$$\hat{\boldsymbol{F}}_{\boldsymbol{i}} \phi_i = \epsilon_i \phi_i \tag{2.12}$$

Its eigenvector, ϕ_i is the molecular spin-orbital of the electron i and its eigenvalue ϵ_i the corresponding orbital energy. The Fock operator can be written as:

$$\hat{\boldsymbol{F}}_{\boldsymbol{i}}(\boldsymbol{r}) = \hat{\boldsymbol{h}}_{\boldsymbol{i}}(\boldsymbol{r}) + \sum_{j=1}^{N} |\hat{\boldsymbol{J}}_j(\boldsymbol{r}) - \hat{\boldsymbol{K}}_j(\boldsymbol{r})| \tag{2.13}$$

The one-electron core Hamiltonian $\hat{h}_i(\mathbf{r})$ is composed of the kinetic energy of the electron i and the nucleus-electron potential energy:

$$\hat{\boldsymbol{h}}_{\boldsymbol{i}}(\boldsymbol{r}) = -\frac{1}{2} \bigtriangledown_i^2 - \sum_{K=1}^{N} \frac{Z_K}{r_{iK}} \tag{2.14}$$

The second part of the equation 2.13 is composed by the two one-electron operators. The Coulomb operator J_j, corresponds to the classic representation of the repulsion between two electrons (i and j). The second operator is the non-classical exchange operator and arises from the indiscernability of the electrons and the anti-symmetry of the wave-function. It forbids electrons with identical spins to occupy the same spatial position. Applying the exchange and Coulomb operators on ϕ_j gives:

$$\hat{\boldsymbol{J}}_j\phi_i(\boldsymbol{r_i}) = \left[\int \frac{\phi_j^*(\boldsymbol{r_j})\phi_j(\boldsymbol{r_j})}{\boldsymbol{r_{ij}}} d\boldsymbol{r_j}\right]\phi_i(\boldsymbol{r_i}) \tag{2.15}$$

$$\hat{\boldsymbol{K}}_j\phi_i(\boldsymbol{r_i}) = \left[\int \frac{\phi_j^*(\boldsymbol{r_j})\phi_i(\boldsymbol{r_j})}{\boldsymbol{r_{ij}}} d\boldsymbol{r_j}\right]\phi_j(\boldsymbol{r_i}) \tag{2.16}$$

Thus the eigenvalue ϵ_i of the eigenfunction ϕ_i in the equation 2.12 is:

$$\epsilon_i = \langle\phi_i|\,\hat{\boldsymbol{F}}_{\boldsymbol{i}}\,|\phi_i\rangle = \langle\phi_i|\,\hat{\boldsymbol{h}}_{\boldsymbol{i}}\,|\phi_i\rangle + \langle\phi_i|\sum_{j=1}^{N}(\hat{\boldsymbol{J}}_j - \hat{\boldsymbol{K}}_j)\,|\phi_i\rangle \tag{2.17}$$

Finally, the whole energy Hartree-Fock is:

$$\boldsymbol{E}_{HF} = \sum_{i=1}^{N} h_{ii} + \frac{1}{2}\sum_{i=1}^{N}\sum_{j=1}^{N}(\boldsymbol{J}_{ij} - \boldsymbol{K}_{ij}) = \sum_{i=1}^{N}[\epsilon_i - \frac{1}{2}\sum_{j=1}^{N}(\boldsymbol{J}_{ij} - \boldsymbol{K}_{ij})] \tag{2.18}$$

Where N remains the number of electrons and ϵ_i, $\boldsymbol{J}_{ij}$ and $\boldsymbol{K}_{ij}$ follow the description of the equations 2.17 and:

$$\boldsymbol{J}_{ij} = \int \phi_i^*\hat{J}_i\phi_i; \boldsymbol{K}_{ij} = \int \phi_i^*\hat{K}_i\phi_i \tag{2.19}$$

One can note that the total energy Hartree-Fock is not the sum or the energy of the spin-orbitals of the equation 2.17 otherwise the electronic repulsion would be counted twice for each electron.

2.2.2 The problem of Electron Correlation

Definition

As mentioned above, in the HF approximation, the instantaneous electron-electron interaction was replaced by an average potential while this approximation can yield to a fairly good representation of the physical systems. It is, nevertheless, still far from the exact solution as far as physico-chemical process are concerned. The missing interactions are what is referred as electronic

correlation E_{corr} [11] which is defined as the difference between the total exact non relativistic energy of the system E_{tot} and the Hartree-Fock one E_{HF} (for a given basis set limit, see Section 2.5):

$$E_{corr} = E_{tot} - E_{HF} \tag{2.20}$$

Though electron correlation represents only 5 to 10% of the total energy of the system it can change the whole picture of the wave function and impact molecular properties and thus cannot be neglected [12]. From a physical point of view, electronic correlation is due to two types of instantaneous repulsions. The first one is the repulsion between the two negative charges, leading to the Coulomb hole. The second type of repulsion prevents two particules with the same spin to be at the same position corresponding to the Fermi hole.

One can distinguish between the dynamical and non-dynamical (or static) electronic correlation. The static correlation, occurring in case of near orbitals degeneracy, implies that the wave function has to be described by more than one Slater determinant. The dynamical correlation, is connected to the instantaneous correlation of the electron motions and is accounted for by post-Hartree-Fock methods discussed after.

Møller-Plesset Perturbation Theory

In order to include dynamical correlation into a single reference wavefunction, Perturbation Theory (PT) [13] can be used. One can rewrite the Schrödinger equation as:

$$\hat{H}\psi = E\psi \tag{2.21}$$

with :

$$\hat{H} = \hat{H}_0 + \hat{H}' \tag{2.22}$$

where $\hat{H}_0$ is the HF Hamiltonian and $\hat{H}'$ the perturbation one defined in the equation 2.26.

The energy and the wave function can be written as Taylor expansion of λ (being the strength of the perturbation) since E_{PT} and ψ are continuous functions between zero and infinity:

$$E_{PT} = \lambda^{(0)} E_0 + \lambda^{(1)} E_1 + \lambda^{(2)} E_2 + ... \tag{2.23}$$

$$\psi = \lambda^{(0)} \psi_0 + \lambda^{(1)} \psi_1 + \lambda^{(2)} \psi_2 + ... \tag{2.24}$$

If λ = 1, the n-th order energy and wavefunction are of all the terms with indices $\leq$ n.

In the Møller-Plesser (MP) Perturbation Theory, $\hat{H}_0 = \hat{H}_{HF}$ thus it consists in the introduction of a perturbation to a reference (HF) wave function. In other words, excited Slater determinants are included.

We will focus on Møller-Plesset to the 2^{nd} order (MP2), for which double excitations are included. Since it is easily proven that MP1 (Møller-Plesser to the 1^{st} order) is actually equivalent to HF [10] with the Brillouin theorem. The Brillouin theorem stating that the singly excited configurations do not contribute to the 1^{st} order correction to the wave function. By single excitation, one has to understand the promotion of one electron to an unoccupied orbital is allowed (see Figure 2.1), for double excitations, it is two electrons. The number of excited determinants is directly linked to the size of the basis set implying that, the computational cost will be also dependent on it (see Table 2.1 and Section 2.5.1 for the definition of a basis set). Let us have a look at E_{MP2} starting from λ = 1 and equation 2.23 .

$$E_{MP2} = E_0 + E_1 + E_2 = \sum_i \epsilon_i - \frac{1}{2} \sum_{ij} \langle ij| \, |ij\rangle \tag{2.25}$$

As mentioned before, MP2 includes single and double excitations (if non-canonical/open-shell orbitals are used). The matrix elements with singly excited determinants Φ_i^a are:

$$\begin{aligned}\langle\Phi_0|\,\hat{H}'\,|\Phi_i^a\rangle &= \langle\Phi_0|\,\hat{H}_0 - \sum_j^{N_{elec}} \hat{\boldsymbol{F}}_j\,|\Phi_i^a\rangle \\ &= \langle\Phi_0|\,\hat{H}_0\,|\Phi_i^a\rangle - \langle\Phi_0|\sum_j^{N_{elec}} \hat{\boldsymbol{F}}_j\,|\Phi_i^a\rangle \\ &= \langle\Phi_0|\,\hat{H}_0\,|\Phi_i^a\rangle - \left(\sum_j^{N_{elec}} \epsilon_j\right)\langle\Phi_0|\Phi_i^a\rangle\end{aligned} \tag{2.26}$$

Where the subscript of Φ, *i,j, ...* are the occupied orbitals the electron is promoted from and *a, b, ...* the virtual orbitals. Φ_0 and Φ_i^a are two orthogonal states so the second term is equals to zero. For the first term, the Brillouin theorem [14] states that (for closed shell systems) if two orthogonal states satisfying HF equation are different by only one orbital then: $\langle\Phi_0|\,\hat{H}_0\,|\Phi_i^a\rangle$ = 0, so that $\langle\Phi_0|\,\hat{H}'\,|\Phi_i^a\rangle$ = 0. Thus, E_2 only involves doubly excited determinants:

$$E_2 = \sum_{i<j}^{occ}\sum_{a<b}^{vir} \frac{\langle\Phi_0|\,\hat{H}'\,|\Phi_{ij}^{ab}\rangle\,\langle\Phi_{ij}^{ab}|\,\hat{H}'\,|\Phi_0\rangle}{E_0 - \epsilon_{ij}^{ab}} \tag{2.27}$$

Because of the Koopmans' Theorem [15] the difference in total energy between two Slater determinants is the difference in Molecular Orbitals (MO) energies thus the second-order energy for a closed-shell system can be written with a sum over the spatial orbitals a, b, r and s as:

$$E(MP2) = 2\sum_{abrs}^{N/2} \frac{\langle ab|\,|rs\rangle - \langle rs|\,|ab\rangle}{\epsilon_a + \epsilon_b - \epsilon_r - \epsilon_s} - \sum_{abrs}^{N/2} \frac{\langle ab|\,|rs\rangle - \langle rs|\,|ba\rangle}{\epsilon_a + \epsilon_b - \epsilon_r - \epsilon_s} \tag{2.28}$$

The two main advantages of MP2 are the low computational cost compared to variational methods (such as CI see Section 4.2.1) and its size extensivity [1].

[1] Size-extensivity is a mathematical concept introduced by Bartlett [16] to characterised a method with a linear scaling between the energy and the number of electrons. The size consistency is also a property of a method, refering to the fact that if A and B are two subsystems sharing no electrons the following equality is true: E(A + B) = E(A) + E(B).This property is particularly important when a dissociation curve is explored.

Higher orders of perturbation such as MP3 (with the third order energy) or MP4 (with the fourth order energy) allow to include more dynamical correlation but at a greater cost. However, it has been shown that MP perturbation theory may not always converge [17], converge slowly or even oscillate. The issue of convergence, as well as the fact that other approaches such as coupled cluster have a similar cost than MP3, MP4 etc... but are more reliable, means that these approaches are mow seldom used.

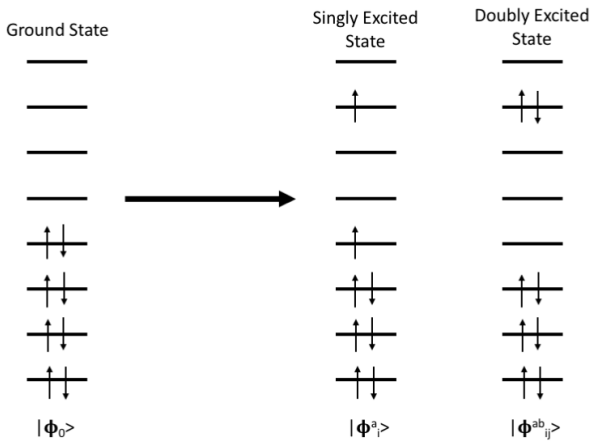

FIGURE 2.1: Single Excitation from a Ground State [17]

TABLE 2.1: Computational Cost and Amount of Correlation Included In the different Møller-Plesser Perturbation Theories. (see section 2.5.1 for the definition of M_{basis})

Method	Computational Cost	Amount of Correlation Included
MP2	M^5_{basis}	80 - 90 %
MP3	M^6_{basis}	90 - 95 %
MP4	M^7_{basis}	95 - 97 %

Coupled Cluster Method

The coupled cluster (CC) method [18–21] is an approach based on the Many-Body Perturbation Theory where high-order excitations are included efficiently. Thus, the Schrödinger equation can be written as:

$$\hat{H}\Psi_{CC} = E\Psi_{CC} \tag{2.29}$$

Ψ_{CC} is defined with an excitation operator $\hat{T}$ acting on a reference wave function:

$$\Psi_{CC} = e^{\hat{T}}\Psi_0 \tag{2.30}$$

The exponential term can be expanded as:

$$e^{\hat{T}} = 1 + \hat{T} + \frac{1}{2!}\hat{T}^2 + \frac{1}{3!}\hat{T}^3 + ... = \sum_{k=0}^{\infty}\frac{1}{k!}\hat{T}_k \tag{2.31}$$

the excitation operator $\hat{T}$ is the sum:

$$\hat{T} = \sum_{i=1}^{N}\hat{T}_i \tag{2.32}$$

the subscript being the excitation order and N the number of electrons in the system. The excitation order corresponds to the number of electrons excited from an occupied to an unoccupied orbital, for example:

$$\hat{T}_1\Psi_0 = \sum_{i}^{occ}\sum_{a}^{virtual} t_i^a\Phi_i^a \tag{2.33}$$

and

$$\hat{T}_2\Psi_0 = \sum_{i<j}^{occ}\sum_{a<b}^{virtual} t_{ij}^{ab}\Phi_{ij}^{ab} \tag{2.34}$$

represent single and double excitations, where t_i^a and t_{ij}^{ab} are the amplitudes of the excitations and so on. Here, the variational principle generally used to find the energy cannot be applied. Indeed, non-vanishing terms all the way up to the order of N arise because of the expansion in equation 2.31. Therefore, the energy is determined by projecting equation 2.29 onto the reference

wave function Φ_0. The coupled-cluster E_{CC} energy is then expressed as:

$$E_{CC} = \langle \Phi_0 | \, e^{-\hat{T}} \hat{H} e^{\hat{T}} \, | \Phi_0 \rangle \tag{2.35}$$

This method, similar to MP2 in the idea, retrieves the dynamical correlation of the system but still describes it with a single reference determinant. However, in contrast to MP2, the single excited T_1 operators are known to introduce orbital relaxation [22] and make CC method more reliable than MP2 in cases the HF orbitals are not optimal

If no constraints on the excitation order are put in place, one would arrive at the FCI calculation and the method 4.2.1 would only be applicable for very small systems, so a truncated form was developed including only the single and double electrons excitations [23]. This truncated CC, called CCSD, remains size extensive and affordable for medium systems. Higher-order truncations are available such as CCSDT[24] including explicitly the triple excitations or CCSDTQ adding the quadruple ones, but they are too expensive for the gain in electronic correlation retrieved. The triple excitations, that might be important for the description of some wave functions, are then included perturbatively, leading to CCSD(T) being the most wisely used triple variant [25][2].

Unfortunately, the restricted CCSD(T) depicted above is inadequate to describe open-shell molecules such as the ones under study. Thus, one must turn to the unrestricted version of this method UCCSD(T). The first formulations of it [16, 27, 28] use an Unrestricted-HF (UHF) reference wave function. However this idea has the disadvantages of being expensive and leading to spin contamination (artificial mixing of multiple electronic spin states). This is why different studies decided to start with a restricted HF reference [29, 30] but the spin contamination of the wave-function was still present. In 1993, Knowles *et al.* [20, 21] proposed a RHF-UCCSD formulation.

Today, UCCSD(T) is considered as the "gold standard" for single reference cases, but may fail for multi-reference ones. The T_1 [31] and D_1 diagnostics [32, 33] can be used to qualitatively spot a multi-reference character. Defining

[2] CCSD(T) is different from CCSD[T] were the contribution of the single excitations are not taken into account and from CCSD-T where triples corrections are computed as defined by M. J. O. Deegan *et al.*[26]

T_1 with the one-electron excitation amplitudes t_1:

$$T_1 = \frac{||t_1||}{\sqrt{N}} \tag{2.36}$$

And the D_1 for open-shell [34]:

$$D_1 = max(||f_i^a||_2, ||f_x^a||_2, ||f_i^x||_2) \tag{2.37}$$

where the 2-norm of a matrix, $||R||_2$, is the maximum Euclidean norm of the vectors formed by the multiplication of R with a unit vector [35], and the f amplitudes being linked to the t amplitudes by:

$$f_i^a = \frac{t_{i\alpha}^{a\alpha} + t_{i\beta}^{a\beta}}{2} \tag{2.38}$$

$$f_x^a = \frac{t_{x\alpha}^{a\alpha}}{\sqrt{2}} \tag{2.39}$$

$$f_i^x = \frac{t_{i\beta}^{x\beta}}{\sqrt{2}} \tag{2.40}$$

If for lighter elements a T_1 diagnostic higher than 0.02 is usually a sign of multi-reference character the value is raised at 0.05 [36, 37] for systems with transition metals and other heavy elements.

2.3 Density Functional Theory

At the birth of quantum chemistry in the 1960's, the limited computational power raised difficulties to perform accurate calculations using large basis sets (see Section 2.5.1) or including many atoms with HF method. In this context, the great adventure of Density Functional Theory (DFT) started in 1964 with Hohenberg and Kohn [38] when they demonstrated that the exact energy of the ground state of any electron gas in an external potential is a functional of the density F [ρ].

$$E[\rho] \equiv \int v(\boldsymbol{r})\rho(\boldsymbol{r})d\boldsymbol{r} + F[\rho] \tag{2.41}$$

where ν would be the Coulomb attraction between the nuclei and the electrons. ρ, the total electron density of N electrons is defined as:

$$\rho(\boldsymbol{r}) = N \int ... \int |\Psi(\boldsymbol{x}_1, \boldsymbol{x}_2, ...\boldsymbol{x}_n)|^2 d\sigma d\boldsymbol{x}_2 ... d\boldsymbol{x}_N \tag{2.42}$$

σ being the arbitrary spin of the electron one, $\boldsymbol{x}_i$ being the map of the spin-spatial coordinated of the other N-1 electrons.

F[ρ] is a universal functional of the total electron density ρ that corresponds to the sum of the two electron energy functional W[ρ] and the kinetic energy terms T[ρ]. Considering F[ρ], it can be rewritten as:

$$F[\rho] = T[\rho] + W[\rho] \tag{2.43}$$

Thus the "only" down side is the determination of the universal functional F[ρ], since the energy is simply obtained by the variational principle. Hohenberg and Kohn stated themselves the problem of obtaining this universal functional in the conclusion of their paper: *"We have developed a theory of electronic ground state which is exact in two cases : The case of a nearly constant density [...] and the case of a slowly varying density. Actual electronic systems do not belong to either of them."*

The answer to this problem arrived one year later in 1965, with Kohn and Sham [39] by proposing that the exchange-correlation term, at the heart of the problem of Hohenberg and Kohn (and more generally in quantum chemistry), can be approximate by using the true chemical potential $\mu(\rho)$ of the homogeneous interacting electron gas.

$$\frac{\delta E}{\delta \rho} = \mu \tag{2.44}$$

First, the density is rewritten as a slater determinant of spin orbitals ϕ_i for a non interacting reference system.

$$\rho(\boldsymbol{r}) = \sum_i^N \phi_i^*(\boldsymbol{r}) \phi_i(\boldsymbol{r}) \tag{2.45}$$

Then, the variational principle is applied to equation 2.41 in order to obtain N coupled one-particle equations for the non-interacting electrons, the so-called the Kohn-Sham equations:

$$\left\{ -\frac{1}{2m} \bigtriangledown^2 + \phi(\boldsymbol{r_i}) + \nu_{xc}(\rho(\boldsymbol{r_i})) \right\} |\phi_i\rangle = \epsilon_i |\phi_i\rangle \tag{2.46}$$

with:

$$\phi(\boldsymbol{r}) = \nu_{ext}(\boldsymbol{r}) + \int \frac{\rho(\boldsymbol{r'})}{|\boldsymbol{r} - \boldsymbol{r'}|} d\boldsymbol{r'} \tag{2.47}$$

and

$$\nu_{xc}(\rho(\boldsymbol{r})) = \frac{\delta E_{xc}[\rho]}{\delta \rho(\boldsymbol{r})} \tag{2.48}$$

Here, the issue is the formulation of E_{xc}. In practice, the exact functional is replaced by an approximated one with a certain number of exact conditions being enforced [10] as listed below:

- For a hydrogen-like system the functional should give the exact exchange energy and a correlation energy equals to zero.
- For solid-state physics, it is important to recover the electron gas solution when the density becomes constant. However, it is less true for molecular densities since as the electron gas model does not properly describe a molecular system.
- Multiplying by a constant factor the molecular coordinates ($\rho\lambda$(x,y,z) = $\lambda^3\rho(\lambda$x, λy, λz)) should result in a linear scaling of the exchange energy. $E_x[\rho_\lambda] = \lambda\ E_x[\rho]$.
- On the contrary, there is no full scaling concerning the correlation energy.
- The exact functional should fulfill the Lieb-Oxford inequality saying that $E_x[\rho] \geq E_{xc}[\rho] \geq 2.273\ E_x^{LDA}[\rho]$ (see Section 2.3.1).
- As $\boldsymbol{r}$ tends to infinity the exchange potential should have an asymptotic behaviour in $-\boldsymbol{r}^{-1}$ while the correlation potential shows a $-\frac{1}{2}\alpha\boldsymbol{r}^{-4}$ behaviour (α being the polarisability of the N_{elec} - 1 system).

A good starting point to find the universal or approximate functional is to separate the exchange term from the correlation one in equation **??**, such as

$E_{xc}[\rho] = E_x[\rho] + E_c[\rho]$, with :

$$E_x[\rho] = \int \rho(\boldsymbol{r})\epsilon_x([\rho], \boldsymbol{r})d\boldsymbol{r} \tag{2.49}$$

$$E_c[\rho] = \int \rho(\boldsymbol{r})\epsilon_c([\rho], \boldsymbol{r})d\boldsymbol{r} \tag{2.50}$$

The exchange energy, by definition, involves only electrons with identical spins while the correlation due to electrons with the same spin is different, and thus separable, from the correlation from electrons with opposite spins:

$$E_x[\rho] = E_x^{\alpha}[\rho_\alpha] + E_x^{\beta}[\rho_\beta] \tag{2.51}$$

$$E_c[\rho] = E_c^{\alpha\alpha}[\rho_\alpha] + E_c^{\beta\beta}[\rho_\beta] + E_c^{\alpha\beta}[\rho_\alpha, \rho_\beta] \tag{2.52}$$

With $\rho = \rho_\alpha + \rho_\beta$ and $\rho_\alpha = \rho_\beta$ for a closed-shell singlet state.

Now that the basis of DFT are exposed, the next part will focus of the expressions of $E_x[\rho]$ and $E_c[\rho]$ and the approximations leading to their formulations.

2.3.1 Local Density Approximation

In the Local Density Approximation (LDA)[39–41], the exchange energy is given by the Dirac formula:

$$E_x^{LDA}[\rho] = -C_x \int \rho(\boldsymbol{r})^{\frac{4}{3}} d^3\boldsymbol{r} \tag{2.53}$$

In the case of an open-shell system where α and β densities are different, LSDA (Local Spin Density Approximation) is used, the exchange energy reads :

$$E_x^{LSDA}[\rho] = -C_x \int (\rho_\alpha(\boldsymbol{r})^{\frac{4}{3}} + \rho_\beta(\boldsymbol{r})^{\frac{4}{3}}) d^3\boldsymbol{r} \tag{2.54}$$

Concerning the correlation part, it is fitted on high precision calculations performed with Quantum Monte Carlo method to a uniform electron gas. The analytic interpolation formula used for this fit defines the functional, for example Vosko, Wilk and Nusair' one [41] (VWN) or the popular PW92 constructed by Perdew and Wang in 1992 [40].

2.3.2 Generalised Gradient Approximation

The goal of the Generalised Gradient Approximation's (GGA) [42] is to improve the exchange and correlation energies by including the electron density and its derivative, at given point (removing the *local* or homogeneous character of LDA) in the functional. For example, in this thesis, we have used the Perdew-Burke-Ernzerhof (PBE) [43] GGA functional defined by its exchange functional:

$$\epsilon_x^{PBE} = \epsilon_x^{LDA} F(x) \tag{2.55}$$

where x is a gradient of the density:

$$x = \frac{|\nabla\rho|}{\rho^{\frac{4}{3}}} \tag{2.56}$$

and

$$F(x) = 1 + a - \frac{a}{1 + bx^2} \tag{2.57}$$

a and b being parameters. The correlation part is expressed as:

$$\epsilon_c^{PBE} = \epsilon_c^{LDA} H(x) \tag{2.58}$$

$$H(x) = c f_3^3 \ln\left[1 + dt^2\left(\frac{1 + At^2}{1 + At^2 + A^2t^4}\right)\right] \tag{2.59}$$

$$A = d\left[exp\left(-\frac{\epsilon_c^{PBE}}{c f_3^3}\right) - 1\right]^{-1} \tag{2.60}$$

$$f_3(\zeta) = \frac{1}{2}\left[(1+\zeta)^{\frac{2}{3}} + (1-\zeta)^{\frac{2}{3}}\right] \tag{2.61}$$

$$t = \left[2(3\pi^3)^{\frac{1}{3}} f_3\right]^{-1} x \tag{2.62}$$

The parameters a, b and c are determined in a non-empirical way. ζ is the relative spin polarisation (= ($n_\uparrow$ - $n_\downarrow$) /n with $n = 3/4\ \pi\ r_s^3$, r_s being the Wigner-Seitz radius that is the radius of a sphere whose volume is equal to the mean volume per atom in a solid).

2.3.3 Hybrid-Generalised Gradient Approximation

Hybrid-GGA functionals combine a LDA part, a GGA part and an exact HF exchange weighted in order to fit experimental data. For example in this work, the well-used B3LYP [44] and PBE0 [45, 46] functionals have been used. The B3LYP functional is:

$$E_{xc}^{B3LYP} = (1-a)E_x^{LSDA} + aE_x^{exact} + b\delta E_x^{B88} + (1-c)E_c^{LSDA} + cE_c^{LYP} \quad (2.63)$$

The LYP and B88 part of the correlation and exchange energies are obtained with the GGA approximtion. E_x^{exact} is obtained when the KS orbitals used are identical to HF one. E_x^{LSDA} is described in the equation 2.54. The default values for a, b and c are 0.2, 0.7 and 0.8 respectively, however most of the quantum chemistry codes allow the user to modify these values. The defaults values are kept in the present work.

PBE0 consists in the addition of 25% of E_x^{exact} to the PBE functional presented in the previous paragraph.

2.3.4 Strengths and Weaknesses of DFT

As one understood, DFT is a great tool for quantum chemists. It is fast and black box once the functional is (smartly) chosen. Its computational cost scales as N^3 (N being the number of orbitals). On the other side, the impossibility to systematically improve results and the problem of describing spin states are severe drawbacks [47, 48]. In a vision restricted to the treatment of actinides, the main deficiency of DFT is its single determinant description, while the large number of unpaired f, s and d actinides electrons may results in a strongly multi-determinantal wave-function.

We can also point out that the exchange-correlation functional does not account for long-range ($\frac{C_6}{R_6}$) correlation corresponding to the London part of the dispersion energy notably present when Van der Waals interaction are important.

Dispersion can be patched to KS energies as proposed by Grimme *et al.* [49–51] with the D3 empirical correction:

$$E_{disp} = E^{(2)} + E^{(3)} \tag{2.64}$$

With the two-body $E^{(2)}$ term defined as:

$$E^{(2)} = \sum_{AB} \sum_{n=6,8,10} s_n \frac{C_n^{AB}}{r_{AB}^n} f_{d,n}(r_{AB}) \tag{2.65}$$

with

$$f_{d,n}(r_{AB}) = \frac{1}{1 + 6(\frac{r_{AB}}{s_{r,n} R_0^{AB}})^{-\alpha_n}} \tag{2.66}$$

C_n^{AB} are tabulated for atom pairs, s_n and $s_{r,n}$ are a scaling factor adjusted for each functional and R_0^{AB} is the cutoff radii

The three-body $E^{(3)}$ term is:

$$E^{(3)} = \sum_{ABC} f_{d,(3)}(\bar{r}_{ABC}) E^{ABC} \tag{2.67}$$

$\bar{r}_{ABC}$ being the geometrically averaged radii of atoms A, B and C and E^{ABC} the triple dispersion term:

$$E^{ABC} = \frac{C_9^{ABC}(3cos\theta_a cos\theta_b cos\theta_c + 1)}{(r_{AB} r_{BC} r_{CA})^3} \tag{2.68}$$

where C_9^{ABC} is a constant and θ_a, θ_b and θ_c are the internal angles of the triangle formed by r_{AB}, r_{BC} and r_{CA}

This dispersion correction can be efficient but still relies on empirical corrections. A second solution is a new type of functionals, the Double Hybrids described in Chapter 5.

2.4 Treatment of relativistic effects

All the methods presented so far were based on the non-relativistic Schrödinger equation. For relatively light atoms (Z < 36), this approximation is fully legitimate but increasing the atomic number of the atom implies for the electrons closer to the nucleus to have a velocity approaching the speed of light [52],

making relativistic effects no longer negligible and affecting their electronic structure.

Relativistic effects can be separated in two types: those independent of the electron spin (or scalar) and those dependent of the electron spin (or spin-orbit). The first steams from the fact that, because of the stronger nuclear attraction (as Z increases), the inner electrons are accelerated and get closer to the nucleus. The consequence is, the contraction and the stabilisation of the *s* and *p* orbitals. Furthermore, as the inner *s* and *p* electrons are drawn towards the core, they increasingly more effective in screening outer shells and as consequence, the *d* and *f* electrons are destabilised. The second category, the spin-orbit one, can be seen, in a classic representation, as the interaction of the electron magnetic moment and the magnetic induction created by the kinetic orbital motion and results in the splitting of orbitals with angular momenta greater than 0.

2.4.1 Dirac equation

According to relativistic theory, since the speed of light and the Physics laws are the same in all inertial frames, the researched equation must be invariant under Lorentz transformation [53][3]. We see, for instance, the time-dependent Schrödinger equation:

$$\frac{-\hbar}{2m}\left[\frac{\partial^2\psi(\boldsymbol{r},t)}{\partial x^2}+\frac{\partial^2\psi(\boldsymbol{r},t)}{\partial y^2}+\frac{\partial^2\psi(\boldsymbol{r},t)}{\partial z^2}\right]=-i\hbar\frac{\partial\psi(\boldsymbol{r},t)}{\partial t} \tag{2.69}$$

does not fulfil this requirement, since the spatial coordinates x, y and z appear as quadratic derivatives while the time appears as its first derivative.

Paul. A. M. Dirac [54] suggested instead an Hamiltonian with linear derivatives of both time and space, introducing the algebraic quantities $\boldsymbol{\alpha}$ and $\boldsymbol{\beta}$. The Dirac equation, in an external electromagnetic potential describes the relativistic motion of an electron as:

$$\left(\beta m_0 c^2+e\phi+\boldsymbol{\alpha}.\boldsymbol{\pi}-ih\frac{\partial}{\partial t}\right)\psi=0 \tag{2.70}$$

[3]Invariant under Lorentz transformation means that the value of a quantity is the same in all Galileen referentials

with

$$\boldsymbol{\pi} = \boldsymbol{p} + e\boldsymbol{A} \tag{2.71}$$

recalling :

$$\boldsymbol{p} \rightarrow p - q\boldsymbol{A}; E \rightarrow -q\phi \tag{2.72}$$

ϕ being the scalar potential and $\boldsymbol{A}$ the vector potential describing the magnetic field and q = -e for an electron and q = +e for a positon. $\boldsymbol{\alpha}$ retains the information about the spin of the particle. Both $\boldsymbol{\alpha}$ and $\boldsymbol{\beta}$ are 4 x 4 matrices defined as:

$$\alpha_x = \begin{pmatrix} 0 & 0 & 0 & 1 \\ 0 & 0 & 1 & 0 \\ 0 & 1 & 0 & 0 \\ 1 & 0 & 0 & 0 \end{pmatrix}, \alpha_y = \begin{pmatrix} 0 & 0 & 0 & -i \\ 0 & 0 & i & 0 \\ 0 & -i & 0 & 0 \\ i & 0 & 0 & 0 \end{pmatrix}, \alpha_z = \begin{pmatrix} 0 & 0 & 1 & 0 \\ 0 & 0 & 0 & -1 \\ 1 & 0 & 0 & 0 \\ 0 & 1 & 0 & 0 \end{pmatrix} \tag{2.73}$$

$$\beta = \begin{pmatrix} 1 & 0 & 0 & 0 \\ 0 & 1 & 0 & 0 \\ 0 & 0 & -1 & 0 \\ 0 & 0 & 0 & -1 \end{pmatrix} \tag{2.74}$$

This can be rewritten with the Pauli matrices, the zero 2 x 2 matrix 0_2 and the 2 x 2 Identity matrix 1_2:

$$\alpha_x = \begin{pmatrix} 0_2 & \sigma_x \\ \sigma_x & 0_2 \end{pmatrix}, \alpha_y = \begin{pmatrix} 0_2 & \sigma_y \\ \sigma_y & 0_2 \end{pmatrix}, \alpha_z = \begin{pmatrix} 0_2 & \sigma_z \\ \sigma_z & 0_2 \end{pmatrix} \tag{2.75}$$

$$\beta = \begin{pmatrix} 1_2 & 0_2 \\ 0_2 & -1_2 \end{pmatrix} \tag{2.76}$$

The Pauli matrices being:

$$\sigma_x = \begin{pmatrix} 0 & 1 \\ 1 & 0 \end{pmatrix}, \sigma_y = \begin{pmatrix} 0 & -i \\ i & 0 \end{pmatrix}, \sigma_z = \begin{pmatrix} 1 & 0 \\ 0 & -1 \end{pmatrix} \tag{2.77}$$

Since $\boldsymbol{\alpha}$ and $\boldsymbol{\beta}$ appears in the equation 2.70 as 4 x 4 matrices the wave function must be a four-component vector:

$$\psi(\boldsymbol{r},t) = \begin{pmatrix} \psi_1(\boldsymbol{r},t) \\ \psi_2(\boldsymbol{r},t) \\ \psi_3(\boldsymbol{r},t) \\ \psi_4(\boldsymbol{r},t) \end{pmatrix} \tag{2.78}$$

Among the four components, two (one for the spin α and one for the β) are the large (L) ones and the other two are the small (S) components (also one for the spin α and one for the β) we can rewrite $\psi(\boldsymbol{r}, \mathrm{t})$ as:

$$\psi(\boldsymbol{r},t) = \begin{pmatrix} \psi^L(\boldsymbol{r},t) \\ \psi^S(\boldsymbol{r},t) \end{pmatrix} = \begin{pmatrix} \psi^L_\alpha(\boldsymbol{r},t) \\ \psi^L_\beta(\boldsymbol{r},t) \\ \psi^S_\alpha(\boldsymbol{r},t) \\ \psi^S_\beta(\boldsymbol{r},t) \end{pmatrix} \tag{2.79}$$

The solution of the time-independent Dirac equation for a free electron can then be found by solving the matrix equation:

$$\begin{pmatrix} mc^2 - E & c(\boldsymbol{\sigma}.\boldsymbol{p}) \\ c(\boldsymbol{\sigma}.\boldsymbol{p}) & -mc^2 - E \end{pmatrix} \begin{pmatrix} \psi^L \\ \psi^S \end{pmatrix} = 0 \tag{2.80}$$

leading to the four two-fold degenerate solutions, corresponding to the large and small components:

$$E^+ = +\sqrt{c^2p^2 + m^2c^4} \tag{2.81}$$

and

$$E^- = -\sqrt{c^2p^2 + m^2c^4} \tag{2.82}$$

indicating that an electron could occupy a positive or negative state. Since the physical meaning of the former states would be a problem, Dirac supposed all the negative states to be occupied [55], That so the electrons would not be able to occupy them due to the Pauli principle. In the presence of a potential such as the nucleus (V = eϕ = $\frac{-Z}{r}$ see equation 2.71), two continuum of states appear, with one corresponding to electronic (positive) states and one for the negative solutions, and bound states in between the continuum.

In this formalism only the one electron equation can be exactly resolved, therefore, some approximations must be made to describe many-electrons systems.

2.4.2 Dirac-Coulomb-Breit Hamiltonian

While multiple electrons are present their motions are dependent from each other. Thus we introduce the many-electron Dirac-Coulomb-Breit Hamiltonian $\hat{H}^{DCB}$ as the sum of the Dirac one-electronic Hamiltonian and the two-electronic Breit correction term g^B_{ij}:

$$\hat{H}^{DCB} = \sum_{i=1}^{N} \hat{h}_i + \sum_{i<j} \hat{g}^B_{ij} \tag{2.83}$$

where

$$\hat{g}^B_{ij} = -\frac{1}{2r_{ij}} \left(\boldsymbol{\alpha}_i . \boldsymbol{\alpha}_j + \frac{(\boldsymbol{\alpha}_i . \boldsymbol{r}_{ij})(\boldsymbol{\alpha}_i . \boldsymbol{r}_{ij})}{r^2_{ij}} \right) \tag{2.84}$$

the first term in parenthesis being the Gaunt interaction [56] and the second the retarded effect important for long distance interactions [57, 58].

2.4.3 Dirac Equation approximations

Since working with the four-component framework can be expensive even for relatively small systems, simplifying the Dirac equation by keeping only two components, the large ones, could save a lot of computational effort. To do so, the large and small components must be separated. It can be done with the elimination of the small components or by decoupling the small and large components with a unitary transformation.

Small Components elimination

In a similar way than in equation 2.80, the time independent Dirac equation for one free electron can be written to take into account an external potential

V (shifting by -mc^2 to set the electronic solutions to zero):

$$\begin{pmatrix} V-E & c(\boldsymbol{\sigma}.\boldsymbol{p}) \\ c(\boldsymbol{\sigma}.\boldsymbol{p}) & V-2mc^2-E \end{pmatrix} \begin{pmatrix} \psi^L \\ \psi^S \end{pmatrix} = 0 \tag{2.85}$$

which is equivalent to resolve the two equations system:

$$\begin{aligned} c(\boldsymbol{\sigma}.\boldsymbol{p})\psi^S + V\psi^L &= E\psi^L \\ c(\boldsymbol{\sigma}.\boldsymbol{p})\psi^L + (V-2mc^2)\psi^S &= E\psi^S \end{aligned} \tag{2.86}$$

Thus it is possible to express ψ^S as a function of ψ^L:

$$\psi^S = K(E)\frac{\boldsymbol{\sigma}.\boldsymbol{p}}{2mc}\psi^L \tag{2.87}$$

with K(E) a local multiplicative operator that depends on the electron energy:

$$K(E) = \left(1 - \frac{V-E}{2mc^2}\right)^{-1} \tag{2.88}$$

By inserting equation 2.87 in the first equation 2.86 we obtained the 2-component equation:

$$\left(\frac{1}{2m}(\boldsymbol{\sigma}.\boldsymbol{p})K(E)(\boldsymbol{\sigma}.\boldsymbol{p}) + V\right)\psi^L = E\psi^L \tag{2.89}$$

This equation allows to retrieve the Schrödinger equation in the non-relativistic limit (c $\rightarrow \infty$ and K $\rightarrow$ 1).

Pauli Hamiltonian

The K(E) term can be expanded as a geometric series as:

$$K(E) = \sum_{k=0}^{\infty}\left(\frac{V-E}{2mc^2}\right)^k \tag{2.90}$$

The Pauli approximation is obtained by retaining the two first terms of the series:

$$K(E) \approx K^{Pauli}(E) = 1 + \frac{V - E}{2mc^2} \tag{2.91}$$

This expansion is only valid if

$$|V - E| << 2mc^2$$

but is not the case in the region close to the nucleus. As r $\rightarrow$ 0 and V = $\frac{-Z}{r} \rightarrow \infty$, making the condition | V - E | < < 2mc^2 not true. Away from the nucleus, K(E) can be expanded to the first order leading to the Pauli Hamiltonian $\hat{H}^{Pauli}$ [59, 60]:

$$\hat{H}^{Pauli} = \hat{T} + V - \frac{1}{8m^2c^2}\boldsymbol{p}^4 + \frac{\hbar^2}{8m^3c^2}(\nabla^2 V) + \frac{\hbar}{4m^2c^2}\boldsymbol{\sigma}.(\nabla V) \times \boldsymbol{p} \tag{2.92}$$

$\hat{T}$ being the kinetic energy operator, V remains the potential created by the nucleus ($-\frac{Ze^2}{r}$) the third term being the mass-speed correction term coming from the relativistic variation of the mass with the speed. The fourth term is a correction due to the fast oscillation of the electron around its mean position. It is also called the Darwin term. Finally the last term is the spin-orbit coupling.

Zeroth Order Relativistic Approximation Hamiltonian

To obtain an approximate Hamiltonian valid in all regions of space one can expanded K(E) differently as:

$$K(E) = \left[1 + \frac{E}{2mc^2 - V}\right]^{-1} = 1 - \frac{E}{2mc^2 - V} + \left[\frac{E}{2mc^2 - V}\right]^2 + ... \tag{2.93}$$

Thus, by keeping the zeroth order of expansion 2.93, we obtain the Zeroth Order Relativistic Approximation (ZORA) Hamiltonian:

$$\hat{H}^{ZORA} = V + (\boldsymbol{\sigma}.\boldsymbol{p})\frac{c^2}{2mc^2 - V}(\boldsymbol{\sigma}.\boldsymbol{p}) \tag{2.94}$$

Of course, this formulation retains the spin-orbit coupling in $\boldsymbol{\sigma}.\boldsymbol{p}$, it is easy to disregard this part to obtain the Scalar Relativistic (SR) ZORA Hamiltonian. In 1998, Christoph van Wüllen [61] showed that the scalar relativistic effects could be fully included in a kinetic operator $\hat{T}_{SR}^{ZORA}$:

$$\hat{T}_{SR}^{ZORA} = \boldsymbol{p}\frac{c^2}{2mc^2 - V}\boldsymbol{p} \tag{2.95}$$

This new operator is really useful when the SOC is small enough to be disregarded and allows to decrease the computational cost.

Decoupling small and large components with unitary transform: the Douglas-Kroll-Hess Hamiltonian

The Douglas-Kroll-Hess (DKH) [62, 63] Hamiltonian does not rely on the elimination of the small components as before but is derived from a unitary transformation U, acting on the Dirac-Coulomb Breit Hamiltonian $\hat{H}^{DCB}$, in order to obtain a diagonal Hamiltonian:

$$U^{\dagger}\hat{H}^{DCB}U = \begin{pmatrix} h_+ & 0 \\ 0 & h_- \end{pmatrix} \tag{2.96}$$

with $U^{\dagger}U = 1$.

The first transformation in the DKH approximation is actually the Foldy Wouthuysen transformation [64] in a free particule case.

$$\hat{U}^{(0)} = \hat{A}_i(a + \boldsymbol{\beta}\boldsymbol{\alpha}\boldsymbol{P}_i) \tag{2.97}$$

with

$$\hat{A}_i = \sqrt{\frac{\hat{E}_i + m_e c^2}{2\hat{E}_i}}; \boldsymbol{P}_i = \frac{c\boldsymbol{p}_i}{\hat{E}_i + m_e c^2} \tag{2.98}$$

with $\hat{E}_i$ the kinetic energy operator for the positive energy states, defined as:

$$\hat{E}_i = \sqrt{m_e^2 c^4 + p_i^2 c^2} \tag{2.99}$$

After this first transformation the resulting Hamiltonian matrix, $\hat{H}^{DKH1}$ is not diagonal but the coupling is already reduced. The potential $\hat{V}$ needs to be now added and the decomposition to be pushed one step further.

$$\hat{U}^{(1)} = \sqrt{1 + \hat{W}_1^2} + \hat{W}_1 \tag{2.100}$$

with

$$\hat{W}_1(i) = \hat{W}_1\phi(\boldsymbol{p}_i) = \int d^3p_j \hat{W}(\boldsymbol{p}_i, \boldsymbol{p}_j)\phi(\boldsymbol{p}_j) \tag{2.101}$$

where:

$$\hat{W}(\boldsymbol{p}_i, \boldsymbol{p}_j) = \int d^3p_j \hat{A}_i(\boldsymbol{\sigma}\boldsymbol{P}_i - \boldsymbol{\sigma}\boldsymbol{P}_j)\hat{A}_j \frac{\hat{V}(\boldsymbol{p}_i, \boldsymbol{p}_j)}{\hat{E}_i + \hat{E}_j}\phi(\boldsymbol{p}_j) \tag{2.102}$$

$\hat{V}(\boldsymbol{p}_i, \boldsymbol{p}_j)$ being the the Fourier transform of the potential energy and $\phi(p_i)$ the (bi-spinor) wave function associated to an electron having the momentum $\boldsymbol{p}_i$. The decoupled Hamiltonian for two particles is thus:

$$\hat{H}^{Decoupled} = \beta\hat{E}_i + \hat{A}_i(\hat{V} + \boldsymbol{\sigma}\boldsymbol{P}_i\hat{V}\boldsymbol{\sigma}\boldsymbol{P}_i)\hat{A}_i - \beta(\hat{W}_1\hat{E}_i\hat{W}_1 + \frac{1}{2}[\hat{W}_1^2, \hat{E}_i]_+) \tag{2.103}$$

Using the Dirac relation $((\boldsymbol{\sigma}.\boldsymbol{u})(\boldsymbol{\sigma}.\boldsymbol{v}) = \boldsymbol{u}.\boldsymbol{v} + \mathrm{i}\,\boldsymbol{\alpha}(\boldsymbol{u} \times \boldsymbol{v}))$, it is possible to separate the terms spin-independent to the spin-dependent leading to the $\hat{H}^{SF}$ and $\hat{H}^{SO}$, respectively.

$$\hat{H}^{SF} = \sum_i \hat{E}_i + \sum_i \hat{V}_{eff}^{SF}(i) + \sum_{i<j} \frac{1}{r_{ij}} \tag{2.104}$$

with

$$\begin{aligned} \hat{V}_{eff}^{SF}(i) &= -\hat{A}_i[V(i) + \boldsymbol{P}_i V(i)\boldsymbol{P}_i]\hat{A}_i - \hat{W}_1(i)\hat{E}_i\hat{W}_1(i) - \frac{1}{2}[\hat{W}_1^2(i), \hat{E}_i] \\ V(i) &= \sum_\alpha \frac{Z_\alpha}{r_{i\alpha}} \end{aligned} \tag{2.105}$$

and $\hat{H}^{SO}$:

$$\begin{aligned}\hat{H}^{SO} =& \alpha\hbar c\Bigg\{ \sum_i \sum_a Z_a \frac{\hat{A}_i}{\hat{E}_i + m_e c^2} \boldsymbol{\sigma}_i \left(\frac{\boldsymbol{r}_{ia}}{r_{ia}^3} \times \boldsymbol{p}_i\right) \frac{\hat{A}_i}{\hat{E}_i + m_e c^2} \\ & - \sum_{i \neq j} \frac{\hat{A}_i \hat{A}_j}{\hat{E}_i + m_e c^2} . \left(\boldsymbol{\sigma}_i \frac{\boldsymbol{r}_{ij}}{r_{ij}^3} \times \boldsymbol{p}_i\right) \frac{\hat{A}_i \hat{A}_j}{\hat{E}_i + m_e c^2} - 2\boldsymbol{\sigma}_i \left(\frac{\boldsymbol{r}_{ij}}{r_{ij}^3} \times \boldsymbol{p}_i\right) \frac{\hat{A}_i \hat{A}_j}{\hat{E}_i + m_e c^2} \Bigg\}\end{aligned} \tag{2.106}$$

This SO Hamiltonian is the sum of one-electron and two-electrons terms. The matrix elements of the SO operator are still expensive to calculate. A solution is to approximate this Hamiltonian. The Atomic Mean Field Approximation (AMFI) is used to reduce the number of integrals to calculate using a "simple" idea since the SO interaction is short range as it behaves (as $\frac{1}{r^3}$), it is relevant to disregard all multi-center two-electron SO integrals [65]. For a balanced treatment of SO effects, it is also appropriate to only include one-center one-electron SO integrals.

To simplify the SO Hamiltonian in a context of CI-SO coupling, Hess *et al.*[65] showed that the doubly excited determinants SO contributions can be negligible if the matrix elements of the SO operator between two Slater determinant that differ from only one single-excitation (from the spin orbital i to the spin orbital j) are modified in a way that defines the effective mean field one-electronic operator as:

$$\begin{aligned}\hat{H}_{ij}^{SO} = & \langle \phi_i(1) | \, \hat{h}^{SO}(1) \, | \phi_j(2) \rangle + \frac{1}{2} \sum_k n_k \Big\{ \langle \phi_i(1) | \, \widetilde{H}_{kk}^{SO}(1) \, | \phi_j(1) \rangle \\ & - \langle \phi_i(1) | \, \widetilde{H}_{kj}^{SO}(1) \, | \phi_k(1) \rangle - \langle \phi_k(1) | \, \widetilde{H}_{ik}^{SO}(1) \, | \phi_j(1) \rangle \Big\}\end{aligned} \tag{2.107}$$

with

$$\langle \phi_i(1) | \, \widetilde{H}_{kk}^{SO}(1) \, | \phi_j(1) \rangle = \langle \phi_i(1) [\phi_k(2) | \, \widetilde{H}_{1,2}^{SO} \, | \phi_k(2)] \phi_j(1) \rangle \tag{2.108}$$

$$\langle \phi_i(1) | \, \widetilde{H}_{kj}^{SO}(1) \, | \phi_k(1) \rangle = \langle \phi_i(1) [\phi_k(2) | \, \widetilde{H}_{1,2}^{SO} \, | \phi_j(2)] \phi_k(1) \rangle \tag{2.109}$$

$$\langle \phi_k(1) | \, \widetilde{H}_{ik}^{SO}(1) \, | \phi_j(1) \rangle = \langle \phi_k(1) [\phi_i(2) | \, \widetilde{H}_{1,2}^{SO} \, | \phi_k(2)] \phi_j(1) \rangle \tag{2.110}$$

and :

$$\hat{h}^{SO}(1) = \alpha\hbar c\left\{ \sum_a Z_\alpha \frac{\hat{A}_1}{\hat{E}_1 + m_e c^2} \boldsymbol{\sigma}_1 \left(\frac{\boldsymbol{r}_{1a}}{r_{1a}^3} \times \boldsymbol{p}_1\right) \frac{\hat{A}_1}{\hat{E}_1 + m_e c^2} \right\} \tag{2.111}$$

$$\widetilde{H}_{1,2}^{SO} = \alpha\hbar c\left\{ \frac{\hat{A}_1\hat{A}_2}{\hat{E}_1 + m_e c^2} . \left(\boldsymbol{\sigma}_1 \frac{\boldsymbol{r}_{12}}{r_{12}^3} \times \boldsymbol{p}_1\right) \frac{\hat{A}_1\hat{A}_2}{\hat{E}_1 + m_e c^2} - 2\boldsymbol{\sigma}_1 \left(\frac{\boldsymbol{r}_{12}}{r_{12}^3} \times \boldsymbol{p}_1\right) \frac{\hat{A}_1\hat{A}_2}{\hat{E}_1 + m_e c^2} \right\} \tag{2.112}$$

n_k is the occupation of spin-orbital k, ϕ_i an occupied and ϕ_j a virtual orbital. Since equation 2.107 describes the valence electrons in a field created by the electrons in the orbitals k $\neq$ i, n_k and ϕ_k must have a physical meaning. For this reason, the AMFI module must be used with atomic natural orbitals such as the relativistic contracted ANO-RCC basis sets (see Section 2.5.1).

2.4.4 Relativistic Effective Core Potential

In chemistry, many molecule's properties involve the valence electrons and eventually the sub-valence shells. It is then possible to speed up the calculation by replacing the core electrons by an effective core potential (ECP) [66]. Since the number of electrons is smaller and the number of functional basis can be reduced, the calculation becomes less expensive. The second advantage of ECP is its convenience because it can be used with DFT and wave function methods. The Hamiltonian is reduced to the sum of the interaction between the valence electrons and the interaction of the former with the nucleus/core electrons and called the valence Hamiltonian $\hat{H}^v$:

$$\hat{H}^v = \sum_i^{n_{valence}} -\frac{1}{2}\hat{\nabla}_i^2 + \sum_{i<j}^{n_{valence}} \frac{1}{r_{ij}} + \sum_i^{n_{valence}} \sum_I^N V_{cv}^I(i) + \sum_{I<J}^N \frac{Q_I Q_J}{R_{IJ}} + V_{CPP} \tag{2.113}$$

The first term is the kinetic energy of the valence electrons. The second is the interaction between the valence electrons, the third one is the interaction between the electron/nuclei and valence electrons. The fourth term is the repulsion between effective cores. The last term is the core polarisation potential (CPP). V_{cv} in equation 2.113 is parametrised to include not only to

the scalar relativistic effects but also the spin-orbit relativistic effects so it is adjusted to reproduce data with great accuracy.

$$V_{cv}^{I}(i) = \sum_{i}^{n_{valence}} \frac{Q_I}{r_{iI}} + \sum_{i}^{n_{valence}} V_{PP}^{I}(i) \tag{2.114}$$

The name of the ECP is given under the form ECPnXY where usually XY represents the level of the fully relativistic method used to generate the target all-electron data to which the ECP parameters are adjusted: MWB for multi-configurational Wood-Boring or MDF for multi-configuration Dirac-Fock [67].

2.5 Basis Sets, Basis Sets Superposition Error and Complete Basis Set Extrapolation

2.5.1 Basis Sets

Back to equation 2.10, the wave-function is described by a Slater determinant composed of orthonormal spin-orbitals. In a molecule, each spin-orbital represents a molecular orbital (MO) ϕ_i which can be represented by a Linear Combination of Atomic Orbitals (LCAO) [68], χ_k.

$$\phi_i = \sum_{j}^{N_{AO}} c_{ij}\psi_i = \sum_{j}^{N_{AO}} c_{ij} \sum_{k}^{Nb} d_{jk}\chi_k \tag{2.115}$$

d_{jk} being the expansion coefficients, χ_k the atomic basis functions, and Nb the number of the basis function used. A minimum basis set contains roughly[4] as much basis function as there are atomic orbitals.

The only restriction for mathematical functions to be used as basis functions is to decay to zero as the distance between the nuclei and the electron increases. In practice, two families of orbitals are used: the Slater Type Orbitals (STO) [69] and the Gaussian Type Orbitals (GTO) [70] both products of a radial part $\mathcal{R}_l(r)$ and a spherical harmonic function $Y_{lm_l}(\theta\phi)$.

[4] sometimes extra orbitals are added for polarization

- Slater Type Orbitals

Slater-type orbitals, the radial part only depends on n as

$$\mathcal{R}_n = N_{Slater} r^{n-1} e^{-\zeta r} \tag{2.116}$$

n being the principal quantum number, N_{Slater} the normalisation constant, r is the distance between the electron and the nucleus and ζ a constant related to the effective charge of the nucleus Z^* such that the energy level of this orbital equals to

$$E_n = \frac{1}{2}\left(\frac{Z^*}{n}\right)^2 \tag{2.117}$$

STO basis are successful for atoms as they describe the cusp at the nucleus. However, their limitation is that two-electrons integrals involving 3 or 4 centres cannot be computed analytically.

- Gaussian Type Orbitals

To overcome the integration issue, GTO (Gaussian Type Orbitals) were introduced defined as:

$$\mathcal{R}_n = N_6(\alpha) r^{n-1} e^{-\alpha r^2} \tag{2.118}$$

for their radial part. If the GTOs allow the calculations to be performed faster, the r^2 dependency alter the description of the electron behaviour near the nucleus [10]. Therefore a larger basis will be needed to reach the same accuracy as with an STO.

Linear combinations (contractions) of primitive GTOs functions are able to approximate the nodal structures of atomic orbitals (AO). The quality of a basis set is linked to the number of Gaussian primitives and to the optimisation of the contraction coefficients.

In the current work, we aim at computing reaction energies with an accuracy of a few kJ.mol^{-1}. Thus the choice of the atomic basis set is crucial. In all the PhD projects, basis sets of at least triple-ζ quality were used to determine the optimal geometries, using correlation consistent Dunning's basis sets [71, 72], aug-cc-pVTZ/aug-cc-pVQZ, and the proper small-core RECP basis sets

for the heavy elements. For the largest molecular complexes (See Chapter 3), efficient computational speed up was achieved with the resolution of the identity algorithm, using Ahlrichs def2-TZVP basis sets and their auxiliary counterparts [73, 74]. Note that for heavy elements, the def2-basis sets are bound to small-core RECPs.

To reach chemical accuracy (or higher) for thermodynamics properties of plutonium gas-phase molecules, the electronic energies were extrapolated to the complete basis set limit, from calculations with the extended all-electron atomic natural orbital relativistic correlation consistent (ANO-RCC) Roos's basis sets [75–77], which offer from triple to quadruple-ζ quality expansions in the Douglas-Kroll-Hess relativistic framework [78].

We will comment on the choice of the basis sets in the appropriate introductory sections of each research project.

2.5.2 Basis Sets Superposition Error

The Basis Sets Superposition Error (BSSE) introduced by Boys and Bernardi [79] occurs when 2 atoms (A and B) are close to each other. The basis set of the atom A will be superposed with the basis set of the atom B describing twice the same stabilising energy. Thus, the total energy is lower than what it should be and must be corrected.

$$E_{corrected} = E_{uncorrected} + E_{BSSE} \tag{2.119}$$

In order to compute the corrected total energy, the energy of atom A has to be calculated in the presence of the basis of the atom B and the energy of atom B in the presence of the basis of the atom A.

$$E_{BSSE} = E_A^A - E_A^{AB} + E_B^B - E_B^{AB} \tag{2.120}$$

where the superscripts refers to the basis set used and the subscripts the atom.

FIGURE 2.2: Theoretical convergence to the complete basis set limite with increasing the number of basis functions

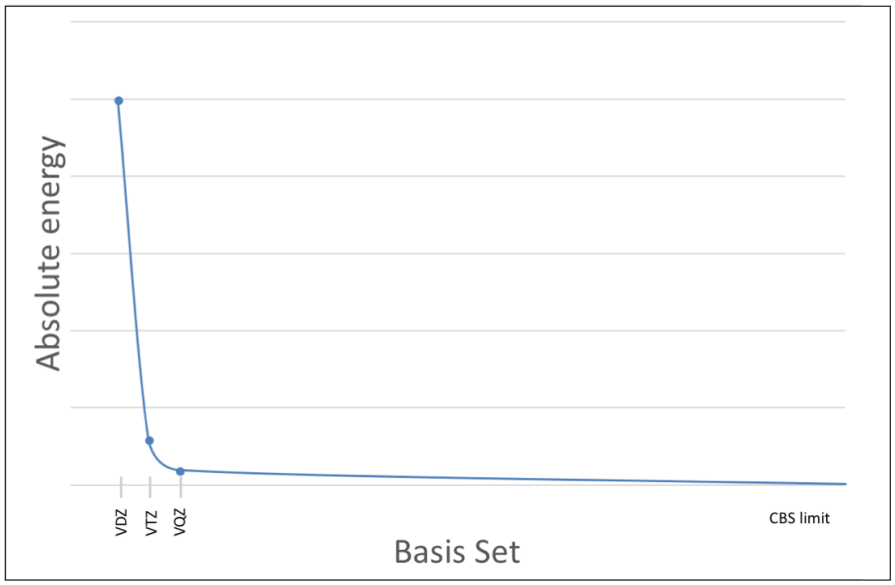

2.5.3 Complete Basis Set Extrapolation

A way to avoid BSSE, among others, is to extrapolate the energy to the Complete Basis Set (CBS) limit *i.e.* to approach the results with infinite basis sets (see Figure 2.2).

In this work we compared two ways of extrapolating energies, one by extrapolating the total energy, the second by extrapolating separately the SCF energy and the correlated energy before summing the two.

The total energy CBS value can be derived from a two-points extrapolation formula [80]:

$$E_{XY}^{CBS} = \frac{X^3 E_X - Y^3 E_Y}{X^3 - Y^3} \tag{2.121}$$

where X and Y are the size of the basis sets (typically n=3 and n=4 for triple and quadruple-ζ basis sets).

Peterson *et. al.* [81] proposed specific formulas for the uncorrelated energy E_{CBS}^{SCF} and the correlated energy E_{CBS}^{Corr} extrapolations:

$$E_n^{SCF} = E_{CBS}^{SCF} + A(n+1)e^{-6.57\sqrt{n}} \tag{2.122}$$

$$E_n^{corr} = E_{CBS}^{corr} + \frac{B}{(n+\frac{1}{2})^4} \tag{2.123}$$

In these formulas n is the size of the basis set (typically n=3 and n=4 for triple and quadruple-ζ basis sets), E^{SCF} is either the SCF or CASSCF energy and E^{corr} the correlation part of the total energy.

2.6 Conclusion

As mentioned before, only a few and basic methods of Quantum Chemistry were depicted here. Nonetheless, it already triggers some general questions at the heart of the modelling of Actinides.
How to properly describe the relativistic effects ?
How the retrieve electronic correlation ?
If the first question is almost answered in the present section, the former question will be addressed more particularly in the Chapter 4. Indeed, a good way to describe the static correlation is to use methods including multiple Slater determinants in the wave function. These methods are called "multi-reference" quantum chemical methods.

Chapter 3

Coordination of Alkyl cations $[(XA_2)X(CH_2SiMe_3)]$ (X = Th, U) or$[(XN_2)Zr(CH_3)]$ with an arene for Ethylene polymerisation: Exploration of the bonding

3.1 Introduction

The amount of polyethylene produced every year implies a constant need for improving the industrial production process. Since the pioneering process by Karl Ziegler and Giulio Natta in the early 1950's on the polymerisation of simple olefins, there had been intense interest in the application of early transition metal catalysts for the selective polymerisation of inexpensive olefins. Following to Ziegler-Natta catalysts [82] , metallocene catalysts were discovered in the late 1980's and resulted in numerous industrial processes for improving the properties of polyolefinic materials along with performance parameters. In particular, beside the requirement of higher activity, research have focused on the control of particle size, particle size distribution, and the morphology of the resultant polyolefin (number of carbon in the chain). In the metallocene family, group 4 transition metal metallocene complexes have the largest activity, such as $[Cp_2ZrMe][B(C_6F_4TBS)_4]$ synthesised by Marks and co-workers [83–91] 1.1 x 10^7g of polyethylene.(mol

of M=Zr)$^{-1}$.h^{-1}.atm^{-1}[92]). The brother complex with Th was also synthesised but is an order of magnitude less active than the Zr-complex (9.2 x 10^5g of polyethylene.(mol of Th)$^{-1}$.h^{-1}.atm^{-1}), suggesting that the nature of the metallic centre may play a key role in the catalytic activity. In the 1990s, new catalysts with well-defined metal complexes and other ligand motifs were summarised as the "post metallocenes" family [93].

During my first-year PhD stay at Mc Master University in Hamilton (Ontario, Canada), discussions were initiated with David Emslie's research group, currently working on the synthesis of cationic metal alkyl complexes, that are open post-metallocene catalysts of electropositive metals. These are typically generated by reaction of a neutral dialkyl complex with strong electrophiles such as $[CPh_3][B(C_6F_5)_4]$, $[HNMe_2Ph][B(C_6F_5)_4]$, $B(C_6F_5)_3$ or $(Al(CH_3)xOy)n$ (Methylaluminoxane-MAO). The subsequent polymerisation is achieved by repeated ethylene coordination and 1,2-insertion steps [1]. These activation and polymerization reactions are commonly conducted in arene or alkane solvents; the former is standard in academic laboratories [2], while the latter is favoured in industry [3, 94]. However, in sterically open post-metallocene catalysts of electropositive metals, arene solvents have significant potential to coordinate, negatively impacting ethylene polymerisation activity. At the same time arene coordination is known to increase the thermal stability of metal alkyl cations prior to exposure to ethylene, which is of key importance for industrial polymerisation processes often conducted at elevated temperatures (140 °C). Therefore, Emslie's group has explored, in a systematic fashion, the suitability of tetravalent actinides, namely Thorium and Uranium, to create thermally robust and highly reactive cationic monoalkyl derivatives, as an alternative to the Zirconium based ones.

The chapter begins with a review of all the Zr, Th, and U complexes that were synthesised and crystallised when possible for structural characterisation. We will also present the evaluated ethylene polymerisation activities at room and elevated (70-80 °C) temperatures. The experimental work scanned several arene solvents, from benzene, toluene, to halogenated derivatives of benzene (bromo-benzene, fluoro-benzene and di fluorobenzene), with different electron donor capabilities, noting for example that Hayes *et al.* showed a good activity for a scandium complex in Bromobenzene [95, 96]. In an

attempt to link the catalytic properties with the complexes structures and coordination, the second part will present the quantum chemical calculations that allow an in-depth discussion of the influence of the cation and the impact of arene solvent coordination. We finally investigate the strength of the interaction between cationic metal alkyl complex with ethylene to shed some light on the competition between ethylene and arene coordination in the initial steps of the catalytic reaction.

3.2 Systems presentation and theoretical studies

3.2.1 Catalysts synthesis strategy, structures and catalytic power

Using a neutral dialkyl **1-X** (X = Th, U or Zr) the arene-coordinated alkyl cations could be derived, where the arene (benzene, toluene, bromo-benzene, fluorobenzene or the (o)-difluoro-benzene) is introduced by the solvent. The catalytic power and the robustness of the compounds were tested by exposing them to ethylene during 30 min at temperatures between 20 and 70 °C (80 °C for **n-Zr**). It is important to note that early transition metal and f-element olefin polymerisation catalysts are frequently generated *in situ* without isolation and characterisation, this lack of information is the main source of uncertainties in the mechanism.

TABLE 3.1: Name of the different ligands, counter ion and arene of the compounds discussed in this Chapter

	Formula	Name
Ligands	XA_2	4,5-bis(2,6-diisopropylanido)-2,7-di-tert-butyl-9,9-dimethylxanthene
Ligands	XN_2	4,5-bis(2,4,6-triisopropylanido)-2,7-di-tert-butyl-9,9-dimethylxanthene
	CH_2SiMe_3	(trimethylsilyl)methyl
Counter ion	$B(C_6F_5)_4^-$	diskal tetrakis(pentafluorophenyl)borate
Arene	C_6H_6	Benzene
	$C_6H_5CH_3$	Toluene
	C_6H_5Br	Bromobenzene
	C_6H_5F	Fluorobenzene
	$C_6H_5F_2$	Difluorobenzene
	C_2H_2	Ethylene

The different metallic centres are chosen first because the literature reports their efficiency (see Section 3.1) and because of their electronic structure in the tetravalent oxidation state. Zr(IV) is a $4d^0$-element with the smallest ionic radius, while Th(IV) is a $5f^0$-element and U(IV) a $5f^2$-element with larger ionic

TABLE 3.2: Numbers and Formula of the different compounds of the present Chapter

Number	Formula	X-ray structure
1-U	$[(XA_2)U(CH_2SiMe_3)_2]$	yes
2-U	$[(XA_2)U(CH_2SiMe_3)(C_6H_6)]^+[B(C_6F_5)_4]^-$	yes
3-U	$[(XA_2)U(CH_2SiMe_3)(C_6H_5CH_3)]^+[B(C_6F_5)_4]^-$	yes
4-U	$[(XA_2)U(CH_2SiMe_3)(C_6H_5Br)]^+[B(C_6F_5)_4]^-$	no
5-U	$[(XA_2)U(CH_2SiMe_3)(C_6H_5F)]^+[B(C_6F_5)_4]^-$	yes
6-U	$[(XA_2)U(CH_2SiMe_3)(C_6H_4F_2)]^+[B(C_6F_5)_4]^-$	no
E-U	$[(XA_2)U(CH_2SiMe_3)(C_2H_2)]^+[B(C_6F_5)_4]^-$	not synthesised
1-Th	$[(XA_2)Th(CH_2SiMe_3)_2]$	no
2-Th	$[(XA_2)Th(CH_2SiMe_3)(C_6H_6)]^+[B(C_6F_5)_4]^-$	yes
3-Th	$[(XA_2)Th(CH_2SiMe_3)(C_6H_5CH_3)]^+[B(C_6F_5)_4]^-$	no
4-Th	$[(XA_2)Th(CH_2SiMe_3)(C_6H_5Br)]^+[B(C_6F_5)_4]^-$	not synthesised
5-Th	$[(XA_2)Th(CH_2SiMe_3)(C_6H_5F)]^+[B(C_6F_5)_4]^-$	no
6-Th	$[(XA_2)Th(CH_2SiMe_3)(C_6H_4F_2)]^+[B(C_6F_5)_4]^-$	not synthesised
2′-Th	$[(XN_2)Th(CH_3)(C_6H_6)]^+[B(C_6F_5)_4]^-$	not synthesised
E-Th	$[(XA_2)Th(CH_2SiMe_3)(C_2H_2)]^+[B(C_6F_5)_4]^-$	not synthesised
2-Zr	$[(XA_2)Zr(CH_2SiMe_3)((C_6H_5CH_3))]^+[B(C_6F_5)_4]^-$	not synthesised
2′-Zr	$[(XN_2)Zr(CH_3)(C_6H_6)]^+[B(C_6F_5)_4]^-$	no
3′-Zr	$[(XN_2)Zr(CH_3)(C_6H_5CH_3)]^+[B(C_6F_5)_4]^-$	yes
4′-Zr	$[(XN_2)Zr(CH_3)\ (C_6H_5Br)]^+[B(C_6F_5)_4]^-$	no
5′-Zr	$[(XN_2)Zr(CH_3)\ (C_6H_5F)]^+[B(C_6F_5)_4]^-$	not synthesised
6′-Zr	$[(XN_2)Zr(CH_3)\ (C_6H_4F_2)]^+[B(C_6F_5)_4]^-$	not synthesised
E′-Zr	$[((XN_2)Zr(CH_3)(C_2H_2)]^+[B(C_6F_5)_4]^-$	not synthesised

radii (see Table 3.3). In the actinides, while the 5f-orbitals are expected to participate into the bonding, the 6d-orbitals in U(IV) complexes may also play a role in the bonding, allowing back donation electron transfer [97].

TABLE 3.3: Ionic Radii of metallic center in Å from [98]

Element	Ionic Radius
Zr	0.72
Th	0.94
U	0.89

The choice of the arene is made in order to tune the donating capacity. This donating power is directly connected to the strength of the cation arene bond. If too strong it could hinder or even shutter ethylene coordination and impact the catalytic activity (see Section 3.2.2).

We start the a survey on Emslie's work with the cation derivatives of the neutral dialkyl **1-Th**. **2-Th**, **3-Th** and **5-Th** cations [99–102]. All of them could be synthesised but only **2-Th** could be characterised with X-ray diffraction (see Figure 3.1). Unfortunately only **5-Th** exhibits a catalytic power but it is not thermally robust (see Table 3.5). **4-Th** could not be synthesised and no attempt was made for the generation of **6-Th**.

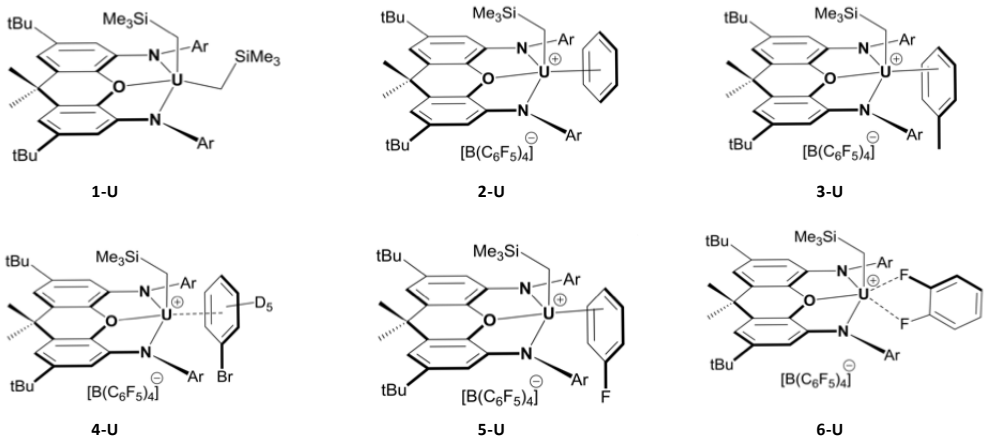

FIGURE 3.1: Structures of the catalysts containing uranium, thorium ones are strictly equivalent.

The benzene **2-U** and toluene **3-U** derivatives of **1-U**, are more soluble than their thorium equivalents [103–107]. Thus it could be crystallised to obtain a deep brown solids (see Figures 3.2 and 3.3 for structure). The distances are, as expected from the ionic radii, shorter in the uranium complexes than in the thorium ones (see Table 3.4). **4-U** (bromobenzene) was readily obtained

but not structurally characterised and catalytically silent.

TABLE 3.4: Important bond lengths in Å and angles in degree for the neutral **1-U** and the cationic **2-U**, **2-Th**, **3-U**, **3'-Zr** and **5-U** given by X-ray diffraction [108].

Compounds	**1-U**	**2-U**	**2-Th**
An-O	2.484(5), 2.504(4)	2.441(2)	2.496(5)
An-N	2.261(5), 2.262(5), 2.272(5), 2.280(5)	2.224(2), 2.236(6)	2.278(3), 2.288(3)
An-C_{arene}	–	3.099(3) - 3.248(3)	3.18 - 3.31
$N_1 \ldots N_2$	4.00, 4.02	3.94	4.04
Arene Bend Angle [1]	17.5, 18.8	18.9	8.7
O-An-C_{apical}	94.8(2),95.0(2)	87.26(8)	91.3(1)
An-C-Si	128.2(3), 130.4(3), 130.5(4), 130.8(3)	133.7(2)	131.0(2)
Compounds	**3-U**	**3'-Zr**	**5-U**
An-O	2.417(9)	2.220	2.431(3)
An-N	2.21(1), 2.22(1)	2.138; 2.122	2.215(3), 2.218(3)
An-C_{arene}	3.05(2) - 3.78(2)	2.697 - 2.840	3.129(5) - 3.598(6)
$N_1 \ldots N_2$	3.98	3.91	3.98
Arene Bend Angle[1]	5.9		7.2
O-An-C_{apical}	88.8(4)		89.6(1)
An-C-Si	136.8(7)	–	134.8(2)

[1] Angle between the carbons of the arene and the planar ligand.

Bromobenzene was then exchanged (conceptually) with fluorobenzene to have an expected less donating ligand character, leading to **5-U** which could be X-ray analysed (see Figure 3.4). This makes it the first 5*f*-element complex bearing a π-coordinated fluoroarene ligand crystallographically characterised. Table 3.4 shows a ressemblance between **5-U** and **3-U** with the same distance N_1-$_2$ (3.98 Å) and the smallest arene bend angle (7.2 °and 5.9°, respectively).

In order to further decrease the coordination between arene and the uranium

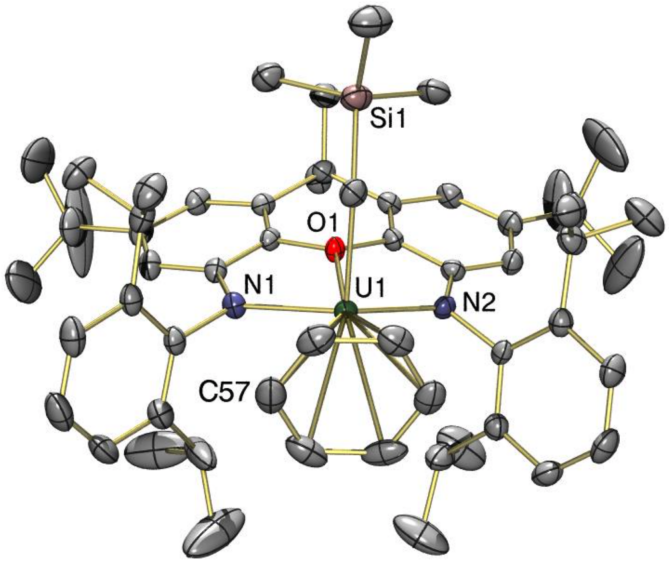

FIGURE 3.2: X-ray crystal structure of η^6**-2-U** [108]. Hydrogen atoms are not represented

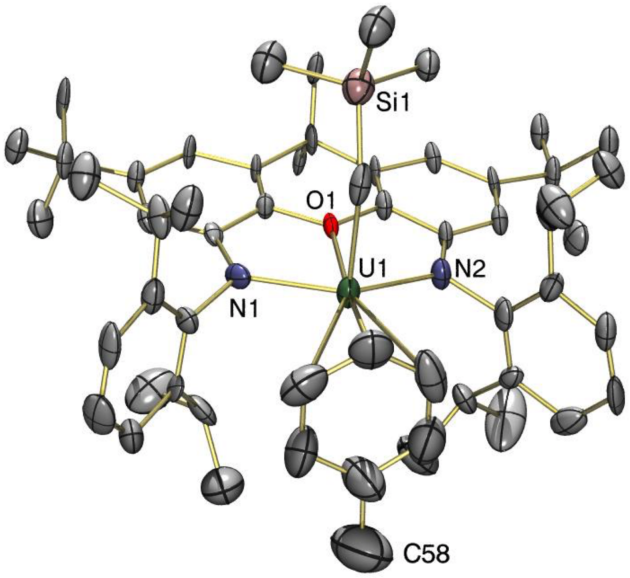

FIGURE 3.3: X-ray crystal structure of η^6**-3-U** [108]. Hydrogen atoms are not represented

mettalic center, the cation with *o*-difluorobenzene was synthesised but could not be crystallised.

The activity of **5-U** is slightly larger than **6-U**, 1.12 x 10^4g of polyethylene.(mol

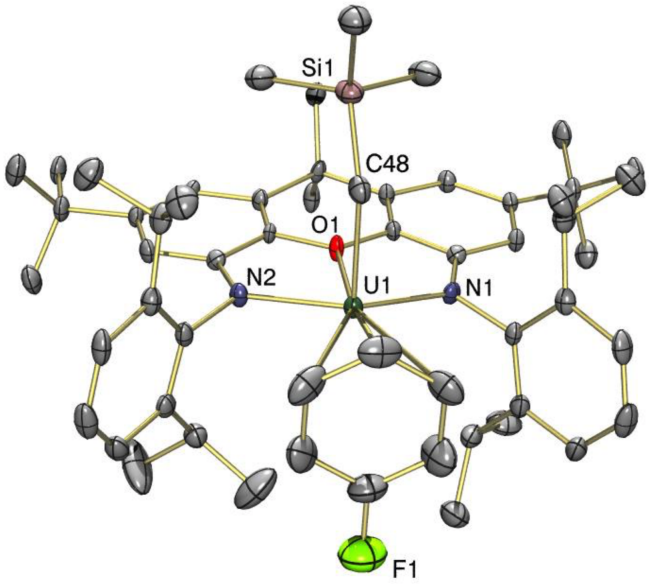

FIGURE 3.4: X-ray crystal structure of η^6-**5-U** [108]. Hydrogen atoms are not represented

of U)$^{-1}$.h^{-1}.atm^{-1} at 20 °C (see Table 3.5). However, at higher temperature (70 °C) no polymerisation is observed, indicating that **6-U** has a reduced thermal stability. An attempt was made to use the *m*-difluorobenzene, unfortunately no polyethylene was formed after 30 minutes at 20 °C.

TABLE 3.5: Activities of complexes at and 1 atm in g of polyethylene.(mol of X=Th, U or Zr)$^{-1}$.h^{-1}.atm^{-1} and after 30 min of ethylene exposure.

Complex	Activity (20°C)	Activity (70°C)[1]
2-U	0	0
3-U	0	0
4-U	0	0
5-U	12 800	39 200
6-U	11 200	0
2-Th	0	0
3-Th	0	0
5-Th	16 800	57 600
2'-Zr	NA	NA
3'-Zr	273 000	113 000
4'-Zr	52 200	NA

At the same time, close equivalents were synthesised with a zirconium center [109].

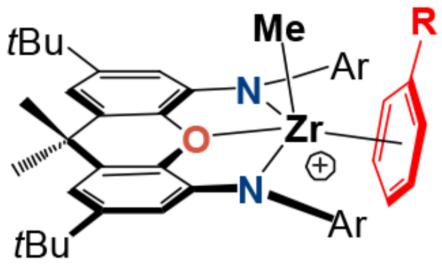

FIGURE 3.5: Structures of the compounds containing zirconium, with R = H, CH_3, F, Br .

2′-Zr polymerises so slowly that its activity is negligible. **3′-Zr** presents excellent performance with an activity of 2.73 x 10^5g.mol $^{-1}$.h^{-1}.atm^{-1} observed after 30 minutes at 20 °C and 1.11 x 10^5g.mol $^{-1}$.h^{-1}.atm^{-1} observed after 30 minutes at 80 °C. The decrease of the activity as the temperature increases can probably be explained by the decomposition of the catalyst. **4′-Zr** could be obtained (see Figure 3.6) and presents an activity close to that of **3′-Zr**. Its structure could not be resolved since the synthesis leads to a mixture of two isomers (see Figure 3.6). There is no report of synthesis concerning **5′-Zr** or **6′-Zr** yet.

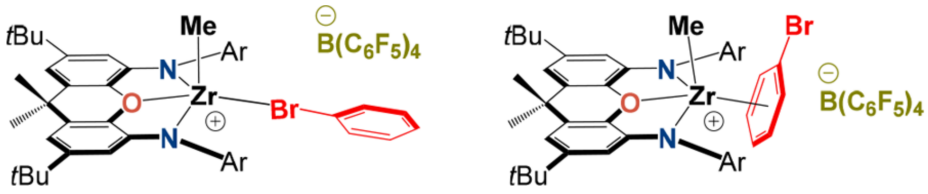

FIGURE 3.6: Possible structures of **4′-Zr** [109]

3.2.2 Finding the catalytic mechanism

The rationalisation of the catalytic mechanism is not easy since several hypotheses can be put forward:

- First, is it a concerted mechanism like in Figure 3.7 where both arene and ethylene are bonded at the same time to the metallic center or not ?

- If not, the relative bonding strengths of ethylene versus arene with the metal will be important. If the arene-metal bond is too strong, the ethylene will not be able to insert itself and the catalysis will not occur.

The success of the zirconium complexes over the actinides ones raises the question on the nature of the arene bonds to the metals. Having the smallest ionic radius Zr could be expected to form stronger bonds than the Th and U, contradicting the observed efficiency.

Gardner *et al.* [110] reported a larger catalytic power for Th complexes ([Th{N(CH_2CH_2 $NSiPri_3)_2(CH_2CH_2NSiPri_2C[H]MeCH_2)$}]) than for the U ones (as for **5-U** and **5-Th**), and proposed as an explanation that electrostatic interactions are dominant in Th-complexes making the Th-ligand bond reacting more easily than the U-ligand one. Conversely, Domeshek *et al.* [111], in their complexes bis(N,N'-bis(trimethylsilyl)-2-pyridylami-dinate)An(μ-Cl)$_2$Li(TMEDA) (An = Th, U) found that U-complexes are more efficient than the Th ones. They proposed three explanations. The first is that the $5f^2$ electrons of uranium can participate to a back-donation leading to an improved coordination to the olefin facilitating the activation of the double bond. The second is that the thorium complexes form stronger bonds with the arene making the insertion of ethylene harder. Another explanation is that the 5f orbitals in the U complex could stabilise the 4-member transition state (Figure 3.7), thus facilitating the catalysis [112].

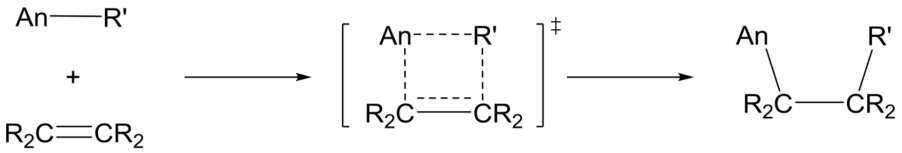

FIGURE 3.7: Four-center transition state in neutral organoactinide-mediated transformation where R' is the arene [108]

The last explanation appears as the simplest, as the larger size of Th(IV) might make it sterically more accessible than the U(IV) .

Of course, the true explanation can be a mixture of these hypothesis calling for a theoretical study of the systems to rationalise their catalytic activities and the mechanism of polymerisation by answering the following questions:

- Why do Zr complexes present such short bonds between the arene and the metal?
- What is the dominant nature of the bonding (electrostatic, covalent?...)?
- What is the participation of d and f orbitals into the bonding?
- What is the strength of the ethylene-metal versus the arene-metal bond?

3.2.3 Theoretical Studies of the Th, U and Zr cationic complexes

The theoretical studies of the complexes cited in the previous section are very limited. One theoretical study explored the catalysis reaction path [110]. It includes a full geometry optimisation followed by an anharmonic frequency calculation with the B3PW91 [113, 114] functional. Scalar relativistic effects were included by the Stuttgart-Dresden RECP [115, 116] and the corresponding basis sets. These articles emphasised the important role of the 5f-orbitals of thorium [110] and uranium [110, 117].

This study confirm that the explanations proposed by experimentalists such as electrostatic interaction, back-donation and strength of the bonds must be tested and assessed by an in-depth exploration of the bond between the various metallic centre and the arene solvents. In this context, we have used the ETS-NOCV bonding analysis [118, 119] that has been proven useful to elucidate the nature of the bonding interaction in multiple transition metal complexes [97, 120–129].

We start by optimising the structures of the complexes and compare the computed geometries to X-ray data, when available. Ultimately our results should address the previous and the following questions:

- How well do quantum chemistry structures agree with X-ray data?
- Is it possible to predict the geometries of the uncrystallised complexes?

- What are the driving forces of the cation interactions? How do they relate to the catalytic activity?

3.3 Optimisation of the Arene-Coordinated Uranium, Thorium or Zirconium Alkyl Cations

The complexes were optimised at the DFT level with the TURBOMOLE package [130]. Def-TZVP with RECP [131] was used for U, Th and Zr, and def2-TZVP basis set [73] for all the other atoms. The resolution of identity for the Coulomb integrals was used to reduce the computational cost. We first considered the pure GGA PBE functional but it was not satisfying. Indeed in the η^6**-2-U** and η^6**-2-Th** benzene complexes, the benzene ended up being tilted in the optimised structured deviating from its expected orientation observed in the crystal. The hybrid PBE0 [45] functional previously reported good geometrical agreement with the experimental data for Actinides containing molecules [132] . In our case PBE0 brought the theoretical structure in excellent agreement with the experimental one. All the geometries provided by Emslie's team are available in Appendix A. The inclusion of the solvent effect with the COSMO continuum solvent model marginally affected the geometries while significantly increasing the computational time. This lead us to consider only gas-phase optimised geometries.

3.3.1 Optimisation of Benzene-Coordinated Alkyl Cations

For η^6**-2-Th** and η^6**-2-U**, X-ray structures were available and were used as starting points (see Table 3.2). For the **2′-Zr** no X-ray structure was available. Thus the X-ray structure of η^6**-3′-Zr** was used by substituting the methyl group of toluene by a hydrogen atom. As a complement of information concerning the influence of the (trimethylsilyl)methyl group, the structure η^6**-2-Zr**, being the strict equivalent of η^6**-2-Th** and the structure η^6**-2′-Th** being the strict equivalent of η^6**-2′-Zr**, were optimised. The starting points of those optimisations were the optimised η^6**-2-Th** and η^6**-2′-Zr** geometries where the Th atom was substituted by a Zr atom and vice versa respectively..

3.3.2 Optimisation of Toluene-Coordinated Alkyl Cations

For η^6**-3-U** and η^6**-3′-Zr**, X-ray structures were available and were used as starting points. Since the X-ray data of η^6**-3-U** and η^6**-3′-Zr** present the arene facing the metallic center (as in the benzene complexes), we only tested the orientation of the methyl group of the arene for the toluene structure η^6**-3-Th**. By convention, as in [96], we will name as "exo" structure the structure where the methyl group is on the same side as the CH_2SiMe_3 group and as "endo" structure, the structure where the methyl group sits on the opposite side of CH_2SiMe_3 as illustrated by Figure 3.8.

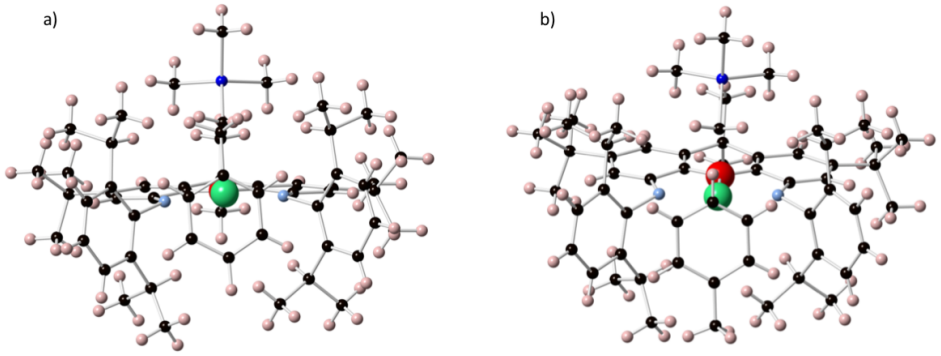

FIGURE 3.8: Starting geometries for the optimisation of the toluene complex η^6**-3-Th** with a) the "exo" starting point b) the "endo" starting point.

3.3.3 Optimisation of Halogeno-Coordinated Alkyl Cations

The X-ray structure of fluorobenzene, η^6**-5-U**, is also presenting a "endo" structure. Thus we also expect a "endo" structure for η^6**-5-Th**. We also explored the orientation of the arene in the fluorobenzene complexes η^1**-5-Th** and η^1**-5′-Zr** having the fluorobenzene of the arene ring facing the metallic centre, with the "horizontal" and the "vertical" orientations as shown in Figure 3.9.

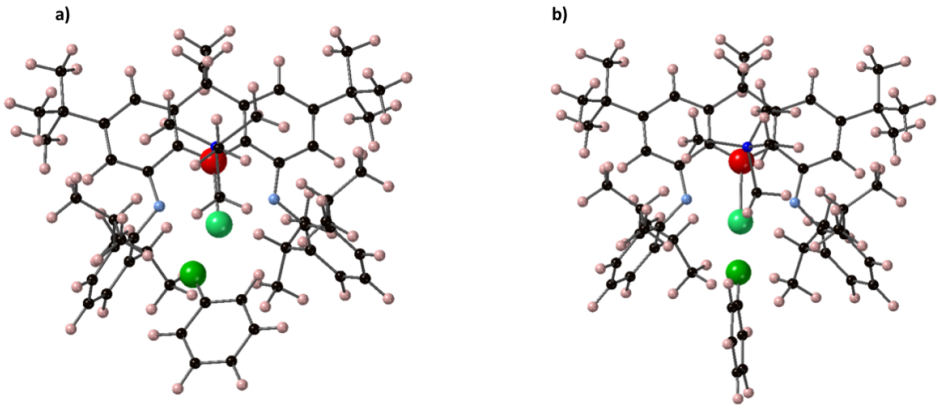

FIGURE 3.9: Starting geometries for the optimisation of η^1**-5-Th** with a) the "horizontal" starting point and b) the "vertical" starting point.

The bromo-benzene **4-U** and fluorobenzene **5-U** were optimised with the η^6**-5-U** X-ray structure as starting point substituting fluorine by bromine.

The η^6**-3-Th**, η^6**-3-U** and η^6**-5-U** have a similar orientation of the methyl group of the toluene or the fluor of the fluorobenzene; all are in the "endo" orientation. Thus the bromo-benzene η^6**-4-Th** and η^6**-4-U** were optimised in the "endo" convention.

For the **4'-Zr**, Motolko *et al.* [109] reported the "exo" and the "horizontal" structures as possible structures and probably a mixing of the two. Thus we tested these two orientations presented in Figure 3.10.

3.3.4 Optimisation of Difluoro-Coordinated Alkyl Cations

For difluoro-benzene complexes, only the **6-Th** was optimised so far. There are no X-ray data for any of the metallic center thus, five orientations were tested. Three correspond to the arene facing Th with different initial positions of the two fluor atoms. Again, we kept the "exo" and "endo" notations, adding the label "side" to the third possibility as it can be seen in Figure 3.11.

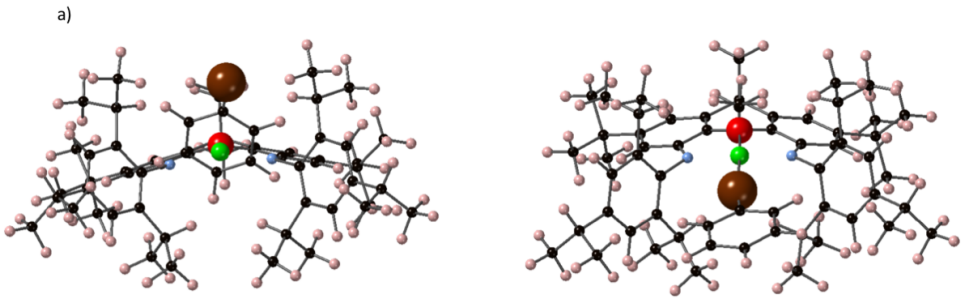

FIGURE 3.10: Starting geometries for the optimisation of the bromobenzene complex **4'-Zr** with a) the "exo" starting point and b) the "horizontal" starting point.

The last two starting points are the "horizontal" and the "vertical" presented earlier.

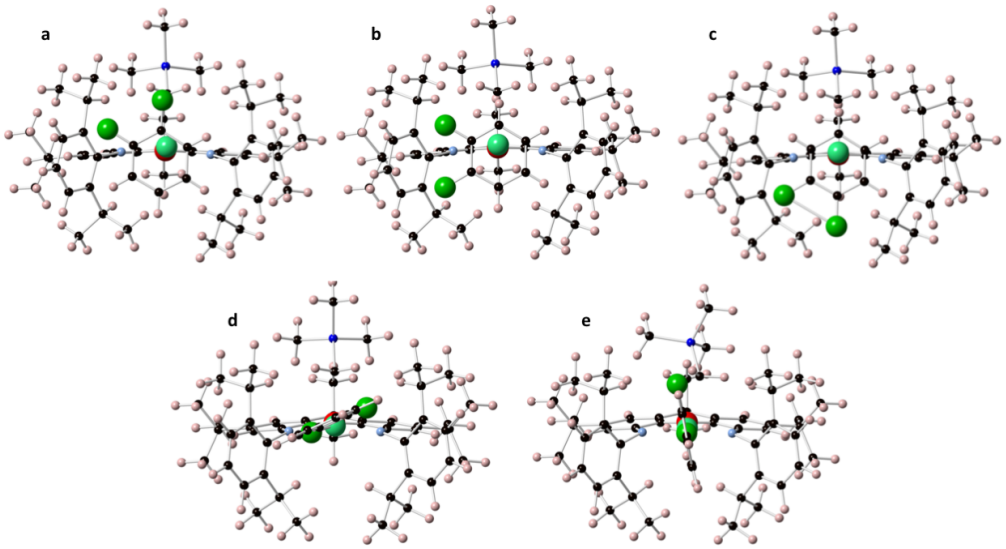

FIGURE 3.11: Starting geometries for the optimisation of **6-Th**: (a) η^6**-6-Th-exo**, (b) η^6**-6-Th-side**, (c) η^6**-6-Th-endo**, (d) η^1**-6-Th-horizontal** and (e) η^1**-6-Th-vertical**.

3.3.5 Optimisation of Ethylene-Coordinated Alkyl Cations

The **E'-Zr**, **E-Th** and **E-U** are optimised with two starting points, one with CH_2 pointing to the metal one with the two carbons of the ethylene facing the metal/actinide centre. The starting structures are the optimised structures of the benzene **2'-Zr**, **2-Th** and **2-U**.

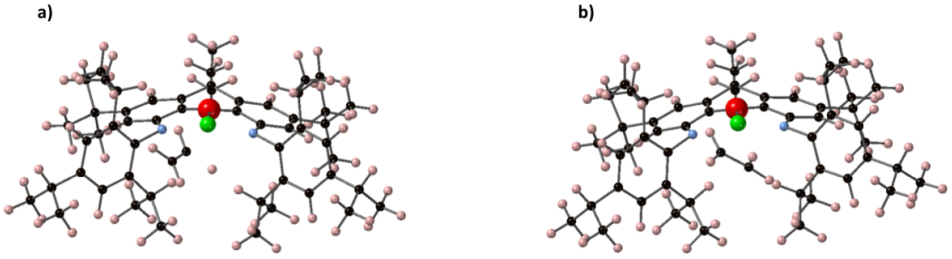

FIGURE 3.12: Starting geometries for the optimisation of **E'-Zr**: (a) η^1-**E'-Zr** and (b) η^2-**E'-Zr**.

3.4 Bonding studies

3.4.1 Dissociation curves - Benzene-Coordinated Alkyl Cations

For the benzene complexes, to quantify the strength and the nature of the benzene cation bonds, interaction curves were computed scanning the cation benzene distance from 2.7 Å to 4.0 Å for Th and U and from 2.2 Å to 3.4 Å in steps of 0.1 Å plus additional points at 4.5, 5, 6 and 10 Å.

Since the curves were smooth and presented only a single minimum (see Figure 3.17), the estimation of the binding energy was done at the structures accounting for the BSSE correction as described in the following paragraph.

3.4.2 Estimation of the binding energies at the equilibrium including BSSE and dispersion

For the BSSE calculation, the complex is divided into two fragments the first one (A) being composed of the catalyst and the second fragment (B) corresponding to the arene. If all the setup from the previous calculation was kept (DFT-TURBOMOLE-PBE0), tests on basis sets, using larger ones, such as def2-QZVP, def2-TZVPP and aug-cc-pVTZ for **2'-Zr** were performed. The interaction energies changed by a few kJ/mol with a largest basis sets proving that def2-TZVP is sufficiently accurate.

Because of the π-coordination of the arene to the metallic center, dispersion effects might be important. They can be captured by the MP2 method at considerable computational cost, or with a DFT-based approach with an empirical dispersion correction, namely the D3 correction [50].

3.4.3 Decomposition of the bond energy: the ETS-NOCV method

The ETS-NOCV method [118, 119], implemented in the ADF package, decomposes the interaction between two fragments within a system chosen by the user, to offer a quantitative picture of the chemical bond.

ETS - Extended Transition State decomposition analysis

The total energy between the interacting fragments is divided in 4 components [133]:

$$\Delta E_{tot} = \Delta E_{dist} + \Delta E_{elstat} + \Delta E_{Pauli} + \Delta E_{orb} \tag{3.1}$$

- ΔE_{dist}: the distorsion term corresponding to the energy between the free fragments and their geometry within the complex.
- ΔE_{elstat}: the electrostatic stabilising interaction between the 2 fragments when they are brought to their position in the final complex.

- ΔE_{Pauli}: the destabilising repulsive interaction between the occupied orbitals of the 2 fragments.
- ΔE_{orb}: the stabilising interaction between the occupied orbitals of one fragment and the unoccupied orbitals of the other one and the mixing of the unoccupied and occupied orbitals of a same fragment (intrafragment polarisation) once the two fragments have been united.

The change in the electronic density $\Delta\rho$ responsible for ΔE_{orb} can be written as:

$$\Delta\rho(1) = \sum_{\lambda}\sum_{\nu}\Delta P_{\lambda\nu}\lambda(1)\nu(1) \tag{3.2}$$

With "(1)" corresponding to the molecular orbital, λ are the occupied orbitals and ν the unoccupied orbitals of the 2 fragments and $\Delta P_{\lambda\nu}$ the deformation density function of λ and ν. Then ΔE_{orb} can be written as:

$$\Delta E_{orb} = \sum_{\lambda}\sum_{\nu}\Delta P_{\lambda\nu}F^{TS}_{\lambda\nu} \tag{3.3}$$

where $F^{TS}_{\lambda\nu}$ is the Kohn-Sham Fock matrix element that can be defined in terms of potential (transition state -TS) that is midway between the combined fragments and the final molecule (this is why it is called transition state).

NOCV - Natural orbitals for chemical valence

Derived from Nalewajski-Mrozek valence theory [134, 135], the deformation density is defined as :

$$\Delta\rho(r) = \rho^{system} - \sum_{i}\rho_i^{frag}(r) \tag{3.4}$$

The deformation density $\Delta\rho$ can be expanded as a sum of pairs of (Ψ_{-k}, Ψ_k) the natural orbitals for chemical valence (NOCV) that provide an orbital representation of the deformation density:

$$\Delta\rho(r) = \sum_{k=1}^{M/2} \nu_k[-\Psi^2_{-k}(r) + \Psi^2_k(r)] = \sum_{k=1}^{M/2} \Delta\rho_k(r) \tag{3.5}$$

In equation 3.5, Ψ_{-k} and Ψ_k NOCV are the eigenvectors of the ΔP matrix corresponding to eigenvalues $\pm\, \nu_k$, where ΔP = P_{AB} - (P_A + P_B), and P_{AB}, P_A and P_B are the molecular, and the fragment charge and bond order matrices [134, 135].

As a result the orbital interaction can be expressed in terms of the NOCV orbitals as:

$$\Delta E_{orb} = \sum_{k=1}^{M/2} \Delta E_{orb}(k) = \sum_{k=1}^{M/2} \nu_k[-F^{TS}_{-k,-k}(r) + F^{TS}_{k,k}(r)] \tag{3.6}$$

where $F^{TS}_{-k,-k}$ and $F^{TS}_{k,k}$ are the diagonal Kohn-Sham matrix elements defined over NOCVs with respect to the TS density. In this expression, only few complementary NOCV pairs (often 2 to 4) contribute significantly to ΔE_{orb}. Each pair represents one charge-transfer contribution $\Delta\rho_k$, with its energy contribution ΔE_{orb}(k). To discuss trends across complexes the same fragment types must be used *i.e.* the fragments A and B must describe the same parts of the molecule.

ETS-NOCV calculations were performed for all the benzene complexes with the PBE0 functional, QZ4P basis sets and included scalar relativistic effects with the ZORA Hamiltonian. As for the BSSE calculation, the first fragment includes the cationic complex and the second one the arene. One has to note that ETS-NOCV analysis cannot be performed with spin-orbit coupling. Nevertheless, for benzene complexes a simple-point calculation with Spin-Orbit ZORA Hamiltonian was ran showing that spin-orbit coupling has no effect on the interaction energy.

3.5 Results and discussions

3.5.1 Geometries of the arene-coordinated uranium, thorium or zirconium alkyl cation with the arene solvent

Geometries of benzene-coordinated alkyl cations

TABLE 3.6: Important bond lengths in Å and angles in degree for η^6**-2-U** (X-ray and optimised structures), η^6**-2-Th** (X-ray and optimised structures),η^6**-2'-Th** (optimised structure), η^6**-2'-Zr** (optimised structure) and η^6**-2-Zr** (optimised structure).

Compounds	η^6**-2-U** X-ray	η^6**-2-U** opt	η^6**-2-Th** X-ray	η^6**-2-Th** opt
M-O	2.441(2)	2.428	2.496(5)	2.487
M-N	2.224(2), 2.236(6)	2.222, 2.231	2.278(3), 2.288(3)	2.278, 2.282
M-C_{arene}	3.099(3) - 3.248(3)	3.028 - 3.795	3.18 - 3.31	3.19 - 3.41
M-Arene Centroid	2.932	3.136	2.950	2.999
$N_1 \ldots N_2$	3.94	3.99	4.04	4.02
Arene Bend Angle[1]	18.9	23.5	8.7	10.8
O-M-C_{apical}	87.26(8)	91.90	91.3(1)	91.4
M-C-Si	133.7(2)	135.7	131.0(2)	132.4
Compounds	η^6**-2'-Th**	η^6**-2'-Zr** opt	η^6**-2-Zr** opt	
M-O	2.500	2.248	2.263	
M-N	2.273, 2.274	2.144, 2.149	2.103, 2.099	
M-C_{arene}	3.171-3.302	2.781 - 2.881	4.43 - 2.699	
M-Arene Centroid	2.925	2.470	3.403	
$N_1 \ldots N_2$	3.963	3.87	3.829	
Arene Bend Angle[1]	0.8	2.4	30.1	
O-M-C_{apical}	82.8	82.2	96.2	
M-C-Si	–	–	132.3	

[1] Angle between the carbons of the arene and the planar ligand.

Table 3.6 gathers all the results for the benzene complexes. The distances between the metal centres and both the oxygen and nitrogen atoms of the XA_2 (4,5-bis(2,4,6-triisopropylanilido)-2,7-di-tert-butyl-9,9-dimethylxanthene) group

almost perfectly vary with respect to the ionic radii variations; for instance the Th-O distance in η^6**-2-Th** comes out 0.22 Å longer the Zr-O one in η^6**-2-Zr**, and 0.06 Å longer than the U-O one in η^6**-2-U**. Contrariwise the metal-arene distances do not follow the ionic radii trends since the Th-C_{arene} distance are about 0.47 Å and 0.17 Å longer than the Zr-C_{arene} and U-C_{arene} ones respectively, suggesting that the various cations interact differently with the benzene ring. The computed structure of η^6**-2'-Zr** is also reported though it could not be crystallised by Emslie *et al.* The difference between η^6**-2'-Zr** and η^6**-2-Zr** is that a methyl group is attached to Zr in the former while the latter carries a bulkier CH_2SiMe_3 group. This is confirmed by the fact that η^6**-2'-Th** present similar O-M-C_{apical} angle and arene bend angle than η^6**-2'-Zr**. As consequences, η^6**-2'-Th** also present a short distance M-Arene Centroid than η^6**-2-Th**. Albeit Zr-O and Zr-N distances are nearly the same in both η^6**-2-Zr** and η^6**-2'-Zr** complexes, the Zr-C_{arene} distance is shorter in the former than in the latter.

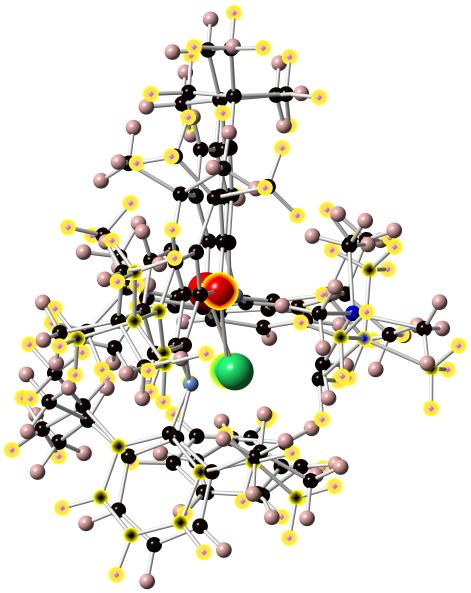

FIGURE 3.13: Superposition of the X-ray and the optimised (yellow atoms) structures of η^6**-2-Th**

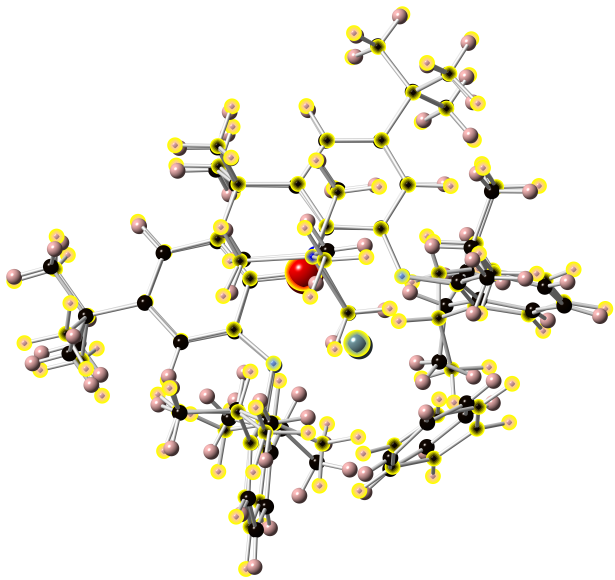

FIGURE 3.14: Superposition of the X-ray and the optimised (yellow atoms) structures of η^6**-2-U**

Geometries of toluene-coordinated alkyl cations

TABLE 3.7: Important bond lengths in Å and angles in degree for η^6**-3-U** (X-ray structures), η^6**-2-Th** (optimised structure) and η^6**-3′-Zr** (X-ray and optimised structures).

Compounds	η^6**-3-U-endo** X-ray	η^6**-3-Th-endo** opt	η^6**-3′-Zr-exo** opt	η^6**-3′-Zr-exo** X-ray
M-O	2.480	2.417(9)	2.247	2.220
M-N	2.21(1), 2.22(1)	2.277, 2.273	2.161, 2.148	2.138, 2.142
M-C_{arene}	3.05(2) - 3.78(2)	3.084 - 4.005	2.747 - 2.908	2.697 - 2.840
M-Arene Centroid	3.138	3.271	2.449	2.383
$N_1 \ldots N_2$	3.98	4.04	3.91	3.91
Arene Bend Angle[1]	11.8	13.4	12.7	
O-M-C_{apical}	5.9	92.20	87.7	81.0
M-C-Si	136.8(7)	133.8	–	–

[1] Angle between the carbons of the arene and the planar ligand.

The structures of η^6**-3-U-endo** and η^6**-3-Th-exo** are not be obtained yet. For those available the computed geometries agree well with the available crystallographic data (see Table 3.7). The main observation is that the M-C_{arene} distances in toluene complexes are slightly shorter than in the benzene ones.

Geometries of halogeno-coordinated alkyl cations

The structures of bromobenzene η^6**-4-U** and the fluorobenzene η^6**-5-U** and η^1**-5-Th-horizontal** are not reported yet.

The fluorobenzene η^6**-5′-Zr-exo** is slightly more stable than η^1**-5-Th-vertical** with a difference in energy of 0.35 kJ.mol^{-1}. This difference is so small that both structures will be kept for the rest of the study. The η^1**-5′-Zr-vertical** relaxed to an "horizontal" orientation but forming an important tilt angle with the molecular plane. The most stable is the optimised **5′-Zr-vertical**, with an energy 4.2 kJ.mol^{-1} lower than that obtained with the η^1**-5′-Zr-horizontal**. The last isomer, η^6**-5′-Zr-exo** is the least stable lying 15.7 kJ.mol^{-1} above η^1**-5′-Zr-vertical**. Nevertheless, as the structures are close in energy both the η^1**-5′-Zr-horizontal** (from the optimised $\eta^{'}$**-5′-Zr-vertical** starting point) and η^1**-5′-Zr-exo** are kept for the next steps of the study. The currently optimised

structures cannot be compared to crystal data, though, they reveal very similar bond distances to the toluene ones.

TABLE 3.8: Important bond lengths in Å and angles in degree for η^6**-5-U** (optimised and X-ray structures), η^6**-5-Th** (optimised structure), η^6**-5′-Zr** (optimised structure) and η^1**-5′-Zr -horizontal** (optimised structure) and the relative energy ΔE in kJ.mol^{-1} with respect to the most stable isomer.

Compounds	η^6**-5-U** X-ray	η^6**-5-Th-endo** opt	η^1**-5-Th-vertical**
M-O	2.431	2.477	2.476
M-N	2.215, 2.218	2.267, 2.275	2.267, 2.270
M-C$_{arene}$	3.128 - 3.598	3.140 - 3.822	–
M-Arene Centroid	3.077	3.204	–
$N_1 \ldots N_2$	3.98	4.033	4.040
Arene Bend Angle [1]	1.6	8.4	78.9
O-M-C$_{apical}$	89.6	92.3	94.9
M-C-Si	134.8	133.2	132.5
ΔE		0.0	0.3
Compounds	η^6**-5′-Zr-exo** opt	η^1**-5′-Zr -horizontal** opt	
M-O	2.277	2.257	
M-N	2.088, 2.082	2.068, 2.070	
M-C$_{arene}$	2.687 - 4.417	–	
M-Arene Centroid	3.401	–	
$N_1 \ldots N_2$	3.790	3.813	
Arene Bend Angle [1]	10.7	11.1	
O-M-C$_{apical}$	91.3	101.5	
M-C-Si	–	–	
ΔE	15.7	0.0	

[1] Angle between the carbons of the arene and the planar ligand.

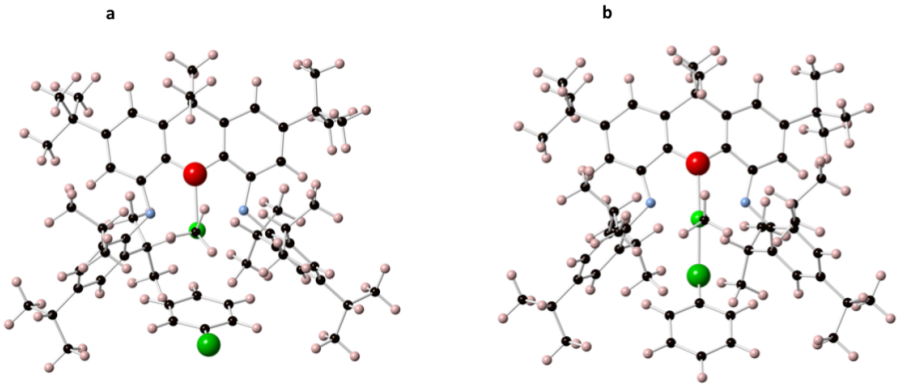

FIGURE 3.15: Optimised geometries for a) η^6**-5′-Zr-exo**, b) η^1**-5′-Zr-horizontal**

TABLE 3.9: Important bond lengths in Å and angles in degree for η^6**-4-Th** (optimised structure) and **4′-Zr** (optimised structures) and the relative energy ΔE in kJ.mol^{-1} with respect to the most stable isomers.

Compounds	η^6**-4-Th-endo** opt	η^6**-4′-Zr-exo** opt	η^1**-4′-Zr-horizontal** opt
M-O	2.472	2.276	2.260
M-N	2.263, 2.263	2.082, 2.088	2.069, 2.077
M-C$_{arene}$	3.058 - 4.335	2.697 - 4.406	–
M-Arene Centroid	3.481	3.390	–
$N_1 \ldots N_2$	4.03	3.789	3.789
Arene Bend Angle [1]	4.9	11.4	13.5
O-M-C$_{apical}$	92.9	91.1	90.8
M-C-Si	133.3	–	–
ΔE		0.0	9.7

[1] The angle between the carbons of the arene and the planar ligand.

In the case of bromobenzene isomers, η^6**-4′-Zr-exo** is more stable than η^1**-4′-Zr-horizontal** by 9.7 kJ.mol^{-1} but since David Emslie suspected the presence of these two isomers from NMR analysis [109], both will be kept for the next steps of the bonding study.

Geometries of difluorobenzene-coordinated alkyl cations

η^1**-6-Th-vertical** and η^1**-6-Th-horizontal** are converging to the same η^1**-6-Th-vertical** structure, thus only this one will be kept for the results. The most stable isomer is the η^1**-6-Th-vertical** and the other three are less than 15 kJ.mol^{-1} higher in energy, forcing us to consider all of them. Nonetheless the final structure of η^1**-6-Th-horizontal**

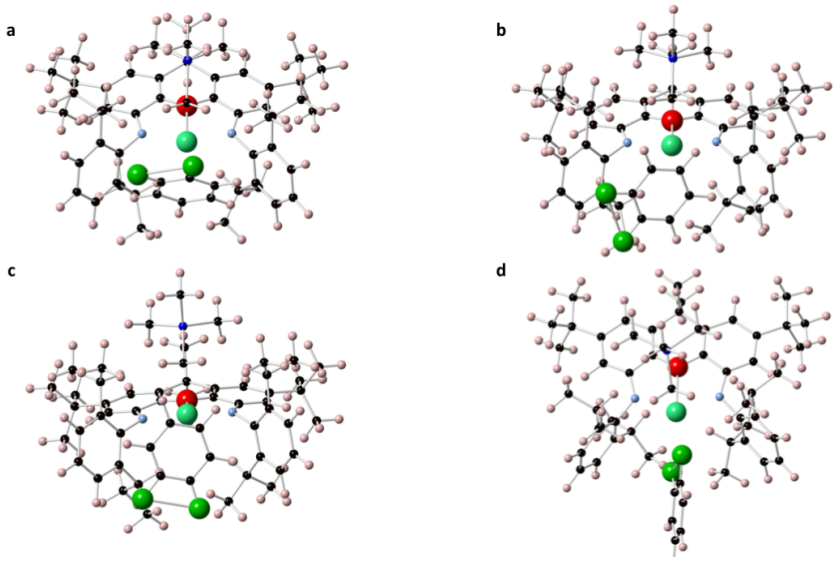

FIGURE 3.16: Optimised geometries for a) η^6**-6-Th-exo**, b) η^6**-6-Th-side**, c) η^6**-6-Th-endo** and, d) η^1**-6-Th-vertical**

TABLE 3.10: Important bond lengths in Å and angles in degree for η^6**-6-Th-exo**, η^6**-6-Th-side**, η^6**-6-Th-endo**, η^1**-6-Th-horizontal** and η^1**-6-Th-vertical** optimised structures and the relative energies ΔE in kJ.mol^{-1} with respect to the most stable isomer.

Compounds	η^1**-6-Th-vertical** opt	η^6**-6-Th-exo** opt	η^6**-6-Th-side** opt	η^6**-6-Th-endo** opt
M-O	2.46	2.492	2.477	2.475
M-N	2.252, 2.254	2.279, 2.280	2.259, 2.258	2.262, 2.258
M-C$_{arene}$	–	3.060 - 4.298	3.107 - 4.373	3.030 - 4.326
M-Arene Centroid	–	3.461	3.531	3.464
$N_1 \ldots N_2$	4.000	4.036	4.004	4.014
Arene Bend Angle [1]	–	28.6	24.9	13.0
O-M-C$_{apical}$	93.6	93.5	93.3	93.5
M-C-Si	132.3	133.8	132.4	132.3
ΔE	0.0	12.4	15.5	9.6

[1] The angle between the carbons of the arene and the planar ligand.

The arene bend angles in the η^6**-6-Th-exo** and η^6**-6-Th-side** isomers are larger than in the η^6**-6-Th-endo** one because of the steric repulsion of the two fluorine atoms.

Optimisation of Ethylene-Coordinated Alkyl Cations

The **E'-Zr** optimised structures with both starting points are giving the same result with the two carbons of the ethylene facing the zirconium atom. For this reason, for U and Th complexes, the optimisation where the CH_2 is pointing to the actinide is disregarded. The important information on the complexes can be found in Table 3.11

TABLE 3.11: Important bond lengths in Å and angles in degree for η^2**-E'-Zr** and η^2**-E-Th** optimised structures.

Compounds	**E'-Zr**	**E-Th**
M-O	2.268	2.467
M-N	2.070, 2.076	2.251, 2.254
M-$C_{ethylene}$	2.796, 2.842	3.113, 3.094
$N_1 \ldots N_2$	3.790	4.005
Ethylene Bend		
Angle [1]	37.4	12.9
O-M-C_{apical}	92.1	95.6
M-C-Si	–	131.4

[1] The angle between the carbons of the ethylene and the planar ligand.

All the distance M-$C_{ethylene}$ are shorter than in the other complexes thus a stronger bond could be expected. Unfortunately, as I write this lines, no result about η^2**-E-U** is available.

3.5.2 Bonding studies

Dissociation curves - Benzene-Coordinated Alkyl Cations

Figure 3.17 presents the results for the dissociation of benzene from the alkyl Zr, Th and U cations. The curves display only one minimum corresponding to the distance benzene - metallic center found in the geometry optimisations. The bonding energies derived from the curves are -145.5 kJ.mol^{-1}, -90.4 kJ.mol^{-1} and -80.3 kJ.mol^{-1} for η^6**-2'-Zr**, η^6**-2-Th** and η^6**-2-U**, respectively.

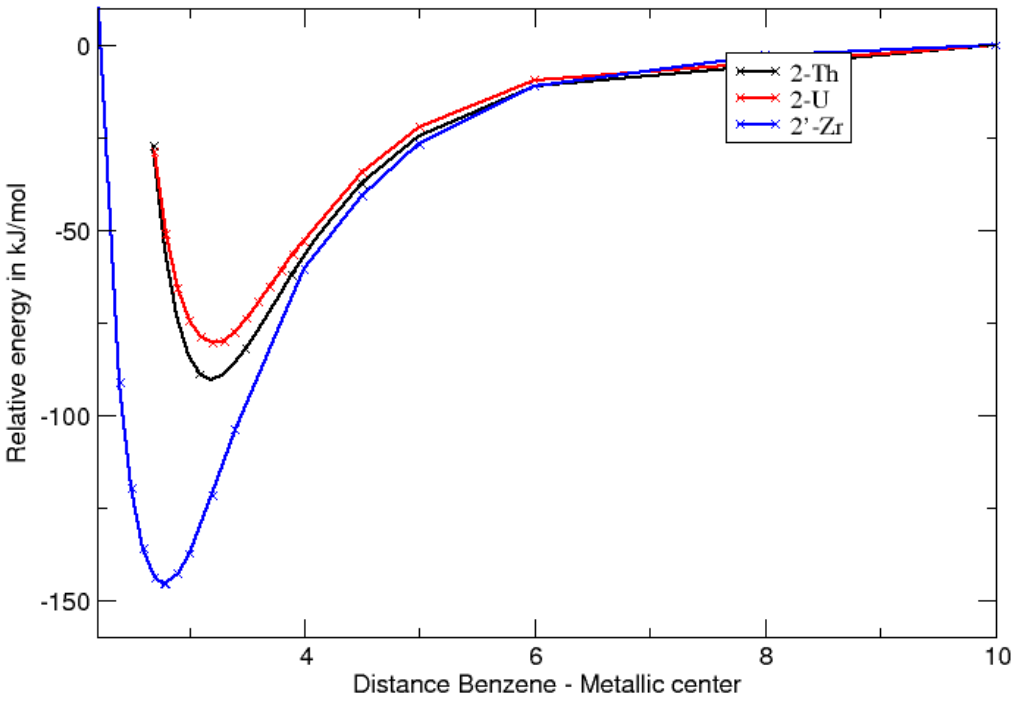

FIGURE 3.17: Dissociation curves for η^6**-2-Th** (black), η^6**-2-U** (red) and η^6**-2'-Zr** (blue) for a benzene - metallic center distance between 2.2 Å and 10 Å

BSSE corrections and decompositions of the bond energies: an ETS-NOCV study

TABLE 3.12: BSSE corrections (in kJ.mol^{-1}) to the benzene interaction energies in η^6**-2'-Zr** computed at different levels of calculation with different basis sets.

	ΔE	ΔE(BSSE)	$\Delta E_{corrected}$
PBE0-def2-TZVP	-147.4	-4.6	-142.8
(PBE0 + D3)-def2-TZVP	-204.4	-4.6	-199.9
MP2-def2-TZVP	-281.9	-42.2	-239.7
MP2-def2-TZVPP	-289.4	-36.9	-252.6
MP2-aug-cc-pVTZ	-305.2	-45.0	-260.2

To evaluate the accuracy of the QM methods on the bonding energies, we have performed PBE0, PBE0 + D3 and MP2 calculations for the η^6**-2'-Zr** complex (see Table 3.12). MP2 energies are somewhat sensitive to the size of the basis set; increasing the basis quality from def2-TZVP to def2-TZVPP and aug-cc-PVTZ increases the binding energy by 13 and 20 kJ.mol^{-1} (< 10% of the total interaction energy), respectively, while expanding significantly the computational time. Thus, the def2-TZVP basis sets are kept for all other complexes.

TABLE 3.13: Bonding energies in kJ.mol^{-1} for the benzene molecules η^6**-2'-Zr**, η^6**-2-Zr**, η^6**-2-Th** and η^6**-2-U** at PBE0, PBE0 + D3 and MP2 levels.

	ΔE			ΔE(BSSE)			$\Delta E_{corrected}$		
	PBE0	PBE0 + D3	MP2	PBE0	PBE0 + D3	MP2	PBE0	PBE0 + D3	MP2
η^6**-2'-Zr**	-147.4	-204.4	-305.2	-4.6	-4.6	-45.0	-142.8	-199.9	-260.2
η^6**-2-Zr**	-92.8	-147.1	-190.5	-3.2	-3.2	-29.1	-89.6	-143.8	-161.5
η^6**-2-Th**	-92.5	-141.7	-189.7	-3.5	-3.5	-25.7	-89.0	-138.1	-164.1
η^6**-2-U**	-77.8	-128.0		-3.5	0.2		-74.2	-128.2	

From Table 3.13, we note that for both Zr and Th complexes, the MP2 energies are larger than the PBE0 ones. Assuming that PBE0 with D3 correction captures most of the dispersion effects, it is interesting to note that the PBE0 trends across the metal centres match the MP2 ones. However, the MP2 values come out lower than the PBE0 + D3 ones, which is in line with the fact

that MP2 is known to overestimate dispersion contributions [136, 137].

TABLE 3.14: Bonding energy decomposition in kJ.mol^{-1} for the zirconium cations with the ETS-NOCV method .

	η^2-**E′-Zr**	η^6-**2′-Zr**	η^6-**2-Zr**	η^6-**3′-Zr-exo**
ΔE_{Dist}	29.7	95.4	38.1	112.0
ΔE_{Pauli}	130.8	296.4	137.6	311.7
ΔE_{elstat} [1]	-119.3 (54%)	-200.5 (45%)	-105.6 (45%)	-217.6 (45%)
ΔE_{orb} [1]	-99.6 (46%)	-242.2 (55%)	-126.3 (55%)	-263.2 (55%)
ΔE^{σ}_{orb} [2]	-62.8 (63%)	-45.2 (19%)	–	-46.0 (19%)
$\Delta E^{\pi}1_{orb}$ [2]	-12.5 (13%)	-60.2 (25 %)	-71.1 (56%)	-66.1 (25%)
$\Delta E^{\pi}2_{orb}$ [2]	–	-63.2 (26%)	-13.0 (10%)	-66.9 (25%)
ΔE^{other}_{orb} [2]	-24.7 (24%)	-77.0 (30%)	-41.0 (32%)	-84.1 (31%)
ΔE^{PBE0}_{int}	-88.1	-146.3	-94.3	-169.2
ΔE_{Disp} [3]	-33.1	-52.5	-51.0	-61.9
$\Delta E^{PBE0+D3}_{int}$	**-91.5**	**-103.4**	**-107.2**not finish	**-119.1**
	η^6-**4′-Zr-exo** *	η^1-**4′-Zr-horizontal**	η^6-**5′-Zr-exo**	η^1-**5′-Zr-horizontal**
ΔE_{Dist}	36.3	29.1	30.7	22.3
ΔE_{Pauli}	133.3	115.3	136.7	100.3
ΔE_{elstat} [1]	-95.1 (43%)	-97.5 (48%)	-103.0 (45%)	-108.7 (54%)
ΔE_{orb} [1]	-125.6 (57%)	-105.9 (52%)	-125.3 (55%)	-91.7 (44%)
ΔE^{σ}_{orb} [2]	-73.6 (59%)	-65.5 (62%)	-74.5 (59%)	-44.5 (49%)
$\Delta E^{\pi}1_{orb}$ [2]	-10.5 (8%)	-10.8 (10%)	-9.6 (8%)	-14.2 (15%)
$\Delta E^{\pi}2_{orb}$ [2]	-8.4 (7%)	–	-8.4 (7%)	-9.6 (10%)
ΔE^{other}_{orb} [2]	-33.4 (26%)	-30.2 (28%)	-33.1 (24%)	-23.8 (26%)
ΔE^{PBE0}_{int}	-87.3	-88.1	-91.5	-100.0
ΔE_{Disp} [3]	-55.5	-47.3	-52.5	-36.8
$\Delta E^{PBE0+D3}_{int}$	**-106.5**	**-106.3**	**-113.0**	**-114.5**

* Most stable isomers.

[1] Values in parenthesis give the percentage contribution to the total attractive interaction (ΔE_{elstat} +ΔE_{orb}).

[2] Values in parenthesis give the percentage contribution to the total orbital energy for the σ- and π-donor NOCV-pair contributions.

[3] ΔE_{Disp} is the difference between ΔE^{PBE0}_{int} and $\Delta E^{PBE0+D3}_{int}$ with the BSSE correction.

Tables 3.14 and 3.15 summarise the energy decomposition analysis performed

at the PBE0 level and the dispersion contributions that range from 40 to 70 kJ.mol^{-1}, representing at least 27% of the bonding energy. Thus, dispersion does not change the trends observed but is not negligible. Comparing the benzene η^6**-2'-Zr** and the toluene η^6**-3'-Zr-exo** in Table 3.14, we see that the η^6**-3'-Zr-exo**, which is catalytically more active than η^6**-2'-Zr**, exhibits a stronger bond between Zr and the toluene solvent, which is counter intuitive with the hypothetical mechanism. η^6**-2-Zr** does not present an important σ interaction while η^6**-2'-Zr** does. It can come from the fact that η^6**-2-Zr** presents a large arene bond angle (30.1°) which prevents σ overlaps.

Fluorobenzene **5'-Zr** forms the weakest arene bond to zirconium. In case of the η^6**-5'-Zr-exo** isomer, it can be explained by the fact that the center of the fluorobenzene ring is shifted upwards as a result of hydrogen bonding between fluorine and a hydrogen atom of the CH_2SiMe_3 group.

The weakest bond is observed between the ethylene and the zirconium. Such a weak bond discredits the hypothesis of a competition between the arene from solvent and the ethylene. Nonetheless, the ethylene complexe is presenting a bond different from the one between the arene and the zirconium. Indeed, in present a σ donation from the ethylene carbons to the 4d and 5s orbitals of the zirconium and a π-retrodonation from the 2p orbitals of the carbons around Zr to the 2p orbitals of the ethylene carbons (see Figure **??**). Further explorations of possible transition states involving both ethylene and

the arene are foreseen.

TABLE 3.15: Bonding energy decomposition in kJ.mol^{-1} for the thorium cations with the ETS-NOCV method.

	η^2-**E-Th**	η^6-**2-Th**	η^6-**2′-Th**	η^6-**3-Th-endo**
ΔE_{Dist}	1.4	15.5	29.8	17.3
ΔE_{Pauli}	90.4	143.9	153.5	119.7
ΔE_{elstat} [1]	-87.6 (56%)	-115.6 (49%)	-120.8 (48%)	-102.0 (49%)
ΔE_{orb} [1]	-69.3 ((44%))	-120.9 (51%)	-130.3 (52%)	-104.9 (51%)
ΔE^{σ}_{orb} [2]	-43.1(62%)	-22.6 (19%)	-24.5 (19%)	-10.5 (10%)
$\Delta E^{\pi}1_{orb}$ [2]	-8.7 (12%)	-33.0 (27%)	-35.6 (27%)	-39.7 (38%)
$\Delta E^{\pi}2_{orb}$ [2]	–	-26.4 (22%)	-28.5 (22%)	-20.9 (20%)
ΔE^{other}_{orb} [2]	-17.8 (26%)	-39.7 (33%)	-42.6 (32%)	-34.2 (32%)
ΔE^{PBE0}_{int}	-66.5	-92.6	-97.6	-87.1
ΔE_{Disp} [3]	-25.2	-45.6	-50.5	-52.1
$\Delta E^{PBE0+D3}_{int}$	**-90.2**	**-122.7**	**-118.3**	**-121.9**
	η^6-**4-Th-endo**	η^6-**5-Th-endo**	η^1-**5-Th-verical**	
ΔE_{Dist}	8.1	-0.6	-6.1	
ΔE_{Pauli}	94.4	113.1	63.4	
ΔE_{elstat} [1]	-72.7 (45%)	-91.4 (48%)	-72.4 (55%)	
ΔE_{orb} [1]	-87.8 (55%)	-97.8 (52%)	-59.3 (45%)	
ΔE^{σ}_{orb} [2]	–	-11.7 (12%)	–	
$\Delta E^{\pi}1_{orb}$ [2]	–	-33.5 (34%)	–	
$\Delta E^{\pi}2_{orb}$ [2]	–	-21.3 (22%)	–	
ΔE^{other}_{orb} [2]	-87.8 (100%)	-32.1 (32%)	-59.3 (100%)	
ΔE^{PBE0}_{int}	-66.1	-76.1	-68.3	
ΔE_{Disp} [3]	-50.8	-48.7	-21.3	
$\Delta E^{PBE0+D3}_{int}$	**-108.8**	**-125.4**	**-95.7**	
	η^1-**6-Th-vertical***	η^6-**6-Th-exo**	η^6-**6-Th-side**	η^6-**6-Th-endo**
ΔE_{Dist}	6.5	6.8	6.8	31.8
ΔE_{Pauli}	70.2	97.3	89.6	93.2
ΔE_{elstat} [1]	-80.2 (56%)	-71.4 (45%)	-68.6 (45%)	-69.8 (44%)
ΔE_{orb} [1]	-62.0 (44%)	-87.0 (55%)	-82.2 (55%)	-89.0 (56%)
ΔE^{σ}_{orb} [2]		– -15.5 (18%)	-38.0 (46%)	-41.4 (47%)
$\Delta E^{\pi}1_{orb}$ [2]	–	-39.7 (46%)	-16.2 (20%)	-13.8 (16%)
$\Delta E^{\pi}2_{orb}$ [2]	–	–	–	–
ΔE^{other}_{orb} [2]	-62.0 (100%)	-32.3 (37%)	-28.6 (34%)	-34.4 (37%)
ΔE^{PBE0}_{int}	-72.0	-61.1	-61.2	-65.6
ΔE_{Disp} [3]	-22.7	-45.9	-44.2	-44.4
$\Delta E^{PBE0+D3}_{int}$	**-88.2**	**-100.2**	**-98.6**	**-78.2**

* Most stable isomers.

We can see that the bonding interaction decreases along the arene series of the Th-complexes (see Table 3.15); as the bonding strength decreases, so does the 7s and 5f characters of the acceptor orbital while the 6d character increase in the main deformation densities contributions (See figure 3.18, **??** and the Appendix C).

Regarding the **6-Th** isomers, η^6**-6-Th-vertical** is the most stable one and presents the strongest arene-metal interaction. In η^1**-6-Th-vertical** and η^6**-6-Th-endo** the orbital interaction is composed of multiple small interactions. In η^1**-6-Th-vertical**, the arene ring orientation does not favour any bonding symmetry, while η^6**-6-Th-endo**, the arene ring is shifted perpendicularly to the molecular plane. Just as in Zr complexes, η^2**-E-Th** presents the weakest bond and the π retrodonation from the 2p orbitals of the carbons close to the Th center and the 4d orbitals of the thorium to the 2p orbitals of the ethylene carbons. The same exploration of transition state must then be done to shed light on the mechanism.

Finally the useful complexes to compare the metals are the η^6**-2-Th**, η^6**-2-Zr**, η^6**-2′-Th** and η^6**-2′-Zr** ones (see Tables 3.14 and 3.15 and Figures 3.18, **??**, 3.19 and **??**). The interaction strength is roughly the same comparing metals but the Zr benzene bond is somewhat more covalent than the Th-benzene one (larger ΔE_{orb} percentage). Again the absence of σ interaction in **2-Zr** is explained by the large arene bend angle. Being smaller in the thorium equivalent, the σ donation contributions into the 6d and 5f orbitals of Th amounts to 20% while π-type interactions sums up to 49% of the covalent contribution.

3.6 Conclusion and Perspectives

Although a lot of information have been already collected, the catalytic mechanism could not be revealed. So far we have shown that our QM calculations are able to reproduce X-ray data and certainly predict the geometries of uncrystallised complexes. We have seen that the Zr-cations have a bonding interaction slightly more covalent than the Th-ones, in which the arene interaction is electrostatically driven. The stronger bonds in thorium systems

mainly involve 7s and 5f orbitals while the weakest involve mainly 6d orbitals. The study of hypothetic transition states will be done to explore the possible reaction paths.

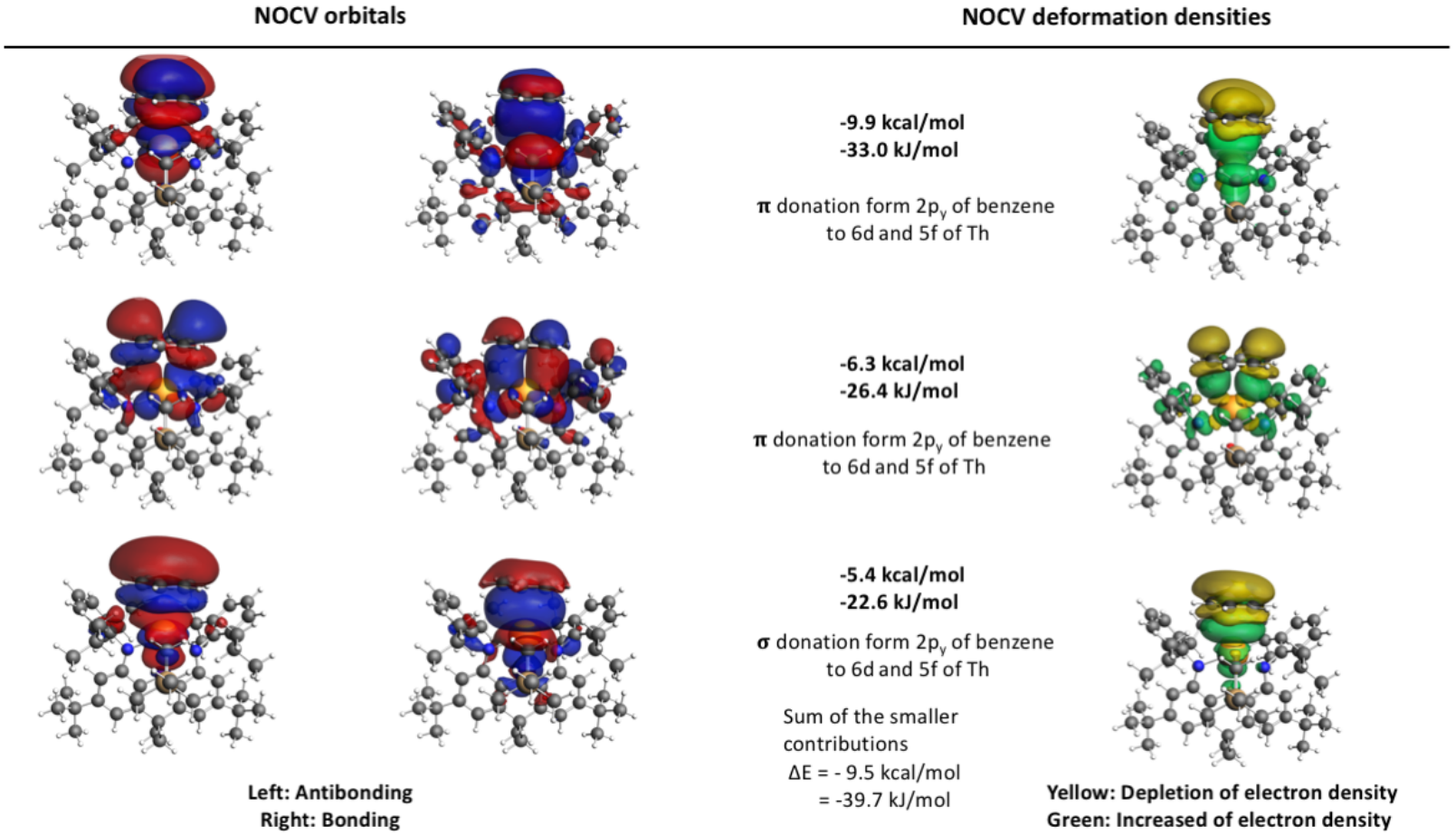

FIGURE 3.18: On the left hand side: the NOCV Orbitals (with isosurfaces set to 0.01) and on the right hand side ETS-NOCV deformation density contributions, Increased (green) and decreased (yellow) electron density is presented relative to that in the isolated fragments (isosurfaces are set to 0.0001) for the molecule η^6**-2-Th**.

FIGURE 3.19: On the left hand side: the NOCV Orbitals (with isosurfaces set to 0.01) and on the right hand side ETS-NOCV deformation density contributions, Increased (green) and decreased (yellow) electron density is presented relative to that in the isolated fragments (isosurfaces are set to 0.0001) for the molecule η^6-**2-Zr**.

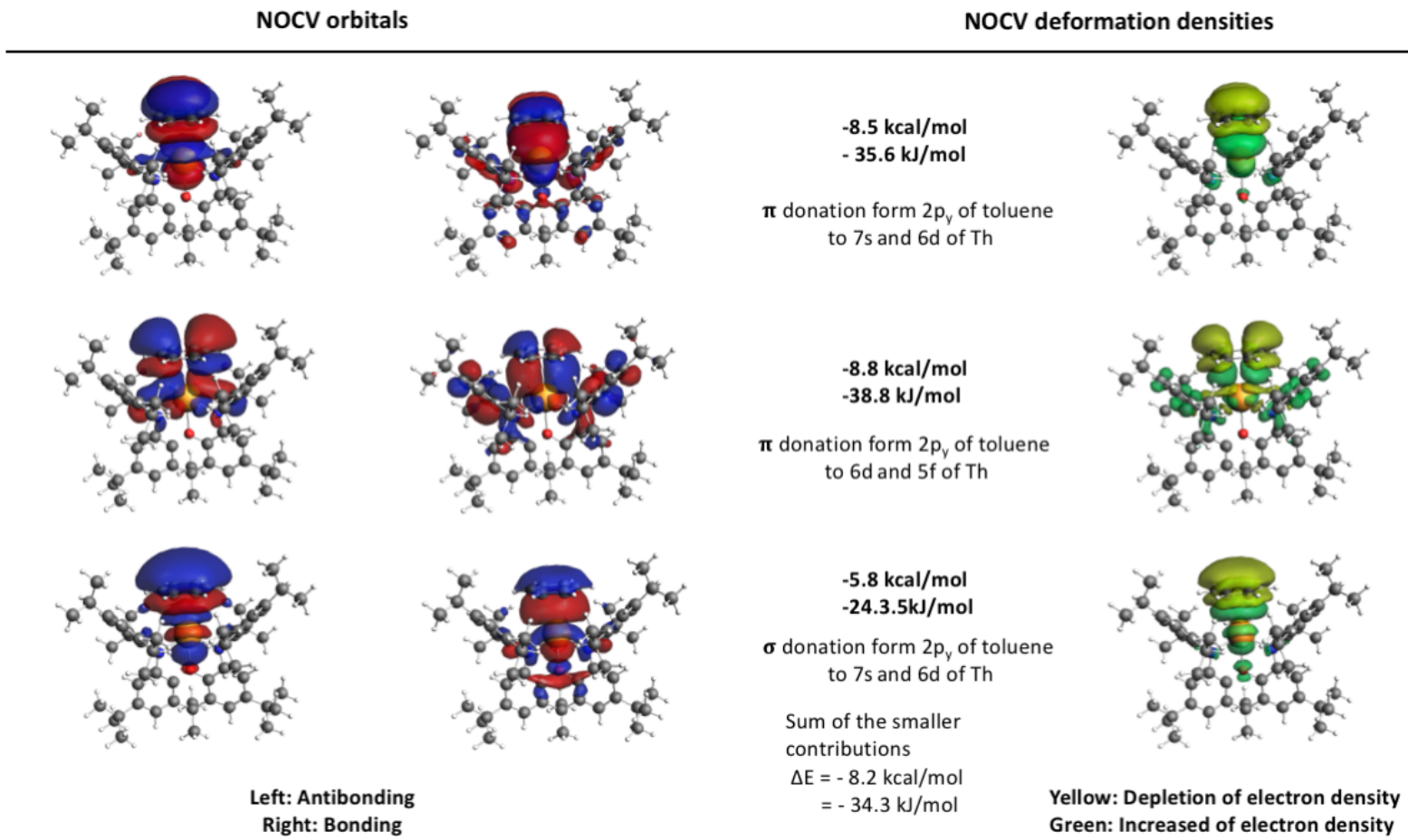

FIGURE 3.20: On the left hand side: the NOCV Orbitals (with isosurfaces set to 0.01) and on the right hand side ETS-NOCV deformation density contributions, Increased (green) and decreased (yellow) electron density is presented relative to that in the isolated fragments (isosurfaces are set to 0.0001) for the molecule η^6**2′-Th**.

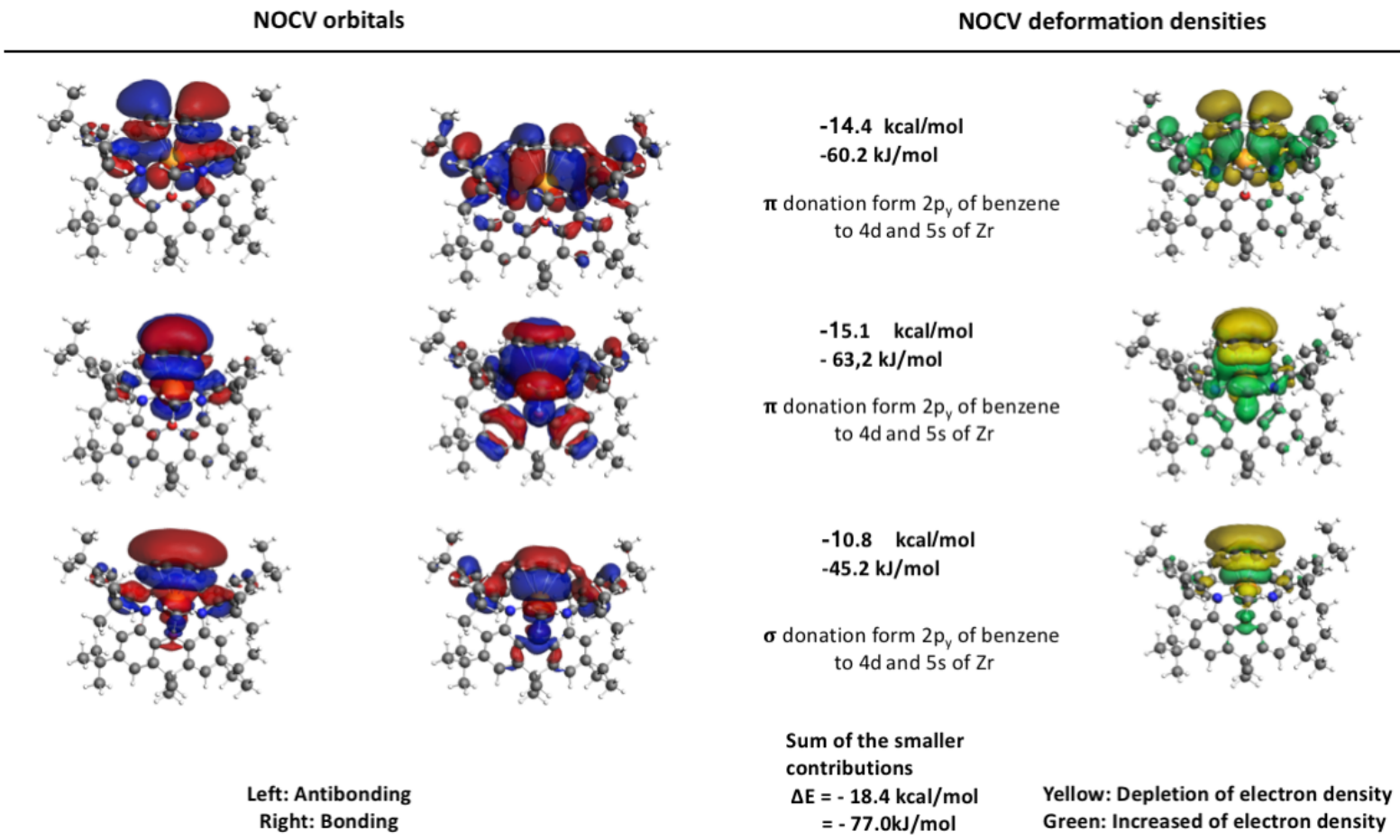

FIGURE 3.21: On the left hand side: the NOCV Orbitals (with isosurfaces set to 0.01) and on the right hand side ETS-NOCV deformation density contributions, Increased (green) and decreased (yellow) electron density is presented relative to that in the isolated fragments (isosurfaces are set to 0.0001) for the molecule η^6**2'-Zr**.

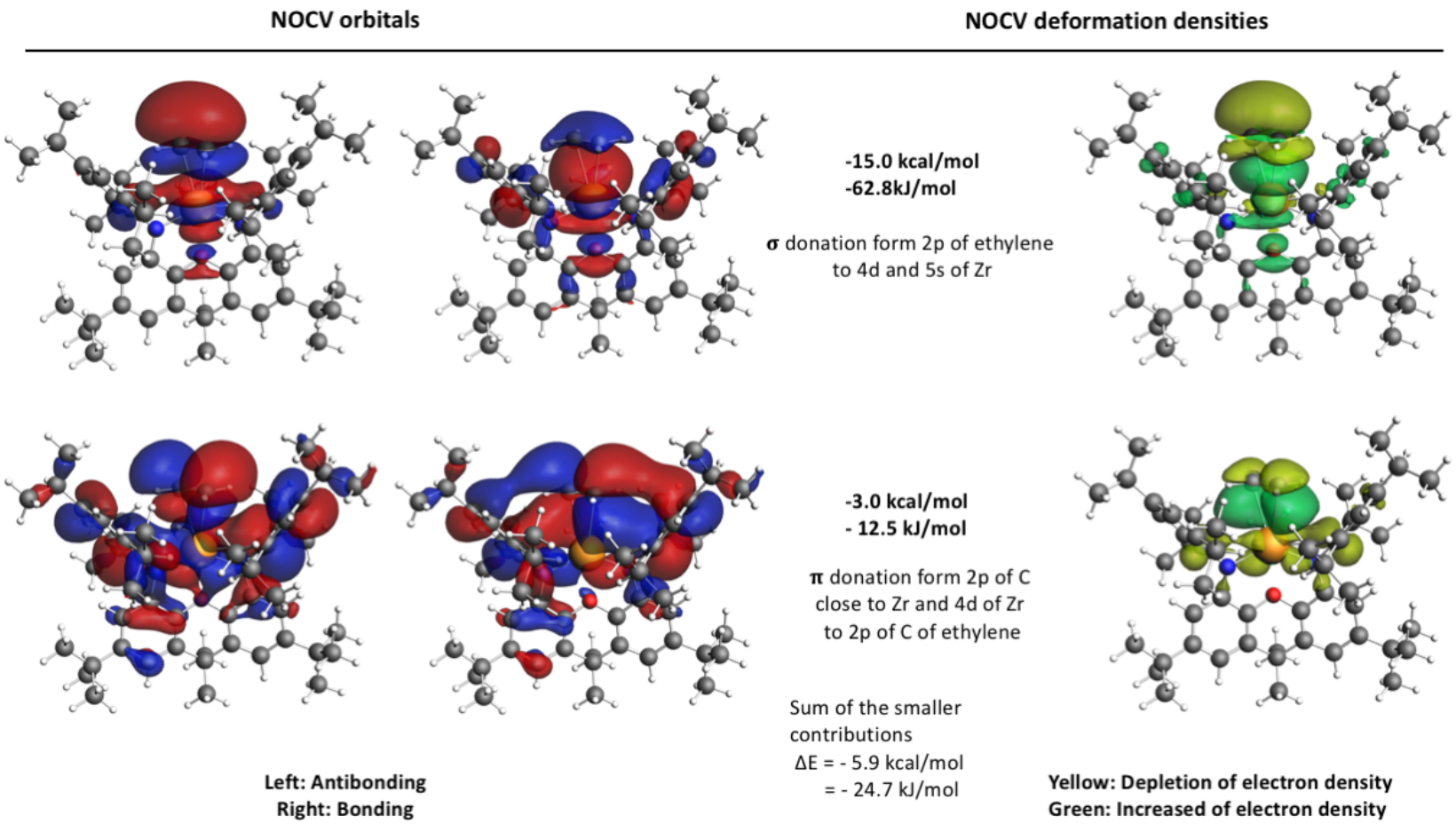

FIGURE 3.22: On the left hand side: the NOCV Orbitals (with isosurfaces set to 0.01) and on the right hand side ETS-NOCV deformation density contributions, Increased (green) and decreased (yellow) electron density is presented relative to that in the isolated fragments (isosurfaces are set to 0.0001) for the molecule η^2-**E′-Zr**.

FIGURE 3.23: On the left hand side: the NOCV Orbitals (with isosurfaces set to 0.01) and on the right hand side ETS-NOCV deformation density contributions, Increased (green) and decreased (yellow) electron density is presented relative to that in the isolated fragments (isosurfaces are set to 0.0001) for the molecule η^2-**E-Th**.

Chapter 4

Thermodynamic properties and electronic structures of Plutonium Oxides

Contents

As mentioned previously a nuclear accident would release numerous compounds. To confine this compounds would first imply to know the amount of the species released. This is what the IRSN (French Institute for Radioprotection and Nuclear Safety) aims to do. They decided to focused on Plutonium and its oxide because of its toxicity and volatility mentioned in the Introduction. In order to make a good prediction, the enthalpies of formation, the heat capacity and the entropy of each molecule involved must be known with the highest possible accuracy. In this Chapter, the enthalpies of formation of PuO_2, PuO_3 and $PuO_2(OH)_2$ will be discussed. Before a discussion of the computational protocol used and of the results obtained for these species, the existing experimental and theoretical results are reviewed below.

4.1 Review of available data for Plutonium Oxides

4.1.1 Experimental data

From a number of experimental investigations on PuO_2 [138–144], the most rescent which adresses the determination of $\Delta_f H^\ominus$ is that of Gotcu-Freis *et al.* [138]. They carried out the measurements of the vapour pressure with a Knudsen cell coupled with a quadrupole mass spectrometer. This apparatus is designed for the study of radioactive materials at high temperature and built in a glove box shielded by 5 cm thick lead bricks. This simple description of the experimental setup is enough to emphasize the difficulty of manipulating plutonium. Gotcu-Freis *et al.* extracted the values $\Delta_f H^\ominus$ = -(428.7 $\pm$ 7.0) kJ.mol^{-1} and $\Delta_f H^\ominus$ = -(440$\pm$ 7.0) kJ.mol^{-1}, using the 2^{nd} and 3^{rd} law of thermodynamics, respectively. Previously the values reported in the thermodynamic databases were slightly higher $\Delta_f H^\ominus$ = -(412 $\pm$ 20.0) kJ.mol^{-1}

[139] and $\Delta_f H^\ominus$ = -(410± 20.0) kJ.mol^{-1} [140]. Konings in his 2014's review [141] selected $\Delta_f H^\ominus$ = -(428.7 ± 20.0) kJ.mol^{-1} as the preferred value.

Unfortunately, the thermodynamic properties of PuO_3 and $PuO_2(OH)_2$ are not as much documented (see Table 4.1). The first molecule was observed in a small amount by Ronchi *et al.* [145] after sublimation of free surfaces of PuO_2 in presence of oxygen but no thermodynamic data was reported. Krikorian *et al.* [146] favoured the transpiration method starting from a PuO_2 solid sample and flows of O_2 or H_2O to generate PuO_3 and $PuO_2(OH)_2$ molecules respectively. They reported the values of standard enthalpy of formation of -(562.8 ± 5.0) kJ.mol^{-1} for PuO_3 and -(1 018.2 ± 3.3) kJ.mol^{-1} for $PuO_2(OH)_2$. This study is the unique source of experimental data for $PuO_2(OH)_2$. Konings *et al.* [141] reported the value of $\Delta_f H^\ominus$ = -(567.6 ± 15.0) kJ.mol^{-1} for PuO_3. One can note that the measurement of $\Delta_f H^\ominus$ is never direct as they are derives from measured reaction quantities (such as the partial vapour pression) for a given chemical reaction. Thus the validity of the results on $PuO_2(OH)_2$ and PuO_3 needs to be confirmed.

Accounting for the fact that the manipulation plutonium is neither easy or safe, a reasonable alternative is to determine the enthalpies of formation with accurate relativistic correlated quantum chemical methods.

However, simulations of such systems remain challenging and to prove the capabilities of *ab initio* methods one has to answer to the following questions:

- Is it possible to reproduce the $\Delta_f H^\ominus$ value for PuO_2 ?
- Can we confirm the values of $\Delta_f H^\ominus$ for PuO_3 and $PuO_2(OH)_2$?

4.1.2 Computational protocol for prediction of thermochemistry data

On the quantum chemical side, these molecules have been studied from a structural point of view but, predictions of enthalpies of formation are lacking, justifying our study.

Since our goal is to calculate the enthalpies of formation $\Delta_f H^\ominus$ of different species, we need to define the target quantities. The enthalpy H is defined as:

$$H = U + pV \tag{4.1}$$

U being the internal energy of the system, p its pressure and V its volume. The enthalpy of formation of a molecule is then the change in enthalpy to form one mole of the molecule. Hess law states that the enthalpy of a given reaction is the sum of standard enthalpies of formation of products minus the sum of the reactants.

$$\Delta_r H^\ominus = \sum_i \nu_i \Delta_f H^\ominus \tag{4.2}$$

with ν_i the stoechiometric number.

In practice $\Delta_r H^\ominus$ is calculated as:

$$\Delta_r H^\ominus = \sum_i (E_i + ZPE_i + H_{corr,i}) \tag{4.3}$$

summing up the electronic energy E_i, the Zero Point Energy (ZPE) and the thermal correction to enthalpy $H_{corr,i}$.

The enthalpy of formation of the molecule of interest can thus be extracted by the computation of the $\Delta_r H^\ominus$ for a chosen reaction as in the equation 4.4 and the subtraction of the known $\Delta_f H^\ominus$ of the other reactants and products (see Table 4.2). For example for the reaction : A + Pu $\rightarrow$ PuX + C we can obtain $\Delta_f H^\ominus$ as:

$$\Delta_f H^\ominus(PuX) = \Delta_r H^\ominus - \Delta_f H^\ominus(A) - \Delta_f H^\ominus(Pu) + \Delta_f H^\ominus(C) \tag{4.4}$$

where $\Delta_f H^\ominus$(Pu), $\Delta_f H^\ominus$(A) and $\Delta_f H^\ominus$(C) are tabulated. Sing the enthalpy of formation is path independent, the results from the reactions R_1 to R_5 should be close to each other. The average of the results will be our final $\Delta_f H^\ominus$ and the mean deviation the reported error.

Since it is established that DFT is able, even for open-shell systems, to yield good geometries and vibrational frequencies that contribute to the Zero Point Energy (ZPE) and the thermal correction to the enthalpy (H_{corr}), this will be

the method of choice to estimate these thermodynamic contributions. However, the accurate estimation of the electronic energy of each molecules remains the most sensitive part, in particular for Pu and its derivatives since one can expect large contributions of the electron correlation as well as the relativistic effects. This will thus concentrate most of our attention in the following paragraphs.

Among the prior theoretical investigations on Pu oxides [147–152], the only one that focussed on the trioxide and oxyhydroxide molecules is that of Boguslawski *et al.* [147] employing the spin-free DMRG method which underlines the complexity of the electronic structure of $PuO_2(OH)_2$, PuO_2 and PuO_3. This method, allowing to include all the valence orbitals in the active space for the DMRG wave-function, can indicate which orbitals are important for the description of the correlation *via* an entanglement figure (see section 4.2.3). The entanglement diagrams show that the 5f-orbitals plutonium orbitals and the p-orbitals of bonded oxygens are important for the description of the non-dynamical correlation and that the wave-function has a strong multi-reference character.

This study, however, only provides a partial picture of the problem as it lacks the treatment of SOC in order to establish the true nature of the ground state.

While there are no subsequent theoretical investigations for $PuO_2(OH)_2$ reported in the literature, for PuO_3, a study, based on CASSCF/CASPT2 + RASSI simulations by Kovacs *et al.* [148] represents a priori a good starting point for a deeper understanding of its electronic structure. Despite a different active space from what Boguslawski *et al.* predicted, they reached an agreement on the nature ground state (spin-free $^3B_2$ in the symmetry C_{2v}).

Concerning PuO_2, its electronic structure was studied by Liao *et al.* [149], Moskaleva *et al.* [152] and Archibong *et al.* [150] using single reference approaches, U-DFT for the two first and U-CCSD(T) for the last one, and only including the scalar relativistic effects. The only theoretical study of PuO_2 including the SOC was carried out by La Macchia *et al.* [151]. While all spin-free studies (i.e all aforementioned papers including the one using DMRG) proposed that the lowest $^5\Sigma_g$ state as the molecule's ground state, La Macchia *et al.* found that the SOC effect is so important that the ground state is no longer mainly composed of the $^5\Sigma_g$, as there is a strong contribution of the

$^5\Phi_u$, and that the geometry of the molecule is strongly modified compared to the spin-free on, with SOC being responsible for a decrease of the Pu-O bond length of 0.048 Å.

TABLE 4.1: $\Delta_f H^\ominus$ (kJ/mol) of the different compounds given in the literature.

Molecule	References	$\Delta_f H^\ominus$
PuO_2	Gotcu-Freis *et al.* [138]	-(428.7 $\pm$ 7)
	Gotcu-Freis *et al.* [138]	-(440$\pm$ 7)
	Glushko *et al.* [139]	-(412 $\pm$ 20)
	Cordfunke *et al.* [140]	-(4120 $\pm$ 20)
	Konings *et al.* [141]	-(428.7 $\pm$ 20)
PuO_3	Krikorian *et al.* [146]	-(562.8 $\pm$ 5)
	Konings *et al.* [141]	-(567.6 $\pm$ 15)
$PuO_2(OH)_2$	Krikorian *et al.* [146]	-(1 018.2 $\pm$ 3.3)

The results discussed above raise a few questions that will condition our capability of computing the desired thermodynamics:

- What is the geometry and nature of ground state of PuO_2 ?
- What is the ground state electronic structure of PuO_3 and $PuO_2(OH)_2$?
- Have static and dynamical correlation effects been treated properly before?

An appealing choice would be to use four-component-based multireference methods, such as 4c-FSCC [153–155] or EOM-CC [156] to answer these questions. Unfortunately, the relativistic FSCC implementation at our disposal at this time, cannot be used to investigate PuO_3 and $PuO_2(OH)_2$; it requires that the reference wave function to be a single determinant. For these systems, such a reference is a very poor choice. For PuO_2, on the other hand, once SOC is included self-consistently in the calculation as it is done in four-component approach, the ground state can be represented by a single determinant and the CCSD(T) method (and EOM-CC) applied.

Another option would be to extend the work of Boguslawski *et al.* and include a better description of the electronic correlation, in particular the dynamic contribution, and also include the effect of the spin-orbit coupling.

Recent developments make it now possible to use DMRG-SCF and DMRG-NEVPT2 to include, respectively static and dynamic correlation, with an active space up to 50 electrons in 50 orbitals. Though, SOC is still only included via State Interaction (see Section 4.2.2). Preliminary calculations, however, were not successful and require further investigation that will pursued beyond this thesis.

For these reasons, the only generally applicable method to treat such highly correlated systems in a relativistic framework is the CASPT2 method, combined with a posteriori treatment of SOC.

In this chapter, we provide a detailed description of the CASSCF approach that relies on the selection of important orbitals (active space) for the treatment of the static correlation. The choice of the active space is at the heart of this work and will be discussed in details for the three molecules.

4.2 Multireference Approaches

All the quantum chemical methods listed so far in Chapter 2 refer to single determinant wave function, thus not applicable for the foreseen multi-reference gas-phase plutonium molecules. Indeed, partial population of the valence 7s, 5f and 6d orbitals can induce significant multi-reference contributions to the wave functions and connected to the presence of quasi-degenerated electronic states, reflected by strong static correlation. We will now describe the various multi-reference methods that can account for static and dynamical correlation.

4.2.1 The ideal multi reference method: Full Configuration Interaction

The most complete way to capture electronic correlation, for the ground state or excited states, is to use the Full Configuration Interaction (FCI) method, for which the wave function is written as a linear combination of all the possible determinants created by single up to N-excitations from the HF determinant, N being the number of electrons:

$$|\psi_{FCI}\rangle = c_0 |\Phi_{HF}\rangle + \sum_{a,r} c_a^r |\Phi_a^r\rangle + \sum_{\substack{a<b \\ r<s}} c_{ab}^{rs} |\Phi_{ab}^{rs}\rangle + \sum_{\substack{a<b<c \\ r<s<t}} c_{abc}^{rst} |\Phi_{abc}^{rst}\rangle + ... \quad (4.5)$$

One recognises Φ_{HF} the HF solution the excited determinants from the HF one. Φ_a^r is a singly excited (S-type) determinant generated by the promotion of one electron from the spin orbital a to the spin orbital r; the ψ_{ab}^{rs} is a doubly excited (D-type) determinant created by the promotion of two electrons from the spin orbitals a and b to the spin orbitals r and s etc...

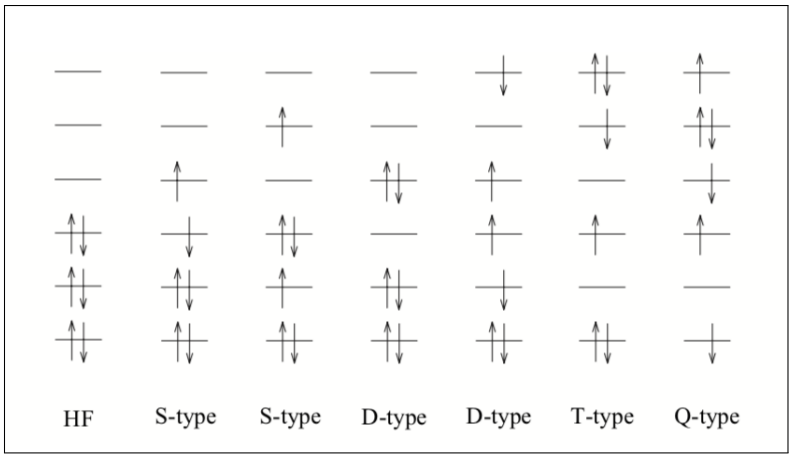

FIGURE 4.1: Various Excited Slater determinants generated from a HF reference [10]

The expansion coefficients are determined from a variational procedure in order to minimise the energy. In order to find the expansion coefficients all the possible excited determinants must be generated but also all the combinaisons of them : the Configurational State Functions (CSFs). It is the number of CSFs that will limit the use of this method. Indeed it was shown [10] that just for singlet the number of generated CSFs is:

$$\frac{M!(M+1)!}{(\frac{N}{2})!(\frac{N}{2}+1)!(M-\frac{N}{2})!(M-\frac{N}{2}+1)!} \quad (4.6)$$

M being the number of basis functions and N the number of electrons. If one takes the plutonium atom as example, the number of electron is 94 and the chosen basis set is the contracted ANO-RCC-TZP corresponding to 87 basis

functions, the number of CSFs is $4.461\,424\,5 \times 10^{48}$ only for singlet configurations (!!). For this reason, one is forced to cut the number of excitations to obtain a *truncated*-CI expansion or reduce the number of determinants by selecting the orbitals that can participate into the excited determinants.

4.2.2 Multiple-steps correlated methods

Inclusion of static correlation: Complete Active Space Self Consistent Field

The main idea of the Complete Active Space Self Consistent Field (CASSCF) method is to proceed to a FCI calculation but only with a set of selected orbitals forming the so-called active space. The molecular orbitals are thus divided in three groups: the inactive orbitals, lowest in energy and doubly occupied, the active space containing at most 18 electrons in 18 active orbitals. The occupations of the active orbitals can vary between zero and two electrons. The third and last type of orbitals are the unoccupied orbitals also called virtual orbitals (see Figure 4.2) which will remain unoccupied.

CASSCF is far from "black box" being a method since the selection of the active space is in general not trivial especially due to the constraint of the number of electrons and the active obitals. The choice of active space, and making sure it accurately represents the physics of the system, represent the main challenges if this type of calculation. That said, one can follow the rules proposed by Roos *et al.* [157] to built an active space suitable for the ground state or excited states of a given system:

- the orbitals participating to the target state.
- the valence orbitals (*i.e.* first row for light atoms; 7s, 5f and 6d for an actinide atom).
- orbitals with an occupation between 0.05 and 1.95 electron from the MP2 first-order density matrix.
- if bonding orbitals are taken, the corresponding anti-bonding should be included as well.

Certainly, the number of electrons and orbitals corresponding to the point above can quickly be greater than 18. So, the choice of the orbitals to exclude is left to the appreciation of the user, nonetheless, this choice must be argued.

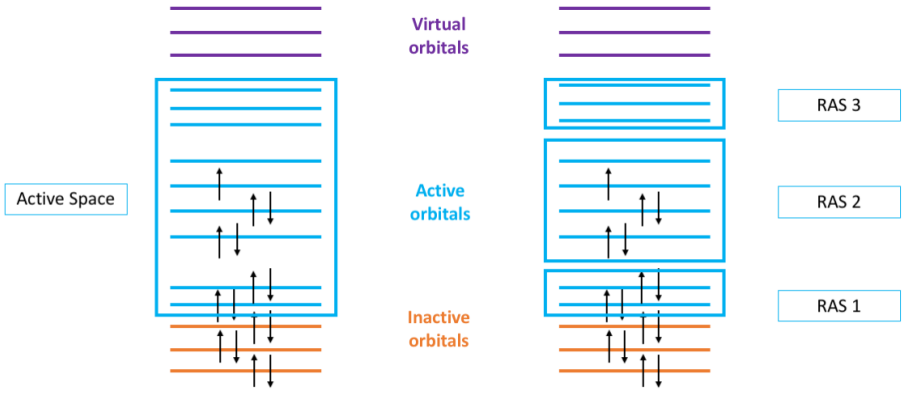

FIGURE 4.2: Representation of the CASSCF and RASSCF approaches. On the left hand side, the CASSCF method within the active space (9;9) on the right hand side, the RASSCF method with the active spaces: RAS1(4;2), RAS2(5;4);, RAS3(0,3).

One solution to extend the size of the active space is to use the Restricted Active Space Self Consistent Field (RASSCF) method, Figure 4.2. The RAS1 is composed of doubly occupied orbitals, the RAS2 is the full CI active space and RAS3 includes unoccupied orbitals. A FCI will be done in the RAS2 space and excitations from RAS1 orbitals to RAS3 ones are added with a user-defined constrain on the maximum numbers of holes and particles in RAS1 and RAS3, respectively.

In order to compute the Spin-Orbit Coupling (SOC) in the system not only the ground state is needed but also some of the excited states (this need will be explain in the section 4.2.2) that can be coupled by the SO operator. If only one state is computed at a time, we refer to a State Specific (SS) calculation, for a ground or excited state. The SS approach has the main disadvantages to be computationally expensive since a specific set of orbitals is optimised for each state. Instead, it is faster to use the SA procedure for which a set of common orbitals to several state sharing the same multiplicity and symmetry is optimised.

Note that SA-CASSCF energies will be higher than the SS ones but as we often only consider energy differences, the errors on the individual energies will compensate.

This multi-reference method CASSCF or RASSCF thoroughly includes the static electronic correlation but only a limited part of the dynamical correlation, since only double excitations are included within the active space. A rather economical way of including dynamical correlation, due to the excitations from active space to the virtual orbitals, is to use second-order perturbation theory.

Multi-Reference Perturbation Theory at the 2^{nd} order

The Complete Active Space Perturbation Theory at the 2^{nd} order or CASPT2 is, as indicated by his name a perturbative method. It allows to account for the dynamical correlation to the wave function, starting from a CASSCF calculation by adapting the MP2 approach introduced in Section 2.2.2. The contributing single and double excitations are represented in Figure 4.3. They are classified according to the number of holes and particules. It is useful to by-pass the diagonalisation problem of the operator $\hat{H}'$. Instead of the diagonalisation of the full $\hat{H}'$ will be done by block *i.e.* for each excitation type at a time.

Originally, the Hamiltonian used was the Zeroth-Order Hamiltonian with the standard Fock matrix formulation [158]:

$$\hat{H}_0 = \hat{P}_0\hat{F}\hat{P}_0 + \hat{P}_k\hat{F}\hat{P}_k + \hat{P}_{SD}\hat{F}\hat{P}_{SD} + \hat{P}_{TQ...}\hat{F}\hat{P}_{TQ...} \tag{4.7}$$

where $\hat{P}_0$ in the projector on the one-dimensional space V_0, spanned by the CAS reference wave function ϕ_0 under consideration, $\hat{P}_k$ is the projector on the space V_k, spanned by the orthogonal complement to ϕ_0 in the restricted FCI subspace used to generate the CAS wave function. $\hat{P}_{SD}$ is the projector on the space V_{SD}, spanned by all the single and double replacement states generated from V_0, finally $\hat{P}_{TQ...}$ in the projector on the space V_{TQ}, spanned by all higher excitation not included in V_k and V_{SD}.

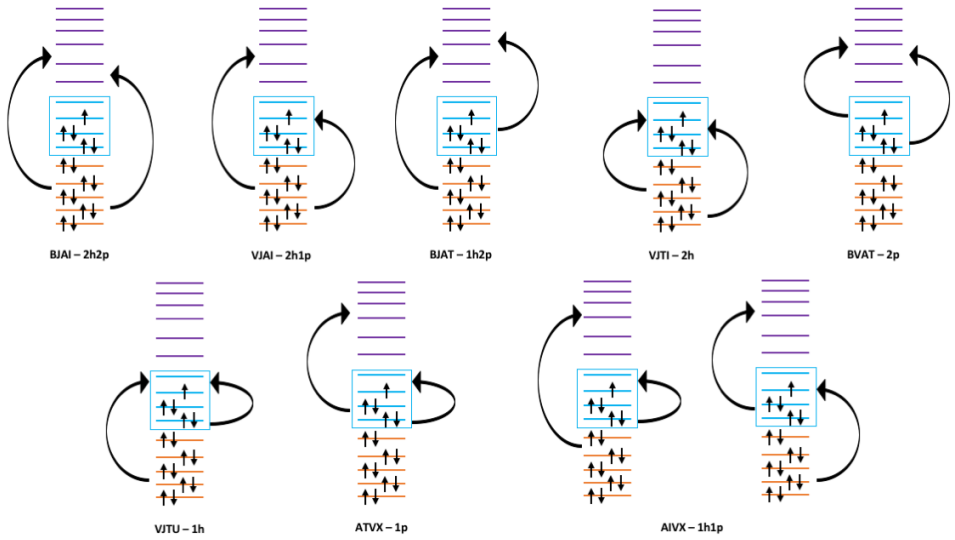

FIGURE 4.3: Representation of the possible di-excitation in CASPT2 method. NAME of the excitation in CASPT2 method - number of ***h***oles (electron(s) outside the active space promoted to the active or virtual orbitals) number of ***p***articule (electron occupying a virtual orbital - outside the active space - after the perturbation).

This formulation raises the intruder state problem [159]. When excited determinants are close in energy to the reference ones, their contribution will diverge due to a denominator approaching zero. Those intruder states can be spotted by a low (< 0.60) value of the weight of the CAS/RAS wave function in the final wave function. To eliminate this problem a level shift of the active orbitals was introduced. Based on the Ionisation Potential (IP) and Electronic affinity (EA) [160], the IPEA shift was determined thanks to a benchmark on atomic data. During our study IPEA value was kept at its default value: 0.25 a.u.. Since it is known that the higher states are much more sensitive to the value of the level shift [159] it was decided to use the available "imaginary shift". It actually uses real quantities to treat the potential energy function differently from the IPEA level shift in order to reduce the sensitivity of the energies to the size of the imaginary shift. It was fixed at 0.05 a.u., the smallest value reported by Forsberg *et al.* [159] to reach accurate results.

Finally, another possibility to fix the problem of intruder states is to use the Hamiltonian by Angeli *et al.* [161] which is based on the generalised zeroth

order Hamiltonian by Dyall [162]. It behaves as a true many-body Hamiltonian inside the CAS subspace, including all two-electrons interactions, while the CASPT2 method uses the monoelectronic Fock Hamiltonian. N-Electron Valence state Perturbation Theory at the 2^{nd} order (NEVPT2) method is intrinsically intruder state free; however, current implementations limit its use to active spaces of 14 electrons in 14 orbitals, thus inapplicable to our systems.

A posteriori treatment of spin orbit coupling : the RASSI method

The Restricted Active Space State Interaction (RASSI) methods is able to compute the coupling elements for any one-electron operator between CASSCF/RASSCF wave-function that can be non-orthogonal. In our case, the one-electron operator is SOC, computed with the atomic mean field spin-orbit operator described by equation 2.106 in Section 2.4.3, that couples states of different spins and spatial symmetries. In order to also include the dynamical correlation, the method was adapted by Malmqvist *et al.* [163] to use the CASPT2 wave-functions as basis. So the diagonal RASSI matrix [65] is dressed with the CASPT2 energies while the spin orbit matrix elements (V_{SO}) appear as off-diagonal elements. The so-constructed matrix is diagonalised to obtain the SO-eigenstates.

The lowest eigenvalue is the energy of ground state at spin-orbit CASPT2 (SO-CASPT2) level. Every SO-state is expressed as a linear combinaison of the Spin-Free (SF) states that constituted the basis. The SOC contribution to the molecule total energy is thus energy difference between the lowest SO state and the lowest SF state.

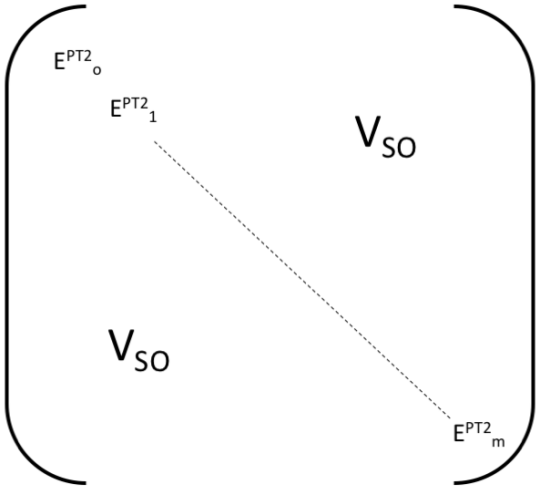

FIGURE 4.4: Matrix representation with, in diagonal, the CASPT2 energies and outside the diagonal, the spin orbit element.

TABLE 4.2: $\Delta_f H^{\ominus}$ of the different compounds given in kJ/mol

Species	$\Delta_f H^{\ominus}$	$\Delta\Delta_f H^{\ominus}$
O (^{3}P)	249.23 [164]	0.00
H (^{1}S)	218.00 [165]	0.01
Pu (^{5}F)	349.00 [166]	3.0
H_2 (1S)	0.00[165]	0
H_2O	-241.81[164]	0.03
H_2O_2	-135.88 [167]	
O_2	0.00[165]	0.00
OH	37.36 [164]	0.13

TABLE 4.3: Reactions used to calculate $\Delta_r H^\ominus$

	PuO_2	PuO_3	$PuO_2(OH)_2$
R_1	$Pu + O_2 \longrightarrow PuO_2$	$Pu + \frac{3}{2} O_2 \longrightarrow PuO_3$	$Pu + O_2 + 2\,H_2 \longrightarrow PuO_2(OH)_2$
R_2	$Pu + 2\,O \longrightarrow PuO_2$	$Pu + 3\,O \longrightarrow PuO_3$	$Pu + 4\,O + 2\,H \longrightarrow PuO_2(OH)_2$
R_3	$Pu + H_2O_2 \longrightarrow PuO_2 + H_2$	$Pu + \frac{3}{2} H_2O_2 \longrightarrow PuO_3 + \frac{3}{2} H_2O$	$Pu + 3\,H_2O_2 \longrightarrow PuO_2(OH)_2 + 2\,H_2O$
R_4	$Pu + OH \longrightarrow PuO_2 + 2\,H$	$Pu + 3\,OH \longrightarrow PuO_3 + 3\,H$	$Pu + 4\,OH \longrightarrow PuO_2(OH)_2 + 2\,H$
R_5	$Pu + 2\,H_2O \longrightarrow PuO_2 + 2\,H_2$	$Pu + 3\,H_2O \longrightarrow PuO_3 + 3\,H_2$	$Pu + 4\,H_2O \longrightarrow PuO_2(OH)_2 + 2\,H_2$

4.2.3 Opening the active spaces to include electronic correlation: the Density Matrix Renormalisation Group

4.3 Technical Considerations and Computational details

4.3.1 Geometries, enthalpic corrections and basis sets

The first information a computational chemist needs is the geometry of the system under study. In our case, all the geometries (except PuO_2 see section 4.3.1) were optimised with DFT (see section 2.3) and the B3LYP functional [168, 169] using the GAUSSIAN09 [170] package. The plutonium atom was described by a relativistic effective core potential (RECP) ECP60MWB [171] with the corresponding basis set of quadruple ζ [71] quality, while for the lighter atoms by augmented triple ζ (aug-cc-pVTZ) basis sets were used. This basis set quality is known to reproduce properly the geometries and the enthalpic corrections. All the geometries are available in Annex A. The calculation of harmonic frequencies is necessary to compute the zero point energy (ZPE) and the thermal corrections to the enthalpy of equation 4.3 and the entropy. Anharmonic frequencies were also computed but no significant difference in the value of the entropies S were seen in comparison to the harmonic ones, thus only contributions obtained at the harmonic level were kept.

Once the geometries of the different molecules were obtained and to reach accurate electronic energies for the determination of $\Delta_f H^\ominus$, two methods were used. The first is the UCCSD(T) method which represents the gold standard for single-reference wave function. The second is the multi-reference wave-function method that involves CASSCF plus CASPT2 calculations to check whether the wave function has a multi-reference character or not. In

both cases, the scalar relativistic effects are included via the DKH2 Hamiltonian and the SOC was calculating with the RASSI procedure and added to the UCCSD(T) and CASPT2 spin free energies. All atoms are described with the ANO-RCC basis sets [172, 173] with qualities sequentially increased from triple-ζ (n=3) to quadruple-ζ (n=4) to extrapolate the energies to the CBS limit with the total energy extrapolation (CBS-TE) and the extrapolation separating the uncorrelated and correlated energies (CBS-CE). The two extrapolation methods yield to small differences of a few kJ.mol^{-1} for the reaction energies.

Geometry of PuO_2

Because of disagreement in literature [147, 149, 152, 174] concerning the distance Pu-O and the nature of the ground state, a more accurate exploration of the potential energy surface was needed. It was first done with the State Specific-Spin-Free-CASPT2 method for the lowest quintet A_g and A_u states in D_{2u} symmetry. Scanning distances from 1.724Å to 1.884Å in steps of 0.02 Å.

In addition to the CASPT2 calculations, Andre Gomes performed calculations based on the molecular mean-field [175] approximation to the Dirac–Coulomb ($^2DC^M$) Hamiltonian, at MP2, CCSD and CCSD(T) [176, 177] levels of theory with the DIRAC electronic structure code [178] using $D_{\infty h}$ symmetry. The Dyall basis sets [179, 180] of triple- and quadruple-zeta qualities were employed for the plutonium atom, and Dunning's aug-cc-pVXZ (X=T, Q) sets[181] for the oxygen atoms. In all calculations, the $(SS|SS)$-type two-electron integrals were approximated by a point-charge model [182]. Electrons in molecular spinors with energies comprised between -3 and 100 au were included in the correlated treatment, which amounted to correlating 28 electrons for PuO_2.

The SCF calculations were closed-shell ones, with 52 and 58 electrons in g and u irreducible representations, respectively. The equilibrium structure and spectroscopic constants for each electronic structure method were determined via a polynomial fit of the potential energy surface constructed from single-point calculations for Pu-O internuclear distances between 1.750 Å and 1.880 , in steps of 0.005 . Energies and potential energy curves at the

complete basis set limit were obtained with the two-point extrapolation (see equation 2.121).

4.3.2 Results of the single-reference gold standard method: UCCSD(T)

The UCCSD(T) [183] calculations were performed with the Molpro Quantum Chemistry software [156]. The frozen orbitals were the 1*s* orbital of O and 1*s* to 5*d* (included) orbitals of Pu. No core-valence correlation was considered here due to the excessive computational cost and that we expect them not to exeed few kJ mol^{-1} for actinide molecules [184].

In order to look at the influence of the inclusion of the spin-orbit *a priori*, ^{2}DC^M-CCSD(T) calculation were performed (by Andre Gomes). It could be done on Pu, PuO_2, H_2, OH, H_2O and H_2O_2 allowing us to obtain the energies for reactions R_3, R_4 and R_5 for PuO_2. The setup from the PES exploration of PuO_2 was kept (see Section 4.3.1).

In addition, thanks to the recent implementation made by Andre Gomes used recent implementation in DIRAC code [185] of variant of EOM-CCSD, we were able to compute the ionization potential for atomic Pu and PuO_2 (EOM-IP-CCSD) and the excitation energies (EOM-EE-CCSD) for PuO_2.

In the case of EOM-IP-CCSD for Pu, we requested the number of states as follows: five $\Omega = 1/2_g$, two $\Omega = 3/2_g$, one $\Omega = 5/2_g$, three $\Omega = 1/2_u$, two $\Omega = 3/2_u$ and one $\Omega = 5/2_u$, whereas for PuO_2 we requested two $\Omega = 1/2_g$, one $\Omega = 3/2_g$, three $\Omega = 1/2_u$, two $\Omega = 3/2_u$ and one $\Omega = 5/2_u$ states. In the case of EOM-EE-CCSD we requested the number of states as follows: six $\Omega = 0_g$, four $\Omega = 1_g$, three $\Omega = 2_g$, two $\Omega = 3_g$, one $\Omega = 4_g$, one $\Omega = 5_g$, ten $\Omega = 0_u$, nine $\Omega = 1_u$, seven $\Omega = 2_u$, five $\Omega = 3_u$, three $\Omega = 4_u$, and one $\Omega = 5_u$.

4.3.3 Multi-reference calculations: Actives Spaces, Number of States and Shifts

Actives spaces

All the multi-reference wave-function calculations were performed with the MOLCAS software [186]. As previously mentioned the choice of active space is crucial since a poor choice of active space can lead not only to poor accuracy but to false results. The easiest choice of active space is the one for the atomic plutonium. One would be tempted to wisely but simply consider the 5f-orbitals. The Paris-Sud database [167] reports the nonet ^{9}H, involving the 6d and 7s orbitals, as the closest in energy to the septuplet ground state. Thus the former orbitals were also included to lead to an active space of 8 electrons in 13 orbitals (8,13). First calculations yield for the appearance of a spurious orbital in the CAS, making us reconsider our previous active space. Finally, we proposed the following organisation: the 7s orbital in the RAS1 with 1 hole allowed, the 5f orbitals in the RAS2 and the 6d orbitals in the RAS3 with one particule permitted. Concerning the molecules with no plutonium atom, the active space is simply composed of the oxygen valence orbitals. For those molecules, spin-orbit coupling was not imputed as it is expected to be negligible.

Concerning the plutonium oxides and oxyhydroxides, the choice of the active space was guided by the DMRG study of Boguslawski *et al.* [147], to which our research team contributed. This study followed the rules laid out in the Section 4.2.2 to define the 'full valence" space. The analysis of the entanglement diagrams lead to the definition of "optimal active spaces" listed in Table 4.4.

TABLE 4.4: Full active space and optimal active space presented in the article of Boguslawski *et al.* [147]

Molecules	Full Valence	Optimal Active Space
PuO_2	(28,25)	(18,17)
PuO_3	(34,26)	(14,14)
$PuO_2(OH)_2$	(42,35)	(20,22)

Note that neither orbital optimisation nor SOC were included in [147]. The suggested optimal active space for $PuO_2(OH)_2$ is too large for the CASSCF

method. Instead, we restricted ourselves to a minimal active space of 2 electrons in 4 orbitals (see Figure 4.5). Concerning PuO_3 and PuO_2 attempts to use the optimal active spaces was made but turned out unsuccessful as these are suited for the ground state only but do not apply for the excited states. Thus the active spaces had to be modified.

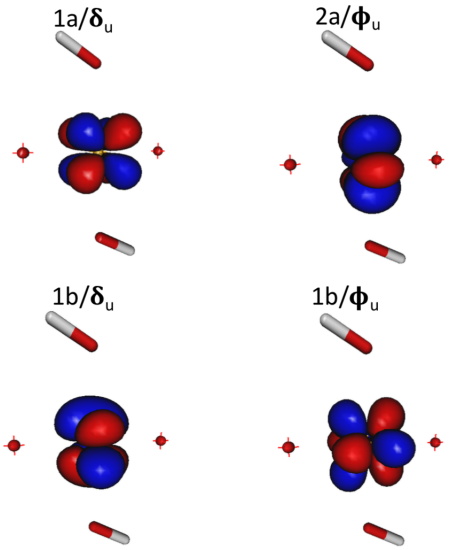

FIGURE 4.5: Molecular orbitals of $PuO_2(OH)_2$ at the CASSCF level. Isosurface = 0.05 a.u.

- **PuO_2 active space**

For PuO_2, the optimal active space matches the MO diagram of the uranyl moleculeproposed by Denning *et al.* [187]. This paper emphasised the mixing of the 5f, 6d and the 2p-orbitals of the oxygens, thus a chemically relevant model should include (14, 18) which is already approaching the limit of the CASSCF code. Moreover we would like to add the 7s orbitals that have been proven important for the description of plutonium and for PuO_2 [147], bringing the active space to 16 electrons in 19 orbitals, which is undoable.

After a close look at the DFT-B3LYP results for PuO_2, it appears that the lowest orbitals of the (16;19) active space are the degenerate π_g orbitals formed by the combination of Pu's 6d and oxygen 2p-orbitals. These orbitals did not appear as strongly entangled to the other valence orbitals in the entanglement diagram on the Figure 3 in [147] and can thus be eliminated from the active space cutting it down to a CAS(12, 17) (see Table 4.5 for details). This

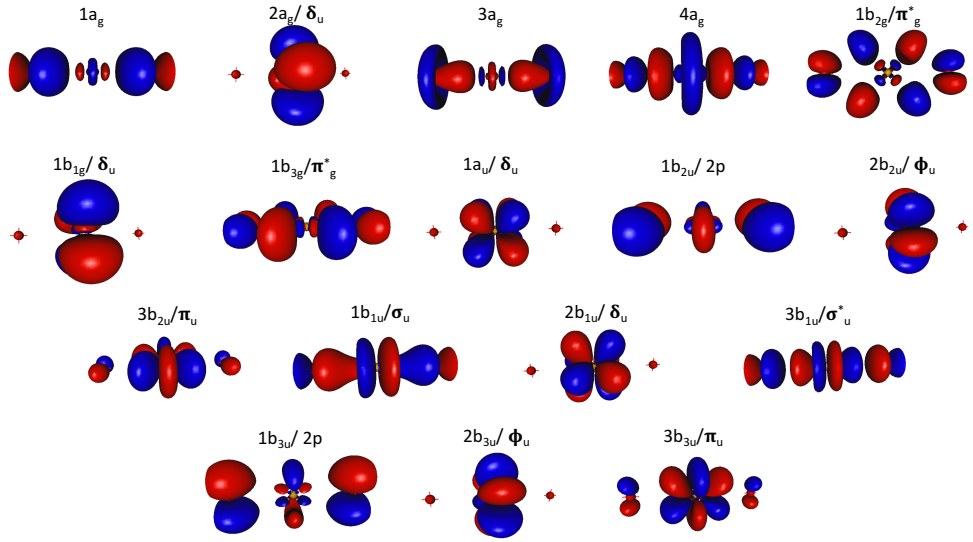

FIGURE 4.6: Molecular orbitals of PuO_2 at the CASSCF level; Isosurface = 0.05 a.u.

is slightly larger than the one used in the study of La Macchia *et al.* but the results can still be comparable.

TABLE 4.5: Active spaces for the various plutonium oxides and oxyhydroxides.

Molecule	Active Space (electron, orbitals)	Orbitals
PuO_2	(12,17)	$\pi_u(2)$, $\pi_g(2)$, σ_g, σ_u, $\pi_u^*(2)$, $\pi_g^*(2)$, σ_g^*, σ_u^*, $f_\delta(2)$, $f_\phi(2)$
PuO_3	(14,13)	$1a_1/\pi_u$,$2a_1$, $4a_1/p_x^o$,$5a_1/\phi_u$, $6a_1/\pi_u$, $1b_1/\phi_u$, $2b_1/\pi_u$, $1b_2/p_z^o$,$2b_2/\sigma_u$, $3b_2/\delta_u$, $4b_2/\sigma_u^*$, $1a_2/\delta_u$
$PuO_2(OH)_2$	(4,4)	$1a/\delta$, $2a/\phi$, $1b/\delta$, $2b/\phi$
Pu	(8,13)	7s, 5f, 6d
O	(6,4)	2s, $2p_x$, $2p_y$, $2p_z$
O_2	(12, 8)	σ_{2s}, σ_{2s}^*, $\sigma_{2p}(3)$, $\sigma_{2p}^*(3)$
OH	(7,5)	σ, σ_{nb}, $2p_x^O$, $2p_y^O$, σ^*,
H_2O_2	(14, 10)	1 σ^{O-O}, 1 σ^{*O-O}, σ^{O-H} (2), 2 σ^{O-O}, π^{O-O}, $2p^O$, $1\sigma^{*O-O}$, $\sigma^{O-H}(2)$
H_2O	(8,6)	$2a_1$,$1b_2$, $3a_1$, $1b_1$, $4a_1$, $1b_2$
H_2	(2, 2)	σ,σ^*
H	(1,1)	1s

- **PuO_3 active space**

Concerning PuO_3, from a chemical view point, assuming Pu to be in oxidation state (VI), we can depict it as a plutonyl PuO_2^{2+} in interaction with a O^{2-} anion. Thus from the PuO_2 active space we selected all the orbitals that could mix with the 2p-orbitals of the apical oxygen, leading to an active space of 12 electrons in 10 orbitals ($2p_x$ and $2p_z$ of the oxygen plus the $2b_{2u}/\phi_u$, $2b_{3u}/\phi_u$, $1b_{1u}/\sigma_u$, $2b_{1u}/\delta_u$, $3b_{1u}/\sigma_u^*$, $1a_u/\delta_u$, $3b_{3u}/\pi_u$ and $3b_{3u}/\pi_u$ of PuO_2). It is enough for the description of the ground state but not for the excited states. Thus, 2 electrons and 3 orbitals (corresponding to the $1a_g$, $1b_{2u}/2p$ and the visible of Figure 4.6 and the $1a_g$ of Figure 4.7) were added to obtain the active space mentionned in the Table 4.5 or in Figure 4.7.

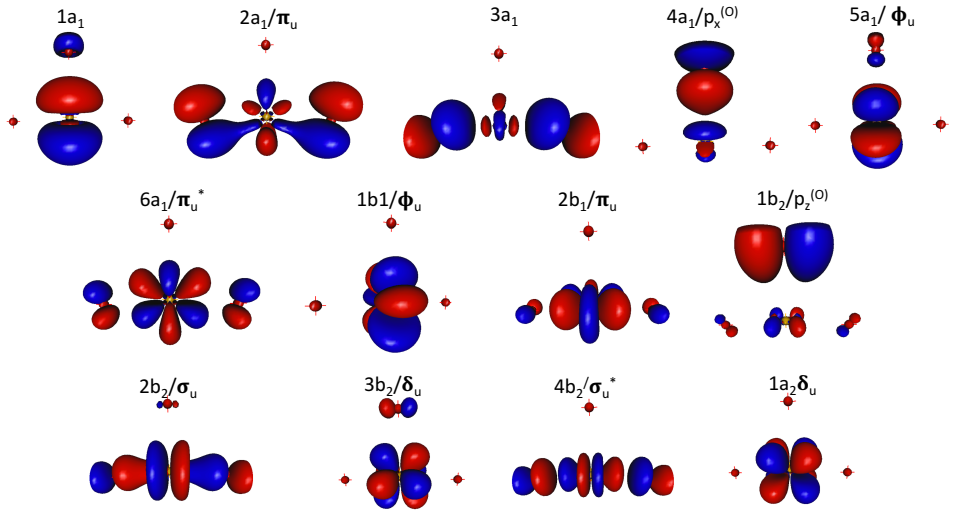

FIGURE 4.7: Active CASSCF orbitals of PuO_3 at the CASSCF level; Isosurface = 0.05 a.u.

- **CASPT2 - Numbers of state computed**

The number of states that are computed at CASSCF levels was dependent on the number of states that could be described properly (with a significant (> 0.6) reference weight) at the CASPT2 level. To keep high reference weights, beside the default IPEA value (0.25 a.u.), an imaginary shift had to be added. Indeed the Molcas manual recommends its use to improve the description of CASPT2 excited states results when transition metals or actinides are involved to avoid intruder state problems. Since the computation of PuO_2 is quite expensive, tests on the value of the imaginary shift was done on Pu,

TABLE 4.6: Totale energy of the ground state of Pu, PuO_3 and $PuO_2(OH)_2$ for different value of the imaginary shift.

Molecule	0.01	0.05	0.01	No Imaginary shift
Pu	-29539.80490586	-29539.80507744	-29539.80592767	-29539.80604535
PuO_3	-29765.45793749	-29765.45814830	-29765.45837134	-29765.45737950
$PuO_2(OH)_2$	-29841.93260283	-29841.93266384	-29841.93267515	-29841.93267545

PuO_3 and $PuO_2(OH)_2$ only with smaller active spaces, (6,7), (12,10) and (2,4) for Pu, PuO_3 and $PuO_2(OH)_2$, respectively.

As shown in [159] the total energy is barely modified and the minimal value of the shift with noticeable effect on the description of the excited states is 0.05 a.u.. This is the value kept in all the CASPT2 calculations since the 0.01 does not increase the number of states properly described and the value 0.1 impact the total energies and the excitation energies.

TABLE 4.7: Number of electronic states at CASSCF level of calculations

Multiplicity	Pu (C_i)	PuO_2 (D_{2h})								PuO_3 (C_{2v})				$PuO_2(OH)_2$ (C_2)	
symmetry	A_g	A_g	B_{2g}	B_{1g}	B_{3g}	A_u	B_{2u}	B_{1u}	B_{3u}	A_1	B_1	B_2	A_2	A	B
Singulet	0	5	5	5	5	5	5	5	5	20	20	20	20	7	4
Triplet	50	5	10	10	10	7	10	7	10	20	20	20	20	2	4
Quintuplet	120	5	5	5	5	5	5	5	5	20	20	20	20	0	0
Septuplet	110	0	0	0	0	0	0	0	0	0	0	0	0	0	0
Nonet	35	0	0	0	0	0	0	0	0	0	0	0	0	0	0

TABLE 4.8: Number of electronic states at CASPT2 level of calculations

Multiplicity	Pu (C_i)	PuO_2 (D_{2h})								PuO_3 (C_{2v})				$PuO_2(OH)_2$ (C_2)	
symmetry	A_g	A_g	B_{2g}	B_{1g}	B_{3g}	A_u	B_{2u}	B_{1u}	B_{3u}	A_1	B_1	B_2	A_2	A	B
Singulet	0	2	0	2	0	3	3	3	3	10	9	7	7	7	4
Triplet	27	2	3	3	3	6	7	6	7	16	15	13	14	2	4
Quintuplet	113	4	3	2	3	4	4	4	4	8	7	6	7	0	0
Septuplet	103	0	0	0	0	0	0	0	0	0	0	0	0	0	0
Nonet	35	0	0	0	0	0	0	0	0	0	0	0	0	0	0

Concerning the number of states included in the CASPT2, all of the 16 states were incorporated for $PuO_2(OH)_2$. Nonetheless, it was not possible for the atom of Pu or for the di and tri oxides (see Table 4.9). Thus we set a limit at 3 eV from the ground state for PuO_3 and only 2 eV for Pu and PuO_2. Even if these limits can seem arbitrary, they ensure a good description of all states introduced in the SO-RASSI calculations and which couple to the spin-free ground states.

TABLE 4.9: Number of states available for computation and states taken for computation for the plutonium atom and the various plutonium oxides and oxyhydroxides.

	Pu	PuO_2	$PuO_2(OH)_2$	PuO_3
Number of available states	20 825	136 634 576	16	2 740 106
Number of states included in RASSI	278	81	16	119

4.4 Results and Discussions

4.4.1 Electronic Structures Analysis

Atomic Pu

TABLE 4.10: Fine structure transition energies (cm^{-1}) of atomic Pu computed at the SO-CASPT2 with the ANO-RCC-TZVP basis set, and analysis of the various J-states in terms of the dominating LS terms.

Exp.[188–190]	This work	J-value	Weight of LS states
0	0	0	54% ^7F , 38% ^5D , 7% ^3P
2204	1806	1	64% ^7F , 32% ^5D
4300	4208	2	82% ^7F , 17% ^5D
6145	6353	3	88% ^7F , 10% ^5D
7775	8091	4	93% ^7F
9179	9552	5	90% ^7F
10 238	11 010	6	85% ^7F , 10% ^5G
9773	12 499	0	44% ^7F , 21% ^5D , 8% ^3P
13 528	13 612	1	66% ^9H , 9% ^7F , 7% ^7G

To compute the enthalpies of formation of the plutonium molecules, an accurate description of the plutonium atom, i.e. its electronic structure, is mandatory. Thus, in Table 4.10 (the higher excited states can be found in the Appendix B), the SO-CASPT2 calculations are reported and compared to available data from the literature [188–190]. The *ab initio* energy levels are able to accurately reproduce the experimental assignments with errors between 91 and 397 cm^{-1} for the first five excited states under 9500 cm^{-1}. Deviations between our results and the available data appear after the sixth state. The experimental assignment predicts the sixth state at 9773 cm^{-1} with a $J = 0$

while such state is found at 12 488 cm^{-1} in the current study though uncertainties remain for the attribution of this electronic state. The computed seventh state with $J = 6$ is about 800 cm^{-1} higher energy than the experimental value. Looking closely at the nature of the Pu low-lying states, one can first notice the remarkable mixing between the ^7F, ^5D and ^3P spin-orbit free states and that the contribution of the ^5D state decreases as the energy increases. Finally, the most important result is the overall good reproduction of the SO splitting of ^7F spin-free state, making us confident for the exploration of the other plutonium molecules.

PuO_3 and $PuO_2(OH)_2$

For PuO_3, at the spin-orbit level, we report the description of the ground state and the six lowest excited states in Table **??**, (the higher excited states can be found in the Appendix B). It is noteworthy that the $1a_g$, $2a_g/\delta_u$ and $3a_g$ orbitals are doubly occupied in all the calculated spin-free states. The PuO_3 orbitals are composed of a mixture of orbitals belonging to the plutonyl subunit and the distant oxygen. Thus, for the sake of clarity, we labelled these orbitals with the labels associated to those of the PuO_2^{2+} ion (with linear energy D_{2h} notations), and those of the distant oxygen atom are denoted by $p^{(O)}_{x,y,z}$. The SO ground state is composed of 47% $^3B_2$, 24% $^3A_2$ and 14% $^3B_1$ spin-free states. The composition is similar to the one previously reported by Kovács [191] (52% $^3B_2$ and 24% $^3A_2$). More striking is the difference between our computed vertical excitation energies with that of Kovács's SO-CASPT2 spectrum [191]. While we predict the first excited state to be at 1235 cm^{-1}, he places it at 471 cm^{-1}. The overall determined spectrum from our calculations is much denser and lower by about 4000 cm^{-1} than his. Such discrepancy may find its origin in the description of the spin-free states. We agree with Kovács that the spin-free ground state has $^3B_2$ symmetry, though with a different orbital character. Indeed, the $^3B_2$ exhibits a strong multi-determinantal character with 57% corresponding to the configuration in which the $4a_1/p^{(O)}_z$ and $2b_2/\sigma_u$ orbitals are doubly occupied (See Table **??** and Figure 4.7) and the singly occupied orbitals $5b_1/\Phi_u$, $1b_2/p^{(O)}_z$, $3b_2/\delta_u$ and $1a_2/\delta_u$ and 22% from the electronic configuration in which of the $4a_1/p^{(O)}_z$, $1b_2/p^{(O)}_z$ and $2b_2/\sigma_u$ orbitals are doubly occupied and the $5b_1/\Phi$ and $1a_2/\delta_u$ singly occupied. Kovács, however, finds the ground state to be mainly composed of plutonyl

orbitals (79%). Such a difference can be explained by the fact that the considered active spaces are different (a CAS(10,16) in his case and CAS(14,13) in our work). Looking closely at the entanglement diagram of PuO_3 derived from DMRG calculations [147] (Figure 6a, Full-Valence CAS) there is a strong correlation within the non-bonding plutonyl-like orbitals ($5f_\delta$, $5f_\phi$) and also between the $b_2/p^{(O)}$ and the $5f_{\delta_u}$ orbitals, in agreement with our analysis of the $^3B_2$ ground-state wave function.

Concerning $PuO_2(OH)_2$, the low energy part of the vertical spectrum including SO coupling reported in the Table **??** shows two close-lying states separated by about 323 cm^{-1}, followed by a state at 2222 cm^{-1}. The analysis of the two lowest states shows that they correspond to a fifty-fifty combination of $^3A(1)$ and $^3B(1)$ spin-free states, with a small contribution (6% in each case) of the $^3B(2)$. The next three states also have strong SO-mixings between triplet states but also singlet excited states of $^1A(1)$ and $^1B(1)$ symmetries, placed at the spin-free level at about 5764 and 7444 cm^{-1}, respectively.

PuO_2 molecule

- PuO_2 Geometry

As explained in the section 4.1 La Macchia *et al.* showed that the spin-orbit coupling was of great importance not only to describe the electronic structure but also the geometry of PuO_2. In their study, the spin-free results gave a $^5\Sigma_g^+$ as ground state with a Pu-O distance of 1.792 Å. At the spin-orbit level, the ground state was found to be a 1_u composed by 96% of the $^5\Phi_u$ with a bond length of 1.744 Å. At the latter, our SO-CASPT2 calculation predicted a 0_g ground state.

The $^5\Sigma_g^+$ is the lowest at SF level as found in La Macchia's study by the similarities stop here. The equilibrium distance is here longer with 1.804 Å(versus 1.792 Åof La Macchia *et al.*). At this distance, the energy gap to the $^5\phi_u$ state is estimated to 7992 cm^{-1}, while it was equal to 1800 cm^{-1} in La Macchia's study. In spite of this disagreement, the "reduction" of the bond distance while the spin orbit is included might be true and must be tested.

At the $^2DC^M$ level, the PuO_2 ground-state is found to be well-described a closed-shell ($\Omega = 0_g$) determinant, corresponding to occupied $f_{3/2}$ and $f_{5/2}$

TABLE 4.11: Lowest electronic levels in cm^{-1} of PuO_3, computed at the SF-CASPT2 and SO-CASPT2 levels with the ANO-RCC-TZVP basis set, and analysis of the various states.

	No.	Term Symbol	ΔE	Character : % [orbital(number of electron)]
SF	1	$^3B_2(1)$	0	36% [$4a_1/p^{(O)}(2)$, $1b_1/\Phi_u(1)$, $1b_2/p^{(O)}(\bar{1})$, $2b_2/\sigma_u(2)$, $3b_2/\delta_u(1)$, $1a_2/\delta_u(1)$]
				21% [$4a_1/p^{(O)}(2)$, $1b_1/\Phi_u(1)$, $1b_2/p^{(O)}(1)$, $2b_2/\sigma_u(2)$, $3b_2/\delta_u(\bar{1})$, $1a_2/\delta_u(1)$]
				22% [$4a_1/p^{(O)}(2)$,$1b_1/\Phi_u(1)$,$1b_2/p^{(O)}(2)$,$2b_2/\sigma_u(2)$,$1a_2/\delta_u(1)$]
	2	$^3A_2(1)$	3161	43% [$4a_1/p^{(O)}(2)$, $5a_1/\Phi_u(1)$,$1b_2/p^{(O)}(\bar{1})$,$2b_2/\sigma_u(2)$,$3b_2/\delta_u(1)$,$1a_2/\delta_u(1)$]
				23% [$4a_1/p^{(O)}(2)$, $5a_1/\Phi_u(1)$,$1b_2/p^{(O)}(1)$,$2b_2/\sigma_u(2)$,$3b_2/\delta_u(\bar{1})$,$1a_2/\delta_u(1)$]
				17% [$4a_1/p^{(O)}(2)$, $5a_1/\Phi_u(1)$,$1b_2/p^{(O)}(2)$,$2b_2/\sigma_u(2)$,$1a_2/\delta_u(1)$]
	3	$^3B_1(1)$	4663	38% [$4a_1/p^{(O)}(2)$,$5a_1/\Phi_u(1)$,$1b_1/\Phi_u(1)$,$1b_2/p^{(O)}(\bar{1})$,$2b_2/\sigma_u(2)$,$3b_2/\delta_u(1)$]
				12% [$4a_1/p^{(O)}(2)$, $5a_1/\Phi_u(1)$, $2b_1/\pi_u(1)$,$1b_2/p^{(O)}(\bar{1})$,$2b_2/\sigma_u(2)$,$3b_2/\delta_u(1)$]
				12% [$4a_1/p^{(O)}(2)$, $5a_1/\Phi_u(1)$,$1b_1/\Phi_u(1)$,$2b_1/\pi_u(2)$,$1b_2/p^{(O)}(2)$]
	4	$^1A_1(1)$	7239	32% [$4a_1/p^{(O)}(2)$,$1b_2/p^{(O)}(1)$,$2b_2/\sigma_u(2)$,$3b_2/\delta_u(\bar{1})$,$1a_2/\delta_u(2)$]
				28% [$4a_1/p^{(O)}(2)$,$1b_2/p^{(O)}(2)$,$2b_2/\sigma_u(2)$,$1a_2/\delta_u(2)$]
				11% [$4a_1/p^{(O)}(1)$, $5a_1/\Phi_u(\bar{1})$,$1b_2/p^{(O)}(2)$,$2b_2/\sigma_u(2)$,$1a_2/\delta_u(2)$]
	5	$^3A_2(2)$	7287	20% [$4a_1/p^{(O)}(2)$,$1b_1/\Phi_u(1)$,$1b_2/p^{(O)}(1)$,$2b_2/\sigma_u(2)$,$3b_2/\delta_u(2)$]
				18% [$4a_1/p^{(O)}(1)$,$5a_1/\Phi_u(\bar{1})$,$1b_1/\Phi_u(1)$,$1b_2/p^{(O)}(2)$,$2b_2/\sigma_u(2)$,$3b_2/\delta_u(1)$]
				17% [$4a_1/p^{(O)}(2)$,$1b_1/\Phi_u(1)$,$1b_2/p^{(O)}(2)$,$2b_2/\sigma_u(2)$,$3b_2/\delta_u(1)$]
	6	$^3B_1(2)$	8038	31% [$4a_1/p^{(O)}(1)$,$5a_1/\Phi_u(\bar{1})$,$1b_2/p^{(O)}(2)$,$2b_2/\sigma_u(2)$,$3b_2/\delta_u(1)$,$1a_2/\delta_u(1)$]
				11% [$4a_1/p^{(O)}(2)$,$5a_1/\Phi_u(1)$,$2b_1/\pi_u(1)$,$1b_2/p^{(O)}(\bar{1})$,$2b_2/\sigma_u(2)$,$3b_2/\delta_u(1)$]
				10% [$4a_1/p^{(O)}(2)$,$1b_2/p^{(O)}(2)$,$2b_2/\sigma_u(2)$,$3b_2/\delta_u(1)$,$1a_2/\delta_u(1)$]
				10% [$4a_1/p^{(O)}(2)$,$1b_1/\Phi_u(1)$,$2b_1/\pi_u(1)$,$1b_2/p^{(O)}(\bar{1})$,$2b_2/\sigma_u(2)$,$1a_2/\delta_u(1)$]
SO		X	0	47% $^3B_2(1)$ + 24% $^3A_2(1)$ + 14% $^3B_1(1)$
		a	1235	59% $^3B_2(1)$ + 25% $^3A_2(1)$
		b	1783	73% $^3B_2(1)$
		c	3777	51% $^3A_2(1)$
		d	5660	24% $^3B_1(1)$ + 18% $^1A_1(1)$ + 17% $^3A_2(2)$ + 10% $^3B_1(2)$

TABLE 4.12: Lowest electronic levels in cm^{-1} of $PuO_2(OH)_2$, computed at the SF-CASPT2 and SO-CASPT2 levels with the ANO-RCC-TZVP basis set, and analysis of the various states.

	State	ΔE	Character : % [orbital(number of electron)]
SF	$^3B(1)$	0	49% [2a/Φ_u(1) ,1b/δ_u(1)]
			48% [1a/δ_u(1) , 2b/Φ_u(1)]
	$^3A(1)$	889	41% [1a/δ_u(1) , 2a/Φ_u(1)]
			59% [1b/δ_u(1) , 2b/Φ_u(1)]
	$^3B(2)$	2136	75% [1a/δ_u(1) , 1b/δ_u(1)]
			20% [2a/Φ_u(1) , 2b/Φ_u(1)]
	$^3A(2)$	4698	59% [1a/δ_u(1) , 2a/Φ_u(1)]
			41% [1b/δ_u(1) , 2b/Φ_u(1)]
	$^3B(3)$	5351	52% 2a/Φ_u(1), 1b/δ_u(1)
			46% [1a/δ_u(1), 2b/Φ_u(1)]
	$^1A(1)$	5764	[58% 1b/δ_u(1) , 2b/$\Phi_u(\bar{1})$]
			30% [1a/δ_u(1) , 2a/$\Phi_u(\bar{1})$]
			5%[2a/Φ_u(2)]
	$^1B(1)$	7444	50% [1a/δ_u(1), 1b/$\delta_u(\bar{1})$]
			28% [2a/Φ_u(1), 2b/$\Phi_u(\bar{1})$]
			16%[1a/δ_u(1), 2b/$\Phi_u(\bar{1})$]
	$^1A(2)$	9626	39% [1a/δ_u(1) , 2a/$\Phi_u(\bar{1})$]
			29 % [2a/Φ_u(2)]
			13% [1b/δ_u(1) , 2b/$\Phi_u(\bar{1})$]
			10% [1a/δ_u(2)]
			7 %[2a/Φ_u(2)]
SO	X	0	46% $^3A(1)$, 41% $^3B(1)$, 6% $^3B(2)$
	a	323	45.% $^3B(1)$, 45% $^3A(1)$, 6% $^3B(2)$
	b	2222	35% $^3B(2)$, 25% $^3B(1)$, 14% $^1A(1)$, 13% $^3A(2)$, 10% $^3B(3)$
	c	3757	40% $^3A(2)$, 25% $^3B(2)$, 19% $^1B(1)$, 7% $^3B(1)$, 6% $^3A(1)$
	d	4158	36% $^3B(3)$, 34% $^3B(2)$, 14% $^1A(2)$, 11% $^3B(1)$,

TABLE 4.13: Comparison of CBS extrapolated $^2DC^M$-EOM-CCSD and SO-CASPT2 PuO_2 vertical transition energies in cm^{-1} computed at the 1.744 and 1.808 Å Pu−O distances.

	d(Pu-O)=1.744 Å			d(Pu-O)=1.808 Å	
Ω	$^2DC^M$-EOM-CCSD	SO-CASPT2		$^2DC^M$-EOM-CCSD	SO-CASPT2
	This work	This work	Ref. [192]	This work	
0_g	0	0	1794	0	0
1_g	2435	1438	2315	2325	2462
2_g	6012	4235	4131	5378	5904
1_u	5721	1778	0	8548	5851
2_u	5926	1805	535	8782	6265
3_u	6622			9882	
4_u	12 751			15 471	

TABLE 4.14: CBS extrapolated Ionization Potentials of PuO_2 in eV computed at the $^2DC^M$-EOM-CCSD level (d(Pu-O)= 1.808 Å) and comparison with experiments.

$^2DC^M$-EOM-CCSD		Exp			
State	IP	[[193]]	[[194]]	[[195]]	[[196]]
		9.4	10.1	7.03	6.6
$3/2_u$	7.65				
$5/2_u$	7.90				
$1/2_u$	9.81				
$3/2_u$	10.81				

spinors. This allowed us to employ accurate single-reference approaches such as CCSD(T) to determine the optimal Pu−O bond length, which is equals to 1.808 Å after extrapolation, with a corresponding harmonic vibrational frequency of 793 cm^{-1}. We note that the CBS-$^2DC^M$-CCSD(T) Pu−O bond length is longer than the one predicted by La Macchia et al. [192] at the SO-CASPT2 level.

Furthermore, our $^2DC^M$-EOM-EE-CCSD calculations (see Table 4.13) confirm that, at the CBS-$^2DC^M$-CCSD(T) equilibrium structure, the $\Omega = 0_g$ state is indeed the ground-state: it is sufficiently well-separated from the lowest-lying states of both g ($\Omega = 1_g$, by over 2000 wavenumbers) and u ($\Omega = 1_u$, by over 5000 wavenumbers), and considering a shorter bond length–namely

TABLE 4.15: Lowest electronic levels in cm^{-1} of PuO_2, computed at the SF-CASPT2 and SO-CASPT2 levels (d(Pu-O)= 1.808 Å) with the ANO-RCC-TZVP basis set, and analysis of the various states.

	State	ΔE	Character : % [orbital(number of electron)]
SF	$^5\Sigma_g^+$	0	84% [$1a_u/\delta_u(1)$, $2b_{2u}/\Phi_u(1)$, $2b_{1u}/\delta_u(1)$, $2b_{3u}/\Phi_u(1)$]
	$^5\Sigma_g$	4798	45% [$1a_u/\delta_u(1)$, $3b_{2u}/\pi_u(1)$, $2b_{1u}/\delta_u(1)$, $2b_{3u}/\Phi_u(1)$]
			45% [$1a_u/\delta_u(1)$, $2b_{2u}/\Phi_u(1)$, $2b_{1u}/\delta_u3(1)$, $3b_{3u}/\pi_u(1)$]
	$^5\Phi_{u(1)}$ ($^5B_{3u}(1)$)	5421	85% [$3a_g(1)$, $1a_u/\delta_u(1)$, $2b_{1u}/\delta_u(1)$, $2b_{3u}/\Phi_u(1)$]
	$^5\Phi_{u(2)}$ ($^5B_{2u}(1)$)	5421	85% [$3a_g(1)$, $1a_u/\delta_u(1)$, $2b_{1u}/\delta_u(1)$, $2b_{3u}/\Phi_u(1)$]
	$^5\Delta_{u(1)}$ ($^5A_u(1)$)	7452	79% [$3a_g(1)$, $2b_{2u}/\Phi_u(1)$, $2b_{1u}/\delta_u(1)$, $2b_{3u}/\Phi_u(1)$]
	$^5\Delta_{u(2)}$ ($^5B_{1u}(1)$)	7462	80% [$3a_g(1)$, $1a_u/\delta_u(1)$, $2b_{2u}/\Phi_u0(1)$, $2b_{3u}/\Phi_u(1)$]
	$^3\Sigma_g^-$	10 308	24% [$1a_u/\delta_u(1)$, $2b_{2u}/\Phi_u(2)$, $2b_{1u}/\delta_u(1)$]
			24% [$1a_u/\delta_u(1)$, $2b_{1u}/\delta_u(1)$, $2b_{3u}/\Phi_u(2)$]
			19% [$2b_{2u}/\Phi_u(1)$, $2b_{1u}/\delta_u(2)$, $2b_{3u}/\Phi_u(1)$]
			16% [$1a_u/\delta_u(1)$, $2b_{2u}/\Phi_u(1)$, $2b_{3u}/\Phi_u(1)$]
SO	0_g^-	0	48% $^5\Sigma_g^+$, 22% $^3\Sigma_g^-$
	1_g	2462	67% $^5\Sigma_g^+$, 15% $^3\Sigma_g^-$
	1_u	5851	27% $^5\Phi_{u(1)}$, 27% 21% $^5\Phi_{u(2)}$, 13% $^5\Delta_{u(1)}$, 13% $^5\Delta_{u(2)}$
	2_g	5904	85% $^5\Sigma_g^+$
	2_u	6265	21% $^5\Phi_{u(1)}$, 21% $^5\Phi_{u(2)}$, 24% $^5\Delta_{u(1)}$
	3_u	7195	38.85% $^5\Phi_{u(1)}$, 24.97% $^5\Phi_{u(2)}$

1.744 Å, as was proposed by La Macchia et al. [192] for the ground state from SO-CASPT2–does not alter this picture. Thus, our results differ qualitatively from La Macchia et al., since they suggest the PuO_2 ground-state is of $\Omega = 1_u$ symmetry, and corresponding mainly to the occupation of the two $5f_\delta$, one $5f_\phi$ and the 7s orbitals (See Figure 4.6).

From Table 4.13, we observe significant variations for the u states (of nearly 3000 wavenumbers) when the internuclear distance is varied from 1.808 Å to 1.744 Å, while the g states remain more or less at the same energies. With this, at the longer distance, the $\Omega = 2_g$ state becomes lower than the $\Omega = 1_u$ one.

- PuO_2 Electronic Structure

The SO-CASPT2 transition energies computed at the $^2DC^M$ optimal bond length are reported in Table 4.15 (the higher excited states can be found in

the Appendix B). The spin-orbit 0_g ground state is composed by the spin-free ground state $^5\Sigma_g^+(1)$ up to 48% and by the $^3\Sigma_g(1)$ up to 22%, which lies 10.308 cm above it. La Macchia *et al.* also found large SO effects this with a SO-value of 8548 cm^{-1}. Note that the vertical transition energies computed at the SO-CASPT2 level are in very good agreement with the $^2DC^M$ ones for the g-states, but the u-states come out about 2300 cm^{-1} lower in energy at the SO-CASPT2 than at the $^2DC^M$-EOM-CCSD level. However, we note that the electronic state spacing within either the g or u symmetries agrees with the SO-CASPT2 calculations. This thus points out to the importance of the choice of the active space to accurately predict the relative energies of g states involving mostly non-bonding 5f Pu atomic-centered orbitals, versus the u states involving the more diffuse plutonium 7s orbital.

Finally, for the computed ionization energies for PuO_2 (IPs, see Table 4.14), our calculations could be grouped into three regions with respect to their energies: one below 8 eV, one between 8 and 10 eV and the last at energies higher than 10 eV. We see that, if one considers only the lowest EOM-IP-CCSD state ($\Omega = 3/2_u$), we observe a good agreement with the results of Rauh et al. [193] (and to a lesser extent, with the results of Capone et al. [194]) but poor agreement with a second measurement of Capone et al. [196] and of Santos et al. [195]. However, if we compare the first $\Omega = 1/2_u$ state to this second measurement of Capone, and the second $\Omega = 3/2_u$ state with that of Santos et al. [195], we see an overall good agreement between the calculated and experimental values. This leads us to suggest that experiments may have measured PuO_2^+ in different electronically excited states, something that would explain the rather different experimental values.

- Spin-free calculations

Beside calculations including spin-orbit coupling, it is informative to discuss the nature of PuO_2 ground-state at the scalar relativistic level (spin free). In our study, CASPT2 and UCCSD(T) calculations give the $^5\Sigma_g$ state ($(5f_\delta)^2(5f_\phi)^2$ occupations) lower in energy than the $^5\Phi_u$ state ($(5f_\delta)^2(5f_\phi)^1(7s)^1$) by 7994 cm^{-1} at the distance Pu-O of 1.804 Å, as found in the previous studies [174, 192]. With the ANO-RCC AVTZ basis set, the equilibrium Pu−O distance is 1.818 Å and 1.808 Å at UCCSD(T) and CASPT2 levels, respectively, distances that are close to the fully-relativistic ones. These values are also in line with the SF-CASPT2 (CAS(12,14)) of La Macchia (d(Pu-O))= 1.792 Å),

but significantly shorter by about 0.4/0.5 Å than the estimations Archibong and Ray [174]. These large discrepancies are probably related to the choice of a large-core RECP (78 electrons), which was proven to yield too long bond distances for actinide molecules [197], while the small-core ECP gives exactly the same distances that the all-electron Douglas-Kroll relativistic approach.

The ground state $^5\Sigma_g^+(1)$ is dominated up to 84% by the configuration that corresponds to the occupation of the two $5f_\delta$ and two $5f_\Phi$ orbitals carrying one electron each. It corresponds to the description of the ground state of Boguslawski *et al* [147]. and also to the $^5\Sigma_g^+(1)$ reported by La Macchia et al. [192]. The former study places the first excited state at 1800 cm^{-1} corresponding to $^5\Phi_u$ state, while in our SO-CASPT2 it appears at higher energy, of 5421 cm^{-1}. We note that in our SF-CASPT2 calculation, the spin-free spectrum is less dense than La Macchia's results [192]. Such differences can be explained by the choice of different active space, the fact that we computed a larger number of spin-free states, and most likely the change in the interatomic Pu−O distance. SO-coupling is not expected to change the energy of the $\Lambda = 0$ $^5\Sigma_g^+$ state, while it lifts the degeneracy of the $^5\Phi_u$ state. Given the small energy gap of 1800 cm^{-1} between the $^5\Sigma_g^+$ and $^5\Phi_u$ state, the 1_u state becomes the ground state in their study, while in our work, it remains a state of g symmetry.

TABLE 4.17: Standard enthalpies of formation $\Delta_f H^\circ$ of PuO_2, $PuO_2(OH)_2$, PuO_3 in kJ mol^{-1} in the gas phase calculated at various level of theory and extrapolated to the CBS-CE limit, and from the average of five reactions listed in Table 4.3, except for $^2DC^M$-CCSD(T). The standard deviations $\Delta\Delta_f H^\circ$ includes the uncertainty on the average value as well as the experimental error bars.

$\Delta_f H^\circ$	PuO_2	$PuO_2(OH)_2$	PuO_3
UCCSD + ΔE_{SO}	-348.4 ± 28.2		
UCCSD(T) + ΔE_{SO}	-404.3 ± 22.6	-518.8 ± 32.9	+599.1 ± 28.3
CASPT2 + ΔE_{SO}	-364.4 ±17.8	-1008.7 ± 34.3	-539.8 ± 24.1
Reference	-410 ± 20 [198] ; -412 ± 20 [139] ; -440± 7 [138]; -428.7 ± 7[138]; -428.7 ± 20 [141];	-1018.2 ±3.3[199]	-562.8 ±5[199] ; -567.6 ± 15 [141]

4.4.2 Thermodynamic properties

TABLE 4.16: Standard enthalpies of formation $\Delta_f H^\circ$ of PuO_2, $PuO_2(OH)_2$, PuO_3 in kJ mol^{-1} in the gas phase calculated at various level of theory and extrapolated to the CBS-TE limit, and from the average of five reactions listed in Table 4.3, except for $^2DC^M$-CCSD(T). The standard deviations $\Delta\Delta_f H^\circ$ includes the uncertainty on the average value as well as the experimental error bars.

$\Delta_f H^\circ$	PuO_2	$PuO_2(OH)_2$	PuO_3
ΔE_{SO} [1]	34.4	46.9	59.0
B3LYP[1] + ΔE_{SO}	-304.1 ± 16.4	-787.0 ± 30.1	-397.3 ± 21.6
$^2DC^M$-CCSD(T)	-432		
UCCSD + ΔE_{SO}	-347.6± 21.1		
UCCSD(T) + ΔE_{SO}	-406.6 ± 9.3	-260.9 ± 26.9	+438.0 ± 8.5
CASPT2 + ΔE_{SO}	-367.3±17.1	-1009.3 ± 44.5	-545.0 ± 23.3
Reference	-410 ± 20 [198] ; -412 ± 20 [139] ; -440± 7 [138]; -428.7 ± 7[138]; -428.7 ± 20 [141];	-1018.2 ±3.3[199]	-562.8 ±5[199] ; -567.6 ± 15 [141]

[1] ΔE_{SO} is estimation of the SO contribution.

All the values of enthalpy of formation can be found in the Table 4.16. From

our discussion of the electronic structures of the different Pu molecules detailed in section 4.4.1, one will not be surprised to see that the single-reference methods, here DFT and CCSD(T), fail at describing $PuO_2(OH)_2$ and PuO_3 thermodynamic properties, while they should be in principle usable for PuO_2 molecule. Thus, for this methods, we will focus only on the PuO_2 molecule. One can observe that the enthalpy obtained with the B3LYP functional and the $+\Delta E_{SO}$ correction gives a value about 25% off the experimental one (100 kJ mol^{-1}). A change in the density functional will not ensure a better agreement with experience as observed previously for actinide systems [200] or for transition metal molecules [201]. The $\Delta_f H^{\ominus}$(298.15 K) computed with ^{2}DC^M approach (^{2}DC^M) is in almost perfect agreement with the available results [138, 141]. Note that the absence of error value is because the calculation was done only for the reaction R_4, as the other reactions involved species with a multi-determinantal character. UCCSD+ΔE_{SO} result (-385.0$\pm$21.1kJ mol^{-1}) is lower than ^{2}DC^M-CCSD(T) one, while the UCCSD(T)+ΔE_{SO} agrees with the best theoretical estimations and the experimental data, thus highlighting the importance of the perturbative triple contributions. For the reaction 4, UCCSD(T) + ΔE_{SO} and CASPT2 + ΔE_{SO} give -416.22 kJ mol^{-1} and -387.7 kJ mol^{-1}, respectively. The SO-CASPT2 value deviates by about 40 kJ mol^{-1} from both ^{2}DC^M-CCSD(T) and experiments, probably because of the incompleteness of the active space. Nevertheless, the SO-CASPT2 results for $PuO_2(OH)_2$ and PuO_3 show great agreement with the experiment values by Krikorian et al. [199].

4.5 Conclusion and Perspectives

Concerning PuO_2, where the static correlation is not important and the wave function can be described by single-reference methods that include the dynamic correlation such as UCCSD(T) the $\Delta_f H^{\ominus}$ could be reproduced. The distance Pu-O found for the linear PuO_2 is 1.808 Å and the ground state a 0_g mainly composed by the spin-free state ^5A_g.

About $PuO_2(OH)_2$, SO-CASPT2 method is enough to reproduce the only experimental data available but the enthalpy of formation given by this method for PuO_3 is smaller than expected. Since the detection of PuO_3 is complicated one could argue on the validity of the two measurements but we would

rather point out the fact that our active space size might not be large enough and could lead to a mistreatment of the static correlation. In order to improve the description, larger active spaces can be handled with the DMRG method recently implemented in Molcas. Exploratory DMRG calculations will be performed in coming weeks.

Our thermodynamics data are about to be implemented by our IRSN colleagues (F. Virot) in the accident simulation code to quantify the amounts of each volatile Pu species released.

Chapter 5

How well are the f-elements described by a Double-Hybrid Functional ?

Contents

Our interest here is to see how double hybrids work for the geometries and thermochemistry of species containing actinides and lanthanides. This project was triggered by two reasons: the first is that we have seen that the B3LYP is not accurate to compute the thermochemistry of PuO_2, thus raising the question of whether other functionals and double hybrids in particular could be more accurate for such f-element complexes. The second, because we are involved in the implementation and benchmarking of double-hybrids four-component-based methods in Dirac in a collaboration with Benjamin Helmich-Paris (Mulheim) and Lucas Visscher (Amsterdam); therefore, we want to investigate if there are significant changes between spin-free (Molpro) and SOC (Dirac) calculations. This chapter presents the first step of the study. It consists in a systematic comparison of structural and thermodynamic properties computed at the spin-free level with the state of the art CCSD(T) method as reference. This is, to the best of our knowledge, the first application of double-hybrid B2-BLYP to actinide chemistry. However, we can refer to recent assessments of double hybrid, in particular B2-PLYP for transition metal thermochemistry [202, 203], leading to average uncertainties of up to 8 kcal.mol^{-1}, which is about 4 kcal.mol^{-1} better than B3LYP. After a brief description of the current development of double-hybrids and the B2-PLYP functional and a review of the available thermodynamic data, we will reach the aim of this chapter and present the first results regarding the f element properties.

5.1 Motivations for double-hybrid functionals

One of the biggest weakness of DFT is not accounting for the dispersion effects as we have seen in the Section 2.3.4. A widely used solution is the

Grimme dispersion correction [49–51] which we have used in the Chapter 3. We have seen that even if it lead to good qualitative results, this correction could not be used as quantitative method for such a large system. When the system has a reasonable size, MP2 is a good but expensive solution to include dispersion effects.

The idea of double-hybrids (B2-PLYP) [204] is to add non-locality responsible for dispersive (van der Waals) interactions to hybrid functionals by considering virtuals orbitals and having a well-balanced performance for properties (energetics, etc). It relies on a combination of KS-DFT (Kohn Sham Density Functional Theory) and Perturbation Theory (PT) where the exchange-correlation energy is expressed as:

$$E_{xc} = (1 - a_x)E_x^{GGA} + a_x E_x^{HF} + bE_c^{GGA} + cE_c^{PT2} \tag{5.1}$$

where

$$E_c^{PT2} = \frac{1}{4}\sum_{ia}\sum_{jb}\frac{[(ia|jb) - (ib|ja)]^2}{\epsilon_i + \epsilon_j - \epsilon_a - \epsilon_b} \tag{5.2}$$

with ϵ_i being the KS eigenvalue of the orbital i, the bracket terms corresponding to the two electrons integrals over the KS orbitals. The parameters a_x, b and c were parametrised to reproduce thermodynamic properties of light elements namely the G2/97 set of heat of formation. During this parametrisation, the relation $b + c = 1$ was found and confirmed [205] and $c \leq a_x$, leading to only two parameters with a value of 0.53 and 0.27 for a_x and c, respectively. The GGA functional used is the BLYP one. Multiple rigorous analysis were done concerning the parametrisation [205–207] and showing that the value of a_x and c are very close to a theoretical optimum.

Even if it is not used in this thesis we can note that it is also possible to perform TDDFT with double hybrid [208, 209] or to add long-range dispersion [210].

During the past 10 years the development of many other double-hybrid functionals was done [207, 211–233] and listed and compared in a review of Grimme *et al* [234]. This work exposes the functional DSD-BLYP-D3 [221] and PWPB95-D3 [203] as the most accurate and robust ones though we have not evaluated them in this thesis.

Most specific performances are also tested such as: spin-state energetics [235], ionisation energies and aqueous redox potentials of organic molecules [236], non-linear optical properties [237] and thermochemistry of 3d transition metals [202]. This last study is particularly interesting since it states that the Mean Average Deviation (MAD) of B2-PLYP is 32.6 kJ.mol^{-1} for the determination of enthalpies of formation. Since the DIRAC implementation concerns only the B2-PLYP functional, it will be compared to HF, CCSD(T), B3LYP hybrid functional, PBE GGA functional and the limiting cases of B2-PLYP, MP2 and BLYP functional.

5.2 Literature review of the available enthalpies of formation $\Delta_r H^{\ominus}$.

The enthalpies of formation theoretical and experimental of the reactions listed in the Table 5.1 are only reported for reaction including UF_6. The enthalpies are extracted from the work of Peterson *et al.* and [184] Privalov *et al*. The former study includes four-component CCSD(T) calculations with a pseudopotential (PP) [179] or all electron basis sets [238]. The latter one includes SCF, MP2, B3LYP and CCSD(T) single point energy using geometries obtained at the HF level with a scalar relativistic pseudopotential or experimental data.

All the reactions were chosen for the fact that they involve close shell species and because the information about the structures are readily accessible.

TABLE 5.1: Reactions used to calculate $\Delta_r H^\ominus$ and their previously reported values.

Reactions	$\Delta_r H^\ominus$ in kJ.mol^{-1}
R_1: $H_2 + F_2 \longrightarrow 2\,HF$	
R_2: $La^{3+} + H_2O \longrightarrow LaH_2O^{3+}$	
R_3: $CeF_4 + CeO_2 \longrightarrow 2\,CeOF_2$	
R_4: $ThF_4 + ThO_2 \longrightarrow 2\,ThOF_2$	
R_5: $UO_2^{2+} + H_2O \longrightarrow UO_2(H_2O)^{2+}$	
R_6: $Ac^{3+} + H_2O \longrightarrow AcH_2O^{3+}$	
R_7: $UF_6 + SO_3 \longrightarrow UO_3 + SF_6$	4C-CCSD(T): 525.5 [1], 527.2 [2] [184] Exp: 528.9 [184]
R_8: $UF_6 + 3\,H_2O \longrightarrow UO_3 + 6\,HF$	4C-CCSD(T): 481.6 [1], 479.9 [2] [184] SCF: 539 ; MP2: 487, 534[*]; CCSD(T): 558, 464[*] [239] B3LYP: 627, 500 [*]; Exp: 435 [239]
R_9: $UF_6 + H_2O \longrightarrow UOF_4 + {}_2HF$	
R_{10}: $UF_6 + 2\,H_2O \longrightarrow UO_2F_2 + {}_4HF$	4C-CCSD(T): 204.2[1], 202.1 [2] [184] SCF: 170; MP2: 232, 263 [*]; CCSD(T): 232, 263 [*] [239] B3LYP: 332, 246[*]; Exp: 187 [239]
R_{11}: $UO_2^{2+} + 4\,H_2O \longrightarrow UO_2(H_2O)_4^{2+}$	
R_{12}: $PaO_2^{+} + H_2O \longrightarrow PaO_2(H_2O)^{+}$	

[1] Values FC-CCSD(T)/CBS with pseudo potential.
[2] Values FC-CCSD(T)/CBS with the all electron basis sets.
[*] Corrected values

We aim to reproduce results as close as possible to the experimental ones or to the corresponding method in use.

Concerning the geometries of the molecules, when possible it will be compared to experimental data, otherwise the quantum chemical method used to determined them will be specified.

5.3 Computational details

As in the previous Chapters, the geometry of the molecules under interest is a key information for the description of thermodynamic properties. Therefore the different molecules were first optimised for each of the quantum chemistry methods at the spin-free level with the Molpro2015.1 package [156], followed by an harmonic frequency calculation. The reaction enthalpies are computed as in Chapter 4 in equation 4.3:

$$\Delta_r H^{\circ} = \sum_i (E_i + ZPE_i + H_{corr,i}) \tag{5.3}$$

The light elements (first and second rows) are described with aug-cc-pVQZ basis sets [cite], for actinides the scalar relativistic effects were included with the relativistic pseudopotential with 60 e- in core, namely ECP60MDF [cite] with the corresponding quadruple-ζ quality basis sets[cite]. For lanthanides,the small-core relativistic pseudo potential with 28 e - in core, namely ECP28WB, [171, 240] and the corresponding quadruple-ζ basis sets were used. Peterson *et al.* [184] reportes that quadruple-ζ basis sets used are close enough from the CBS for us to overcome the need of CBS extrapolations. Since all the molecules involved in the reactions under study (see Table 5.1) are closed-shell, no spin state problem should appear and spin-orbit coupling is expected to be negligible [184].

In most of the reactions the bonding picture changes a lot from the reactants to the products resulting in large differences of dynamical correlation across the reactions making it then relevant for benchmarking correlation methods. A particular attention will be paid to the R_1 since its enthalpy of reaction is computationally challenging because as mentioned in the reference [239], Privalov *et al.* could not reproduce it.

5.4 Results and Discusions

The optimisations of $UO_2(H_2O)_4^{2+}$ are still in progress, thus, the results of the reaction R_{11} will not be reported. Table 5.2 presents the reported geometries of molecules with an f-element with the corresponding reference data.

5.4.1 Geometries and total energies

TABLE 5.2: Geometries of the various molecules under study, the distance are given in Å and angles in degree symmetry is given in parenthesis.

Molecule		CCSD(T)	MP2	B2PLYP	B3LYP	BLYP	PBE	HF	Literature
ThF_4 (Td)	r(Th-F)	2.112	2.113	2.116	2.117	2.132	2.113	2.116	Exp: 2.124 [241]
	angle(F-Th-F)	109.5	109.5	109.5	109.5	109.4	109.4	109.5	107.2
$ThOF_2$ (Cs)	r(Th-O)	1.890	1.896	1.895	1.888	1.906	1.890	1.870	Exp: 1.886 [242]
	r(Th-F)	2.138	2.136	2.139	2.141	2.152	2.130	2.154	Exp: 2.157
	angle(F-Th-F)	106.9	120.6	106.0	106.1	104.8	103.8	110.6	107
	angle(F-Th-O)	106.9	120.6	106.0	106.1	104.8	103.8	110.6	
ThO_2 (C_{2v})	r(Th-O)	1.907	1.912	1.913	1.905	1.923	1.906	1.891	CCSD(T): 1.905 [243]
	angle(O-Th-O)	117.0	114.4	117.8	119.9	119.0	119.2	120.4	117
UF_6 (O_h)	r(U-F)	2.000	1.999	2.016	2.014	2.041	2.022	1.984	Exp: 1.999 [244]
UO_3 (C_{2v})	r(U-O_{apical})	1.8	1.865 [1]	1.871[1]	1.81162	1.880	1.863	1.747	4C-CCSD(T): 1.801[184]
	r(U-O)	1.9	1.865[1]	1.871[1]	1.852977	1.854	1.829	1.828	1.852
	angle(O_{apical}-U-O)	99.4	119.9[1]	120[1]	101.4286	106.5	103.1	97.7	99.5
UO_2F_2 (C_{2v})	r(U-O)	1.769	1.788	1.798	1.788	1.816	1.816	1.713	4C-CCSD(T): 1.768 [184]
	r(U-F)	2.076	2.073	2.077	2.073	2.093	2.093	2.092	2.075
	angle(O-U-O)	169.1	169.5	166.4	169.5	163.9	163.9	170.2	169.2
	angle(F-U-F)	114.0	112.8	111.7	112.8	118.6	118.6	118.9	114.1
$UO_2H_2O^2+$ (Cs)	r(U-O)	1.713	1.732	1.734	1.716	1.748	1.733	1.660	CCSD(T): 1.789 [243]
	r(U-OH_2)	2.324	2.317	2.325	2.330	2.343	2.314	2.373	2.453
	angle(O-U-O)	89.8	88.8	89.5	90.1	90.1	89.4	90.7	90.0
LaF_3 (C_{3v})	r(La-F)	2.120	2.120	2.123	2.123	2.134	2.112	2.138	Exp: 2.12 [245]
	angle(F-La-F)	116.2	115.9	115.8	115.8	115.1	114.3	119.5	
CeO_2 (C_{2v})	r(Ce-O)	1.821	1.822	1.819	1.835	1.850	1.829	1.790	HF: 1.82 [246]
	angle(O-Ce-O)	121.8	115.4	128.4	139.1	132.6	132.9	116.6	132
CeF_4 (Td)	r(Ce-F)	2.028	2.026	2.036	2.042	2.070	2.049	2.031	CISD: 2.04 [247]
$CeOF_2$ (C_s)	r(Ce-O)	1.786	1.787	1.804	1.791	1.832	1.811	1.748	B3LYP: 1.794 [248]
	r(Ce-F)	2.082	2.078	2.087	2.090	2.109	2.086	2.098	2.091
	angle(F-Ce-F)	110.5	110.7	109.0	109.6	109.2	108.3	114.9	110.5
AcF_3 (C_{3v})	r(Ac-F)	2.195	2.195	2.197	2.197	2.209	2.186	2.210	MP2: 2.272 [249]
	angle(F-Ac-F)	113.4	113.3	113.0	112.7	111.6	110.9	116.7	
PaO_2^+ ($D_{\infty h}$)	r(Pa-O)	1.773	1.794	1.784	1.775	1.799	1.784	1.738	CCSD(T): 1.776 [243]
$PaO_2H_2O^+$ ($D_{\infty h}$)	r(Pa-O)	1.789	1.799	1.801	1.791	1.816	1.800	1.754	CCSD(T): 1.788 [243]
	r(Pa-OH_2)	2.449	2.441	2.455	2.465	2.475	2.442	2.511	2.447
	angle(O-Pa-OH_2)	88.7	88.7	89.1	89.6	88.5	88.8	90.6	98.5

[1] The symmetry is D_{3h}

Looking at Table 5.2 the B2-PLYP presents good performances at reproducing the literature data. This is highligted in Figures 5.1 and 5.2 presenting the bond length and angular deviation with respect to CCSD(T). Unfortunately, B2-PLYP and MP2 predict the wrong symmetry for UO_3 giving it as a D_{3h} symmetry for the molecule instead the expected C_{2v}.

Concerning the distances, it is the functional B3LYP that is the closest to CCSD(T) with a MAD of 0.006 Å followed by MP2 with 0.012 Å. B2-PLYP functional arrives third with an average error of 0.014 Å. However, while UO_3 is taken out of the set, the MAD of MP2 and B2-PLYP are reduced to 0.007 Å and 0.008 Å, respectively.

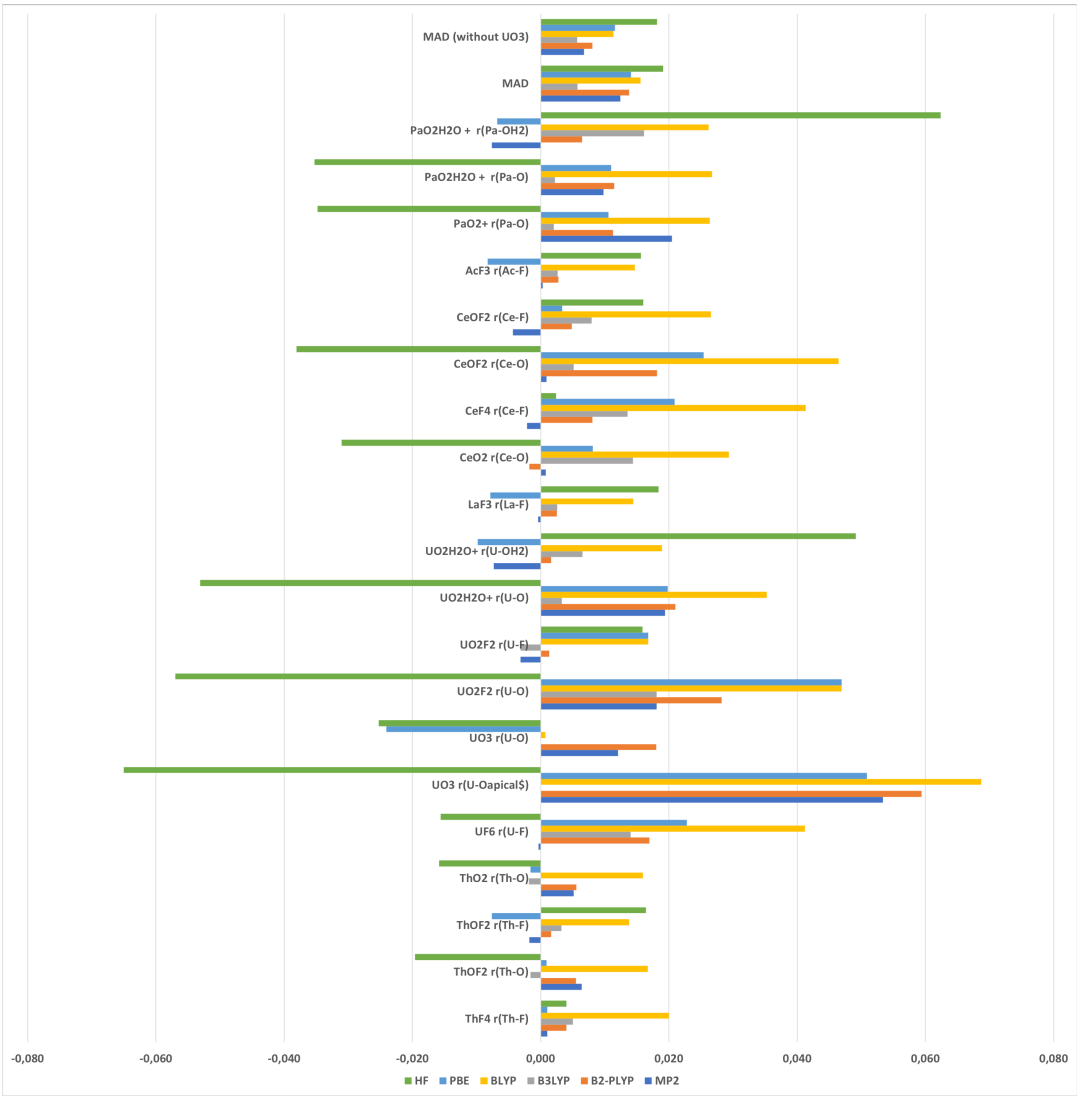

FIGURE 5.1: Error in the bond length in Å with respect to CCSD(T) values and MAD over all complexes

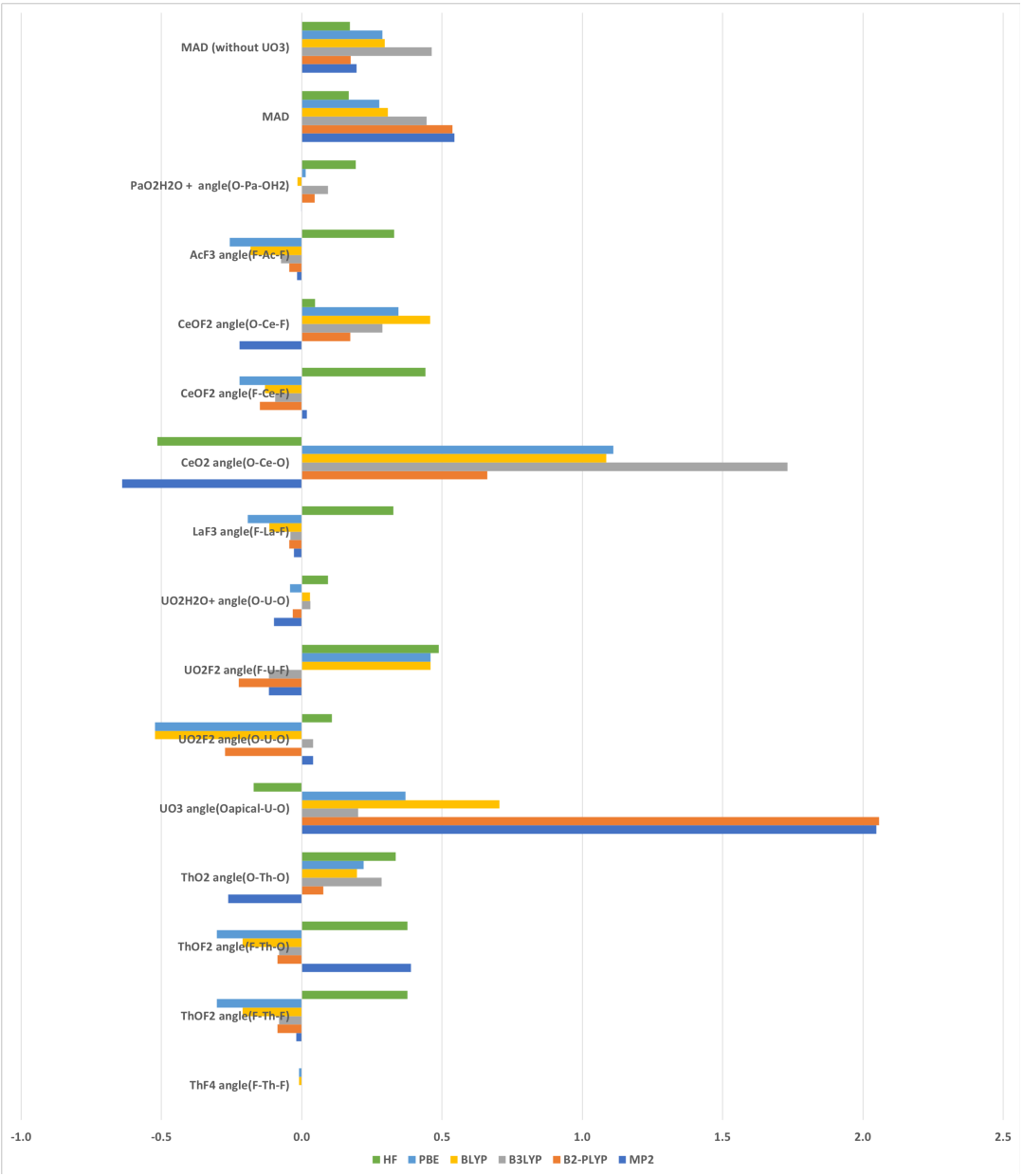

FIGURE 5.2: Differences in the angles (in degrees) with respect to CCSD(T) and the MAD over all complexes

For the intramolecular angles, MP2 and B2-PLYP perform the worst with a MAD of 5.4 due to the bad description of UO_3. While this molecule is taken off the set the MAD of B2-PLYP is the best with 1.7 degrees and MP2 the second best value with MADs of 2.0 degrees. Explanations about the failure of MP2 and B2-PLYP to describe UO_3 are still under investigation.

This small B2-PLYP MAD makes use confident about its capability in giving very accurate geometries while MP2 is performing well.

In Table 5.3, we reported the difference in total energies. One can note that the behaviour of each method/functional depends on the actinide/lanthanide present. Nonetheless, in every cases containing an heavy atom, the B2-PLYP is the closest to CCSD(T) after MP2. MP2 underestimates the total energies while all other methods overestimate it. So far, the smallest MAD is obtained with B2-PLYP attesting its good performance.

5.4.2 Enthalpies of Reactions

As mentioned previously, only scarce experimental values of reaction enthalpies are available for f elements. The only ones to benchmark with are those studying reactions R7, R8, R10 and R12. Thus, we will start the discussion by scrutinize the results obtained for these four reactions. For the reactions R_8 and R_{10} we could see that computed reaction enthalpies were far from the experimental values (see Table 5.3) . This was already noticed in [184] by Peterson *et al.*, thus we decided to correct the results in the same way they did. Peterson *et al.* attributed the error to the description of HF, and because of that they took the difference between the experimental value and theirs for reaction R_{10}. This difference was then divided by 4 (the number of HF molecules in reaction R_{10}) to obtain the correction factor for each HF molecule. This correction was then apply to each reaction involving HF.

Table 5.3 presents the enthalpies of reaction of the chosen reactions. The results obtained on reactions R_8 and R_{10} validate our correction since in reaction R_8 we are closer to the experimental enthalpy of reaction. Figure 5.3 exposes the differences in between the enthalpies of reactions with respect to

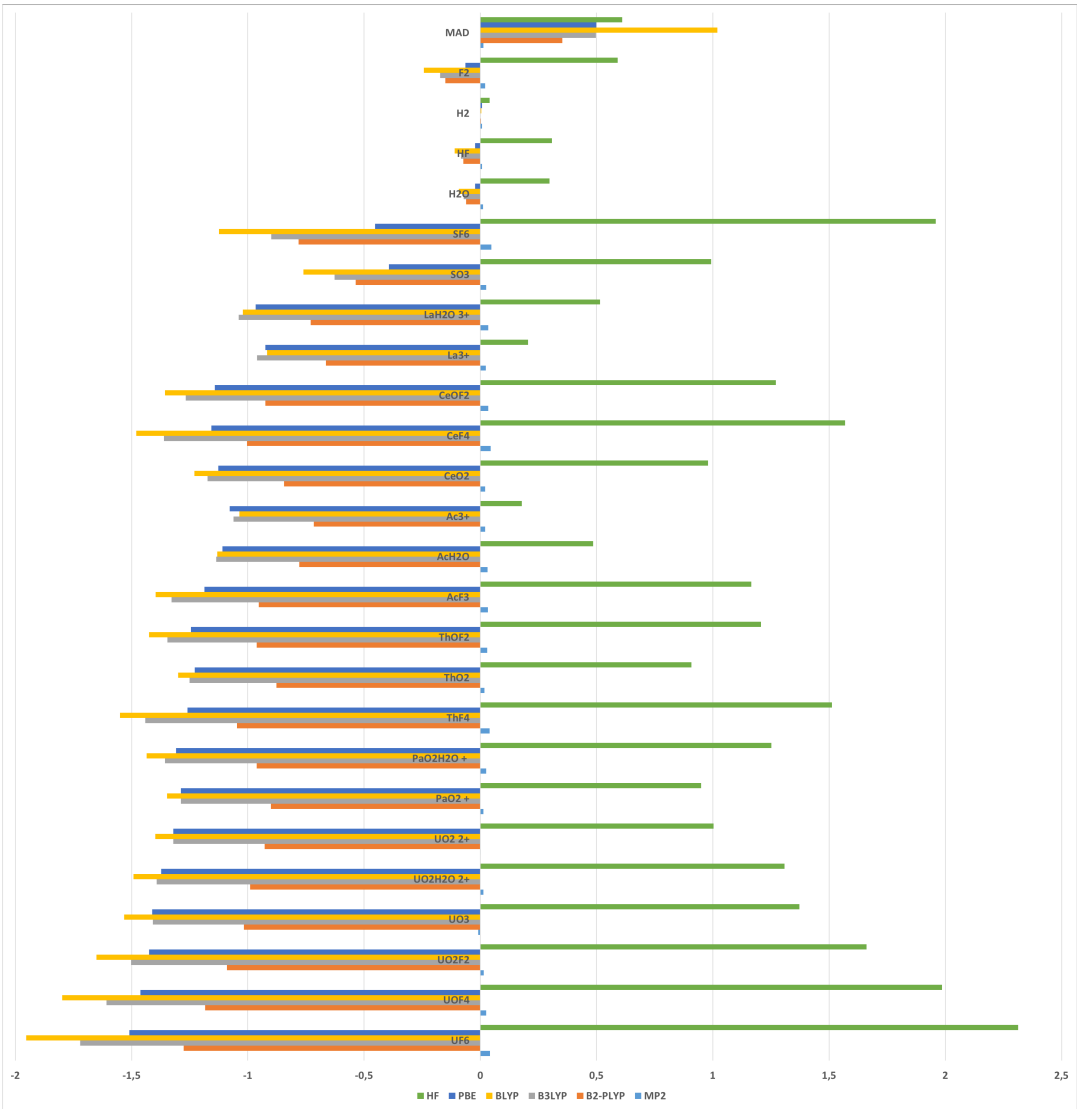

FIGURE 5.3: Difference in energy between the total energy given by the CCSD(T) and the considered method and functionals in a.u.

TABLE 5.3: $\Delta_r H^\circ$ in kJ.mol^{-1} for the reaction under study.

	CCSD(T)	MP2	B2-PLYP	B3LYP	BLYP	PBE	HF	Exp
R_1	-547.3	-612.6	-578.1	-563.5	-533.0	-544.5	-617.7	
R_2	-381.0	-383.4	-391.7	-401.0	-413.7	-428.5	-345.8	
R_3	-146.0	-136.1	-147.6	-148.0	-162.2	-143.8	-164.5	
R_4	13.3	16.4	13.6	11.0	11.2	11.4	2.8	
R_5	-275.9	-276.8	-276.8	-278.3	-280.5	-356.1	-250.2	
R_6	-338.2	-340.4	-344.6	-347.1	-348.9	-360.9	-310.4	
R_7	539.2	457.1	570.2	643.6	686.7	635.2	604.6	539.3
R_8	468.7	356.0	472.2	545.0	553.2	553.2	527.9	
$R_{8,corrected}$	456.9	424.9	401.6	420.2	553.2	377.9	550.8	435
R_9	43.7	56.4	110.3	140.3	158.6	160.4	75.5	
$R_{9,corrected}$	39.8	79.4	86.8	98.7	99.1	102.0	83.2	
R_{10}	194.9	141.1	234.1	270.2	306.1	303.8	171.7	
$R_{10,corrected}$	187.0	187.0	187.0	187.0	187.0	187.0	187.0	187
R_{12}	-152.4	-155.6	-151.3	-146.8	-117.6	-149.7	-132.8	

CCSD(T) values. So far the smallest MAD is HF's with 27.8 kJ.mol^{-1}. The second lowest MAD is the one is given by the B2-PLYP functional (with 28.4 kJ.mol^{-1}). All the other MADs are above 35 kJ.mol^{-1}.

5.5 Conclusion and Perspectives

Even if we can observe in B2-PLYP some imperfection of MP2, such as the inaccuracies in the description of the geometry of UO_3, it still yields to good results in the description of the geometry. The thermodynamic properties of f-element are even better describe with B2-PLYP than MP2, which is what was desired. The MAD reported for B2-PLYP (28.4 kJ.mol^{-1}) is smaller than the one found in the study of Wilson *et al.* on transition metals (32.6 kJ.mol^{-1}). All of this, demonstrate that this double hybrid is suitable to answer this kind of problems. The follow-up of the current work will be to use the double-hybrid implementation in DIRAC program to assess the importance of SOC to our results.

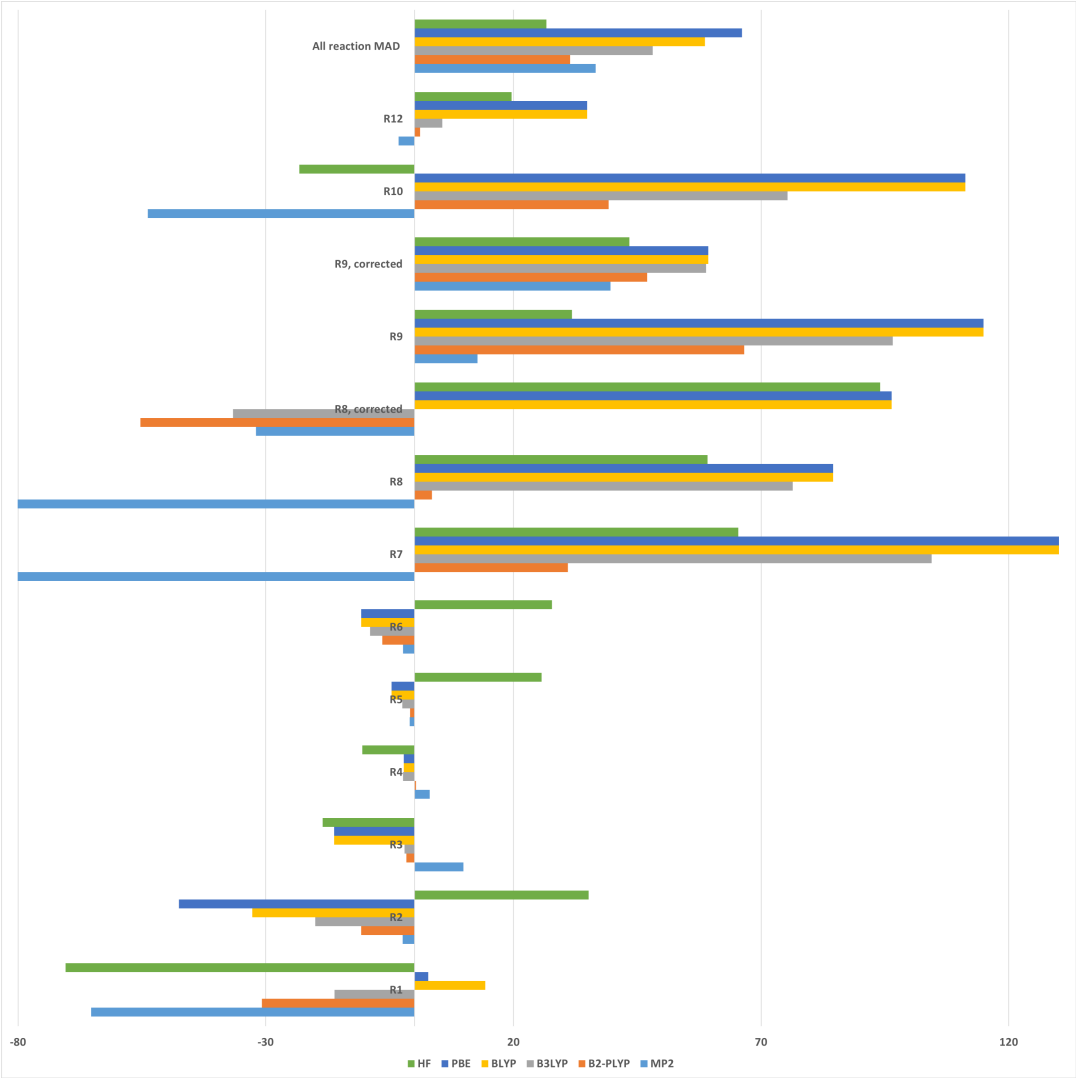

FIGURE 5.4: Differences in the enthalpies of reaction with respect to CCSD(T) values in kJ.mol^{-1}

Chapter 6

Conclusions and perspectives

With respect to the quantum chemical methods used in this thesis to study actinides several conclusions need to be drawn. First, for closed-shell systems or for systems with a dominant single reference character, DFT with hybrid methods, such as semi-empirical dispersion corrections or double hybrid functional, performs well. For large systems it is cheap and efficient. With B2-PLYP, enough correlation can be included to describe properly closed-shell systems. Nonetheless, DFT is still failing for multireference systems. For this type of systems, we chose the CAS method. This method is neither black-box nor cheap. The choice of active space can be tedious and we have seen that in cases, where very accurate results are wanted, this method may fail because of the limited size of active space and probably a lack of accurate dynamic electron correlation treatment.

To the question raised in the introduction about the efficiency of the available tools to describe the structure, the bonding and the thermodynamics of actinide systems, we can not give a simple answer.

First, concerning the geometries, the three studies showed that the structures of actinides and f-elements systems can have their geometries reproduced or unravelled. We have seen that the X-ray structures were well reproduced for the catalysts in Chapter 3 as well as structural experimental values in Chapter 5 with the double-hybrid (B2-BLYP) functional, proving its capability, in most cases, at being as accurate as other quantum chemistry methods but also being predictive. It is worth noticing the failure of the DFT at converging to the expected triplet state for the uranium complexes in Chapter 3. In Chapter 5, only UO_3 structure turned out to be problematic both at MP2 and

B2-PLYP levels; and the explanations of this failure are expected soon. Finally, for PuO_2, in Chapter 4 we reported a bond length and a ground state different from what was reported before at spin-orbit level [151].

Chapters 3 and 4 were focusing on the bonding. In the case of closed-shell systems, the exploration of the bonding via the determination of the electronic structure is rather easy and the ETS-NOCV is a powerful tool to analyse and explore the metal arene chemical bonds and determine the main forces driving them. In particular we have seen that the zirconium-arene bond was mainly covalent while the thorium-arene one was mostly driven by electrostatic forces. In cases of open-shell systems, like in Chapter 4, the electronic wave functions are more difficult to describe. The CAS methods present the main disadvantages to include a limited number of orbitals in the active space thus requiring a thorough analysis of results. For example, in PuO_3, the full valence active space is (34; 26) but we could only compute a active space of (14,14) which might not be large enough.

The third properties we wanted to reproduce were thermodynamics. This part is particularly satisfactory in Chapter 5 where the double hybrid B2-PLYP already exhibits great performances at the spin-free level, compared to either experimental or state-of-the-art CCSD(T) data. In Chapter 4, multireference methods were needed to predict the enthalpies of formation of plutonium oxyhydroxide $PuO_2(OH)_2$ and trioxide PuO_3. The enthalpy of formation of $PuO_2(OH)_2$ was within very good agreement with experimental data but its uniqueness imposes to confirm this value with another method. For PuO_2, the single reference method UCCSD(T) perform very well. Regarding PuO_3 and PuO_2, the results with SO-CASPT2 method are good but not excellent, demonstrating the limit of actual relativistic multireference method accuracy.

As perspectives, the study of the alkyl cation catalysts calls for a further investigation of the possible transition states to have a better comprehension of the catalytic mechanism. Concerning the thermodynamic properties of plutonium oxides and oxyhydroxyde, in the next weeks, we will use the DMRG methods to be able to handle all valence orbitals in the active space to confirm our conclusions on PuO_3 and $PuO_2(OH)_2$. With DMRG we can expect to also be able to predict other thermodynamic values such as the one of uranyl complexes or RuO_2 (also important for nuclear safety) for which it is not easy

to properly describe because of a ground and first excited states close to each other in energy [201].

To shed light on the possible formation of PuO_3 we wait for the results of IRSN on accident simulation. At the moment, the double hybrid B2-PLYP is tested on PuO_2 hoping to obtain results as good as the one computed with UCCSD(T) method. In addition we plan to benchmark the implementation of the double hybrid in the DIRAC package to have results in the fully relativistic context.

Finally, the broad range of uses and theoretical challenges to describe actinides makes them a wonderful subject for the development of both experimental and computational chemistry.

Appendix A

Geometries

Contents

A.1 Geometries from the Chapter Coordination of Alkyl cations [$(XA_2)X(CH_2Y)$] (X = Th, U or Zr; Y = $SiMe_3$, H) with an arene for Ethylene polymerisation: Exploration of the bonding

A.1.1 X-Ray structures of Alkyl cations containing Thorium

X-Ray structure of η^6-2-Th

Th	13.572531	10.195293	14.464022	H	10.792612	4.709827	11.921041
Si	13.448412	7.436393	17.277993	N	15.572197	9.327770	13.767395
O	13.505595	7.925594	13.428804	C	9.770801	6.390663	12.427868
N	11.533051	9.429158	13.797651	C	9.943419	7.681786	12.928914
C	10.901366	5.592226	12.256356	H	9.184008	8.241008	13.042613

C	11.204383	8.166551	13.264229
C	15.830055	8.022389	13.295063
C	17.066703	7.444156	13.025269
H	17.857644	7.959021	13.135114
C	17.163700	6.111844	12.593599
C	15.992251	5.394201	12.387399
H	16.053977	4.497544	12.079063
C	13.429707	5.120134	12.400889
C	12.203748	6.048476	12.562765
C	12.283644	7.315836	13.063811
C	14.695748	7.239794	13.098499
C	14.706170	5.945503	12.620578
C	13.455092	4.557743	10.957491
H	14.231605	3.970005	10.849573
H	13.515482	5.299149	10.319620
H	12.633689	4.050799	10.791760
C	13.364508	3.990600	13.406835
H	14.146097	3.409198	13.296990
H	12.548182	3.469398	13.260375
H	13.357828	4.361303	14.314499
C	8.348976	5.918571	12.065573
C	7.779819	6.834239	10.992178
H	8.336952	6.780376	10.188578
H	7.767795	7.756243	11.323640
H	6.867297	6.553835	10.776343
C	7.451151	6.026297	13.322042
H	6.543973	5.726883	13.102353
H	7.423094	6.957806	13.624597
H	7.815893	5.462322	14.035069
C	8.306757	4.470612	11.572236
H	8.871372	4.380313	10.776343
H	7.383012	4.228230	11.348692
H	8.638899	3.874953	12.275627
C	18.537694	5.516184	12.265992
C	18.968436	6.042139	10.890042
H	19.001303	7.021174	10.909313
H	18.322590	5.749062	10.211703
H	19.856375	5.690446	10.668426
C	19.586226	5.912234	13.316261
H	19.631919	6.889686	13.381782
H	20.462942	5.562126	13.052248
H	19.332644	5.538363	14.185383
C	18.498147	3.962084	12.196616
H	17.836267	3.681681	11.531766
H	18.253115	3.600887	13.073446
H	19.380741	3.623065	11.938385
C	10.472762	10.428789	13.873193
C	10.172685	11.186036	12.726568
C	9.254284	12.234777	12.826778
H	9.026354	12.740136	12.055938
C	8.673102	12.538943	14.058195
H	8.101807	13.294606	14.133351
C	8.919737	11.759517	15.162423
H	8.481245	11.960710	15.981440
C	9.815959	10.660082	15.104610
C	10.781122	10.877117	11.366036
H	11.297639	10.024818	11.460464
C	9.726444	10.645824	10.302277
H	10.164668	10.450967	9.446644
H	9.173319	11.449013	10.211703
H	9.162631	9.886992	10.562435
C	11.757240	11.941700	10.901605
H	12.117974	11.696149	10.024774
H	12.492068	12.016157	11.547183
H	11.292295	12.803504	10.834156
C	9.943419	9.745998	16.303266
H	10.739170	9.161429	16.151025
C	8.720398	8.835083	16.416965
H	8.582785	8.366160	15.569041
H	7.928121	9.373711	16.627019
H	8.866028	8.179225	17.131919
C	10.164668	10.484236	17.638746
H	10.950266	11.065637	17.563589
H	10.311634	9.828377	18.353700
H	9.376399	11.024448	17.848800
C	16.641839	10.305221	13.803817
C	16.846522	11.122668	12.674537
C	17.778016	12.168240	12.782454
H	17.943151	12.724294	12.030885
C	18.463142	12.405870	13.969548
H	19.054745	13.147276	14.036996
C	18.287585	11.566244	15.052578
H	18.774175	11.726248	15.852325
C	17.389492	10.468394	14.985130
C	16.145630	10.888207	11.350619
H	15.295100	10.403441	11.558746
C	15.757374	12.150814	10.599050
H	15.225626	12.729047	11.184888
H	15.228298	11.910016	9.808939
H	16.567020	12.626074	10.317693
C	16.978523	9.955113	10.454518
H	17.216340	9.148755	10.955564
H	17.793514	10.417699	10.171234
H	16.452120	9.706393	9.666334
C	17.314406	9.490942	16.152952
H	16.553660	8.865183	15.975659
C	18.583654	8.652900	16.289776
H	18.771503	8.199819	15.441852
H	18.458867	7.984368	16.995095
H	19.335316	9.235886	16.522955
C	17.031965	10.205416	17.496141
H	16.991884	9.543221	18.216876
H	16.176893	10.679092	17.442182
H	17.748088	10.848602	17.681143
C	13.547547	9.235886	16.700249
H	14.365210	9.589163	17.131919
H	12.791343	9.684215	17.155044
C	14.955744	6.496804	16.715665
H	14.894285	5.568463	17.020147
H	15.760046	6.911865	17.095304
H	15.009186	6.518983	15.738626
C	11.928254	6.550667	16.636654
H	11.925582	5.627078	16.964261
H	11.938943	6.549083	15.655760
H	11.123952	7.011669	16.952699
C	13.372792	7.379204	19.153447
H	13.320419	6.446110	19.450220
H	12.580247	7.865553	19.463710
H	14.178163	7.795848	19.525377
C	14.776713	12.922319	15.844616
H	15.589031	12.871625	16.334100
C	14.819467	13.261338	14.414708
H	15.634457	13.438769	13.963767
C	13.654431	13.302527	13.796109
H	13.670464	13.348469	12.847976
C	12.434617	13.285101	14.391583
H	11.639668	13.468868	13.904027
C	12.398544	12.980935	15.784876
H	11.562177	12.987272	16.237745
C	13.560908	12.672016	16.503684
H	13.528842	12.315571	17.384369

A.1.2 X-Ray structures of Alkyl cations containing Uranium

X-Ray structure of η^6-2-U

U	26.777247	13.503446	-5.391782
C	25.497402	16.315921	-4.020626
C	27.893793	16.400190	-4.055059
C	25.430473	17.597350	-3.505585
C	26.632399	18.515068	-3.328096
C	27.914952	17.674466	-3.553844
O	26.717354	15.703364	-4.374315
Si	26.631072	16.262875	-8.133831
C	24.096018	18.044889	-3.237884
H	23.961710	18.921763	-2.897945
C	30.257583	16.196670	-4.027539
H	31.048407	15.690409	-4.171598
C	29.183435	18.242011	-3.352548
H	29.244576	19.142671	-3.056607
C	23.158568	15.962366	-3.969999
H	22.400133	15.407714	-4.110156
C	29.007950	15.612476	-4.269500
N	28.754519	14.348168	-4.765203
C	30.354856	17.521319	-3.574698
C	24.403820	15.486983	-4.276868
C	26.755000	14.493941	-7.517706
H	27.582991	14.155731	-7.942175
H	26.014113	14.031340	-7.983711
C	22.984861	17.224017	-3.464068
C	26.656266	19.034331	-1.896880
H	25.852805	19.570197	-1.730358
H	27.452665	19.589755	-1.764128
H	26.678646	18.277243	-1.275016
C	21.507655	19.145925	-2.621513
H	20.581249	19.405101	-2.434346
H	21.882572	19.742619	-3.302546
H	22.038066	19.213498	-1.800228
C	32.136413	17.576864	-1.871746
H	32.160015	16.597673	-1.903774
H	31.477376	17.866163	-1.206623
H	33.021484	17.917039	-1.624046
C	29.814411	13.343790	-4.831172
C	26.579170	19.651369	-4.322192
H	25.768992	20.181213	-4.169628
H	26.565710	19.288665	-5.232495
H	27.368347	20.221366	-4.209327
C	32.773442	17.694354	-4.294861
H	32.799566	16.715508	-4.334237
H	33.655035	18.034497	-4.035020
H	32.532489	18.050408	-5.175523
C	20.679690	17.628652	-4.399922
H	19.773461	17.946297	-4.204289
H	20.641089	16.697617	-4.703401
H	21.076323	18.185034	-5.102414
C	31.739727	18.132602	-3.271332
C	21.540230	17.718094	-3.127766
C	21.880182	11.161747	-5.093721
H	21.309073	10.407725	-5.181944
C	30.161611	13.499830	-8.495930
H	30.124018	14.174566	-9.205638
H	29.294009	13.049366	-8.427158
H	30.855745	12.841255	-8.707738
C	30.028630	12.532901	-3.691824
C	30.498085	14.192065	-7.136667
H	29.750695	14.825877	-6.937473
C	30.568704	13.211348	-5.982792
C	23.382822	12.479164	-3.740216
C	29.288062	12.758400	-2.363339
H	28.420965	13.210892	-2.571568
C	22.127932	11.928080	-6.176361
H	21.683459	11.738521	-6.994313
C	23.479803	13.182263	-8.621181
H	24.294972	12.647655	-8.520836
H	23.601289	13.830272	-9.346231
H	22.726360	12.592456	-8.833046
C	31.705241	19.675266	-3.193034
H	31.461049	20.041413	-4.068639
H	32.589621	20.009073	-2.934462
H	31.043203	19.953795	-2.526301
C	31.661489	11.272571	-4.984758
H	32.262332	10.539710	-5.051257
C	24.012019	12.762677	-2.362468
H	24.560907	13.592982	-2.458987
C	30.954213	11.502818	-3.788722
H	31.113026	10.944549	-3.036663
C	21.928421	14.794371	-7.448177
H	21.753414	15.271735	-6.610376
H	21.165420	14.217298	-7.660837
H	22.059889	15.442003	-8.171844
C	31.745780	15.016128	-7.290026
H	31.958778	15.448323	-6.436657
H	31.602658	15.700958	-7.976267
H	32.489374	14.436399	-7.557159
C	22.448796	11.451407	-3.829330
H	22.198153	10.955051	-3.059089
C	23.048285	13.020830	-6.113177
C	31.476420	12.117041	-6.057834
H	31.962150	11.966677	-6.860292
C	23.189072	13.937936	-7.294136
H	23.957727	14.552269	-7.115890
C	20.956590	16.798913	-2.077153
H	20.050732	17.095963	-1.850022
H	21.518646	16.821537	-1.274675
H	20.922369	15.883851	-2.426315
C	25.101379	17.176726	-7.485641
H	25.116140	17.184210	-6.505788
H	24.291945	16.720178	-7.796677
H	25.105468	18.098108	-7.819462
N	24.756569	14.219735	-4.803727
C	23.685898	13.247855	-4.894962
C	26.550285	16.284225	-9.996505
H	27.327675	15.813040	-10.362619
H	26.551612	17.211739	-10.312920
H	25.729063	15.839122	-10.292976
C	30.108673	13.705849	-1.494609
H	30.289149	14.530998	-1.991562
H	30.956523	13.277097	-1.254409
H	29.607625	13.918315	-0.679593
C	28.969588	11.466217	-1.616584
H	28.468832	10.863644	-2.205283
H	28.430628	11.671200	-0.824164
H	29.804747	11.033975	-1.340758
C	28.129862	17.204837	-7.576894
H	28.938128	16.746716	-7.888707
H	28.139472	17.254471	-6.598197
H	28.103473	18.110796	-7.949675
C	22.932561	13.064852	-1.345834
H	23.345893	13.263844	-0.479850
H	22.342390	12.287750	-1.255243
H	22.410354	13.838636	-1.644066
C	24.938240	11.680020	-1.885629
H	25.315200	11.931837	-1.016786
H	25.663250	11.561272	-2.534237
H	24.440404	10.840785	-1.794868
C	25.637524	10.440018	-5.444645
H	24.825993	10.249767	-4.988849
C	28.009889	10.501915	-5.432921
H	28.839978	10.383985	-4.986235
C	25.574737	10.778353	-6.701535
H	24.732888	10.854368	-7.135190
C	27.995367	10.828474	-6.763773
H	28.812288	10.915857	-7.240763
C	26.776345	11.033079	-7.419501
H	26.751681	11.334091	-8.320222
C	26.829335	10.342762	-4.735580
H	26.831194	10.172242	-3.801014

X-Ray structure of η^6-3-U-endo

U	26.475973	25.967895	3.207091
Si	26.597014	23.130531	0.474077
O	26.538359	23.792852	4.259045
N	24.504125	25.166614	3.840404
N	28.481946	25.255346	3.786880
C	24.048222	21.259237	5.310425
H	23.984236	20.362409	5.620104
C	22.872472	22.003952	5.071475
C	22.987114	23.307995	4.618426
H	22.200615	23.824542	4.480790
C	24.205522	23.867324	4.368006
C	28.855200	24.003590	4.354625
C	30.092271	23.499720	4.627984
H	30.857441	24.030527	4.436824
C	30.273566	22.232120	5.176613
C	29.135141	21.430363	5.409828
H	29.252449	20.549381	5.746270
C	26.607678	20.975611	5.337187
C	25.333282	21.839164	5.094414
C	25.338614	23.081412	4.593575
C	27.751435	23.102010	4.606956
C	27.802091	21.904128	5.149850
C	26.676997	19.864877	4.362271
H	25.906494	19.270689	4.488437
H	26.663666	20.227727	3.452350
H	27.506154	19.357837	4.499906
C	26.610344	20.497092	6.790003
H	26.565020	21.271913	7.388334
H	25.834509	19.918750	6.944843
H	27.434169	19.996390	6.969694
C	21.502097	21.374905	5.390712
C	21.038195	21.912050	6.730744
H	20.166380	21.523848	6.954401
H	21.688724	21.672791	7.422743
H	20.955546	22.888102	6.681042
C	20.462318	21.761523	4.278161
H	20.763587	21.414517	3.414118
H	19.587837	21.374905	4.499906
H	20.385001	22.737575	4.228459
C	21.563417	19.798328	5.425121
H	21.864686	19.465583	4.553431
H	22.189950	19.509949	6.120943
H	20.670273	19.441815	5.618192
C	31.689265	21.763108	5.572314
C	31.739921	20.352902	6.065507
H	31.364000	19.755546	5.384977
H	32.670389	20.100967	6.241374
H	31.217365	20.275262	6.891318
C	32.270474	22.716977	6.616048
H	32.227817	23.635987	6.277694
H	31.750585	22.650427	7.443770
H	33.203609	22.476133	6.793826
C	32.585074	21.896206	4.301100
H	32.555747	22.819969	3.976128
H	33.510211	21.660115	4.528580
H	32.254478	21.292511	3.603366
C	23.429687	26.152173	3.796438
C	23.240394	27.003049	4.897519
C	22.304593	28.069418	4.782823
H	22.149959	28.655683	5.513054
C	21.606074	28.245297	3.557488
H	21.006202	28.974167	3.452350
C	21.792701	27.378576	2.544340
H	21.296807	27.508505	1.745291
C	22.664516	26.313792	2.601688
C	22.768494	25.302881	1.470020
H	23.515002	24.669081	1.678385
C	21.440776	24.478941	1.317092
H	21.536756	23.837218	0.581126
H	21.256815	23.995668	2.148638
H	20.699600	25.087388	1.122109
C	23.080428	26.017490	0.086022
H	23.141748	25.344078	-0.623182
H	22.363247	26.649706	-0.124254
H	23.930914	26.500763	0.152928
C	23.901587	26.768543	6.237551
H	24.760071	26.293193	6.046391
C	23.056433	25.803583	7.147472
H	23.515002	25.675238	8.003869
H	22.171288	26.194954	7.306135
H	22.952455	24.936861	6.700158
C	24.280173	28.048819	7.028953
H	24.701417	27.795299	7.877704
H	24.909372	28.585965	6.501352
H	23.472344	28.573289	7.208644
C	29.564383	26.263088	3.689388
C	29.828327	27.045831	4.811497
C	30.777458	28.126459	4.668127
H	31.009409	28.684204	5.402182
C	31.366667	28.322938	3.337654
H	31.963873	29.047054	3.192372
C	31.070729	27.498998	2.324506
H	31.475977	27.663785	1.481490
C	30.220243	26.435798	2.429644
C	30.084272	25.456577	1.278860
H	29.313769	24.848129	1.468109
C	31.353336	24.612039	1.169899
H	31.265355	23.979823	0.426287
H	32.123839	25.198304	1.009325
H	31.489307	24.116090	2.003357
C	29.806998	26.201292	-0.032497
H	29.721683	25.553232	-0.764640
H	28.975175	26.711501	0.049702
H	30.548174	26.812909	-0.223657
C	29.191129	26.747944	6.164910
H	28.724561	25.863794	6.103739
C	30.278898	26.641783	7.264080
H	30.929426	25.954110	7.015572
H	30.734801	27.505336	7.355837
H	29.860320	26.402524	8.116654
C	28.156682	27.803221	6.505175
H	27.754101	27.598821	7.376864
H	28.585924	28.682619	6.541495
H	27.455498	27.807975	5.818910
C	26.517031	24.898833	1.110640
H	25.714535	25.260099	0.661414
H	27.284867	25.331402	0.655679
C	28.159348	22.157648	1.118286
H	28.156682	22.148141	2.098937
H	28.132687	21.237054	0.781844
H	28.972509	22.598139	0.797137
C	26.655668	23.116271	-1.372529
H	26.695659	22.189338	-1.691766
H	25.853172	23.548839	-1.729998
H	27.450166	23.601128	-1.678385
C	25.066672	22.141803	1.022706
H	25.013350	22.137050	1.999534
H	24.258844	22.558526	0.653767
H	25.135991	21.221208	0.693911
C	26.319739	28.335614	1.288418
H	26.314407	27.849172	0.472165
C	27.476827	28.606563	1.856164
H	28.284655	28.354628	1.422230
C	27.535481	29.267300	3.096792
H	28.367304	29.392475	3.542195
C	26.378393	29.722051	3.664537
C	25.167984	29.420996	3.052825
H	24.354824	29.685608	3.465731
C	25.133325	28.725400	1.825578
H	24.309500	28.538429	1.389733
C	26.429049	30.560252	4.859287
H	25.517243	30.796342	5.128823
H	26.866290	30.067472	5.585695
H	26.935608	31.376269	4.666216

X-Ray structure of η^6-5-U-endo

O	-0.156498	15.730261	3.745891	C	-2.385402	19.952003	0.987550
U	-0.224668	17.934927	4.767428	H	-3.212190	20.381636	0.683543
Si	-0.080636	15.164970	7.520860	H	-1.827579	19.728530	0.213371
N	-2.182485	17.109810	4.142043	H	-1.896545	20.564191	1.576680
N	1.792832	17.216825	4.188683	C	-3.917227	17.260890	6.521981
C	-2.629433	13.191173	2.747389	H	-3.177707	16.618800	6.321828
H	-2.694950	12.297283	2.430165	C	-5.216161	16.453556	6.669264
C	-3.796538	13.913524	2.975866	H	-5.960190	17.064171	6.852423
C	-3.704761	15.241769	3.425267	H	-5.124649	15.819335	7.409454
H	-4.496004	15.750090	3.561221	H	-5.392553	15.964120	5.838438
C	-2.457020	15.816188	3.670739	C	-3.595212	17.951766	7.838084
C	2.133414	15.964120	3.655633	H	-2.793093	18.502579	7.730455
C	3.403436	15.499864	3.338408	H	-3.437653	17.278201	8.531068
H	4.159136	16.060119	3.474362	H	-4.347464	18.521464	8.100550
C	3.574522	14.206241	2.819142	C	2.832615	18.217730	4.301411
C	2.462856	13.408350	2.615212	C	3.138450	18.984146	3.155249
H	2.586197	12.533345	2.265888	C	4.053566	20.035411	3.302532
C	-0.069761	12.936225	2.720954	H	4.283804	20.567339	2.549124
C	-1.349862	13.745133	2.973978	C	4.630221	20.310817	4.539329
C	-1.328112	15.030886	3.440373	H	5.204225	21.061496	4.633741
C	1.064718	15.108000	3.415826	C	4.379029	19.509779	5.621290
C	1.153046	13.844279	2.907890	H	4.816958	19.689186	6.444563
C	-0.003183	11.777945	3.716056	C	3.484337	18.422318	5.538208
H	-0.029178	12.132039	4.629964	C	3.340571	17.484363	6.705140
H	0.830236	11.279066	3.581991	H	2.567630	16.876895	6.518204
H	-0.769228	11.181494	3.576327	C	4.597861	16.615653	6.867529
C	-0.089655	12.396429	1.282115	H	4.747993	16.102610	6.046144
H	-0.877981	11.829879	1.155603	H	4.474784	16.000316	7.619048
H	0.721483	11.869223	1.119726	H	5.371333	17.191645	7.039359
H	-0.122015	13.147108	0.651443	C	3.055692	18.224025	8.028796
C	-5.172129	13.310778	2.654865	H	3.822267	18.793723	8.255385
C	-6.205282	13.724674	3.716056	H	2.912456	17.569345	8.744439
H	-5.920402	13.395760	4.595976	H	2.254634	18.777985	7.926832
H	-7.076897	13.340679	3.489468	C	2.522272	18.696150	1.793828
H	-6.275839	14.701973	3.740603	H	2.116703	17.783375	1.833481
C	-5.615364	13.841131	1.280227	C	1.416440	19.670301	1.472827
H	-5.625974	14.821578	1.295333	H	0.681695	19.553844	2.111052
H	-6.514565	13.509070	1.076297	H	1.087529	19.505058	0.564584
H	-4.989371	13.531103	0.592907	H	1.758614	20.586224	1.535139
C	-5.141095	11.766929	2.598218	C	3.570278	18.680413	0.713755
H	-4.554360	11.478933	1.867469	H	3.867360	19.596335	0.532484
H	-6.047723	11.426999	2.441494	H	3.190970	18.290122	-0.101965
H	-4.801043	11.414409	3.446038	H	4.334201	18.140616	1.008320
C	5.005021	13.753001	2.481147	C	-0.198142	16.931976	6.892076
C	5.575576	14.687809	1.425621	H	0.546417	17.391511	7.356583
H	6.517217	14.464336	1.263233	H	-1.023869	17.275054	7.320706
H	5.509263	15.614748	1.739069	C	1.435008	14.266044	6.886411
H	5.068947	14.588663	0.592907	H	1.432355	14.270765	5.906415
C	5.888572	13.850574	3.736827	H	1.424398	13.339105	7.209300
H	5.572924	13.213205	4.409040	H	2.241371	14.714563	7.213077
H	5.838175	14.760201	4.099369	C	0.005040	15.189835	9.397770
H	6.816951	13.644413	3.498909	H	0.769228	15.732779	9.682895
C	5.056480	12.308299	1.954328	H	0.114058	14.273913	9.731989
H	4.790433	11.691389	2.668083	H	-0.822278	15.573830	9.756536
H	5.968148	12.098990	1.665428	C	-1.594159	14.203094	6.995929
H	4.442954	12.213874	1.195256	H	-2.389912	14.602826	7.401901
C	-3.244550	18.098125	4.197558	H	-1.506626	13.273008	7.290495
C	-4.012452	18.241336	5.364490	H	-1.673734	14.231421	6.019709
C	-4.911388	19.330371	5.428690	C	-0.328911	20.403669	6.686258
H	-5.421730	19.470435	6.216086	H	-0.342174	20.025969	7.558625
C	-5.055684	20.186491	4.369387	C	-1.509278	20.693239	6.042368
H	-5.639236	20.932449	4.446805	H	-2.339514	20.527995	6.476663
C	-4.361257	19.983478	3.177908	C	-1.499199	21.225166	4.756477
H	-4.514572	20.554749	2.435830	H	-2.310336	21.404574	4.295746
C	-3.434470	18.930639	3.072166	C	-0.297081	21.483261	4.174899
C	-2.726250	18.678839	1.748510	C	0.901853	21.182675	4.771582
H	-1.867367	18.205140	1.948664	H	1.721479	21.325886	4.316517
C	-3.572931	17.753474	0.872367	C	0.885938	20.664911	6.055586
H	-3.684336	16.889485	1.319880	H	1.705564	20.487078	6.506875
H	-3.127309	17.619705	0.011329	F	-0.272413	22.093876	2.962649
H	-4.453564	18.159501	0.723196				

A.1.3 X-Ray structures of Alkyl cations containing Zirconium

X-Ray structure of η^6-3′-Zr-exo

Zr	7.285954	8.774163	15.782526
O	8.282123	10.391022	14.632517
N	6.037782	10.513949	15.737937
N	8.621293	7.924604	14.345425
C	7.683726	13.944571	13.954353
H	8.083844	14.707173	13.554143
C	6.413363	14.079126	14.540962
C	5.844292	12.955691	15.147673
H	4.984944	13.030522	15.547883
C	6.501660	11.731730	15.178739
C	9.525022	8.743962	13.625413
C	10.531792	8.332530	12.766515
H	10.671907	7.404743	12.623974
C	11.343474	9.257527	12.106808
C	11.096220	10.627797	12.284070
H	11.640386	11.257814	11.827209
C	9.764440	12.571519	13.303783
C	8.378486	12.736923	13.939733
C	7.752986	11.682390	14.572028
C	9.358702	10.107644	13.766126
C	10.070439	11.091258	13.115556
C	9.834116	13.312058	11.969750
H	9.634537	14.260729	12.110463
H	10.734898	13.220060	11.591469
H	9.179132	12.929556	11.348419
C	10.797486	13.166765	14.268673
H	10.611125	14.119810	14.400249
H	10.744894	12.702701	15.131226
H	11.695268	13.057588	13.892220
C	12.440608	8.749381	11.182122
C	13.324447	7.701830	11.956958
H	13.740545	8.134607	12.731793
H	12.761565	6.958546	12.260313
H	14.023335	7.358586	11.361211
C	11.825687	8.061895	10.014386
H	11.207569	7.370662	10.330534
H	11.335317	8.715614	9.471636
H	12.529310	7.648445	9.471636
C	13.413114	9.838731	10.772775
H	13.789554	10.258385	11.575022
H	14.135691	9.446844	10.239162
H	12.943058	10.511657	10.240989
C	5.689633	15.432942	14.502585
C	6.524951	16.475573	15.222598
H	7.412773	16.524700	14.809596
H	6.085299	17.350191	15.154982
H	6.615473	16.228322	16.165558
C	4.317907	15.369288	15.149500
H	3.771037	14.697344	14.690812
H	4.413528	15.121533	16.094288
H	3.883354	16.243402	15.083712
C	5.517302	15.862992	13.031494
H	4.977773	15.196934	12.558186
H	5.065259	16.732238	12.996773
H	6.396836	15.935524	12.607527
C	4.635503	10.649064	16.114390
C	4.260817	10.961367	17.426494
C	2.913795	11.137363	17.715230
H	2.652761	11.333561	18.608849
C	1.934866	11.036785	16.730238
C	2.325160	10.725841	15.440063
H	1.660592	10.635369	14.767565
C	3.667875	10.537688	15.094677
C	4.020244	10.264885	13.632723
H	5.013773	10.190733	13.552315
C	3.534732	11.429597	12.735448
H	3.766245	11.240789	11.801625
H	2.561892	11.521268	12.819511
H	3.967172	12.261118	13.018702
C	3.391500	8.966358	13.128348
H	3.640094	8.826729	12.190870
H	3.716534	8.215453	13.667444
H	2.416275	9.025349	13.203274
C	5.298783	11.151457	18.550371
H	6.087771	10.578845	18.329250
C	5.793157	12.598983	18.628951
H	6.121621	12.880460	17.749951
H	5.053736	13.180551	18.904895
H	6.518045	12.660645	19.285003
C	4.786192	10.718832	19.930090
H	4.468725	9.792612	19.882577
H	5.512989	10.781503	20.582487
H	4.048384	11.303261	20.202379
C	0.476312	11.367248	17.050041
H	0.375806	11.343025	18.044169
C	0.167541	12.787874	16.595007
H	0.818146	13.405717	16.987907
H	0.220425	12.837202	15.617325
H	-0.735038	13.033770	16.885571
C	-0.505722	10.357198	16.467086
H	-0.273983	9.458964	16.781406
H	-1.414166	10.580861	16.757650
H	-0.458407	10.382440	15.489404
C	8.724414	6.550147	13.901357
C	7.912949	6.118556	12.826820
C	8.096091	4.819031	12.346203
H	7.544826	4.513116	11.635328
C	9.052372	3.957291	12.870679
C	9.808169	4.402191	13.950698
H	10.450845	3.813735	14.330806
C	9.663728	5.672445	14.497103
C	6.864113	7.023863	12.198180
H	6.530177	7.631103	12.918193
C	7.428729	7.903651	11.098060
H	6.714230	8.464996	10.728916
H	8.134606	8.476678	11.465376
H	7.801984	7.342060	10.387184
C	5.647374	6.247618	11.660912
H	5.283776	5.679046	12.371787
H	4.960606	6.881427	11.364866
H	5.924244	5.689371	10.904351
C	10.476433	6.072451	15.719662
H	9.989020	6.820522	16.171041
C	11.869091	6.582939	15.366966
H	12.345549	6.825247	16.187488
H	12.364905	5.883029	14.895486
H	11.790337	7.372226	14.789494
C	10.597018	4.916060	16.741203
H	11.127022	5.215100	17.510556
H	9.703872	4.651283	17.042731
H	11.038640	4.151161	16.317236
C	9.260431	2.545222	12.327929
H	10.246890	2.386918	12.364477
C	8.642170	1.500104	13.241650
H	8.911817	1.676107	14.168163
H	7.666109	1.541500	13.172207
H	8.951510	0.610315	12.974843
C	8.883953	2.312729	10.968311
H	9.290919	2.995402	10.394494
H	9.193640	1.425966	10.690540
H	7.908521	2.357655	10.886076
C	8.775268	9.430622	17.320502
H	8.307558	9.853784	18.069754
H	9.275254	8.652146	17.643959
H	9.398000	10.073301	16.918465
C	6.607178	7.309345	18.119095

C	7.250882	6.408794	17.260196	H	4.138094	7.994394	16.019363
H	8.069384	6.017177	17.537968	C	5.427308	7.904468	17.607411
C	6.744188	6.074138	16.035810	H	4.960818	8.539566	18.139196
H	7.186440	5.422365	15.504024	C	7.083585	7.573345	19.498814
C	5.590706	6.675344	15.562502	H	6.495514	8.231630	19.926435
H	5.258827	6.458109	14.698122	H	7.071395	6.740065	20.014153
C	4.931415	7.581915	16.339165	H	7.998037	7.924672	19.467747

A.1.4 Optimised geometries of Alkyl cations containing Thorium

Optimised geometry of η^6-2-Th and the name of the fragment f in the ETS-NOCV in which each atom belongs

Th	13.5411509	10.1377154	14.5509358 f=U	H	17.7678338	4.0709094	10.7278683 f=U
Si	13.4112173	7.5322504	17.4978204 f=U	H	18.0861434	3.5483540	12.3932988 f=U
O	13.4985180	7.8349960	13.6124273 f=U	H	19.4228595	3.8776437	11.2937161 f=U
N	11.5227749	9.3960006	13.7995967 f=U	C	10.5226752	10.4095246	13.7394240 f=U
C	10.9455192	5.5470351	12.3276461 f=U	C	10.3924842	11.1763814	12.5587559 f=U
H	10.8362841	4.5394039	11.9548734 f=U	C	9.4745988	12.2211291	12.5401612 f=U
N	15.5376637	9.3173458	13.8106982 f=U	H	9.3631736	12.8172040	11.6410803 f=U
C	9.8258568	6.3633255	12.4096511 f=U	C	8.6829065	12.5007577	13.6402780 f=U
C	9.9815248	7.6658022	12.8964944 f=U	H	7.9697568	13.3162732	13.6040570 f=U
H	9.1316192	8.3345344	12.9572021 f=U	C	8.7817089	11.7146781	14.7742515 f=U
C	11.2234660	8.1309948	13.3013923 f=U	H	8.1297067	11.9162214	15.6167982 f=U
C	15.7913673	8.0286696	13.3459828 f=U	C	9.6845539	10.6577207	14.8487296 f=U
C	17.0187729	7.5006963	12.9720467 f=U	C	11.1667063	10.8589817	11.2945455 f=U
H	17.8956188	8.1335073	13.0341862 f=U	H	11.8752658	10.0584404	11.5264475 f=U
C	17.1226427	6.1945221	12.4820930 f=U	C	10.2305495	10.3306062	10.2068517 f=U
C	15.9685601	5.4300640	12.3804617 f=U	H	10.8007652	10.0548590	9.3166019 f=U
H	16.0374282	4.4192964	12.0068144 f=U	H	9.5010599	11.0900207	9.9142923 f=U
C	13.4451964	5.0751477	12.6312720 f=U	H	9.6858193	9.4486246	10.5451961 f=U
C	12.2213251	5.9770285	12.7095653 f=U	C	11.9584772	12.0530811	10.7679995 f=U
C	12.3047788	7.2583693	13.1939544 f=U	H	12.5061723	11.7733943	9.8652660 f=U
C	14.6742893	7.2043935	13.2214293 f=U	H	12.6859752	12.4209590	11.4964693 f=U
C	14.7078764	5.9193695	12.7389865 f=U	H	11.3042754	12.8873466	10.5044660 f=U
C	13.4425255	4.2973168	11.3110614 f=U	C	9.6856998	9.7777687	16.0817399 f=U
H	14.3003684	3.6274961	11.2517737 f=U	H	10.5426491	9.1050062	16.0069246 f=U
H	13.4715311	4.9718018	10.4535549 f=U	C	8.4251433	8.9127275	16.1276204 f=U
H	12.5523668	3.6736791	11.2287250 f=U	H	8.3418233	8.2784856	15.2451328 f=U
C	13.4074615	4.0789474	13.8032364 f=U	H	7.5263993	9.5319572	16.1895833 f=U
H	14.2796188	3.4222287	13.7710610 f=U	H	8.4433803	8.2625803	17.0056007 f=U
H	12.5082246	3.4614699	13.7473022 f=U	C	9.8119876	10.5679219	17.3819215 f=U
H	13.4059143	4.5973764	14.7637199 f=U	H	10.7036482	11.1984294	17.3977057 f=U
C	8.4395024	5.8845547	11.9793421 f=U	H	9.8739262	9.8845784	18.2319737 f=U
C	7.9176908	6.7810542	10.8503947 f=U	H	8.9464597	11.2129345	17.5505540 f=U
H	8.5838292	6.7503773	9.9846807 f=U	C	16.6044161	10.2635307	13.8450668 f=U
H	7.8214859	7.8214193	11.1686322 f=U	C	16.7787840	11.1528864	12.7545679 f=U
H	6.9292862	6.4430363	10.5290679 f=U	C	17.7877195	12.1065971	12.8322780 f=U
C	7.4777847	5.9633618	13.1704677 f=U	H	17.9362931	12.7967494	12.0117006 f=U
H	6.4876781	5.6046543	12.8780991 f=U	C	18.6182955	12.1910936	13.9374748 f=U
H	7.3622998	6.9872296	13.5318342 f=U	H	19.4005878	12.9405693	13.9717481 f=U
H	7.8299581	5.3480955	14.0018572 f=U	C	18.4522472	11.3108758	14.9886070 f=U
C	8.4539888	4.4440075	11.4745932 f=U	H	19.1161199	11.3728628	15.8433492 f=U
H	9.0968831	4.3240268	10.5991082 f=U	C	17.4577070	10.3361746	14.9682044 f=U
H	7.4433857	4.1532997	11.1803993 f=U	C	15.9297148	11.0708127	11.4977558 f=U
H	8.7837445	3.7442284	12.2464610 f=U	H	14.9128837	10.7741860	11.7951912 f=U
C	18.4863186	5.6656603	12.0377325 f=U	C	15.8265003	12.3878320	10.7349313 f=U
C	18.9881421	6.5088337	10.8587986 f=U	H	15.5639355	13.2360915	11.3706355 f=U
H	19.0965641	7.5610272	11.1309185 f=U	H	15.0700117	12.3039652	9.9530766 f=U
H	18.2996336	6.4479457	10.0124772 f=U	H	16.7676868	12.6329311	10.2376493 f=U
H	19.9653575	6.1483343	10.5274803 f=U	C	16.4421692	9.9914081	10.5407292 f=U
C	19.4892647	5.7671788	13.1915918 f=U	H	16.4464425	9.0022685	10.9946364 f=U
H	19.6540149	6.8018053	13.4986825 f=U	H	17.4630052	10.2261678	10.2276067 f=U
H	20.4560660	5.3615223	12.8833908 f=U	H	15.8179199	9.9548450	9.6445553 f=U
H	19.1473189	5.2033597	14.0628291 f=U	C	17.3648884	9.3733850	16.1341247 f=U
C	18.4249925	4.2074922	11.5900877 f=U	H	16.4718301	8.7616463	15.9910548 f=U

```
C    18.5702046    8.4333869   16.1724097 f=U
H    18.6555576    7.8490821   15.2572107 f=U
H    18.4762324    7.7339345   17.0065442 f=U
H    19.4997500    8.9918326   16.3103739 f=U
C    17.2415441   10.0901175   17.4769903 f=U
H    17.1033516    9.3630039   18.2805042 f=U
H    16.3937546   10.7770891   17.5005999 f=U
H    18.1402206   10.6649430   17.7121421 f=U
C    13.4931435    9.2830186   16.8053328 f=U
H    14.3816515    9.7454179   17.2697837 f=U
H    12.6316977    9.8147787   17.2471611 f=U
C    14.9126528    6.5317840   16.9803795 f=U
H    14.8187365    5.5078077   17.3538912 f=U
H    15.8303965    6.9446519   17.4074739 f=U
H    15.0428410    6.4776692   15.8967079 f=U
C    11.8474905    6.6589310   16.9367496 f=U
H    11.8420964    5.6339427   17.3191504 f=U
H    11.7489874    6.6064370   15.8496706 f=U
H    10.9543500    7.1515076   17.3302000 f=U
C    13.3884479    7.6116642   19.3749136 f=U
H    13.3422745    6.6090710   19.8097699 f=U
H    12.5222756    8.1700561   19.7406040 f=U
H    14.2860040    8.0995391   19.7649674 f=U
C    14.9635327   13.0048072   15.1370528 f=B
H    16.0276938   13.0028906   14.9293386 f=B
C    14.0518998   13.2555576   14.1108529 f=B
H    14.4129924   13.4643714   13.1114026 f=B
C    12.6851956   13.2744506   14.3762951 f=B
H    11.9749179   13.4871561   13.5868063 f=B
C    12.2238385   13.0253003   15.6668106 f=B
H    11.1596929   13.0395968   15.8654698 f=B
C    13.1300729   12.7600194   16.6864401 f=B
H    12.7760406   12.5675868   17.6921270 f=B
C    14.4981855   12.7588473   16.4235351 f=B
H    15.2011788   12.5782390   17.2268758 f=B
```

Optimised geometry of η^6-2′-Th and the name of the fragment f in the ETS-NOCV in which each atom belongs

```
 C     6.448660     8.349540   15.663848 f=B
 C     7.300386     9.148847   14.911264 f=B
 C     6.925039    10.448375   14.570928 f=B
 C     5.699877    10.954523   14.987350 f=B
 C     4.845149    10.153568   15.744930 f=B
 C     5.217007     8.854583   16.079916 f=B
 H     8.256217     8.763558   14.578559 f=B
Th     7.164431    10.644975   17.851354 f=U
 C     9.379337    10.971753   16.902655 f=U
 O     8.269407    11.505852   19.921606 f=U
 C     8.688510    10.620761   20.908436 f=U
 C     9.324873    11.041861   22.054830 f=U
 C     9.682854    12.512835   22.223304 f=U
 C     8.678455    13.348153   21.439599 f=U
 C     8.078501    12.823486   20.321152 f=U
 C     8.365939     9.300966   20.626994 f=U
 C     8.713481     8.339491   21.572384 f=U
 C     9.353649     8.701681   22.755722 f=U
 C     9.650656    10.046886   22.973504 f=U
 C     8.355137    14.672802   21.748207 f=U
 C     7.480591    15.423653   20.971475 f=U
 C     6.917940    14.836237   19.833472 f=U
 C     7.203610    13.520925   19.493551 f=U
 C     9.736427     7.670919   23.817652 f=U
 C     9.081644     8.043433   25.153185 f=U
 N     7.699676     9.092247   19.423501 f=U
 C     7.296067     7.779314   19.050671 f=U
 C     8.212604     6.884735   18.461359 f=U
 C     7.754086     5.636466   18.050225 f=U
 C     6.433287     5.239485   18.194469 f=U
 C     5.549754     6.133385   18.792223 f=U
 C     5.948273     7.386616   19.238601 f=U
 N     6.689588    12.792345   18.424627 f=U
 C     5.804834    13.415369   17.499156 f=U
 C     4.411124    13.178389   17.596127 f=U
 C     3.571541    13.739065   16.642895 f=U
 C     4.046292    14.544896   15.611789 f=U
 C     5.411699    14.775050   15.549290 f=U
 C     6.308386    14.229095   16.463696 f=U
 C     7.088977    16.853075   21.347217 f=U
 C     7.854314    17.363808   22.565489 f=U
 C     9.714309    12.913093   23.695877 f=U
 C    11.079816    12.742952   21.614541 f=U
 C     9.681194     7.215740   18.284940 f=U
 C    10.126998     7.102465   16.828350 f=U
 C     5.978854     3.873659   17.737045 f=U
 C     4.915656     3.964707   16.644952 f=U
 C     4.961000     8.267096   19.984546 f=U
 C     3.505638     8.065806   19.579893 f=U
 C     3.819112    12.378437   18.744211 f=U
 C     2.457881    11.761962   18.444061 f=U
 C     3.108121    15.160683   14.601050 f=U
 C     2.122265    16.121320   15.262480 f=U
 C     7.782213    14.549984   16.314864 f=U
 C     8.319906    14.149930   14.942119 f=U
 C     7.371238    17.801557   20.177554 f=U
 C     5.590301    16.887479   21.672558 f=U
 C    11.260601     7.659871   23.985513 f=U
 C     9.285294     6.260050   23.448736 f=U
 C     5.098534     8.071927   21.496682 f=U
 C    10.562128     6.323028   19.159695 f=U
 C     5.488537     3.024870   18.908129 f=U
 C     3.715116    13.226717   20.013531 f=U
 C     8.059835    16.032898   16.559612 f=U
 C     2.373532    14.098188   13.786825 f=U
 H    10.152131    10.330023   23.888875 f=U
 H     8.450525     7.308436   21.378778 f=U
 H     6.221636    15.391464   19.216544 f=U
 H     8.801289    15.121396   22.622734 f=U
 H    10.459639    12.330648   24.238107 f=U
 H    10.002900    13.958665   23.806240 f=U
 H     8.744294    12.767600   24.174469 f=U
 H    11.824988    12.142624   22.141416 f=U
 H    11.103007    12.465198   20.558827 f=U
 H    11.358488    13.796020   21.696255 f=U
 H     8.428081    17.782964   19.900585 f=U
 H     6.782925    17.546487   19.293858 f=U
 H     7.112413    18.826152   20.456160 f=U
 H     4.984813    16.574685   20.818948 f=U
 H     5.357082    16.227597   22.511691 f=U
 H     5.286129    17.901841   21.943617 f=U
 H     8.933574    17.373606   22.393645 f=U
 H     7.546741    18.388853   22.782707 f=U
 H     7.650387    16.766923   23.457643 f=U
 H    11.640703     8.634550   24.297409 f=U
 H    11.550679     6.930088   24.745862 f=U
 H    11.756464     7.390254   23.049753 f=U
 H     8.200520     6.195917   23.330624 f=U
 H     9.755592     5.905573   22.528094 f=U
 H     9.569888     5.568591   24.244652 f=U
 H     7.992544     8.059968   25.064985 f=U
 H     9.348778     7.310570   25.918811 f=U
 H     9.404244     9.024079   25.507326 f=U
 H     8.457690     4.940785   17.603033 f=U
 H     4.518457     5.831085   18.931744 f=U
 H     5.219483     9.316942   19.783169 f=U
```

H	4.397689	8.719048	22.029836	f=U
H	4.869599	7.036302	21.762049	f=U
H	6.105086	8.298043	21.846915	f=U
H	2.880197	8.812384	20.072817	f=U
H	3.345861	8.153629	18.502933	f=U
H	3.132745	7.088407	19.893355	f=U
H	9.832313	8.249140	18.605377	f=U
H	10.302822	6.411946	20.214725	f=U
H	10.466955	5.272560	18.873125	f=U
H	11.611734	6.604369	19.047000	f=U
H	9.526918	7.732119	16.168719	f=U
H	11.169676	7.411654	16.726623	f=U
H	10.053588	6.074735	16.464599	f=U
H	6.854906	3.374881	17.308324	f=U
H	6.253572	2.933285	19.681652	f=U
H	4.597109	3.460537	19.367043	f=U
H	5.227143	2.020410	18.567851	f=U
H	5.272237	4.536188	15.784462	f=U
H	4.641388	2.967195	16.294703	f=U
H	4.005624	4.444141	17.016024	f=U
H	2.505624	13.557923	16.711566	f=U
H	5.794312	15.410401	14.756373	f=U
H	4.509890	11.552785	18.975309	f=U
H	3.298689	12.635573	20.832968	f=U
H	4.681936	13.614883	20.330078	f=U
H	3.048178	14.075460	19.840086	f=U
H	2.443194	11.181806	17.518788	f=U
H	2.166043	11.098397	19.259802	f=U
H	1.681735	12.526691	18.367518	f=U
H	8.328201	13.979937	17.070267	f=U
H	9.130050	16.234179	16.471880	f=U
H	7.543497	16.656840	15.825489	f=U
H	7.742040	16.343841	17.554241	f=U
H	9.397846	14.319703	14.894657	f=U
H	8.138224	13.095654	14.726289	f=U
H	7.860456	14.737197	14.143512	f=U
H	3.726010	15.742515	13.908517	f=U
H	3.071820	13.431188	13.275369	f=U
H	1.726274	13.487868	14.422540	f=U
H	1.741605	14.566840	13.029173	f=U
H	2.640904	16.899829	15.825484	f=U
H	1.498399	16.605965	14.508211	f=U
H	1.457184	15.594541	15.951904	f=U
H	9.871404	10.025805	16.646618	f=U
H	9.413709	11.606802	16.011060	f=U
H	10.003158	11.456396	17.663952	f=U
H	7.590831	11.058690	13.973750	f=B
H	5.407176	11.967868	14.736753	f=B
H	3.884992	10.544719	16.056569	f=B
H	4.550204	8.224420	16.654750	f=B
H	6.736682	7.341461	15.938480	f=B

Optimised geometry of η^6-3-Th-endo and the name of the fragment f in the ETS-NOCV in which each atom belongs

Th	26.469113	25.919467	3.054570	f=Th
Si	26.498129	23.187135	0.209239	f=Th
O	26.545771	23.688876	4.136458	f=Th
N	24.479648	25.075114	3.757777	f=Th
N	28.517924	25.221841	3.760973	f=Th
C	24.105598	21.278497	5.415433	f=Th
H	24.052209	20.284913	5.836461	f=Th
C	22.935505	22.003301	5.237570	f=Th
C	23.021269	23.288249	4.689001	f=Th
H	22.129472	23.886926	4.549660	f=Th
C	24.244585	23.822236	4.316302	f=Th
C	28.834930	23.976126	4.298954	f=Th
C	30.095976	23.511931	4.639610	f=Th
H	30.946854	24.165120	4.489640	f=Th
C	30.271912	22.231574	5.176165	f=Th
C	29.152555	21.435039	5.371738	f=Th
H	29.274497	20.444078	5.784788	f=Th
C	26.640519	20.976713	5.274151	f=Th
C	25.365650	21.783038	5.072275	f=Th
C	25.380943	23.041064	4.525425	f=Th
C	27.754998	23.120629	4.514888	f=Th
C	27.858350	21.862623	5.053187	f=Th
C	26.668153	19.821188	4.259757	f=Th
H	25.803826	19.169318	4.401271	f=Th
H	26.648363	20.196642	3.234743	f=Th
H	27.572801	19.223325	4.386791	f=Th
C	26.670432	20.405166	6.697648	f=Th
H	26.651614	21.203516	7.441974	f=Th
H	25.815150	19.752300	6.873370	f=Th
H	27.568157	19.807784	6.858219	f=Th
C	21.565837	21.440444	5.616069	f=Th
C	20.892009	22.367916	6.633781	f=Th
H	19.915904	21.967019	6.917791	f=Th
H	21.495885	22.461869	7.539534	f=Th
H	20.728952	23.368796	6.228016	f=Th
C	20.690088	21.347737	4.361113	f=Th
H	21.148432	20.701537	3.608780	f=Th
H	19.711579	20.932108	4.615291	f=Th
H	20.524517	22.327814	3.909266	f=Th
C	21.661712	20.047701	6.233881	f=Th
H	22.092698	19.321863	5.540052	f=Th
H	22.256036	20.047567	7.150917	f=Th
H	20.660483	19.696860	6.492125	f=Th
C	31.679939	21.758846	5.537326	f=Th
C	31.690734	20.333640	6.084065	f=Th
H	31.307353	19.614486	5.356066	f=Th
H	32.716728	20.044169	6.320659	f=Th
H	31.106100	20.243909	7.002891	f=Th
C	32.268408	22.686666	6.606896	f=Th
H	32.339373	23.718410	6.255516	f=Th
H	31.657825	22.678132	7.513038	f=Th
H	33.276153	22.359312	6.874867	f=Th
C	32.571260	21.798332	4.290836	f=Th
H	32.672828	22.810963	3.895951	f=Th
H	33.574293	21.439714	4.535737	f=Th
H	32.168149	21.163421	3.498296	f=Th
C	23.437643	26.045708	3.736822	f=Th
C	23.193232	26.811633	4.899734	f=Th
C	22.251709	27.832567	4.840704	f=Th
H	22.052590	28.425707	5.726678	f=Th
C	21.550486	28.094794	3.676630	f=Th
H	20.820296	28.895638	3.649621	f=Th
C	21.758117	27.308521	2.557807	f=Th
H	21.170142	27.492155	1.666019	f=Th
C	22.679653	26.264577	2.564402	f=Th
C	22.752016	25.336264	1.369209	f=Th
H	23.644763	24.718343	1.483349	f=Th
C	21.543678	24.396568	1.366107	f=Th
H	21.603724	23.704147	0.522898	f=Th
H	21.492525	23.805016	2.280166	f=Th
H	20.611991	24.960193	1.271014	f=Th
C	22.833622	26.056432	0.026414	f=Th
H	22.931493	25.326972	-0.780787	f=Th
H	21.934328	26.641345	-0.179127	f=Th
H	23.689098	26.732023	-0.040362	f=Th
C	23.882047	26.522059	6.217689	f=Th
H	24.563594	25.682679	6.062735	f=Th
C	22.873655	26.093737	7.283140	f=Th
H	23.391056	25.834750	8.209990	f=Th
H	22.169142	26.897423	7.509556	f=Th

```
 H    22.301963    25.222208     6.962220 f=Th
 C    24.703823    27.707821     6.711773 f=Th
 H    25.221499    27.453694     7.639612 f=Th
 H    25.456603    28.016314     5.981290 f=Th
 H    24.071507    28.575248     6.916668 f=Th
 C    29.534589    26.220856     3.708390 f=Th
 C    29.742928    27.052520     4.833574 f=Th
 C    30.701983    28.055733     4.751219 f=Th
 H    30.877429    28.696796     5.607479 f=Th
 C    31.453602    28.241287     3.604421 f=Th
 H    32.200623    29.025774     3.564420 f=Th
 C    31.264721    27.406359     2.519459 f=Th
 H    31.876719    27.539654     1.634518 f=Th
 C    30.319452    26.384784     2.546155 f=Th
 C    30.216109    25.460988     1.351702 f=Th
 H    29.349086    24.815817     1.506254 f=Th
 C    31.446241    24.558303     1.250698 f=Th
 H    31.355726    23.889038     0.391749 f=Th
 H    32.356540    25.148614     1.117881 f=Th
 H    31.566469    23.942200     2.141915 f=Th
 C    30.025468    26.218907     0.039455 f=Th
 H    29.851268    25.518546    -0.780545 f=Th
 H    29.177639    26.906995     0.078308 f=Th
 H    30.910057    26.805036    -0.220261 f=Th
 C    29.008315    26.849444     6.143433 f=Th
 H    28.164802    26.176540     5.954794 f=Th
 C    29.909590    26.164717     7.172527 f=Th
 H    30.266565    25.198930     6.815215 f=Th
 H    30.778685    26.788618     7.397685 f=Th
 H    29.364612    26.001022     8.105411 f=Th
 C    28.457855    28.149350     6.722713 f=Th
 H    27.861080    27.941690     7.613142 f=Th
 H    29.258894    28.827417     7.024926 f=Th
 H    27.826359    28.679312     6.006731 f=Th
 C    26.484300    24.957442     0.858341 f=Th
 H    25.609820    25.448510     0.394133 f=Th
 H    27.365781    25.442901     0.403947 f=Th
 C    28.047737    22.290222     0.770925 f=Th
 H    28.154622    22.260180     1.858087 f=Th
 H    28.022145    21.257050     0.412318 f=Th
 H    28.950212    22.749567     0.359284 f=Th
 C    26.484766    23.216983    -1.668929 f=Th
 H    26.497324    22.202336    -2.077350 f=Th
 H    25.591738    23.716558    -2.054552 f=Th
 H    27.356506    23.743600    -2.067007 f=Th
 C    24.987683    22.236778     0.789041 f=Th
 H    24.893503    22.203574     1.877209 f=Th
 H    24.064604    22.661076     0.385989 f=Th
 H    25.048904    21.204938     0.430768 f=Th
 C    26.827615    28.441463     1.316750 f=A
 H    27.085837    27.949098     0.386075 f=A
 C    27.820063    28.983913     2.131822 f=A
 H    28.865567    28.874316     1.869306 f=A
 C    27.470234    29.689727     3.274113 f=A
 H    28.253011    30.128912     3.882477 f=A
 C    26.133457    29.867310     3.638993 f=A
 C    25.150973    29.272326     2.846033 f=A
 H    24.105505    29.373111     3.116053 f=A
 C    25.490418    28.582979     1.686483 f=A
 H    24.702520    28.189350     1.055050 f=A
 C    25.764723    30.726492     4.805827 f=A
 H    24.755135    30.515800     5.157193 f=A
 H    26.459298    30.603577     5.638495 f=A
 H    25.799387    31.780010     4.512007 f=A
```

Optimised geometry of η^6-4-Th-endo and the name of the fragment f in the ETS-NOCV in which each atom belongs

```
 C    -0.405504    20.474935     6.472660 f=B
 H    -0.451964    19.897584     7.391840 f=B
 C    -1.580961    20.887258     5.843236 f=B
 H    -2.548584    20.589392     6.230125 f=B
 C    -1.525375    21.714859     4.730646 f=B
 H    -2.437800    22.049040     4.254497 f=B
 C    -0.289387    22.128361     4.248432 f=B
 C     0.890761    21.705107     4.846807 f=B
 H     1.848502    22.028407     4.460721 f=B
 C     0.828943    20.882566     5.963866 f=B
 H     1.751910    20.590332     6.451028 f=B
Br    -0.214734    23.294165     2.778681 f=B
 O    -0.137029    15.618435     3.854669 f=Th
Th    -0.207254    17.846730     4.922957 f=Th
Si    -0.118522    15.157580     7.798293 f=Th
 N    -2.193952    17.020068     4.221336 f=Th
 N     1.830457    17.131702     4.248284 f=Th
 C    -2.590922    13.195811     2.629948 f=Th
 H    -2.649661    12.196827     2.222161 f=Th
 C    -3.759238    13.920825     2.819720 f=Th
 C    -3.667255    15.213281     3.349689 f=Th
 H    -4.558044    15.812622     3.494180 f=Th
 C    -2.438551    15.756988     3.687913 f=Th
 C     2.153015    15.892179     3.702890 f=Th
 C     3.412718    15.428971     3.359864 f=Th
 H     4.264951    16.080615     3.510567 f=Th
 C     3.584121    14.146308     2.825456 f=Th
 C     2.462686    13.351421     2.632720 f=Th
 H     2.583210    12.359043     2.222378 f=Th
 C    -0.052978    12.900052     2.731413 f=Th
 C    -1.326425    13.706023     2.946988 f=Th
 C    -1.306004    14.970620     3.477839 f=Th
 C     1.070082    15.041016     3.483720 f=Th
 C     1.168536    13.781983     2.949052 f=Th
 C    -0.017853    11.736482     3.735730 f=Th
 H    -0.029700    12.103119     4.763913 f=Th
 H     0.885644    11.139244     3.596541 f=Th
 H    -0.882813    11.084915     3.595519 f=Th
 C    -0.034995    12.340189     1.302920 f=Th
 H    -0.892939    11.689904     1.129312 f=Th
 H     0.861273    11.743464     1.130502 f=Th
 H    -0.059071    13.144276     0.565289 f=Th
 C    -5.133420    13.357466     2.459291 f=Th
 C    -6.023893    13.339843     3.706953 f=Th
 H    -5.581815    12.728508     4.497247 f=Th
 H    -7.003768    12.922166     3.462486 f=Th
 H    -6.185632    14.343492     4.105414 f=Th
 C    -5.780717    14.244655     1.389207 f=Th
 H    -5.918110    15.270121     1.739052 f=Th
 H    -6.765218    13.852638     1.121674 f=Th
 H    -5.170988    14.274494     0.482843 f=Th
 C    -5.051963    11.934404     1.913275 f=Th
 H    -4.461375    11.881833     0.995315 f=Th
 H    -6.056915    11.579727     1.675306 f=Th
 H    -4.624376    11.241402     2.642110 f=Th
 C     4.991460    13.666076     2.472793 f=Th
 C     5.605641    14.606920     1.429624 f=Th
 H     6.611113    14.269476     1.165878 f=Th
 H     5.689967    15.629811     1.802986 f=Th
 H     5.005237    14.626711     0.516798 f=Th
 C     5.863277    13.672319     3.733919 f=Th
 H     5.445883    13.018721     4.503511 f=Th
 H     5.958830    14.674531     4.156801 f=Th
 H     6.869528    13.318038     3.496458 f=Th
 C     4.995106    12.251723     1.898777 f=Th
 H     4.601785    11.521239     2.610039 f=Th
 H     6.020457    11.958932     1.663655 f=Th
 H     4.415627    12.184283     0.974691 f=Th
```

C	-3.237475	17.989542	4.256989	f=Th
C	-4.030672	18.149565	5.415555	f=Th
C	-5.001467	19.147346	5.425738	f=Th
H	-5.621181	19.275276	6.305987	f=Th
C	-5.207280	19.962933	4.328997	f=Th
H	-5.976300	20.726544	4.355224	f=Th
C	-4.442450	19.787016	3.189331	f=Th
H	-4.626331	20.416672	2.326806	f=Th
C	-3.455403	18.810081	3.123461	f=Th
C	-2.699432	18.621235	1.823636	f=Th
H	-1.814047	18.009960	2.034213	f=Th
C	-3.546606	17.848541	0.810246	f=Th
H	-3.840670	16.870516	1.190998	f=Th
H	-2.986463	17.698609	-0.115853	f=Th
H	-4.453714	18.407897	0.566263	f=Th
C	-2.233279	19.937665	1.209300	f=Th
H	-3.075021	20.541094	0.863108	f=Th
H	-1.603845	19.742514	0.338989	f=Th
H	-1.658794	20.545727	1.911388	f=Th
C	-3.908763	17.243891	6.622137	f=Th
H	-3.024594	16.619234	6.479860	f=Th
C	-5.115906	16.310986	6.727828	f=Th
H	-6.041430	16.878823	6.853081	f=Th
H	-5.010901	15.650904	7.592229	f=Th
H	-5.217683	15.685165	5.840912	f=Th
C	-3.743717	18.023576	7.925264	f=Th
H	-2.909258	18.729106	7.886016	f=Th
H	-3.560794	17.337950	8.755902	f=Th
H	-4.642262	18.594119	8.171093	f=Th
C	2.801737	18.172617	4.277836	f=Th
C	2.987104	18.971199	3.124594	f=Th
C	3.880039	20.034852	3.186067	f=Th
H	4.035063	20.650536	2.307169	f=Th
C	4.586737	20.313735	4.342532	f=Th
H	5.281749	21.145330	4.368413	f=Th
C	4.424848	19.510406	5.456396	f=Th
H	5.008658	19.715130	6.346571	f=Th
C	3.550639	18.426862	5.449285	f=Th
C	3.499367	17.521187	6.661331	f=Th
H	2.662577	16.833095	6.525282	f=Th
C	4.772863	16.678442	6.753621	f=Th
H	4.912909	16.065453	5.862802	f=Th
H	4.723898	16.009073	7.615874	f=Th
H	5.654796	17.312999	6.873193	f=Th
C	3.289628	18.282035	7.968393	f=Th
H	4.139740	18.926328	8.203837	f=Th
H	3.179184	17.580687	8.798633	f=Th
H	2.396106	18.911775	7.947592	f=Th
C	2.292167	18.676893	1.811438	f=Th
H	1.574111	17.869313	1.983082	f=Th
C	1.528826	19.884834	1.276874	f=Th
H	0.798356	20.263812	1.996235	f=Th
H	0.994162	19.621003	0.361992	f=Th
H	2.200758	20.710783	1.033392	f=Th
C	3.290381	18.176866	0.766672	f=Th
H	4.036423	18.942970	0.540609	f=Th
H	2.773134	17.930509	-0.163594	f=Th
H	3.813374	17.283323	1.109274	f=Th
C	-0.186655	16.922252	7.134223	f=Th
H	0.666802	17.451565	7.594321	f=Th
H	-1.089616	17.373716	7.581814	f=Th
C	1.445115	14.287914	7.233342	f=Th
H	1.548189	14.256041	6.145824	f=Th
H	1.438215	13.255484	7.595246	f=Th
H	2.341017	14.763455	7.640635	f=Th
C	-0.122014	15.200019	9.675767	f=Th
H	0.740214	15.748334	10.065100	f=Th
H	-0.084483	14.188510	10.090308	f=Th
H	-1.023474	15.682360	10.063522	f=Th
C	-1.613888	14.177721	7.228798	f=Th
H	-2.542246	14.587068	7.635410	f=Th
H	-1.533799	13.147503	7.588106	f=Th
H	-1.712607	14.141432	6.140946	f=Th

Optimised geometry of η^6-5-Th-endo and the name of the fragment f in the ETS-NOCV in which each atom belongs

O	-0.113290	15.647010	3.880077	f=Th
Th	-0.166280	17.900891	4.905746	f=Th
Si	-0.087969	15.235443	7.805776	f=Th
N	-2.165704	17.090403	4.182502	f=Th
N	1.866667	17.148530	4.243142	f=Th
C	-2.582531	13.236490	2.659033	f=Th
H	-2.647753	12.231946	2.266731	f=Th
C	-3.744286	13.977853	2.822147	f=Th
C	-3.642578	15.277400	3.331435	f=Th
H	-4.527883	15.890055	3.450659	f=Th
C	-2.411730	15.815317	3.675216	f=Th
C	2.177651	15.904927	3.703822	f=Th
C	3.429527	15.439816	3.335895	f=Th
H	4.284286	16.093500	3.460955	f=Th
C	3.589099	14.153768	2.806751	f=Th
C	2.463456	13.358168	2.644887	f=Th
H	2.575219	12.362194	2.241297	f=Th
C	-0.051179	12.912731	2.797166	f=Th
C	-1.316937	13.737753	2.983853	f=Th
C	-1.287019	15.010633	3.495873	f=Th
C	1.087975	15.057754	3.505926	f=Th
C	1.175797	13.793946	2.980461	f=Th
C	-0.022519	11.789710	3.847225	f=Th
H	-0.029347	12.196750	4.860118	f=Th
H	0.876608	11.181124	3.729836	f=Th
H	-0.893001	11.140054	3.734421	f=Th
C	-0.040024	12.295266	1.392980	f=Th
H	-0.902325	11.644219	1.247149	f=Th
H	0.850499	11.684131	1.243645	f=Th
H	-0.059345	13.068393	0.622849	f=Th
C	-5.119217	13.426088	2.446149	f=Th
C	-6.039502	13.454456	3.671479	f=Th
H	-5.623928	12.862134	4.490162	f=Th
H	-7.017604	13.039826	3.415047	f=Th
H	-6.200833	14.471030	4.035639	f=Th
C	-5.727284	14.295041	1.338655	f=Th
H	-5.854070	15.331563	1.658642	f=Th
H	-6.712233	13.912474	1.059194	f=Th
H	-5.097090	14.290747	0.445920	f=Th
C	-5.047940	11.988066	1.939097	f=Th
H	-4.440792	11.902783	1.034528	f=Th
H	-6.053188	11.641543	1.690572	f=Th
H	-4.644479	11.308689	2.694082	f=Th
C	4.988060	13.671321	2.425766	f=Th
C	5.581391	14.610664	1.369169	f=Th
H	6.580098	14.271050	1.083497	f=Th
H	5.675937	15.633130	1.741149	f=Th
H	4.960728	14.632329	0.470099	f=Th
C	5.885668	13.677860	3.668690	f=Th
H	5.484188	13.024211	4.446653	f=Th
H	5.989379	14.680056	4.089744	f=Th
H	6.886933	13.323698	3.410802	f=Th
C	4.978106	12.256545	1.852919	f=Th
H	4.600553	11.526823	2.573438	f=Th
H	5.997753	11.962887	1.595146	f=Th
H	4.377755	12.188769	0.942284	f=Th
C	-3.232968	18.037255	4.205087	f=Th
C	-4.047439	18.169601	5.351552	f=Th

C	-5.047945	19.137940	5.350668	f=Th
H	-5.683965	19.244069	6.222313	f=Th
C	-5.262442	19.950175	4.253546	f=Th
H	-6.053750	20.690938	4.270148	f=Th
C	-4.477767	19.797994	3.123648	f=Th
H	-4.670010	20.423302	2.259974	f=Th
C	-3.461474	18.850414	3.068484	f=Th
C	-2.686820	18.683362	1.775485	f=Th
H	-1.760730	18.142998	2.005339	f=Th
C	-3.470813	17.825691	0.779073	f=Th
H	-3.694297	16.837867	1.180846	f=Th
H	-2.897702	17.696742	-0.142317	f=Th
H	-4.415323	18.311951	0.520501	f=Th
C	-2.312948	20.009436	1.119460	f=Th
H	-3.194104	20.538000	0.749816	f=Th
H	-1.669647	19.828636	0.256191	f=Th
H	-1.782123	20.680727	1.796939	f=Th
C	-3.918135	17.263826	6.558240	f=Th
H	-3.021209	16.656145	6.422648	f=Th
C	-5.108788	16.309217	6.655917	f=Th
H	-6.045253	16.859893	6.776672	f=Th
H	-4.996685	15.650719	7.520671	f=Th
H	-5.194104	15.681975	5.768721	f=Th
C	-3.777868	18.042059	7.864942	f=Th
H	-2.946677	18.750839	7.837847	f=Th
H	-3.603172	17.355608	8.696696	f=Th
H	-4.683927	18.606127	8.098320	f=Th
C	2.840200	18.187015	4.265407	f=Th
C	3.047763	18.953298	3.095430	f=Th
C	3.896610	20.052422	3.158550	f=Th
H	4.059220	20.652462	2.270186	f=Th
C	4.546634	20.388381	4.333813	f=Th
H	5.202499	21.250933	4.365176	f=Th
C	4.386708	19.598153	5.458293	f=Th
H	4.940889	19.840506	6.357663	f=Th
C	3.556916	18.479574	5.448482	f=Th
C	3.541588	17.557385	6.650437	f=Th
H	2.690467	16.882410	6.539847	f=Th
C	4.807905	16.696664	6.659002	f=Th
H	4.896362	16.103399	5.748857	f=Th
H	4.792615	16.007682	7.506909	f=Th
H	5.701321	17.320076	6.749304	f=Th
C	3.412374	18.278769	7.988585	f=Th
H	4.275761	18.914900	8.195622	f=Th
H	3.352749	17.549112	8.799206	f=Th
H	2.518608	18.904182	8.048089	f=Th
C	2.400678	18.593323	1.773874	f=Th
H	1.888765	17.637203	1.900539	f=Th
C	1.363050	19.627863	1.350755	f=Th
H	0.560101	19.731821	2.088269	f=Th
H	0.901674	19.343836	0.402473	f=Th
H	1.808500	20.617403	1.223588	f=Th
C	3.442791	18.400287	0.673786	f=Th
H	3.967942	19.330621	0.445382	f=Th
H	2.959241	18.061882	-0.245333	f=Th
H	4.185743	17.653395	0.957927	f=Th
C	-0.160675	16.994646	7.128982	f=Th
H	0.680462	17.537292	7.596724	f=Th
H	-1.072379	17.438398	7.565636	f=Th
C	1.477541	14.358441	7.256920	f=Th
H	1.590072	14.320769	6.170590	f=Th
H	1.464248	13.327870	7.623986	f=Th
H	2.371390	14.832884	7.669985	f=Th
C	-0.097001	15.293656	9.683222	f=Th
H	0.763556	15.846266	10.070285	f=Th
H	-0.059517	14.285856	10.106740	f=Th
H	-1.000217	15.778226	10.064110	f=Th
C	-1.582102	14.249737	7.242728	f=Th
H	-2.510253	14.662636	7.646296	f=Th
H	-1.502411	13.222293	7.609940	f=Th
H	-1.681352	14.205223	6.155251	f=Th
C	-0.653737	20.458107	6.769763	f=F
H	-0.802646	20.044086	7.759425	f=F
C	-1.744219	20.879930	6.011475	f=F
H	-2.752289	20.766436	6.389852	f=F
C	-1.551659	21.460755	4.766006	f=F
H	-2.387660	21.804933	4.170855	f=F
C	-0.257589	21.607648	4.291723	f=F
C	0.846552	21.174993	5.010291	f=F
H	1.845147	21.305425	4.609919	f=F
C	0.637143	20.613982	6.267054	f=F
H	1.496325	20.321749	6.858551	f=F
F	-0.068418	22.190126	3.114084	f=F

Optimised geometry of η^1-5-Th-vertical and the name of the fragment f in the ETS-NOCV in which each atom belongs

F	3.119340	-0.636733	0.186344	f=F
C	2.014853	-0.687149	1.035935	f=F
C	1.700597	0.445550	1.745456	f=F
C	0.593352	0.379012	2.581655	f=F
C	-0.145619	-0.791110	2.675385	f=F
C	0.212898	-1.907548	1.933512	f=F
C	1.315831	-1.867080	1.090968	f=F
H	-1.008557	-0.832425	3.328262	f=F
H	0.310538	1.251594	3.157492	f=F
H	2.291261	1.348372	1.649296	f=F
H	1.616679	-2.720310	0.496932	f=F
H	-0.367118	-2.819419	2.004548	f=F
C	4.109276	1.348825	-3.220747	f=Th
C	5.101309	0.353378	-3.075817	f=Th
C	4.981896	-0.877438	-3.766851	f=Th
C	3.868138	-1.085298	-4.570686	f=Th
C	2.884339	-0.121193	-4.700504	f=Th
C	3.009147	1.080217	-4.030536	f=Th
N	6.200583	0.550602	-2.193367	f=Th
C	7.470551	0.855122	-2.671320	f=Th
C	8.509243	0.643006	-1.763948	f=Th
C	9.836814	0.844015	-2.042634	f=Th
C	10.123126	1.343938	-3.319057	f=Th
C	9.135744	1.602238	-4.260843	f=Th
C	7.802587	1.338081	-3.925835	f=Th
O	8.054338	0.176101	-0.536288	f=Th
C	8.991264	-0.369642	0.333479	f=Th
C	10.344190	-0.245064	0.146417	f=Th
C	10.923629	0.553459	-1.015309	f=Th
C	11.152432	-0.871807	1.102749	f=Th
C	10.628904	-1.591390	2.168493	f=Th
C	9.237881	-1.679481	2.302074	f=Th
C	8.397146	-1.065383	1.387935	f=Th
Th	5.638157	-0.067164	-0.105750	f=Th
N	7.006346	-1.067641	1.375915	f=Th
C	6.241745	-1.808171	2.321446	f=Th
C	5.901495	-1.245931	3.574189	f=Th
C	5.120501	-1.993551	4.449196	f=Th
C	4.665589	-3.253578	4.113293	f=Th
C	4.984336	-3.792908	2.881007	f=Th
C	5.771922	-3.098067	1.968828	f=Th
C	11.477026	1.884262	-0.478818	f=Th
C	12.059239	-0.237780	-1.675428	f=Th
C	11.521915	-2.305854	3.182466	f=Th
C	11.251282	-3.813960	3.113269	f=Th
C	9.457161	2.164247	-5.645014	f=Th
C	8.740421	3.508102	-5.823638	f=Th
C	6.373052	0.122556	4.013963	f=Th

C	7.475555	0.022295	5.068638	f=Th
C	6.161005	-3.775823	0.668605	f=Th
C	7.457071	-4.571961	0.836244	f=Th
C	6.039514	-1.958288	-3.692289	f=Th
C	5.447996	-3.309395	-3.300225	f=Th
C	4.234459	2.718295	-2.590626	f=Th
C	4.590786	3.765419	-3.646902	f=Th
C	5.380478	2.084610	0.936174	f=Th
Si	6.586760	3.519221	1.137846	f=Th
C	5.733265	4.944052	2.014684	f=Th
C	8.068775	2.997617	2.165803	f=Th
C	7.185553	4.128737	-0.532651	f=Th
C	13.006470	-2.074558	2.913146	f=Th
C	11.209640	-1.801578	4.595647	f=Th
C	10.952872	2.391555	-5.846906	f=Th
C	8.972531	1.185563	-6.721003	f=Th
C	5.227287	0.979348	4.552066	f=Th
C	5.067161	-4.677179	0.106418	f=Th
C	6.802168	-2.077842	-5.011726	f=Th
C	2.973444	3.136102	-1.837771	f=Th
H	12.224542	-0.790430	0.997994	f=Th
H	8.797646	-2.244560	3.114924	f=Th
H	7.009004	1.505719	-4.644286	f=Th
H	11.155768	1.536107	-3.572384	f=Th
H	10.691904	2.475491	-0.003748	f=Th
H	11.903692	2.474509	-1.292638	f=Th
H	12.260406	1.700796	0.259655	f=Th
H	12.861150	-0.435421	-0.963686	f=Th
H	12.497338	0.325262	-2.499861	f=Th
H	11.700636	-1.192661	-2.063707	f=Th
H	11.371860	-0.723895	4.674046	f=Th
H	11.859943	-2.295894	5.321670	f=Th
H	10.178051	-2.011493	4.885263	f=Th
H	10.210704	-4.050631	3.345842	f=Th
H	11.880578	-4.342493	3.833882	f=Th
H	11.473106	-4.206509	2.117891	f=Th
H	13.309291	-2.456498	1.935134	f=Th
H	13.597312	-2.600926	3.665640	f=Th
H	13.271260	-1.015787	2.970150	f=Th
H	9.199021	1.578924	-7.715184	f=Th
H	7.893633	1.023996	-6.669715	f=Th
H	9.466364	0.215883	-6.620761	f=Th
H	9.062271	4.227903	-5.067339	f=Th
H	7.655977	3.403263	-5.749219	f=Th
H	8.965376	3.925969	-6.808159	f=Th
H	11.356882	3.110821	-5.130232	f=Th
H	11.126408	2.794355	-6.846933	f=Th
H	11.522107	1.462210	-5.765337	f=Th
H	4.864216	-1.577139	5.416301	f=Th
H	4.059349	-3.818053	4.812273	f=Th
H	4.622356	-4.781875	2.630661	f=Th
H	6.371557	-2.996093	-0.078895	f=Th
H	8.282693	-3.938901	1.161342	f=Th
H	7.739590	-5.044894	-0.107411	f=Th
H	7.318435	-5.360952	1.580171	f=Th
H	4.910659	-5.557293	0.732995	f=Th
H	5.353072	-5.041284	-0.881110	f=Th
H	4.108492	-4.159270	0.015172	f=Th
H	6.796481	0.623345	3.140931	f=Th
H	7.115790	-0.498071	5.960250	f=Th
H	7.798398	1.020792	5.373451	f=Th
H	8.348981	-0.508823	4.691395	f=Th
H	4.368458	0.995917	3.876609	f=Th
H	5.564066	2.007833	4.701832	f=Th
H	4.873618	0.614392	5.519097	f=Th
H	3.769718	-2.019910	-5.111020	f=Th
H	2.023116	-0.304910	-5.332371	f=Th
H	2.243110	1.837275	-4.151726	f=Th
H	5.063609	2.682650	-1.880322	f=Th
H	5.530565	3.525093	-4.146533	f=Th
H	4.697625	4.751023	-3.187300	f=Th
H	3.809476	3.834332	-4.408152	f=Th
H	2.134978	3.306497	-2.516800	f=Th
H	3.146004	4.070953	-1.299125	f=Th
H	2.654951	2.379898	-1.114592	f=Th
H	6.764722	-1.670735	-2.924705	f=Th
H	4.858407	-3.246758	-2.382183	f=Th
H	6.244384	-4.041422	-3.146204	f=Th
H	4.792273	-3.702770	-4.080098	f=Th
H	6.129983	-2.365536	-5.824199	f=Th
H	7.578559	-2.842665	-4.933536	f=Th
H	7.280938	-1.136547	-5.283185	f=Th
H	4.495565	2.496989	0.419390	f=Th
H	5.041364	1.824459	1.953486	f=Th
H	7.682408	3.350048	-1.117148	f=Th
H	7.903993	4.941016	-0.388200	f=Th
H	6.366284	4.528934	-1.135367	f=Th
H	4.873490	5.305651	1.443879	f=Th
H	6.416696	5.787062	2.151182	f=Th
H	5.373528	4.646483	3.003464	f=Th
H	7.785475	2.771763	3.196918	f=Th
H	8.793504	3.816215	2.204449	f=Th
H	8.582200	2.121517	1.760960	f=Th

Optimised geometry of η^1-6-Th-vertical and the name of the fragment f in the ETS-NOCV in which each atom belongs

C	4.078764	1.565437	-3.050514	f=Th
C	5.030930	0.527165	-2.946449	f=Th
C	4.836050	-0.691409	-3.642015	f=Th
C	3.684864	-0.846600	-4.403004	f=Th
C	2.734396	0.156473	-4.485450	f=Th
C	2.934893	1.347033	-3.815138	f=Th
N	6.162369	0.670264	-2.095322	f=Th
C	7.430896	0.913081	-2.610829	f=Th
C	8.483694	0.653722	-1.732622	f=Th
C	9.810616	0.795029	-2.047467	f=Th
C	10.084329	1.280235	-3.332383	f=Th
C	9.084245	1.583530	-4.246690	f=Th
C	7.749982	1.380733	-3.874439	f=Th
O	8.040745	0.213266	-0.491716	f=Th
C	8.977886	-0.343145	0.370068	f=Th
C	10.329551	-0.273421	0.150201	f=Th
C	10.913483	0.456930	-1.052797	f=Th
C	11.136795	-0.894597	1.111143	f=Th
C	10.612384	-1.557060	2.212713	f=Th
C	9.222070	-1.594250	2.376417	f=Th
C	8.383198	-0.984963	1.457557	f=Th
Th	5.636555	0.132242	0.028979	f=Th
N	6.993453	-0.939845	1.471774	f=Th
C	6.220227	-1.657165	2.427791	f=Th
C	5.896511	-1.074947	3.675143	f=Th
C	5.097548	-1.794245	4.558420	f=Th
C	4.613341	-3.046480	4.235518	f=Th
C	4.921946	-3.608331	3.009891	f=Th
C	5.725620	-2.942906	2.090410	f=Th
C	11.577514	1.758740	-0.574766	f=Th
C	11.964343	-0.428668	-1.734546	f=Th
C	11.502358	-2.263437	3.234948	f=Th
C	11.185153	-3.763964	3.223550	f=Th
C	9.392734	2.134550	-5.638229	f=Th
C	8.743624	3.515727	-5.788870	f=Th
C	6.407116	0.283407	4.103825	f=Th
C	7.480844	0.158208	5.185059	f=Th
C	6.103149	-3.642394	0.798155	f=Th

```
 C     7.408332    -4.425175     0.961629 f=Th
 C     5.852038    -1.814352    -3.616612 f=Th
 C     5.228428    -3.148810    -3.215350 f=Th
 C     4.293886     2.930944    -2.434616 f=Th
 C     4.639183     3.956515    -3.515604 f=Th
 C     5.620042     2.325287     1.011215 f=Th
Si     6.938723     3.661012     1.147061 f=Th
 C     6.222560     5.169963     2.007215 f=Th
 C     8.392545     3.044094     2.163031 f=Th
 C     7.541505     4.189147    -0.550068 f=Th
 C    12.987905    -2.087212     2.931452 f=Th
 C    11.232233    -1.700966     4.634799 f=Th
 C    10.891620     2.283058    -5.885091 f=Th
 C     8.824362     1.189687    -6.703267 f=Th
 C     5.280708     1.189373     4.600252 f=Th
 C     5.014271    -4.569271     0.268321 f=Th
 C     6.557403    -1.948440    -4.966379 f=Th
 C     3.093561     3.407109    -1.620197 f=Th
 H    12.208586    -0.853680     0.980892 f=Th
 H     8.780525    -2.116841     3.216411 f=Th
 H     6.945245     1.587587    -4.569907 f=Th
 H    11.117635     1.425217    -3.613421 f=Th
 H    10.853809     2.414681    -0.087310 f=Th
 H    12.011851     2.297453    -1.419600 f=Th
 H    12.375117     1.540513     0.138528 f=Th
 H    12.777492    -0.666422    -1.048109 f=Th
 H    12.406044     0.081888    -2.590747 f=Th
 H    11.523895    -1.364632    -2.082675 f=Th
 H    11.427004    -0.626483     4.671786 f=Th
 H    11.881587    -2.188819     5.366067 f=Th
 H    10.200708    -1.869758     4.950247 f=Th
 H    10.142049    -3.960210     3.481174 f=Th
 H    11.810755    -4.286365     3.951852 f=Th
 H    11.377434    -4.197386     2.239015 f=Th
 H    13.261049    -2.512648     1.962659 f=Th
 H    13.576756    -2.604336     3.691920 f=Th
 H    13.284984    -1.035580     2.945536 f=Th
 H     9.043208     1.575581    -7.702110 f=Th
 H     7.740150     1.087110    -6.621436 f=Th
 H     9.267039     0.193917    -6.621330 f=Th
 H     9.127029     4.212860    -5.040090 f=Th
 H     7.658080     3.468032    -5.680088 f=Th
 H     8.959433     3.926795    -6.778373 f=Th
 H    11.354732     2.977804    -5.180085 f=Th
 H    11.056027     2.679185    -6.889378 f=Th
 H    11.412924     1.324563    -5.821879 f=Th
 H     4.853451    -1.362474     5.522080 f=Th
 H     3.993886    -3.589217     4.940224 f=Th
 H     4.537993    -4.591784     2.770733 f=Th
 H     6.292596    -2.874550     0.033839 f=Th
 H     8.235989    -3.781799     1.258826 f=Th
 H     7.677063    -4.916187     0.023104 f=Th
 H     7.287128    -5.199781     1.723594 f=Th
 H     4.897848    -5.451873     0.900632 f=Th
 H     5.283562    -4.928152    -0.726187 f=Th
 H     4.042611    -4.074482     0.202487 f=Th
 H     6.869724     0.754782     3.234024 f=Th
 H     7.081457    -0.328732     6.078620 f=Th
 H     7.839505     1.148091     5.477433 f=Th
 H     8.338687    -0.417041     4.837217 f=Th
 H     4.450282     1.244452     3.892156 f=Th
 H     5.655793     2.202610     4.762568 f=Th
 H     4.876331     0.840262     5.553245 f=Th
 H     3.529299    -1.770865    -4.947950 f=Th
 H     1.842714     0.012878    -5.084808 f=Th
 H     2.198488     2.137326    -3.904363 f=Th
 H     5.157083     2.863906    -1.768336 f=Th
 H     5.536758     3.669606    -4.065705 f=Th
 H     4.818721     4.936989    -3.067869 f=Th
 H     3.820816     4.060831    -4.232634 f=Th
 H     2.222873     3.591417    -2.253632 f=Th
 H     3.327995     4.346190    -1.113450 f=Th
 H     2.794779     2.680269    -0.859331 f=Th
 H     6.615762    -1.562552    -2.874836 f=Th
 H     4.691691    -3.081667    -2.266555 f=Th
 H     6.004046    -3.911970    -3.115653 f=Th
 H     4.521149    -3.503737    -3.968456 f=Th
 H     5.844227    -2.205432    -5.753937 f=Th
 H     7.308716    -2.740665    -4.924660 f=Th
 H     7.058284    -1.022465    -5.249815 f=Th
 H     4.747326     2.800377     0.530224 f=Th
 H     5.297204     2.117033     2.045484 f=Th
 H     7.979068     3.367171    -1.122148 f=Th
 H     8.307811     4.962700    -0.444202 f=Th
 H     6.732680     4.618500    -1.147378 f=Th
 H     5.381798     5.586728     1.445801 f=Th
 H     6.974278     5.957904     2.109915 f=Th
 H     5.861564     4.923797     3.009556 f=Th
 H     8.099523     2.844076     3.197231 f=Th
 H     9.175338     3.807654     2.193349 f=Th
 H     8.837228     2.130146     1.760861 f=Th
 F     3.345025    -1.481475    -0.490926 f=F
 C     2.119049    -1.320570     0.075798 f=F
 C     1.980962    -0.294753     0.983390 f=F
 C     0.784881    -0.050183     1.611934 f=F
 C    -0.288853    -0.875503     1.301136 f=F
 C    -0.149713    -1.908246     0.384984 f=F
 C     1.067182    -2.143236    -0.243382 f=F
 H    -1.243297    -0.704784     1.782551 f=F
 H     0.701750     0.763088     2.321850 f=F
 F     3.078675     0.469421     1.224273 f=F
 H     1.200370    -2.939922    -0.964282 f=F
 H    -0.996023    -2.541678     0.151729 f=F
```

Optimised geometry of η^6-6-Th-exo and the name of the fragment f in the ETS-NOCV in which each atom belongs

```
Th      -0.281113      17.831764      4.911994       f=Th    C      2.47734 13.379133      2.641788       f=Th
C       -0.248155      16.989317      7.160963       f=Th    C      3.57822 14.209343      2.802916       f=Th
Si      -0.24196       15.23722       7.860108       f=Th    C      3.380938       15.488882      3.334663       f=Th
C       -1.754947      14.280659      7.296585       f=Th    C      2.115015       15.92237       3.69658 f=Th
O       -0.164173      15.574553      3.903963       f=Th    C      -5.100945      13.269596      2.369893       f=Th
C       -1.318106      14.91378       3.501055       f=Th    C      -4.988055      11.860749      1.793468       f=Th
C       -1.312083      13.649344      2.969776       f=Th    N      -2.241223      16.948176      4.2235  f=Th
C       -0.022972      12.855171      2.808123       f=Th    C      -3.245783      17.954284      4.205437       f=Th
C       1.179131       13.774005      2.984742       f=Th    C      -3.991708      18.246676      5.372253       f=Th
C       1.054975       15.034538      3.512378       f=Th    C      -4.865779      19.330257      5.345308       f=Th
C       -2.464197      15.689364      3.676764       f=Th    C      -5.040672      20.088579      4.20115 f=Th
C       -3.676546      15.142323      3.290531       f=Th    C      -4.347868      19.763923      3.048091       f=Th
C       -3.741652      13.848166      2.76099 f=Th           C      -3.44775       18.704281      3.022264       f=Th
C       -2.562585      13.130362      2.612753       f=Th    N      1.76643 17.166117      4.218433       f=Th
```

```
C       2.732905        18.210672       4.294504        f=Th
C       2.856484        19.118901       3.212685        f=Th
C       3.778295        20.154575       3.317757        f=Th
C       4.572619        20.301384       4.440955        f=Th
C       4.452285        19.408963       5.488504        f=Th
C       3.542185        18.356762       5.444033        f=Th
C       4.986747        13.778283       2.395037        f=Th
C       5.026606        12.343647       1.875173        f=Th
C       0.02478 11.756221       3.883116        f=Th
C       0.017556        12.207192       1.419024        f=Th
C       -3.951601       17.358069       6.598062        f=Th
C       -3.92761        18.122359       7.918485        f=Th
C       -2.748502       18.370494       1.721278        f=Th
C       -1.914368       19.539057       1.205064        f=Th
C       2.075338        18.957791       1.92197 f=Th
C       2.849176        18.099312       0.918023        f=Th
C       3.497213        17.389482       6.607388        f=Th
C       3.326807        18.101479       7.948185        f=Th
C       1.303546        14.318728       7.321671        f=Th
C       -0.260035       15.312201       9.736378        f=Th
C       -6.001784       13.209024       3.609237        f=Th
C       -5.75538        14.166961       1.313112        f=Th
C       5.493951        14.7054 1.283616        f=Th
C       5.927876        13.874592       3.600798        f=Th
C       -3.751143       17.921202       0.658789        f=Th
C       -5.146988       16.401185       6.586023        f=Th
C       4.750558        16.514524       6.649415        f=Th
C       1.699775        20.283493       1.26817 f=Th
H       -2.602629       12.130476       2.205642        f=Th
H       -4.575276       15.736566       3.404082        f=Th
H       4.215594        16.169515       3.451285        f=Th
H       2.619199        12.38852        2.234932        f=Th
H       -0.004211       12.18446        4.886884        f=Th
H       0.941742        11.170719       3.788102        f=Th
H       -0.826733       11.080924       3.775273        f=Th
H       -0.826217       11.530886       1.280256        f=Th
H       0.923554        11.614261       1.292158        f=Th
H       -0.012956       12.961481       0.630822        f=Th
H       -5.559367       12.580722       4.385874        f=Th
H       -6.975508       12.7884 3.345799        f=Th
H       -6.174942       14.199875       4.034494        f=Th
H       -5.927582       15.178463       1.687297        f=Th
H       -6.724998       13.756196       1.020849        f=Th
H       -5.133574       14.236883       0.41727 f=Th
H       -4.378992       11.838134       0.886366        f=Th
H       -5.982982       11.496944       1.52869 f=Th
H       -4.564572       11.157096       2.514345        f=Th
H       6.502625        14.412677       0.981197        f=Th
H       5.535299        15.746676       1.61056 f=Th
H       4.848104        14.652528       0.403747        f=Th
H       5.581759        13.242885       4.422376        f=Th
H       6.012054        14.898128       3.971398        f=Th
H       6.931326        13.545533       3.319558        f=Th
H       4.695699        11.626595       2.630632        f=Th
H       6.052482        12.084893       1.605048        f=Th
H       4.412005        12.215142       0.980827        f=Th
H       -5.44129        19.570313       6.231481        f=Th
H       -5.734165       20.921685       4.202689        f=Th
H       -4.512585       20.344411       2.147274        f=Th
H       -2.075264       17.529096       1.904839        f=Th
H       -4.329667       17.060317       0.996199        f=Th
H       -3.228245       17.638182       -0.257597       f=Th
H       -4.449483       18.723644       0.408664        f=Th
H       -2.535591       20.406589       0.971254        f=Th
H       -1.388597       19.255214       0.29084 f=Th
H       -1.166225       19.866104       1.933001        f=Th
H       -3.04863        16.747082       6.536484        f=Th
H       -6.088161       16.956609       6.613188        f=Th
H       -5.118174       15.746689       7.460443        f=Th
H       -5.147701       15.77017        5.697109        f=Th
H       -3.117166       18.853664       7.974199        f=Th
H       -3.797397       17.424474       8.748503        f=Th
H       -4.862626       18.657729       8.09746 f=Th
H       3.886251        20.857989       2.502037        f=Th
H       5.29168 21.110866       4.493911        f=Th
H       5.088496        19.52232        6.358975        f=Th
H       2.640493        16.729379       6.457757        f=Th
H       4.861795        15.92641        5.738864        f=Th
H       4.698659        15.819438       7.490939        f=Th
H       5.649484        17.123481       6.775975        f=Th
H       4.211344        18.687144       8.208871        f=Th
H       3.177128        17.372161       8.74767 f=Th
H       2.471649        18.781537       7.948544        f=Th
H       1.146756        18.416474       2.151127        f=Th
H       1.201931        20.969888       1.955569        f=Th
H       1.030363        20.104885       0.425196        f=Th
H       2.577412        20.795753       0.868861        f=Th
H       3.796011        18.582884       0.6631  f=Th
H       2.273597        17.98332        -0.003543       f=Th
H       3.068113        17.106852       1.310168        f=Th
H       0.643776        17.48359        7.584048        f=Th
H       -1.114091       17.499365       7.62023 f=Th
H       1.42187 14.278972       6.235756        f=Th
H       1.26273 13.288474       7.687351        f=Th
H       2.206297        14.771139       7.740047        f=Th
H       0.612141        15.845947       10.123696       f=Th
H       -0.251521       14.307574       10.168866       f=Th
H       -1.152619       15.823456       10.107362       f=Th
H       -2.677746       14.715474       7.688992        f=Th
H       -1.698561       13.255714       7.675054        f=Th
H       -1.84645        14.226011       6.208844        f=Th
H     0.595273    20.216477     7.644759 f=F
H    -1.724150    19.942888     6.795392 f=F
H    -2.381456    20.956813     4.618841 f=F
F     1.674463    22.764851     4.116384   f=F
H     2.239873    21.564320     6.332672   f=F
C     1.226557    21.414600     5.981901   f=F
C     0.310571    20.648822     6.693492   f=F
C    -0.983923    20.477976     6.209266   f=F
C    -1.370641    21.058694     4.999987   f=F
C    -0.455906    21.828848     4.306887   f=F
C     0.834873    22.010228     4.799450   f=F
F    -0.797031    22.418000     3.173317   f=F
```

Optimised geometry of η^6-6-Th-side and the name of the fragment f in the ETS-NOCV in which each atom belongs

```
C     3.5195    18.3662     5.4188 f=Th
C     2.7095    18.2118     4.2703 f=Th
C     2.8311    19.1136     3.1830 f=Th
C     3.7529    20.1500     3.2812 f=Th
C     4.5473    20.3045     4.4031 f=Th
C     4.4278    19.4196     5.4563 f=Th
N     1.7483    17.1617     4.2002 f=Th
C     2.1015    15.9165     3.6854 f=Th
C     1.0439    15.0252     3.5055 f=Th
C     1.1700    13.7640     2.9799 f=Th
C     2.4691    13.3710     2.6379 f=Th
C     3.5684    14.2038     2.7982 f=Th
C     3.3687    15.4847     3.3259 f=Th
O    -0.1754    15.5628     3.8986 f=Th
C    -1.3279    14.9029     3.4919 f=Th
C    -1.3210    13.6386     2.9604 f=Th
C    -0.0314    12.8436     2.8055 f=Th
C    -2.5709    13.1211     2.5989 f=Th
```

```
 C    -3.7499    13.8398     2.7440 f=Th
 C    -3.6857    15.1336     3.2747 f=Th
 C    -2.4739    15.6793     3.6644 f=Th
Th    -0.2921    17.8204     4.9105 f=Th
 N    -2.2490    16.9363     4.2129 f=Th
 C    -3.2448    17.9495     4.2049 f=Th
 C    -3.9851    18.2377     5.3762 f=Th
 C    -4.8335    19.3418     5.3692 f=Th
 C    -4.9881    20.1259     4.2400 f=Th
 C    -4.3056    19.8036     3.0799 f=Th
 C    -3.4329    18.7221     3.0337 f=Th
 C     0.0141    11.7507     3.8868 f=Th
 C     0.0124    12.1876     1.4204 f=Th
 C    -5.1084    13.2624     2.3482 f=Th
 C    -5.7586    14.1606     1.2894 f=Th
 C     4.9781    13.7740     2.3931 f=Th
 C     5.9169    13.8740     3.6005 f=Th
 C    -3.9619    17.3294     6.5874 f=Th
 C    -5.1780    16.3993     6.5659 f=Th
 C    -2.7521    18.3861     1.7234 f=Th
 C    -3.7733    17.9355     0.6788 f=Th
 C     2.0465    18.9466     1.8950 f=Th
 C     1.6891    20.2710     1.2282 f=Th
 C     3.4768    17.4061     6.5883 f=Th
 C     4.7386    16.5444     6.6435 f=Th
 C    -0.2605    16.9679     7.1552 f=Th
Si    -0.2301    15.2151     7.8508 f=Th
 C    -0.2439    15.2851     9.7273 f=Th
 C    -1.7380    14.2495     7.2880 f=Th
 C     1.3214    14.3103     7.3068 f=Th
 C    -4.9949    11.8536     1.7718 f=Th
 C    -6.0135    13.2023     3.5845 f=Th
 C     5.0210    12.3385     1.8760 f=Th
 C     5.4858    14.6999     1.2809 f=Th
 C    -3.9160    18.0764     7.9167 f=Th
 C    -1.9251    19.5511     1.1880 f=Th
 C     2.8050    18.0674     0.8976 f=Th
 C     3.2900    18.1265     7.9222 f=Th
 H    -2.6107    12.1214     2.1914 f=Th
 H    -4.5845    15.7280     3.3870 f=Th
 H     4.2016    16.1677     3.4402 f=Th
 H     2.6132    12.3799     2.2330 f=Th
 H    -0.0171    12.1846     4.8881 f=Th
 H     0.9315    11.1650     3.7971 f=Th
 H    -0.8370    11.0745     3.7809 f=Th
 H    -0.8307    11.5099     1.2838 f=Th
 H     0.9189    11.5942     1.2991 f=Th
 H    -0.0167    12.9370     0.6276 f=Th
 H    -5.5740    12.5737     4.3626 f=Th
 H    -6.9866    12.7823     3.3178 f=Th
 H    -6.1875    14.1932     4.0093 f=Th
 H    -5.9312    15.1721     1.6633 f=Th
 H    -6.7276    13.7508     0.9939 f=Th
 H    -5.1337    14.2303     0.3957 f=Th
 H    -4.3829    11.8306     0.8667 f=Th
 H    -5.9893    11.4907     1.5037 f=Th
 H    -4.5744    11.1494     2.4939 f=Th
 H     6.4953    14.4079     0.9806 f=Th
 H     5.5253    15.7418     1.6060 f=Th
 H     4.8413    14.6446     0.4001 f=Th
 H     5.5705    13.2427     4.4223 f=Th
 H     5.9981    14.8982     3.9699 f=Th
 H     6.9216    13.5467     3.3216 f=Th
 H     4.6902    11.6223     2.6323 f=Th
 H     6.0478    12.0809     1.6080 f=Th
 H     4.4080    12.2073     0.9810 f=Th
 H    -5.4020    19.5802     6.2602 f=Th
 H    -5.6589    20.9772     4.2577 f=Th
 H    -4.4601    20.4018     2.1888 f=Th
 H    -2.0765    17.5446     1.8987 f=Th
 H    -4.3453    17.0747     1.0272 f=Th
 H    -3.2672    17.6520    -0.2468 f=Th
 H    -4.4764    18.7380     0.4422 f=Th
 H    -2.5505    20.4168     0.9573 f=Th
 H    -1.4146    19.2622     0.2668 f=Th
 H    -1.1636    19.8763     1.9027 f=Th
 H    -3.0725    16.7000     6.5137 f=Th
 H    -6.1068    16.9744     6.6065 f=Th
 H    -5.1589    15.7307     7.4298 f=Th
 H    -5.1966    15.7825     5.6673 f=Th
 H    -3.0985    18.7999     7.9661 f=Th
 H    -3.7823    17.3685     8.7376 f=Th
 H    -4.8436    18.6188     8.1124 f=Th
 H     3.8599    20.8493     2.4619 f=Th
 H     5.2607    21.1187     4.4541 f=Th
 H     5.0586    19.5444     6.3287 f=Th
 H     2.6277    16.7359     6.4386 f=Th
 H     4.8622    15.9527     5.7367 f=Th
 H     4.6885    15.8534     7.4885 f=Th
 H     5.6304    17.1633     6.7727 f=Th
 H     4.1622    18.7316     8.1793 f=Th
 H     3.1508    17.4015     8.7276 f=Th
 H     2.4232    18.7914     7.9122 f=Th
 H     1.1103    18.4218     2.1321 f=Th
 H     1.2185    20.9737     1.9187 f=Th
 H     1.0044    20.0966     0.3965 f=Th
 H     2.5718    20.7599     0.8112 f=Th
 H     3.7592    18.5336     0.6379 f=Th
 H     2.2269    17.9526    -0.0226 f=Th
 H     3.0088    17.0751     1.2979 f=Th
 H     0.6127    17.4848     7.5906 f=Th
 H    -1.1450    17.4551     7.6034 f=Th
 H     1.4371    14.2727     6.2205 f=Th
 H     1.2899    13.2794     7.6716 f=Th
 H     2.2214    14.7699     7.7231 f=Th
 H     0.6247    15.8256    10.1133 f=Th
 H    -0.2251    14.2796    10.1573 f=Th
 H    -1.1399    15.7876    10.1021 f=Th
 H    -2.6624    14.6777     7.6842 f=Th
 H    -1.6749    13.2235     7.6626 f=Th
 H    -1.8319    14.1982     6.2003 f=Th
 H     0.7754    20.6094     7.8893 f=F
 H    -1.4835    19.9474     7.0719 f=F
 H    -2.2297    20.6287     4.7985 f=F
 F     2.4289    22.0678     6.5455 f=F
 F     1.6304    22.8049     4.0976 f=F
 C     0.8392    22.0435     4.8297 f=F
 C     1.2567    21.6582     6.1014 f=F
 C     0.4416    20.8740     6.8934 f=F
 C    -0.8098    20.4888     6.4165 f=F
 C    -1.2303    20.8749     5.1448 f=F
 C    -0.3931    21.6493     4.3456 f=F
 H    -0.7026    21.9890     3.3647 f=F
```

Optimised geometry of η^6-6-Th-endo and the name of the fragment f in the ETS-NOCV in which each atom belongs

```
C     3.477468    20.142211     3.344767 f=Th
 C     2.559315    19.088440     3.248252 f=Th
 C     2.482665    18.150969     4.324976 f=Th
 C     3.333864    18.289348     5.460652 f=Th
 C     4.236242    19.361504     5.493746 f=Th
 C     4.311560    20.280776     4.452927 f=Th
 C     3.333017    17.302216     6.618655 f=Th
 C     3.195237    17.995976     7.984193 f=Th
```

N	1.507918	17.101124	4.268571	f=Th
Th	-0.533459	17.819405	4.989196	f=Th
C	-0.494988	17.083987	7.276719	f=Th
Si	-0.482609	15.376207	8.107996	f=Th
C	1.053759	14.398616	7.607217	f=Th
C	1.723698	18.942337	1.979396	f=Th
C	2.406115	18.000503	0.967958	f=Th
C	1.839100	15.830115	3.779553	f=Th
C	0.764358	14.932286	3.667148	f=Th
C	0.862964	13.644140	3.174496	f=Th
C	2.153385	13.234344	2.784401	f=Th
C	3.270364	14.073159	2.868375	f=Th
C	3.097551	15.377150	3.372513	f=Th
C	-0.357375	12.718472	3.099807	f=Th
C	-1.643475	13.546403	3.203586	f=Th
C	-1.631659	14.839892	3.690900	f=Th
O	-0.453344	15.498655	4.083853	f=Th
C	-2.908630	13.037519	2.847794	f=Th
C	-4.084463	13.788390	2.958177	f=Th
C	-3.998495	15.106810	3.446703	f=Th
C	-2.768903	15.653939	3.822391	f=Th
C	4.665638	13.622946	2.401651	f=Th
C	5.123397	14.525285	1.234421	f=Th
C	-0.305112	11.726233	4.290288	f=Th
C	-0.342346	11.923108	1.778110	f=Th
C	-5.456847	13.221585	2.555470	f=Th
C	-6.400777	13.241116	3.777006	f=Th
N	-2.524870	16.943124	4.311358	f=Th
C	-3.538014	17.954380	4.283612	f=Th
C	-4.366001	18.182676	5.421733	f=Th
C	-5.277176	19.246833	5.381445	f=Th
C	-5.396175	20.061272	4.258568	f=Th
C	-4.606308	19.814617	3.137509	f=Th
C	-3.674510	18.768702	3.118195	f=Th
C	-4.347827	17.272961	6.641699	f=Th
C	-4.218406	18.042000	7.965791	f=Th
C	-2.895131	18.496221	1.837869	f=Th
C	-2.320864	19.768224	1.198120	f=Th
C	-6.060843	14.091922	1.431800	f=Th
C	-5.366143	11.775274	2.044181	f=Th
C	5.671972	13.748004	3.565123	f=Th
C	4.678044	12.165473	1.914569	f=Th
C	-5.608046	16.387822	6.677836	f=Th
C	-3.770275	17.744425	0.816452	f=Th
C	1.404077	20.277556	1.293683	f=Th
C	4.604262	16.433185	6.610385	f=Th
C	-0.471427	15.585210	9.985197	f=Th
C	-2.017073	14.385438	7.627230	f=Th
H	-2.965340	12.018332	2.472338	f=Th
H	-4.892167	15.726996	3.527480	f=Th
H	3.942490	16.064544	3.428851	f=Th
H	2.277808	12.224434	2.400483	f=Th
H	-0.316346	12.256778	5.252441	f=Th
H	0.611233	11.120656	4.242804	f=Th
H	-1.170897	11.049255	4.261408	f=Th
H	-1.198757	11.239206	1.722583	f=Th
H	0.560458	11.303783	1.703258	f=Th
H	-0.376553	12.593115	0.908300	f=Th
H	-5.993828	12.638059	4.601693	f=Th
H	-7.382474	12.827017	3.503170	f=Th
H	-6.565281	14.261486	4.151325	f=Th
H	-6.206624	15.133379	1.752528	f=Th
H	-7.043305	13.696531	1.133970	f=Th
H	-5.412471	14.096060	0.543285	f=Th
H	-4.733420	11.693771	1.148039	f=Th
H	-6.370083	11.421296	1.770411	f=Th
H	-4.974774	11.091044	2.811444	f=Th
H	6.122432	14.220084	0.889252	f=Th
H	5.182168	15.581774	1.532878	f=Th
H	4.431354	14.450383	0.382782	f=Th
H	5.364892	13.132712	4.423394	f=Th
H	5.774933	14.786671	3.909533	f=Th
H	6.667068	13.408945	3.241206	f=Th
H	4.383026	11.463745	2.708743	f=Th
H	5.695385	11.895208	1.598171	f=Th
H	4.015051	12.013435	1.050113	f=Th
H	-5.921687	19.429277	6.243422	f=Th
H	-6.118018	20.879785	4.249134	f=Th
H	-4.726458	20.442717	2.253369	f=Th
H	-2.051979	17.829057	2.091184	f=Th
H	-4.140740	16.794486	1.221944	f=Th
H	-3.192679	17.525278	-0.093460	f=Th
H	-4.637390	18.357142	0.527336	f=Th
H	-3.113966	20.430876	0.823727	f=Th
H	-1.691045	19.505138	0.336729	f=Th
H	-1.708584	20.351708	1.901867	f=Th
H	-3.478377	16.606637	6.545334	f=Th
H	-6.517675	16.999610	6.772797	f=Th
H	-5.569561	15.706669	7.540479	f=Th
H	-5.700417	15.775681	5.771744	f=Th
H	-3.333090	18.693837	7.984412	f=Th
H	-4.131997	17.337331	8.805462	f=Th
H	-5.100231	18.669656	8.161716	f=Th
H	3.552629	20.866310	2.533384	f=Th
H	5.023729	21.106360	4.500254	f=Th
H	4.896917	19.474033	6.355028	f=Th
H	2.471925	16.631763	6.484291	f=Th
H	4.703074	15.863125	5.678533	f=Th
H	4.576344	15.713996	7.442063	f=Th
H	5.505725	17.052042	6.733456	f=Th
H	4.085104	18.594790	8.226879	f=Th
H	3.085498	17.244483	8.779482	f=Th
H	2.327291	18.668415	8.030274	f=Th
H	0.762601	18.463715	2.257426	f=Th
H	0.978739	21.022373	1.982710	f=Th
H	0.685747	20.118055	0.478692	f=Th
H	2.301666	20.722697	0.841236	f=Th
H	3.378129	18.416970	0.663404	f=Th
H	1.786247	17.895722	0.065420	f=Th
H	2.577976	17.000976	1.384641	f=Th
H	0.392815	17.627078	7.669152	f=Th
H	-1.378263	17.622782	7.686297	f=Th
H	1.156048	14.285857	6.517678	f=Th
H	1.002177	13.388115	8.041568	f=Th
H	1.974959	14.864700	7.986421	f=Th
H	0.415108	16.143120	10.322337	f=Th
H	-0.461987	14.607667	10.491441	f=Th
H	-1.360338	16.131884	10.334409	f=Th
H	-2.938335	14.847574	8.011473	f=Th
H	-1.954808	13.378425	8.068246	f=Th
H	-2.127379	14.263890	6.539381	f=Th
C	-0.440917	20.878248	4.959267	f=F
C	0.686687	20.974758	5.795315	f=F
C	0.499284	21.108800	7.167083	f=F
C	-0.795351	21.136173	7.709972	f=F
C	-1.910581	21.033135	6.885139	f=F
C	-1.736120	20.905798	5.501965	f=F
H	1.701367	20.979875	5.391659	f=F
F	1.549265	21.222137	7.989030	f=F
H	-0.298818	20.869337	3.875138	f=F
F	-0.939957	21.259180	9.032545	f=F
H	-2.904213	21.072415	7.331658	f=F
H	-2.612225	20.862404	4.852201	f=F

Optimised geometry of η^2-E-Th and the name of the fragment f in the ETS-NOCV in which each atom belongs

C	21.847110	13.218075	0.029437	f=Th
C	22.243178	14.460897	-0.521528	f=Th
C	22.901704	15.420206	0.287493	f=Th
C	23.187838	15.096854	1.609350	f=Th
C	22.835709	13.868886	2.140739	f=Th
C	22.165940	12.947590	1.356963	f=Th
N	22.070791	14.724384	-1.905604	f=Th
Th	23.908423	14.003799	-2.987916	f=Th
C	23.084229	11.927646	-3.860379	f=Th
Si	21.697883	11.549284	-5.081391	f=Th
C	20.052949	12.186872	-4.439322	f=Th
C	23.247791	16.804657	-0.217781	f=Th
C	24.701966	17.176531	0.052609	f=Th
C	21.020343	12.216908	-0.746789	f=Th
C	19.548569	12.316697	-0.339403	f=Th
N	24.791161	14.944346	-4.836444	f=Th
C	24.132397	15.719102	-5.786060	f=Th
C	22.797790	16.006050	-5.492148	f=Th
C	21.977409	16.778136	-6.274645	f=Th
C	22.546441	17.274150	-7.453608	f=Th
C	23.863218	17.019077	-7.812680	f=Th
C	24.651912	16.234930	-6.962407	f=Th
C	20.526660	17.045459	-5.891159	f=Th
C	20.293051	16.664835	-4.434125	f=Th
C	21.190648	15.893936	-3.741004	f=Th
O	22.379862	15.435881	-4.295372	f=Th
C	19.143598	17.044362	-3.730178	f=Th
C	18.922276	16.683373	-2.407646	f=Th
C	19.886205	15.908000	-1.752104	f=Th
C	21.032539	15.497390	-2.411557	f=Th
C	24.479529	17.580554	-9.093641	f=Th
C	25.658547	18.491474	-8.730240	f=Th
C	20.194110	18.526593	-6.103935	f=Th
C	19.611404	16.186171	-6.780334	f=Th
C	17.663067	17.102832	-1.650041	f=Th
C	16.725998	17.950498	-2.506254	f=Th
C	26.189652	14.692150	-4.883797	f=Th
C	26.690753	13.547550	-5.549312	f=Th
C	28.059350	13.297847	-5.510715	f=Th
C	28.925987	14.138571	-4.840708	f=Th
C	28.434409	15.256543	-4.190849	f=Th
C	27.077603	15.560784	-4.195965	f=Th
C	25.807251	12.610126	-6.342315	f=Th
C	25.981023	12.834353	-7.845391	f=Th
C	26.608574	16.837360	-3.524103	f=Th
C	27.441588	17.220654	-2.305338	f=Th
C	21.556337	9.693661	-5.327932	f=Th
C	22.046343	12.342433	-6.747187	f=Th
C	16.899678	15.851437	-1.200520	f=Th
C	18.057876	17.924322	-0.417095	f=Th
C	22.313323	17.851305	0.391058	f=Th
C	21.505198	10.778902	-0.582707	f=Th
C	24.982946	16.428185	-9.970074	f=Th
C	23.480451	18.397508	-9.908823	f=Th
C	26.593957	18.005753	-4.513307	f=Th
C	26.067152	11.141571	-6.010772	f=Th
H	18.403131	17.640124	-4.243753	f=Th
H	25.689493	16.036231	-7.202942	f=Th
H	21.930287	17.876857	-8.104671	f=Th
H	19.750293	15.620154	-0.716474	f=Th
H	23.993529	11.452306	-4.266859	f=Th
H	22.845056	11.369858	-2.937494	f=Th
H	19.153008	18.731197	-5.853497	f=Th
H	20.329780	18.810298	-7.147745	f=Th
H	20.828381	19.166539	-5.488042	f=Th
H	15.846936	18.224247	-1.919149	f=Th
H	16.374447	17.407263	-3.386815	f=Th
H	17.201168	18.877693	-2.836083	f=Th
H	26.437082	17.952507	-8.185970	f=Th
H	25.330448	19.329205	-8.109954	f=Th
H	26.111410	18.899364	-9.637442	f=Th
H	18.563102	16.361530	-6.529147	f=Th
H	19.820358	15.122552	-6.649563	f=Th
H	19.759717	16.436451	-7.832991	f=Th
H	25.760654	15.846775	-9.470707	f=Th
H	25.410792	16.820870	-10.895857	f=Th
H	24.168582	15.749217	-10.233900	f=Th
H	15.991836	16.137915	-0.663641	f=Th
H	17.496537	15.229778	-0.529840	f=Th
H	16.608551	15.239948	-2.057803	f=Th
H	23.068753	13.636711	3.173546	f=Th
H	25.312561	10.509711	-6.484817	f=Th
H	26.043652	10.945384	-4.935711	f=Th
H	27.039597	10.810052	-6.381602	f=Th
H	24.769399	12.841190	-6.093934	f=Th
H	25.570389	16.689314	-3.194245	f=Th
H	21.868676	12.000128	1.790645	f=Th
H	22.572295	10.671456	-0.794024	f=Th
H	20.961852	10.120369	-1.263992	f=Th
H	21.331968	10.403863	0.428502	f=Th
H	22.624717	17.796978	-10.227329	f=Th
H	23.969559	18.773129	-10.809929	f=Th
H	23.110702	19.262915	-9.353352	f=Th
H	29.988937	13.926889	-4.827043	f=Th
H	23.086883	16.821504	-1.300458	f=Th
H	29.126347	15.909962	-3.675236	f=Th
H	19.148036	13.314623	-0.520607	f=Th
H	19.422387	12.085167	0.721474	f=Th
H	18.947403	11.606121	-0.911614	f=Th
H	25.724413	13.853382	-8.134541	f=Th
H	25.334249	12.155574	-8.406482	f=Th
H	27.012710	12.640642	-8.150600	f=Th
H	23.686132	15.824214	2.239806	f=Th
H	28.453622	12.429123	-6.024642	f=Th
H	21.083964	12.484010	-1.803559	f=Th
H	17.163515	18.234697	0.128871	f=Th
H	18.608267	18.823708	-0.703960	f=Th
H	18.680543	17.350762	0.272926	f=Th
H	20.066910	13.256462	-4.213680	f=Th
H	19.737427	11.657622	-3.536595	f=Th
H	19.279202	12.019808	-5.194489	f=Th
H	22.484145	9.270753	-5.722601	f=Th
H	20.756016	9.451336	-6.033046	f=Th
H	21.334188	9.182422	-4.387272	f=Th
H	25.940680	17.813661	-5.363341	f=Th
H	27.603240	18.189088	-4.891442	f=Th
H	26.250345	18.917060	-4.017965	f=Th
H	27.553807	16.398692	-1.593680	f=Th
H	26.974557	18.057049	-1.783747	f=Th
H	28.442603	17.549106	-2.592028	f=Th
H	22.925911	11.905868	-7.227014	f=Th
H	22.201166	13.422959	-6.683780	f=Th
H	21.198410	12.170292	-7.416715	f=Th
H	22.547077	18.843158	-0.002793	f=Th
H	22.425484	17.886803	1.477719	f=Th
H	21.269054	17.635469	0.163155	f=Th
H	24.933030	18.145381	-0.394781	f=Th
H	25.399094	16.440821	-0.357896	f=Th
H	24.906711	17.257959	1.122191	f=Th
C	26.471504	12.963033	-1.559296	f=F
C	25.496519	12.651090	-0.702519	f=F
H	25.203156	13.312913	0.108506	f=F
H	24.991800	11.689823	-0.748135	f=F
H	26.798991	12.274123	-2.333134	f=F
H	27.024737	13.894649	-1.485349	f=F

A.1.5 Optimised geometries of Alkyl cations containing Uranium

Optimised geometry of η^6-2-U

U	26.800801	13.592814	-5.510886
C	25.491564	16.354392	-4.125418
C	27.859184	16.450443	-4.100940
C	25.374046	17.619561	-3.607720
C	26.584983	18.512217	-3.372946
C	27.866905	17.717483	-3.576799
O	26.704269	15.785651	-4.471938
Si	26.748725	16.263684	-8.357543
C	24.072324	18.040990	-3.315238
H	23.936071	19.035812	-2.915692
C	30.220188	16.219437	-3.954170
H	31.115029	15.624078	-4.087968
C	29.126541	18.236029	-3.254768
H	29.177043	19.237272	-2.851155
C	23.154197	15.944873	-4.031913
H	22.310559	15.281382	-4.176239
C	28.996215	15.672194	-4.305170
N	28.755425	14.406473	-4.835895
C	30.300529	17.515419	-3.430218
C	24.425166	15.485274	-4.344659
C	26.778469	14.516861	-7.642928
H	27.657731	14.009038	-8.081075
H	25.897664	14.000468	-8.066364
C	22.962081	17.231350	-3.514712
C	26.545780	19.064114	-1.941638
H	25.642966	19.653100	-1.776663
H	27.397400	19.719182	-1.754472
H	26.566917	18.256036	-1.208279
C	21.519420	19.128052	-2.641993
H	20.489393	19.409663	-2.413867
H	21.897596	19.839603	-3.380282
H	22.099150	19.239753	-1.722441
C	32.345398	17.198517	-2.025562
H	32.506732	16.185276	-2.399907
H	31.744232	17.133317	-1.115349
H	33.322367	17.608172	-1.757125
C	29.805556	13.442668	-4.839113
C	26.552193	19.680812	-4.371123
H	25.642392	20.270138	-4.239342
H	26.579185	19.320344	-5.401177
H	27.409759	20.339120	-4.217147
C	32.544149	18.151328	-4.327783
H	32.714518	17.158779	-4.749780
H	33.520806	18.578219	-4.086297
H	32.083187	18.772426	-5.099434
C	20.657882	17.624523	-4.411195
H	19.651565	17.978086	-4.173094
H	20.564615	16.604010	-4.787757
H	21.055466	18.248659	-5.215074
C	31.669022	18.093653	-3.070331
C	21.547648	17.694299	-3.165275
C	21.808269	11.226944	-4.874431
H	21.050588	10.451720	-4.879614
C	30.412511	13.398266	-8.542697
H	30.335210	14.119434	-9.359476
H	29.540937	12.743199	-8.604023
H	31.297555	12.788620	-8.737350
C	30.049640	12.697456	-3.662349
C	30.510203	14.133732	-7.209000
H	29.627020	14.765887	-7.098002
C	30.576414	13.219479	-6.001855
C	23.567820	12.412978	-3.712184
C	29.348920	12.993585	-2.351449
H	28.623463	13.791967	-2.528938
C	21.980390	12.037195	-5.980298
H	21.345209	11.894524	-6.847401
C	23.250793	13.168848	-8.503801
H	24.144407	12.542989	-8.454812
H	23.369329	13.856229	-9.344718
H	22.404839	12.517532	-8.736037
C	31.569684	19.504055	-2.494917
H	31.131538	20.206564	-3.208142
H	32.570526	19.867326	-2.252717
H	30.980681	19.529486	-1.574720
C	31.712367	11.412966	-4.857821
H	32.446786	10.615850	-4.869923
C	24.350617	12.624722	-2.430434
H	25.254524	13.194362	-2.679122
C	31.003709	11.687375	-3.700574
H	31.202326	11.107937	-2.805781
C	21.762270	14.806669	-7.349048
H	21.603122	15.430853	-6.469947
H	20.874611	14.185137	-7.491402
H	21.846915	15.466632	-8.215871
C	31.732670	15.055063	-7.232214
H	31.802451	15.653685	-6.324210
H	31.674671	15.740739	-8.080969
H	32.654880	14.476800	-7.331643
C	22.592172	11.423751	-3.750368
H	22.432412	10.798651	-2.879927
C	22.937241	13.048575	-5.996127
C	31.505942	12.182604	-5.988417
H	32.100533	11.991274	-6.874219
C	23.020567	13.949256	-7.211135
H	23.864406	14.626238	-7.063852
C	20.969504	16.776983	-2.080826
H	19.956329	17.094454	-1.821588
H	21.577117	16.810911	-1.173131
H	20.915606	15.738034	-2.413315
C	25.184386	17.157574	-7.836846
H	25.071592	17.224607	-6.752064
H	24.291556	16.669657	-8.236224
H	25.197361	18.177318	-8.232864
N	24.768544	14.225881	-4.841291
C	23.752146	13.222525	-4.857619
C	26.772624	16.154835	-10.232090
H	27.672651	15.648994	-10.592301
H	26.752358	17.151948	-10.681267
H	25.907894	15.604016	-10.612132
C	30.341608	13.507969	-1.308866
H	30.864947	14.397379	-1.661677
H	31.088627	12.748095	-1.066251
H	29.819117	13.767429	-0.385121
C	28.592478	11.784703	-1.807714
H	27.835621	11.426989	-2.509936
H	28.086699	12.042829	-0.874627
H	29.266299	10.951369	-1.594781
C	28.248346	17.245122	-7.805123
H	29.176377	16.814151	-8.189238
H	28.336417	17.315384	-6.718361
H	28.180909	18.263558	-8.199184
C	23.549502	13.464920	-1.433089
H	24.129666	13.627673	-0.521457
H	22.627970	12.946131	-1.155389
H	23.281318	14.437698	-1.844433
C	24.782199	11.321412	-1.764336
H	25.438511	11.534204	-0.918324
H	25.317446	10.663177	-2.451053
H	23.927313	10.767982	-1.370276
C	25.594100	9.997042	-5.377091
H	24.761453	9.589362	-4.817891
C	27.942134	10.519101	-5.548983

H	28.943723	10.506546	-5.135160
C	25.379494	10.515147	-6.646812
H	24.382527	10.508200	-7.068628
C	27.728898	11.028977	-6.828773
H	28.572872	11.381829	-7.408480
C	26.446421	11.034485	-7.375398
H	26.290706	11.407912	-8.380757
C	26.871514	10.003360	-4.827268
H	27.039543	9.581841	-3.843284

A.1.6 Optimised geometries of Alkyl cations containing Zirconium

Optimised geometry of η^6-2′-Zr and the name of the fragment f in the ETS-NOCV in which each atom belongs

C	6.765617	8.543203	16.019925	f=B
C	7.594672	9.346129	15.246965	f=B
C	7.196142	10.639722	14.906181	f=B
C	5.972804	11.130791	15.343249	f=B
C	5.154178	10.338319	16.152808	f=B
C	5.548108	9.046473	16.486256	f=B
H	8.549431	8.971886	14.901321	f=B
Zr	7.388531	10.680855	17.780436	f=Z
C	9.476823	11.030952	17.040068	f=Z
O	8.269054	11.440735	19.704398	f=Z
C	8.628986	10.555301	20.706789	f=Z
C	9.220970	10.971548	21.878665	f=Z
C	9.596177	12.436971	22.049428	f=Z
C	8.610252	13.271948	21.243984	f=Z
C	8.051034	12.749072	20.103447	f=Z
C	8.280057	9.255044	20.402336	f=Z
C	8.560596	8.286726	21.368180	f=Z
C	9.155616	8.635298	22.577247	f=Z
C	9.478542	9.973302	22.811748	f=Z
C	8.253111	14.586079	21.549236	f=Z
C	7.383513	15.319339	20.747801	f=Z
C	6.858483	14.724108	19.597930	f=Z
C	7.181169	13.414049	19.256415	f=Z
C	9.461558	7.595019	23.654881	f=Z
C	8.743402	7.979213	24.954065	f=Z
N	7.666527	9.057113	19.160128	f=Z
C	7.320155	7.685229	18.917442	f=Z
C	8.292561	6.787389	18.441989	f=Z
C	7.924372	5.462894	18.219243	f=Z
C	6.643436	4.992255	18.459809	f=Z
C	5.709381	5.895833	18.955297	f=Z
C	6.015533	7.228151	19.204871	f=Z
N	6.709354	12.678854	18.161878	f=Z
C	5.793790	13.422420	17.343529	f=Z
C	4.404791	13.321505	17.575246	f=Z
C	3.544369	14.075971	16.786534	f=Z
C	3.998873	14.939301	15.795797	f=Z
C	5.368096	15.023748	15.598507	f=Z
C	6.282390	14.286679	16.346818	f=Z
C	6.966115	16.747203	21.102858	f=Z
C	7.652049	17.254159	22.368855	f=Z
C	9.607344	12.844484	23.519379	f=Z
C	11.005365	12.649569	21.462693	f=Z
C	9.729930	7.193328	18.175972	f=Z
C	10.162820	6.891034	16.741693	f=Z
C	6.285478	3.546344	18.210695	f=Z
C	5.181821	3.405791	17.165219	f=Z
C	4.956975	8.131120	19.814740	f=Z
C	3.531246	7.793075	19.385413	f=Z
C	3.825036	12.445980	18.672675	f=Z
C	2.467497	11.840098	18.322728	f=Z
C	3.041172	15.761244	14.966304	f=Z
C	2.250963	16.743154	15.828516	f=Z
C	7.760670	14.445703	16.047375	f=Z
C	8.070690	14.297339	14.557208	f=Z
C	7.326302	17.694915	19.953681	f=Z
C	5.450141	16.785160	21.331705	f=Z
C	10.974200	7.554671	23.903527	f=Z
C	9.003939	6.193832	23.258062	f=Z
H	8.284576	7.261235	21.171217	f=Z
H	6.168539	15.273180	18.970894	f=Z
H	8.665378	15.040704	22.437342	f=Z
H	10.337666	12.256421	24.076020	f=Z
H	9.905766	13.887622	23.627945	f=Z
H	8.628259	12.712520	23.983202	f=Z
H	11.735101	12.043939	22.004695	f=Z
H	11.044661	12.367011	20.408760	f=Z
H	11.293617	13.699933	21.544630	f=Z
H	8.401770	17.687980	19.759981	f=Z
H	6.813361	17.427730	19.027610	f=Z
H	7.035820	18.717484	20.207501	f=Z
H	4.897447	16.481220	20.440229	f=Z
H	5.160581	16.122475	22.150918	f=Z
H	5.134555	17.799495	21.588964	f=Z
H	8.739628	17.275510	22.263279	f=Z
H	7.323190	18.274893	22.574635	f=Z
H	7.399525	16.647924	23.242254	f=Z
H	11.356428	8.520654	24.239192	f=Z
H	11.208964	6.817641	24.675722	f=Z
H	11.514543	7.277311	22.995038	f=Z
H	7.925012	6.149437	23.088775	f=Z
H	9.510072	5.835066	22.358283	f=Z
H	9.238419	5.494863	24.063640	f=Z
H	7.661076	8.015551	24.807948	f=Z
H	8.955785	7.241210	25.731701	f=Z
H	9.064587	8.953571	25.326710	f=Z
H	8.671252	4.766910	17.849489	f=Z
H	4.706281	5.543943	19.166778	f=Z
H	5.172311	9.157319	19.494083	f=Z
H	4.263650	8.778327	21.763931	f=Z
H	4.844233	7.109950	21.721998	f=Z
H	5.999277	8.447249	21.711694	f=Z
H	2.848548	8.577403	19.718800	f=Z
H	3.416166	7.685328	18.303492	f=Z
H	3.185581	6.861806	19.839551	f=Z
H	9.805655	8.271329	18.334010	f=Z
H	10.463436	6.757366	20.182720	f=Z
H	10.664756	5.426295	19.035438	f=Z
H	11.720952	6.837195	18.946788	f=Z
H	9.493775	7.335754	16.002418	f=Z
H	11.168315	7.277577	16.559820	f=Z
H	10.188352	5.815982	16.549550	f=Z
H	7.184001	3.061091	17.813897	f=Z
H	6.703419	2.902632	20.248589	f=Z
H	5.000618	3.260531	19.943677	f=Z
H	5.711505	1.773855	19.315796	f=Z
H	5.459866	3.884216	16.223342	f=Z
H	4.980056	2.351711	16.961921	f=Z
H	4.248396	3.858345	17.510703	f=Z
H	2.477136	13.996342	16.958363	f=Z

H	5.739936	15.694090	14.829888	f=Z
H	4.528812	11.622897	18.844284	f=Z
H	3.282134	12.555753	20.767863	f=Z
H	4.659292	13.580684	20.346768	f=Z
H	3.025055	14.059450	19.876922	f=Z
H	2.442099	11.371183	17.335437	f=Z
H	2.196899	11.083883	19.062567	f=Z
H	1.676357	12.592999	18.339442	f=Z
H	8.292559	13.658651	16.586978	f=Z
H	9.365763	15.875988	16.298718	f=Z
H	7.783310	16.618070	16.050233	f=Z
H	8.190092	15.901656	17.615256	f=Z
H	9.150252	14.237740	14.400297	f=Z
H	7.611651	13.408930	14.117843	f=Z
H	7.711329	15.156260	13.986028	f=Z
H	3.648979	16.346516	14.267533	f=Z
H	2.662673	14.200154	13.495038	f=Z
H	1.457407	14.279404	14.785979	f=Z
H	1.460087	15.495549	13.509926	f=Z
H	2.914448	17.396077	16.399301	f=Z
H	1.611544	17.370887	15.203804	f=Z
H	1.605797	16.217401	16.537449	f=Z
H	9.985759	10.086449	16.820017	f=Z
H	9.526360	11.652714	16.141655	f=Z
H	10.043300	11.537249	17.825413	f=Z
C	5.027882	8.119345	21.344000	f=Z
C	10.696641	6.513226	19.146332	f=Z
C	5.906079	2.831771	19.505962	f=Z
C	3.698954	13.206581	19.994957	f=Z
C	8.302917	15.788679	16.537731	f=Z
C	2.104801	14.880875	14.142108	f=Z
H	9.943884	10.244620	23.749566	f=Z
H	7.845085	11.258052	14.300136	f=B
H	5.659133	12.132494	15.081835	f=B
H	4.209622	10.729768	16.504973	f=B
H	4.914149	8.421604	17.099425	f=B
H	7.065048	7.538292	16.286669	f=B

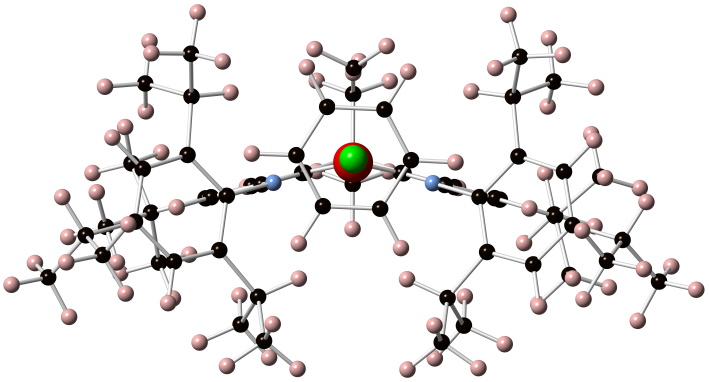

FIGURE A.1: **2′-Zr-a** molecule. Green: Pu; red: O; blue: N; black: C; pink: H

Optimised geometry of η^6-2-Zr and the name of the fragment f in the ETS-NOCV in which each atom belongs

```
;lkjhgfdsdrftghjklp;
```

Optimised geometry of η^6-3′-Zr-exo and the name of the fragment f in the ETS-NOCV in which each atom belongs

Zr	7.241484	8.778722	15.728818	f=Z
O	8.37604	10.43795	14.725539	f=Z
N	6.041734	10.575997	15.687056	f=Z
N	8.580454	7.966974	14.257685	f=Z
C	7.847188	13.982576	14.065712	f=Z
H	8.340867	14.845178	13.639288	f=Z
C	6.548546	14.119205	14.559059	f=Z
C	5.915737	13.007942	15.107004	f=Z
H	4.908206	13.088679	15.487045	f=Z
C	6.560912	11.770446	15.170919	f=Z
C	9.457686	8.790449	13.542351	f=Z
C	10.396445	8.399063	12.592137	f=Z
H	10.488642	7.34834	12.351078	f=Z
C	11.196338	9.338666	11.937741	f=Z
C	11.05044	10.685071	12.256195	f=Z
H	11.667627	11.41714	11.757684	f=Z
C	9.964387	12.575135	13.6375	f=Z
C	8.529419	12.771957	14.104719	f=Z

```
C    7.843191    11.714965    14.662143    f=Z
C    9.369295    10.147382    13.80374     f=Z
C    10.125937    11.125106    13.204583    f=Z
C    10.323614    13.539776    12.511312    f=Z
H    10.230982    14.57351     12.845571    f=Z
H    11.362163    13.407536    12.206714    f=Z
H    9.684256    13.397917    11.638253    f=Z
C    10.903549    12.832114    14.832205    f=Z
H    10.79525    13.860951    15.182735    f=Z
H    10.678964    12.163515    15.665722    f=Z
H    11.942768    12.671409    14.536719    f=Z
C    12.1962    8.858842    10.88479    f=Z
C    13.185709    7.877959    11.52368    f=Z
H    13.742256    8.35351    12.335036    f=Z
H    12.682995    6.997693    11.929344    f=Z
H    13.905614    7.533028    10.77715    f=Z
C    11.440193    8.149451    9.754941    f=Z
H    10.888694    7.279704    10.118005    f=Z
H    10.727811    8.825013    9.275063    f=Z
H    12.143268    7.802524    8.993403    f=Z
C    12.993337    10.009111    10.27525    f=Z
H    13.583338    10.540351    11.026303    f=Z
H    13.68955    9.613599    9.532765    f=Z
H    12.348039    10.729747    9.766824    f=Z
C    5.86003    15.481822    14.481236    f=Z
C    6.682208    16.512038    15.264871    f=Z
H    7.691833    16.618366    14.863564    f=Z
H    6.201045    17.49216    15.215714    f=Z
H    6.76683    16.228464    16.316794    f=Z
C    4.449933    15.454959    15.065231    f=Z
H    3.796974    14.761958    14.528403    f=Z
H    4.45103    15.179758    16.12301    f=Z
H    4.006296    16.449677    14.986067    f=Z
C    5.76314    15.919013    13.014691    f=Z
H    5.176693    15.205728    12.430227    f=Z
H    5.276267    16.895079    12.945114    f=Z
H    6.74679    16.005144    12.549168    f=Z
C    4.660025    10.709227    16.060997    f=Z
C    4.300172    11.057838    17.376605    f=Z
C    2.948951    11.216177    17.674901    f=Z
H    2.66217    11.480989    18.686918    f=Z
C    1.946728    11.061465    16.728534    f=Z
C    2.332178    10.732959    15.4356    f=Z
H    1.569189    10.618426    14.672579    f=Z
C    3.662998    10.560343    15.074594    f=Z
C    3.983874    10.251212    13.623686    f=Z
H    5.052405    10.026627    13.558602    f=Z
C    3.714556    11.460192    12.726124    f=Z
H    3.984213    11.233569    11.691628    f=Z
H    2.654716    11.7277    12.743193    f=Z
H    4.290299    12.330043    13.043208    f=Z
C    3.214969    9.042157    13.093204    f=Z
H    3.522626    8.822293    12.068282    f=Z
H    3.37927    8.142452    13.691201    f=Z
H    2.13874    9.22657    13.073153    f=Z
C    5.328534    11.294083    18.46876    f=Z
H    6.224168    10.726947    18.197704    f=Z
C    5.738926    12.766197    18.558806    f=Z
H    6.185356    13.124851    17.63257    f=Z
H    4.868977    13.389582    18.783206    f=Z
H    6.466102    12.906057    19.362746    f=Z
C    4.866663    10.833415    19.850879    f=Z
H    4.443631    9.825299    19.853821    f=Z
H    5.707009    10.851923    20.549002    f=Z
H    4.105157    11.499925    20.261716    f=Z
C    0.49476    11.25608    17.095625    f=Z
H    0.467841    11.506463    18.16191    f=Z
C    -0.127385    12.421453    16.329699    f=Z
H    0.430775    13.346411    16.488697    f=Z
H    -0.148137    12.222629    15.25485    f=Z
H    -1.15738    12.585655    16.654351    f=Z
C    -0.31574    9.977254    16.898486    f=Z
H    0.102675    9.146664    17.471432    f=Z
H    -1.348565    10.125093    17.221968    f=Z
H    -0.339518    9.682131    15.845967    f=Z
C    8.723797    6.578796    13.92012    f=Z
C    7.933199    6.024248    12.890256    f=Z
C    8.114705    4.686552    12.560278    f=Z
H    7.505573    4.258712    11.772254    f=Z
C    9.050226    3.878302    13.195526    f=Z
C    9.811753    4.450824    14.202076    f=Z
H    10.54556    3.832723    14.709134    f=Z
C    9.67749    5.783626    14.583113    f=Z
C    6.901207    6.83332    12.125691    f=Z
H    6.596811    7.667998    12.76726    f=Z
C    7.484733    7.440819    10.84804    f=Z
H    6.719476    8.012559    10.316729    f=Z
H    8.322596    8.105118    11.055649    f=Z
H    7.835466    6.650299    10.178958    f=Z
C    5.65189    6.030165    11.767412    f=Z
H    5.258706    5.453637    12.608836    f=Z
H    4.865322    6.699292    11.412636    f=Z
H    5.84912    5.321333    10.960095    f=Z
C    10.571936    6.31737    15.685831    f=Z
H    10.126239    7.246935    16.047122    f=Z
C    11.974768    6.651486    15.173733    f=Z
H    12.597962    7.01566    15.994496    f=Z
H    12.454898    5.759762    14.761196    f=Z
H    11.955385    7.417182    14.399607    f=Z
C    10.700352    5.354788    16.866994    f=Z
H    11.163343    5.863011    17.716054    f=Z
H    9.740565    4.947067    17.192041    f=Z
H    11.338864    4.502893    16.622291    f=Z
C    9.235178    2.430524    12.807497    f=Z
H    10.030744    2.030424    13.44568    f=Z
C    7.974383    1.609377    13.067519    f=Z
H    7.66456    1.673585    14.113085    f=Z
H    7.142472    1.954414    12.447563    f=Z
H    8.147306    0.557217    12.83032    f=Z
C    9.68957    2.29021    11.356487    f=Z
H    10.606795    2.852447    11.169614    f=Z
H    9.878672    1.241744    11.115352    f=Z
H    8.925386    2.65484    10.664915    f=Z
C    8.68459    9.195491    17.393953    f=Z
H    8.219318    9.763178    18.20611    f=Z
H    9.140681    8.301301    17.826483    f=Z
H    9.489988    9.810183    16.983148    f=Z
 C    6.399183    7.241748    18.048942 f=t
 C    7.042913    6.322772    17.208383  f=t
 H    7.925389    5.808493    17.567453 f=t
 C    6.563710    6.045666    15.934283 f=t
 H    7.070384    5.316600    15.317068 f=t
 C    5.443818    6.721495    15.442507 f=t
 H    5.069741    6.508599    14.449781 f=t
 C    4.796711    7.643354    16.260262 f=t
 H    3.923633    8.176336    15.908099 f=t
 C    5.277655    7.904809    17.543025 f=t
 H    4.761421    8.632196    18.154469 f=t
 C    6.846925    7.436240    19.457397 f=t
 H    6.599208    8.430215    19.827540    f=t
 H    6.335326    6.708595    20.095550    f=t
 H    7.918576    7.273051    19.566346    f=t
```

Optimised geometry of η^6-4′-Zr-exo and the name of the fragment f in the ETS-NOCV in which each atom belongs

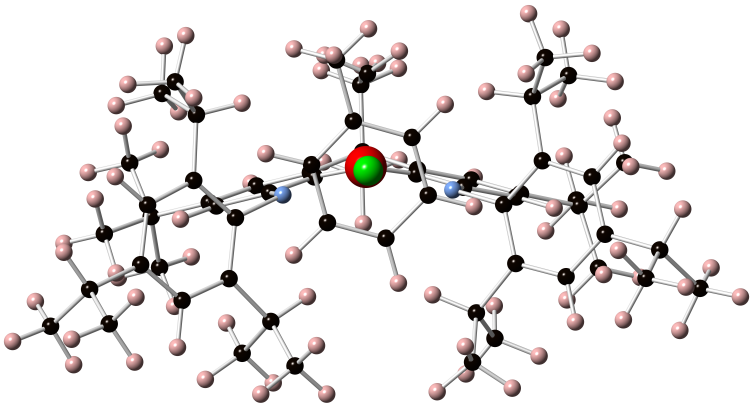

FIGURE A.2: **3′-Zr-a** molecule. Green: Pu; red: O; blue: N; black: C; pink: H

Zr	7.199815	10.734381	18.139199 f=Z	C	10.204199	7.309467	16.849433 f=Z
C	9.010617	10.914767	16.901978 f=Z	C	6.219295	3.912676	17.651095 f=Z
N	6.732466	12.730258	18.505216 f=Z	C	5.172435	3.956146	16.540569 f=Z
C	7.237468	13.496107	19.551206 f=Z	C	4.900485	8.250931	19.839466 f=Z
C	8.127030	12.821728	20.372407 f=Z	C	3.486824	7.958775	19.349525 f=Z
C	8.721761	13.342691	21.493135 f=Z	C	5.818481	13.331859	17.592169 f=Z
C	8.396184	14.670369	21.785527 f=Z	C	6.296126	14.043585	16.472427 f=Z
C	7.524385	15.414368	20.995482 f=Z	C	5.368049	14.582774	15.588096 f=Z
C	6.946060	14.813874	19.871378 f=Z	C	3.997794	14.463192	15.772887 f=Z
C	9.704397	12.492366	22.289867 f=Z	C	3.554159	13.780257	16.900238 f=Z
C	9.311673	11.029192	22.120943 f=Z	C	4.428366	13.215366	17.819975 f=Z
C	8.686371	10.623636	20.964629 f=Z	C	7.770942	14.284981	16.222982 f=Z
O	8.317457	11.509919	19.963324 f=Z	C	8.199296	13.914005	14.804881 f=Z
C	9.579950	10.018531	23.040570 f=Z	C	3.860042	12.547012	19.056172 f=Z
C	9.237008	8.684177	22.809422 f=Z	C	2.702071	11.603131	18.746028 f=Z
C	8.598960	8.345833	21.617138 f=Z	C	3.026833	15.075727	14.791992 f=Z
C	8.306896	9.327319	20.674377 f=Z	C	2.190181	16.173872	15.445218 f=Z
C	7.167156	16.862897	21.330599 f=Z	C	9.091935	6.239915	23.478514 f=Z
C	7.546677	17.770764	20.155282 f=Z	C	8.885200	8.015287	25.192833 f=Z
C	9.727690	12.896902	23.760780 f=Z	C	5.658166	16.967870	21.582322 f=Z
C	11.111337	12.689274	21.693133 f=Z	C	7.893314	17.367613	22.574818 f=Z
C	9.566489	7.636205	23.872515 f=Z	C	10.641991	6.609766	19.208002 f=Z
C	11.085089	7.586506	24.080001 f=Z	C	5.753994	3.030976	18.808193 f=Z
N	7.644696	9.178804	19.459128 f=Z	C	4.963593	8.089279	21.359540 f=Z
C	7.301602	7.866091	19.023120 f=Z	C	3.419369	13.590835	20.084049 f=Z
C	8.278702	7.025886	18.452638 f=Z	C	2.133956	14.020750	14.143082 f=Z
C	7.894025	5.760398	18.020840 f=Z	C	8.140054	15.742239	16.505820 f=Z
C	6.592132	5.296211	18.127032 f=Z	H	10.071961	10.277875	23.968308 f=Z
C	5.647580	6.144083	18.697171 f=Z	H	8.301516	7.325759	21.416671 f=Z
C	5.968379	7.413734	19.158565 f=Z	H	6.249845	15.363208	19.249527 f=Z
C	9.729745	7.432499	18.297428 f=Z	H	8.838922	15.129311	22.656782 f=Z

H	10.454037	12.299617	24.312854 f=Z	H	5.550776	2.017132	18.456356 f=Z
H	10.037240	13.936769	23.869874 f=Z	H	5.511448	4.556798	15.693363 f=Z
H	8.749465	12.774499	24.228994 f=Z	H	4.961723	2.948284	16.176307 f=Z
H	11.837963	12.074331	22.228760 f=Z	H	4.230448	4.379850	16.898827 f=Z
H	11.138670	12.408082	20.638483 f=Z	H	2.487351	13.695155	17.075037 f=Z
H	11.412788	13.735928	21.774913 f=Z	H	5.727005	15.132477	14.723720 f=Z
H	8.616436	17.710773	19.940983 f=Z	H	4.661308	11.961003	19.520064 f=Z
H	7.003500	17.507786	19.245230 f=Z	H	3.029932	13.102346	20.980549 f=Z
H	7.306609	18.810306	20.392142 f=Z	H	4.246706	14.234883	20.382954 f=Z
H	5.078085	16.678940	20.703242 f=Z	H	2.626260	14.221795	19.674087 f=Z
H	5.353573	16.328814	22.414726 f=Z	H	2.962441	10.853683	17.994139 f=Z
H	5.389765	17.997863	21.830443 f=Z	H	2.393472	11.080161	19.653509 f=Z
H	8.978854	17.347302	22.450513 f=Z	H	1.827210	12.143424	18.378647 f=Z
H	7.605515	18.403378	22.766366 f=Z	H	8.332240	13.659450	16.919845 f=Z
H	7.634193	16.787180	23.463695 f=Z	H	9.208527	15.898556	16.339156 f=Z
H	11.481180	8.547794	24.412880 f=Z	H	7.596570	16.419022	15.841223 f=Z
H	11.336491	6.842235	24.839879 f=Z	H	7.916864	16.023364	17.535131 f=Z
H	11.599238	7.313721	23.155124 f=Z	H	9.283159	14.004305	14.706426 f=Z
H	8.008385	6.200588	23.340154 f=Z	H	7.923962	12.890358	14.544636 f=Z
H	9.571459	5.886366	22.562140 f=Z	H	7.751567	14.578374	14.061905 f=Z
H	9.346346	5.533664	24.271503 f=Z	H	3.625286	15.539494	14.000316 f=Z
H	7.799523	8.057223	25.076170 f=Z	H	2.723240	13.248947	13.642200 f=Z
H	9.115235	7.271574	25.959908 f=Z	H	1.496131	13.530410	14.883314 f=Z
H	9.220736	8.985946	25.562437 f=Z	H	1.480029	14.480297	13.398746 f=Z
H	8.642841	5.106947	17.584314 f=Z	H	2.821821	16.947082	15.887089 f=Z
H	4.626910	5.794792	18.793041 f=Z	H	1.540080	16.647416	14.706258 f=Z
H	5.112218	9.310802	19.632402 f=Z	H	1.552126	15.768846	16.235125 f=Z
H	4.198509	8.703377	21.840827 f=Z	H	9.538701	9.964884	16.794549 f=Z
H	4.778847	7.046900	21.632469 f=Z	H	8.710989	11.257021	15.903437 f=Z
H	5.934886	8.377892	21.760609 f=Z	H	9.711156	11.650599	17.307009 f=Z
H	2.790275	8.686098	19.768697 f=Z	C	5.335433	10.773110	15.476623 f=t
H	3.400996	7.992781	18.260272 f=Z	C	5.525781	9.667681	16.313699 f=t
H	3.146781	6.973663	19.676032 f=Z	C	6.337495	8.606945	15.891653 f=t
H	9.817991	8.479446	18.595735 f=Z	C	6.980050	8.669311	14.667198 f=t
H	10.369122	6.720232	20.257812 f=Z	C	6.796046	9.782767	13.856071 f=t
H	10.596780	5.547755	18.953528 f=Z	C	5.974804	10.831879	14.249578 f=t
H	11.678799	6.934698	19.093796 f=Z	Br	7.661406	9.865988	12.196192 f=t
H	9.557871	7.853322	16.157331 f=Z	H	7.603622	7.850533	14.332358 f=t
H	11.216259	7.708092	16.749054 f=Z	H	5.824671	11.681194	13.596222 f=t
H	10.232977	6.266238	16.526185 f=Z	H	4.670173	11.577534	15.768395 f=t
H	7.128336	3.464428	17.235543 f=Z	H	4.901991	9.545096	17.202458 f=t
H	6.509414	2.972740	19.594376 f=Z	H	6.442404	7.722144	16.508373 f=t
H	4.833399	3.416440	19.254391 f=Z				

Optimised geometry of η^6-4′-Zr-horizontal and the name of the fragment f in the ETS-NOCV in which each atom belongs

C	1.148781	9.601211	14.619544 f=Z	C	-3.601916	9.017999	21.106840 f=Z
C	0.673990	10.683643	15.398187 f=Z	C	-2.686008	11.339441	21.226728 f=Z
C	0.555205	11.967135	14.828107 f=Z	Zr	1.952082	10.409557	18.036020 f=Z
C	0.877636	12.126313	13.484817 f=Z	C	0.441767	7.673773	24.211278 f=Z
C	1.327173	11.081041	12.694370 f=Z	C	-0.421839	6.406751	24.224502 f=Z
C	1.468641	9.831507	13.288947 f=Z	N	2.273716	9.444370	19.846307 f=Z
N	0.323648	10.458942	16.760571 f=Z	C	3.601394	8.966923	20.053222 f=Z
C	-1.008264	10.342883	17.141844 f=Z	C	4.557828	9.769887	20.707707 f=Z
C	-1.188772	10.200101	18.510549 f=Z	C	5.842125	9.265130	20.878495 f=Z
C	-2.393944	10.021929	19.139171 f=Z	C	6.211278	7.996550	20.455108 f=Z
C	-3.509981	9.995356	18.296186 f=Z	C	5.244122	7.216088	19.832223 f=Z
C	-3.405406	10.133943	16.915083 f=Z	C	3.946550	7.664689	19.622511 f=Z
C	-2.140558	10.314812	16.342525 f=Z	C	4.223933	11.126257	21.290369 f=Z
C	-2.457356	9.925330	20.660457 f=Z	C	4.200484	11.071998	22.818928 f=Z
C	-1.117508	9.409622	21.175998 f=Z	C	7.607960	7.475617	20.699160 f=Z
C	0.025033	9.602267	20.435973 f=Z	C	7.598198	6.285850	21.656917 f=Z
O	0.018714	10.206175	19.189549 f=Z	C	2.934903	6.713715	19.015303 f=Z
C	1.293988	9.186109	20.798453 f=Z	C	2.511977	5.648498	20.028610 f=Z
C	1.438173	8.561830	22.032834 f=Z	C	0.088374	13.177657	15.608518 f=Z
C	0.325322	8.354522	22.847404 f=Z	C	-1.290949	13.651900	15.151491 f=Z
C	-0.930438	8.773471	22.401611 f=Z	C	1.650904	11.297224	11.235080 f=Z
C	-4.628998	10.060579	16.001102 f=Z	C	3.129182	11.053835	10.939911 f=Z
C	-5.931041	9.908045	16.783116 f=Z	C	1.255845	8.195331	15.184761 f=Z

C	-0.107129	7.502395	15.213686 f=Z	H	5.182185	10.804157	23.217997 f=Z
C	2.117158	12.537237	18.628359 f=Z	H	3.929394	12.048709	23.226782 f=Z
C	-4.726407	11.336766	15.158261 f=Z	H	5.264702	12.251528	19.730738 f=Z
C	-4.484491	8.850128	15.070011 f=Z	H	4.852313	13.192887	21.171175 f=Z
C	-0.048212	8.634482	25.301440 f=Z	H	6.193719	12.056591	21.214065 f=Z
C	1.877829	7.273990	24.539736 f=Z	H	8.169420	8.284706	21.178501 f=Z
C	5.187094	12.214211	20.819768 f=Z	H	7.113650	6.539612	22.601786 f=Z
C	8.324365	7.122831	19.398196 f=Z	H	7.065800	5.434335	21.224844 f=Z
C	3.442650	6.047997	17.740087 f=Z	H	8.618643	5.962380	21.874307 f=Z
C	1.088070	14.330447	15.505460 f=Z	H	8.377564	7.982089	18.725182 f=Z
C	2.262699	7.314899	14.455771 f=Z	H	9.345603	6.793343	19.601906 f=Z
C	0.765447	10.444159	10.329609 f=Z	H	7.815359	6.307713	18.875731 f=Z
H	-1.791650	8.600673	23.033093 f=Z	H	1.828258	9.006228	12.687072 f=Z
H	2.421050	8.229484	22.337577 f=Z	H	0.773115	13.108742	13.035497 f=Z
H	-2.027091	10.404964	15.269053 f=Z	H	1.592295	8.269404	16.233328 f=Z
H	-4.485716	9.858622	18.738007 f=Z	H	-0.015899	6.498803	15.636409 f=Z
H	-3.658924	8.975175	22.194838 f=Z	H	-0.840265	8.054894	15.800117 f=Z
H	-4.560578	9.406600	20.762172 f=Z	H	-0.493622	7.403323	14.195809 f=Z
H	-3.481685	8.002451	20.725676 f=Z	H	3.245736	7.783301	14.375911 f=Z
H	-2.721743	11.308468	22.317984 f=Z	H	2.377135	6.368399	14.985307 f=Z
H	-1.884428	12.019301	20.931235 f=Z	H	1.919015	7.071413	13.447875 f=Z
H	-3.630742	11.745886	20.858792 f=Z	H	0.009751	12.888008	16.658622 f=Z
H	-4.814205	12.222189	15.792557 f=Z	H	-1.598901	14.525375	15.731253 f=Z
H	-3.856136	11.467314	14.511872 f=Z	H	-1.276771	13.941344	14.097500 f=Z
H	-5.608424	11.293276	14.514456 f=Z	H	-2.048440	12.879259	15.282607 f=Z
H	-3.591101	8.922962	14.445997 f=Z	H	0.811792	15.132069	16.194099 f=Z
H	-4.421655	7.921366	15.642244 f=Z	H	2.107569	14.015674	15.739302 f=Z
H	-5.349713	8.781375	14.405696 f=Z	H	1.101130	14.757085	14.499797 f=Z
H	-6.104176	10.751811	17.455766 f=Z	H	1.437713	12.348742	11.014946 f=Z
H	-6.769737	9.868012	16.084993 f=Z	H	3.767928	11.702558	11.544443 f=Z
H	-5.951323	8.986084	17.369386 f=Z	H	3.405091	10.014849	11.141816 f=Z
H	-1.091241	8.920483	25.153255 f=Z	H	3.347912	11.254404	9.888684 f=Z
H	0.029522	8.159731	26.282824 f=Z	H	-0.293501	10.631874	10.517600 f=Z
H	0.551367	9.547839	25.317974 f=Z	H	0.968350	10.665448	9.279369 f=Z
H	2.279856	6.559147	23.817026 f=Z	H	0.949810	9.377701	10.484074 f=Z
H	2.544634	8.139139	24.579362 f=Z	H	3.036382	12.746366	19.183090 f=Z
H	1.905476	6.795820	25.521025 f=Z	H	2.073659	13.210702	17.768137 f=Z
H	-0.093701	5.700011	23.458299 f=Z	H	1.275731	12.787666	19.283410 f=Z
H	-0.347239	5.912075	25.196225 f=Z	Br	4.407454	11.206023	16.741043 f=t
H	-1.475559	6.629163	24.046163 f=Z	C	5.293763	9.833134	15.735801 f=t
H	6.581655	9.877803	21.384232 f=Z	C	5.981724	8.848467	16.418211 f=t
H	5.502852	6.211410	19.515345 f=Z	C	6.668704	7.903664	15.667402 f=t
H	2.039379	7.291088	18.762551 f=Z	C	6.662601	7.965837	14.281666 f=t
H	1.760770	4.985668	19.592276 f=Z	C	5.963600	8.971677	13.630088 f=t
H	3.368241	5.036358	20.324017 f=Z	C	5.262890	9.923889	14.357237 f=t
H	2.086880	6.095926	20.927566 f=Z	H	5.960261	9.024021	12.547885 f=t
H	2.647700	5.450121	17.288330 f=Z	H	7.208921	7.228521	13.706043 f=t
H	3.785214	6.776571	17.002139 f=Z	H	4.709335	10.709690	13.860260 f=t
H	4.274163	5.369710	17.944581 f=Z	H	5.988764	8.812140	17.500800 f=t
H	3.218604	11.391398	20.957663 f=Z	H	7.217446	7.121333	16.177889 f=t
H	3.475617	10.342469	23.183313 f=Z				

Optimised geometry of η^6-5′-Zr-exo and the name of the fragment f in the ETS-NOCV in which each atom belongs

C	5.537644	9.678384	16.311264 f=t	C	3.559163	13.779248	16.892915 f=Z
C	6.329164	8.599653	15.891837 f=t	C	4.003208	14.465242	15.767567 f=Z
C	6.959412	8.638335	14.661669 f=t	C	5.373509	14.586207	15.584190 f=Z
C	6.770844	9.748100	13.854006 f=t	N	6.736627	12.732991	18.501777 f=Z
C	5.973807	10.816795	14.229568 f=t	C	7.240378	13.498687	19.548519 f=Z
C	5.348104	10.777171	15.462709 f=t	C	8.127616	12.823494	20.371745 f=Z
H	7.571843	7.817650	14.310294 f=t	C	8.719851	13.343995	21.494008 f=Z
F	7.367646	9.784202	12.673467 f=t	C	8.394694	14.672015	21.785492 f=Z
H	5.839430	11.651137	13.553299 f=t	C	7.525627	15.416832	20.993315 f=Z
H	4.693620	11.589993	15.755161 f=t	C	6.949279	14.816662	19.867997 f=Z
H	4.912054	9.567614	17.200501 f=t	O	8.318138	11.511676	19.962765 f=Z
H	6.426936	7.721394	16.518662 f=t	C	8.686274	10.624969	20.963944 f=Z
C	6.301309	14.046565	16.468613 f=Z	C	9.308959	11.029850	22.121915 f=Z
C	5.823385	13.333500	17.587476 f=Z	C	9.699312	12.493265	22.294236 f=Z
C	4.432990	13.214396	17.813007 f=Z	C	9.577314	10.018302	23.040606 f=Z

C	9.236923	8.683736	22.807174 f=Z	H	11.477744	8.549562	24.415918 f=Z
C	8.601174	8.346100	21.613473 f=Z	H	11.335605	6.843003	24.839637 f=Z
C	8.309031	9.328402	20.671661 f=Z	H	11.601518	7.317890	23.156354 f=Z
Zr	7.200536	10.736097	18.137230 f=Z	H	8.012671	6.196405	23.331187 f=Z
N	7.648668	9.180079	19.455337 f=Z	H	9.578092	5.887344	22.555793 f=Z
C	7.305780	7.867236	19.019609 f=Z	H	9.350275	5.531005	24.264075 f=Z
C	8.282386	7.028363	18.446250 f=Z	H	7.795475	8.050015	25.069251 f=Z
C	7.898096	5.762522	18.015136 f=Z	H	9.110716	7.265899	25.955056 f=Z
C	6.597061	5.296615	18.124920 f=Z	H	9.213449	8.981120	25.560398 f=Z
C	5.653105	6.143085	18.698077 f=Z	H	8.646520	5.110020	17.576524 f=Z
C	5.973519	7.413241	19.158489 f=Z	H	4.633080	5.792613	18.796756 f=Z
C	9.714604	12.895924	23.765852 f=Z	H	5.120969	9.309471	19.640278 f=Z
C	11.109096	12.692277	21.705024 f=Z	H	4.199801	8.692424	21.843070 f=Z
C	9.566310	7.634770	23.869297 f=Z	H	4.776612	7.035665	21.627247 f=Z
C	9.095842	6.238076	23.471827 f=Z	H	5.935612	8.363186	21.765294 f=Z
C	7.169310	16.865846	21.327293 f=Z	H	2.796710	8.689492	19.766203 f=Z
C	5.659852	16.972833	21.575316 f=Z	H	3.410948	8.003339	18.255863 f=Z
C	9.732527	7.436883	18.287811 f=Z	H	3.149482	6.976848	19.664960 f=Z
C	10.647309	6.618527	19.199803 f=Z	H	9.819225	8.484878	18.582882 f=Z
C	6.224645	3.912821	17.649377 f=Z	H	10.376230	6.732724	20.249673 f=Z
C	5.766506	3.029187	18.807865 f=Z	H	10.602694	5.555521	18.949375 f=Z
C	4.905830	8.249180	19.841030 f=Z	H	11.683557	6.944138	19.082454 f=Z
C	4.964562	8.079041	21.360366 f=Z	H	9.555955	7.849040	16.146453 f=Z
C	3.864048	12.543749	19.047736 f=Z	H	11.215834	7.712571	16.736349 f=Z
C	3.430556	13.585624	20.080671 f=Z	H	10.238110	6.266049	16.520170 f=Z
C	3.032499	15.080256	14.787970 f=Z	H	7.132587	3.466715	17.229142 f=Z
C	2.136596	14.028098	14.138760 f=Z	H	6.525946	2.971328	19.590185 f=Z
C	7.776121	14.289557	16.220646 f=Z	H	4.847569	3.412804	19.259047 f=Z
C	8.144154	15.746347	16.507494 f=Z	H	5.563128	2.015392	18.455984 f=Z
C	9.006617	10.913195	16.891880 f=Z	H	5.506041	4.557714	15.695795 f=Z
C	8.880950	8.010272	25.188540 f=Z	H	4.962473	2.947307	16.179249 f=Z
C	11.084494	7.588027	24.080407 f=Z	H	4.231125	4.376134	16.906999 f=Z
C	7.893123	17.369939	22.573133 f=Z	H	2.492292	13.692200	17.066114 f=Z
C	7.552894	17.772942	20.152692 f=Z	H	5.732714	15.137895	14.721184 f=Z
C	10.205503	7.310334	16.839624 f=Z	H	4.663630	11.952345	19.507924 f=Z
C	5.172468	3.955187	16.543854 f=Z	H	3.040624	13.095507	20.976064 f=Z
C	3.492982	7.962947	19.345178 f=Z	H	4.261410	14.224740	20.380348 f=Z
C	2.701033	11.606301	18.737014 f=Z	H	2.639533	14.221750	19.674652 f=Z
C	2.198950	16.179353	15.443691 f=Z	H	2.955123	10.859998	17.979873 f=Z
C	8.205701	13.923379	14.801733 f=Z	H	2.394102	11.079667	19.642905 f=Z
H	10.067514	10.277122	23.969450 f=Z	H	1.826796	12.152215	18.376552 f=Z
H	8.305760	7.325812	21.411116 f=Z	H	8.337490	13.662454	16.916066 f=Z
H	6.254774	15.366510	19.244677 f=Z	H	9.212542	15.903925	16.341530 f=Z
H	8.835735	15.130606	22.657789 f=Z	H	7.600308	16.424500	15.844586 f=Z
H	10.438410	12.298455	24.321038 f=Z	H	7.920571	16.024505	17.537478 f=Z
H	10.022798	13.935857	23.878013 f=Z	H	9.289211	14.018285	14.703534 f=Z
H	8.733977	12.772169	24.228646 f=Z	H	7.934759	12.899217	14.538856 f=Z
H	11.833525	12.077313	22.243597 f=Z	H	7.755577	14.587825	14.060289 f=Z
H	11.142146	12.412485	20.650162 f=Z	H	3.631026	15.543844	13.996236 f=Z
H	11.409181	13.739091	21.789734 f=Z	H	2.723559	13.255896	13.635752 f=Z
H	8.622978	17.710981	19.940590 f=Z	H	1.498770	13.537821	14.879016 f=Z
H	7.011054	17.510916	19.241567 f=Z	H	1.482549	14.490207	13.396134 f=Z
H	7.314248	18.812943	20.388970 f=Z	H	2.832812	16.950538	15.885919 f=Z
H	5.081491	16.683658	20.695175 f=Z	H	1.548995	16.655395	14.706215 f=Z
H	5.352531	16.335012	22.407664 f=Z	H	1.561048	15.774498	16.233811 f=Z
H	5.392095	18.003396	21.821754 f=Z	H	9.529982	9.961519	16.777541 f=Z
H	8.978940	17.347873	22.451581 f=Z	H	8.702572	11.261323	15.896745 f=Z
H	7.606483	18.406241	22.763508 f=Z	H	9.712619	11.644496	17.295639 f=Z
H	7.630845	16.790308	23.461608 f=Z				

Optimised geometry of η^6-5′-Zr-horizontal and the name of the fragment f in the ETS-NOCV in which each atom belongs

C	4.956835	9.670408	15.943967 f=t	H	7.975236	9.326106	13.689307 f=t
C	6.074845	9.090378	16.485056 f=t	H	3.905863	10.575787	14.308477 f=t
C	7.174465	8.969835	15.644581 f=t	F	3.840492	9.798254	16.789883 f=t
C	7.111237	9.424195	14.334801 f=t	H	6.086304	8.748216	17.513100 f=t
C	5.948883	10.003554	13.846154 f=t	H	8.082719	8.517133	16.023156 f=t
C	4.831654	10.137945	14.661571 f=t	Zr	1.957971	10.200814	17.974402 f=Z
H	5.901550	10.355603	12.822990 f=t	C	2.450817	12.321618	18.285107 f=Z

N	0.315954	10.318194	16.720485 f=Z	H	-3.856965	11.409659	14.512300 f=Z
C	-1.011543	10.271017	17.131581 f=Z	H	-5.614584	11.298342	14.541448 f=Z
C	-1.171727	10.201249	18.508356 f=Z	H	-3.696604	8.853189	14.533858 f=Z
C	-2.372519	10.104767	19.162902 f=Z	H	-4.539262	7.930397	15.783949 f=Z
C	-3.503793	10.083021	18.340215 f=Z	H	-5.459315	8.776705	14.532308 f=Z
C	-3.418946	10.150087	16.952844 f=Z	H	-6.083436	10.892918	17.510817 f=Z
C	-2.158107	10.250734	16.353050 f=Z	H	-6.804828	9.978996	16.189225 f=Z
C	-2.414460	10.086404	20.687169 f=Z	H	-5.996068	9.120695	17.495837 f=Z
C	-1.094992	9.523728	21.203745 f=Z	H	-1.043128	9.160480	25.196734 f=Z
C	0.045315	9.636727	20.444364 f=Z	H	0.053360	8.380801	26.337169 f=Z
O	0.049582	10.193124	19.171042 f=Z	H	0.629775	9.711947	25.324439 f=Z
C	-0.923093	8.920918	22.448425 f=Z	H	2.193092	6.598726	23.897115 f=Z
C	0.316192	8.456899	22.894700 f=Z	H	2.543733	8.185712	24.608442 f=Z
C	1.428025	8.588118	22.063395 f=Z	H	1.851726	6.903954	25.597245 f=Z
C	1.298852	9.180478	20.811920 f=Z	H	-0.223123	5.845359	23.591642 f=Z
C	-4.660352	10.088124	16.062613 f=Z	H	-0.445128	6.122409	25.324658 f=Z
C	-4.723246	11.334359	15.172732 f=Z	H	-1.551308	6.858166	24.164962 f=Z
C	-3.598816	9.268753	21.197396 f=Z	H	6.577157	9.800951	21.411715 f=Z
C	-2.553448	11.537445	21.185548 f=Z	H	5.501027	6.120475	19.570066 f=Z
C	0.416176	7.812628	24.277364 f=Z	H	2.048391	7.208580	18.775639 f=Z
C	-0.013382	8.828766	25.342488 f=Z	H	1.741317	4.915783	19.623133 f=Z
N	2.279183	9.365119	19.844578 f=Z	H	3.340064	4.961611	20.374783 f=Z
C	3.602887	8.884245	20.073960 f=Z	H	2.060793	6.038582	20.950412 f=Z
C	4.559056	9.695379	20.717595 f=Z	H	2.667536	5.347381	17.326643 f=Z
C	5.838225	9.184165	20.910376 f=Z	H	3.804223	6.672452	17.035804 f=Z
C	6.205662	7.909449	20.505403 f=Z	H	4.288866	5.276447	17.995905 f=Z
C	5.241759	7.127195	19.879657 f=Z	H	3.254720	11.357955	20.868128 f=Z
C	3.947203	7.578453	19.657898 f=Z	H	3.380245	10.372287	23.133446 f=Z
C	4.236476	11.073988	21.253058 f=Z	H	5.100957	10.770871	23.225949 f=Z
C	5.250411	12.123041	20.799128 f=Z	H	3.897163	12.060816	23.150004 f=Z
C	7.604569	7.393801	20.748203 f=Z	H	5.400559	12.111028	19.716994 f=Z
C	8.361292	7.188359	19.437332 f=Z	H	4.912857	13.121865	21.084551 f=Z
C	2.938576	6.628517	19.043934 f=Z	H	6.225484	11.966685	21.266337 f=Z
C	3.457552	5.950739	17.779368 f=Z	H	8.132546	8.165908	21.318123 f=Z
C	0.642687	10.501407	15.345133 f=Z	H	7.080004	6.262356	22.531896 f=Z
C	0.582503	11.782891	14.758700 f=Z	H	7.121261	5.292248	21.056099 f=Z
C	0.880813	11.904527	13.405515 f=Z	H	8.628428	5.809061	21.808642 f=Z
C	1.247849	10.824287	12.618656 f=Z	H	8.421725	8.117606	18.865025 f=Z
C	1.330568	9.576793	13.227951 f=Z	H	9.380852	6.848170	19.632193 f=Z
C	1.033743	9.384055	14.570482 f=Z	H	7.873536	6.433073	18.814542 f=Z
C	0.190685	13.027025	15.528276 f=Z	H	1.627538	8.723499	12.630716 f=Z
C	1.189759	14.166133	15.321952 f=Z	H	0.821798	12.885097	12.944358 f=Z
C	1.082086	7.981728	15.150044 f=Z	H	1.376605	8.056921	16.208835 f=Z
C	2.095292	7.071836	14.465544 f=Z	H	-0.255199	6.325269	15.562157 f=Z
C	1.563285	11.007138	11.152977 f=Z	H	-1.034834	7.907335	15.691802 f=Z
C	0.697886	10.117671	10.264513 f=Z	H	-0.655608	7.236020	14.101757 f=Z
C	1.835201	7.353448	24.602246 f=Z	H	3.087826	7.524191	14.405501 f=Z
C	-0.507519	6.590262	24.338905 f=Z	H	2.181156	6.133199	15.014659 f=Z
C	-4.579021	8.838280	15.177185 f=Z	H	1.780248	6.815210	13.451781 f=Z
C	-5.952936	10.016339	16.871308 f=Z	H	0.180323	12.771817	16.590235 f=Z
C	4.146719	11.063438	22.780140 f=Z	H	-1.465301	14.406413	15.714133 f=Z
C	7.604667	6.117442	21.585506 f=Z	H	-1.261269	13.757330	14.085456 f=Z
C	2.492683	5.577057	20.061481 f=Z	H	-1.969342	12.753304	15.358050 f=Z
C	-0.300668	7.328617	15.131634 f=Z	H	0.976357	14.981680	16.016172 f=Z
C	3.048064	10.783840	10.871098 f=Z	H	2.222481	13.848661	15.479827 f=Z
C	-1.210755	13.506898	15.148438 f=Z	H	1.123783	14.577055	14.311841 f=Z
H	-1.784182	8.809318	23.093551 f=Z	H	1.332488	12.049227	10.906964 f=Z
H	2.398468	8.220895	22.368177 f=Z	H	3.669203	11.463874	11.459654 f=Z
H	-2.060312	10.288158	15.274929 f=Z	H	3.343392	9.757665	11.107987 f=Z
H	-4.475842	10.007903	18.804166 f=Z	H	3.268400	10.956848	9.815282 f=Z
H	-3.637572	9.284335	22.286909 f=Z	H	-0.365186	10.282906	10.450359 f=Z
H	-4.540647	9.693696	20.849303 f=Z	H	0.894563	10.327083	9.210776 f=Z
H	-3.543061	8.230137	20.867002 f=Z	H	0.908182	9.058313	10.433046 f=Z
H	-2.569304	11.561846	22.277407 f=Z	H	3.378294	12.432557	18.853548 f=Z
H	-1.721569	12.156096	20.843054 f=Z	H	2.581884	12.812227	17.314974 f=Z
H	-3.481472	11.977436	20.813764 f=Z	H	1.660679	12.854688	18.822414 f=Z
H	-4.771581	12.245514	15.773948 f=Z				

Optimised geometry of η^2-E′-Zr-horizontal and the name of the fragment f in the ETS-NOCV in which each atom belongs

```
C     7.558282     8.854639    16.089291 f=Z
C     8.153290     9.648401    15.078342 f=Z
C     7.667009    10.948369    14.824314 f=Z
C     6.595211    11.412500    15.579647 f=Z
C     5.996834    10.658307    16.576170 f=Z
C     6.502170     9.383756    16.816629 f=Z
N     9.263475     9.130158    14.357418 f=Z
Zr   11.046520     9.240895    15.415755 f=Z
C    11.761421    11.267041    14.913923 f=Z
C     8.251683    11.859960    13.765859 f=Z
C     8.608811    13.234999    14.332718 f=Z
C     4.833615    11.202755    17.369227 f=Z
C     5.162448    11.310860    18.856453 f=Z
C     8.021682     7.434911    16.362634 f=Z
C     7.684915     6.937324    17.762502 f=Z
N    12.807960     8.160428    15.283434 f=Z
C    13.331354     7.589170    14.131490 f=Z
C    12.535474     7.769066    13.008069 f=Z
C    12.792276     7.252753    11.764618 f=Z
C    13.984352     6.528825    11.651876 f=Z
C    14.845998     6.335662    12.727576 f=Z
C    14.505337     6.869671    13.976416 f=Z
C    11.836420     7.522869    10.606950 f=Z
C    10.453085     7.833021    11.170998 f=Z
C    10.322002     8.335418    12.444128 f=Z
O    11.397449     8.502465    13.300421 f=Z
C     9.261147     7.697449    10.461613 f=Z
C     8.019357     8.037219    11.003266 f=Z
C     7.961072     8.536759    12.304033 f=Z
C     9.127244     8.691326    13.045804 f=Z
C    16.148550     5.547313    12.588662 f=Z
C    17.331273     6.447567    12.964526 f=Z
C    11.783222     6.330474     9.653169 f=Z
C    12.337245     8.760653     9.839429 f=Z
C     6.760947     7.848753    10.155921 f=Z
C     6.857185     8.730396     8.904859 f=Z
C    13.411749     7.977729    16.555700 f=Z
C    14.365857     8.901124    17.037096 f=Z
C    14.863913     8.727117    18.323159 f=Z
C    14.475519     7.675444    19.141992 f=Z
C    13.560933     6.760006    18.632358 f=Z
C    13.022924     6.876392    17.358909 f=Z
C    14.899885    10.037793    16.191982 f=Z
C    14.890901    11.374616    16.931186 f=Z
C    12.093599     5.792469    16.850034 f=Z
C    11.071509     5.339423    17.887842 f=Z
C    15.049059     7.523058    20.529803 f=Z
C    15.873489     6.243283    20.655511 f=Z
C     5.490044     8.228339    10.911512 f=Z
C     6.642649     6.379226     9.734524 f=Z
C    16.115175     4.337158    13.529685 f=Z
C    16.371435     5.037955    11.167085 f=Z
C     7.297567    12.033327    12.582954 f=Z
C     3.568930    10.375914    17.146084 f=Z
C     7.469596     6.462294    15.319809 f=Z
C    12.891823     4.584485    16.354046 f=Z
C    13.963181     7.583101    21.601655 f=Z
C    16.315403     9.728787    15.700392 f=Z
H     9.300203     7.312590     9.451316 f=Z
H     7.014344     8.789188    12.761740 f=Z
H    15.143495     6.712897    14.837603 f=Z
H    14.241837     6.108341    10.691156 f=Z
H    11.121463     6.537547     8.811728 f=Z
H    12.767650     6.128993     9.230043 f=Z
H    11.431404     5.428841    10.157404 f=Z
H    11.664110     8.989793     9.010334 f=Z
H    12.387851     9.636361    10.489558 f=Z
H    13.335656     8.577165     9.436234 f=Z
H    17.378093     7.326077    12.316590 f=Z
H    17.267394     6.793030    13.998486 f=Z
H    18.269786     5.897727    12.858675 f=Z
H    16.019334     4.636078    14.575743 f=Z
H    15.280057     3.675013    13.288308 f=Z
H    17.040300     3.762981    13.435112 f=Z
H    16.438687     5.856158    10.445809 f=Z
H    17.312842     4.486385    11.123910 f=Z
H    15.578884     4.356799    10.847533 f=Z
H     7.723304     8.473041     8.292195 f=Z
H     5.964159     8.605085     8.287268 f=Z
H     6.937805     9.786527     9.173617 f=Z
H     5.348799     7.616794    11.806337 f=Z
H     5.485975     9.280829    11.206290 f=Z
H     4.623708     8.068808    10.266280 f=Z
H     6.570689     5.725488    10.607146 f=Z
H     5.745205     6.234887     9.127837 f=Z
H     7.498702     6.053457     9.140850 f=Z
H     6.211869    12.408856    15.384529 f=Z
H     6.045477     8.783068    17.593069 f=Z
H     9.120999     7.403883    16.264222 f=Z
H     7.825124     5.447897    15.516291 f=Z
H     6.377479     6.450296    15.365866 f=Z
H     7.762023     6.737305    14.306907 f=Z
H     8.152145     5.967058    17.934455 f=Z
H     8.020314     7.623258    18.544698 f=Z
H     6.609110     6.794469    17.885221 f=Z
H     9.167373    11.395839    13.392369 f=Z
H     7.071788    11.081971    12.101429 f=Z
H     6.356118    12.486056    12.904716 f=Z
H     7.744535    12.691525    11.834239 f=Z
H     9.210494    13.167229    15.241638 f=Z
H     9.172013    13.810845    13.595138 f=Z
H     7.713058    13.810680    14.576578 f=Z
H     4.640890    12.214298    16.995999 f=Z
H     3.311987    10.317290    16.086547 f=Z
H     3.691240     9.355654    17.519418 f=Z
H     2.724733    10.822073    17.676332 f=Z
H     6.046331    11.929730    19.026742 f=Z
H     4.327298    11.759011    19.399157 f=Z
H     5.348561    10.326569    19.294609 f=Z
H    13.264375     5.918623    19.248369 f=Z
H    15.595102     9.433720    18.701999 f=Z
H    11.548122     6.192245    15.987721 f=Z
H    12.216789     3.813811    15.974068 f=Z
H    13.579450     4.855213    15.553094 f=Z
H    13.472425     4.149515    17.171953 f=Z
H    10.526037     6.176114    18.329495 f=Z
H    10.345594     4.666380    17.426089 f=Z
H    11.541648     4.786226    18.703527 f=Z
H    14.258463    10.128337    15.313193 f=Z
H    16.686876    10.548867    15.081445 f=Z
H    17.002729     9.605699    16.541405 f=Z
H    16.344102     8.818135    15.101172 f=Z
H    15.145093    12.185008    16.244738 f=Z
H    13.916206    11.599404    17.371727 f=Z
H    15.626395    11.394079    17.738594 f=Z
H    15.723516     8.371150    20.690010 f=Z
H    13.390397     8.511226    21.539646 f=Z
H    13.264611     6.747531    21.506611 f=Z
H    14.408551     7.527417    22.597292 f=Z
H    16.669865     6.206345    19.909492 f=Z
H    16.331861     6.182525    21.644996 f=Z
H    15.249334     5.355276    20.525444 f=Z
H    10.939087    11.982021    14.833614 f=Z
H    12.458811    11.627763    15.678074 f=Z
H    12.296647    11.265589    13.958929 f=Z
C    10.924368     9.553377    18.192012 f=t
C    10.128037    10.543560    17.768890 f=t
H    10.525372    11.530788    17.554392 f=t
H     9.054213    10.413600    17.672924 f=t
H    10.518402     8.584812    18.471925 f=t
H    11.988135     9.695550    18.360094 f=t
```

A.2 Geometries from the Chapter Thermodynamic properties and electronic structures of Plutonium Oxides in Angstrom

A.2.1 Molecules containing Plutonium

$PuO_2(OH)_2$ coordinates in Å

Label	x	y	z
Pu	0.000000	0.967853	0.000000
O	-0.017474	0.880968	1.740764
O	0.017474	0.880968	-1.740764
O	1.676305	2.238293	0.001209
O	-1.676305	2.238293	-0.001209
H	2.063158	2.697914	0.750904
H	-2.063158	2.697914	-0.750904

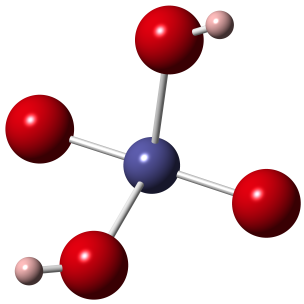

FIGURE A.3: $PuO_2(OH)_2$ molecule.Blue: Pu; red: O: pink; H.

PuO_3 coordinates in Å

Label	x	y	z
Pu	0.000000	0.000000	0.000000

O	1.934000	0.000000	0.000000
O	-0.118952	0.000000	1.762992
O	-0.118952	0.000000	-1.762992

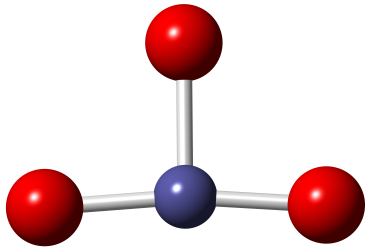

FIGURE A.4: PuO_3 molecule. Blue: Pu; red: O.

PuO_2 coordinates in Å

Label	x	y	z
Pu	0.000000	0.000000	0.000000
O	0.000000	0.000000	1.808000
O	0.000000	0.000000	-1.808000

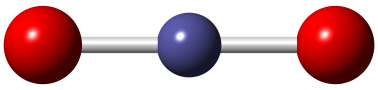

FIGURE A.5: PuO_2 molecule. Blue: Pu; red: O.

A.2.2 Organic Molecules

H_2O_2 coordinates in Å

Label	x	y	z
O	-0.275341	-0.185870	0.687291
O	-0.213172	0.301727	-0.678278
H	0.365257	0.397493	1.116183
H	0.173256	-0.463349	-1.125197

H_2O coordinates in Å

Label	x	y	z
O	0.000000	0.000000	0.000000
H	0.521742	0.000000	0.823124
H	0.521742	0.000000	-0.823124

O_2 coordinates in Å

Label	x	y	z
O	0.000000	0.000000	0.603760
O	0.000000	0.000000	-0.603760

OH coordinates in Å

Label	x	y	z
O	0.000000	0.000000	0.975370
H	0.000000	0.000000	0.000000

H_2 coordinates in Å

Label	x	y	z
H	0.000000	0.000000	0.372000
H	0.000000	0.000000	-0.372000

Appendix B

Electronic levels of Plutonium and Plutonium oxydes

TABLE B.1: Electronic levels (cm-1) of the plutonium atom and analysis of the various states obtained with the ano-cc-TZVP.

J-value	E (cm-1)	Character
0	0	54% ^7F , 38% ^5D , 7% ^3P
1	1806	64% ^7F , 32% ^5D
2	4208	82% ^7F , 17% ^5D
3	6353	88% ^7F , 10% ^5D
4	8091	93% ^7F
5	9552	90% ^7F
6	11010	85% ^7F , 10% ^5G
0	12499	44% ^7F , 21% ^5D , 8% ^3P
1	13612	66% ^9H , 9% ^7F , 7% ^7G
2	14399	82% ^9H , 14% ^7G
1	14845	38% ^5D, 20% ^7F , 9% ^9G
3	15551	89% ^9H , 8% ^7G
4	17026	86% ^9H , 6% ^7G
1	17032	66% ^9D , 29% ^7P

TABLE B.2: Energy electronic states (E < 16 000 cm^{-1}) of $PuO_2(OH)_2$ at SF-CASPT2 and SO-CASPT2 levels obtained with the ano-cc-TZVP.

	Term Symbol	Character : % [orbital(number of electron)]	E (cm^{-1})
SF	$^3B(1)$	49% 2a/Φ_u(1), 1b/δ_u(1)	0
		48% 1a/δ_u(1), 2b/Φ_u(1)	
	$^3A(1)$	41% 1a/δ_u(1) , 2a/Φ_u(1)	889
		59% 1b/δ_u(1) , 2b/Φ_u(1)	
	$^3B(2)$	75% 1a/δ_u(1), 1b/δ_u(1)	2136
		20% 2a/Φ_u(1), 2b/Φ_u(1)	
	$^3A(2)$	59% 1a/δ_u(1) , 2a/Φ_u(1)	4698
		41% 1b/δ_u(1) , 2b/Φ_u(1)	
	$^3B(3)$	52% 2a/Φ_u(1), 1b/δ_u(1)	5351
		46% 1a/δ_u(1), 2b/Φ_u(1)	
	$^1A(1)$	58% 1b/δ_u(1) , 2b/$\Phi_u(\bar{1})$	5764
		30% 1a/δ_u(1) , 2a/$\Phi_u(\bar{1})$	
		5% 2a/Φ_u(2)	
	$^1B(1)$	50% 1a/δ_u(1), 1b/$\delta_u(\bar{1})$	7444
		28% 2a/Φ_u(1), 2b/$\Phi_u(\bar{1})$	
		16% 1a/δ_u(1), 2b/$\Phi_u(\bar{1})$	
	$^1A(2)$	39% 1a/δ_u(1) , 2a/$\Phi_u(\bar{1})$	9626
		29 % 2a/Φ_u(2)	
		13% 1b/δ_u(1) , 2b/$\Phi_u(\bar{1})$	
		10% 1a/δ_u(2)	
		7 % 2a/Φ_u(2)	
	$^1A(3)$	44% 1b/δ_u(2)	10184
		33% 2a/Φ_u(2)	
		12% 2b/Φ_u(2)	
		9% 1a/δ_u(2)	
	$^1B(2)$	66% 2a/Φ_u(1), 2b/$\Phi_u(\bar{1})$	10287
		26% 1a/δ_u(1), 2b/$\Phi_u(\bar{1})$	
		8% 1a/δ_u(1), 1b/$\delta_u(\bar{1})$	
SO	X	46.1% $^3A(1)$, 41.4% $^3B(1)$, 6.4% $^3B(2)$	0
	a	45.3% $^3B(1)$, 44.8% $^3A(1)$, 6.3% $^3B(2)$	323
	b	34.9% $^3B(2)$, 24.7% $^3B(1)$, 14.4% $^1A(1)$, 12.5% $^3A(2)$, 10.1% $^3B(3)$	2222
	c	40.3% $^3A(2)$, 25.4% $^3B(2)$, 18.8% $^1B(1)$, 7.1% $^3B(1)$, 6.1% $^3A(1)$	3757
	d	35.5% $^3B(3)$, 34.3% $^3B(2)$, 14.3% $^1A(2)$, 11.1% $^3B(1)$,	4158
	e	63.5% $^3B(1)$, 30.1% $^3B(2)$	7268
	f	92.8% $^3A(1)$	7575
	g	32.4% $^1A(1)$, 28.1% $^3B(3)$, 27.8% $^3A(2)$, 6.3% $^3B(2)$,	10041
	h	41.1% $^3A(2)$, 24.1% $^3B(3)$, 15.3% $^3B(2)$, 10.5% $^3B(1)$, 6.1% $^1B(1)$	10142
	i	33.5% $^3A(2)$, 26.3% $^3B(2)$, 13.8% $^3B(3)$, 13.1% $^1B(1)$, 8.2% $^3B(1)$	10343
	j	29.3% $^3B(2)$, 25.6% $^3B(3)$, 22.0% $^3B(1)$, 16.6% $^1A(2)$	11089
	k	26.3% $^3B(3)$, 22.9% $^3A(1)$, 17.0% $^3B(1)$, 16.6% $^3A(2)$, 13.0% $^3B(2)$	12269
	l	26.1% $^3A(2)$, 23.6% $^3A(1)$, 21.3% $^3B(3)$, 15.4% $^3B(2)$, 9.6% $^3B(1)$	12311
	m	27.5% $^3B(3)$, 24.6% $^3A(2)$, 22.2% $^3A(1)$, 12.1% $^3B(1)$, 9.7% $^3B(2)$	13782
	n	34.8% $^3B(3)$, 21.8% $^3A(2)$, 17.7% $^3A(1)$, 13.0% $^3B(1)$, 8.5% $^3B(2)$	13783
	o	40.9% $^1A(1)$, 19.7% $^1A(3)$, 15.4% $^3B(2)$, 7.3% $^3B(4)$,	15696

TABLE B.3: Vertical transitions in cm^{-1} of the low-energy ($E < 16\,000\,cm^{-1}$) electronic states of PuO_3 at SF-CASPT2 and SO-CASPT2 levels obtained with the ANO-RCC-TZVP. Orbitals $1a_1$, $2a_1/\pi_u$, $3a_1$ always doubly occupied and do not appear in the following table.

	Term Symbol	Character : % [orbital(number of electron)]	E (cm^{-1})
SF	$^3B_2(1)$	36% [$4a_1/p^{(O)}(2)$, $1b_1/\Phi_u(1)$, $1b_2/p^{(O)}(\bar{1})$, $2b_2/\sigma_u(2)$, $3b_2/\delta_u(1)$, $1a_2/\delta_u(1)$]	0
		21% [$4a_1/p^{(O)}(2)$, $1b_1/\Phi_u(1)$, $1b_2/p^{(O)}(1)$, $2b_2/\sigma_u(2)$, $3b_2/\delta_u(\bar{1})$, $1a_2/\delta_u(1)$]	
		22% [$4a_1/p^{(O)}(2)$,$1b_1/\Phi_u(1)$,$1b_2/p^{(O)}(2)$,$2b_2/\sigma_u(2)$,$1a_2/\delta_u(1)$]	
	$^3A_2(1)$	43% [$4a_1/p^{(O)}(2)$, $5a_1/\Phi_u(1)$,$1b_2/p^{(O)}(\bar{1})$,$2b_2/\sigma_u(2)$,$3b_2/\delta_u(1)$,$1a_2/\delta_u(1)$]	3161
		23% [$4a_1/p^{(O)}(2)$, $5a_1/\Phi_u(1)$,$1b_2/p^{(O)}(1)$,$2b_2/\sigma_u(2)$,$3b_2/\delta_u(\bar{1})$,$1a_2/\delta_u(1)$]	
		17% [$4a_1/p^{(O)}(2)$, $5a_1/\Phi_u(1)$,$1b_2/p^{(O)}(2)$,$2b_2/\sigma_u(2)$,$1a_2/\delta_u(1)$]	
	$^3B_1(1)$	38% [$4a_1/p^{(O)}(2)$,$5a_1/\Phi_u(1)$,$1b_1/\Phi_u(1)$,$1b_2/p^{(O)}(\bar{1})$,$2b_2/\sigma_u(2)$,$3b_2/\delta_u(1)$]	4663
		12% [$4a_1/p^{(O)}(2)$, $5a_1/\Phi_u(1)$, $2b_1/\pi_u(1)$,$1b_2/p^{(O)}(\bar{1})$,$2b_2/\sigma_u(2)$,$3b_2/\delta_u(1)$]	
		12% [$4a_1/p^{(O)}(2)$, $5a_1/\Phi_u(1)$,$1b_1/\Phi_u(1)$,$2b_1/\pi_u(2)$,$1b_2/p^{(O)}(2)$]	
	$^1A_1(1)$	32% [$4a_1/p^{(O)}(2)$,$1b_2/p^{(O)}(1)$,$2b_2/\sigma_u(2)$,$3b_2/\delta_u(\bar{1})$,$1a_2/\delta_u(2)$]	7239
		28% [$4a_1/p^{(O)}(2)$,$1b_2/p^{(O)}(2)$,$2b_2/\sigma_u(2)$,$1a_2/\delta_u(2)$]	
		11% [$4a_1/p^{(O)}(1)$, $5a_1/\Phi_u(\bar{1})$,$1b_2/p^{(O)}(2)$,$2b_2/\sigma_u(2)$,$1a_2/\delta_u(2)$]	
	$^3A_2(2)$	20% [$4a_1/p^{(O)}(2)$,$1b_1/\Phi_u(1)$,$1b_2/p^{(O)}(1)$,$2b_2/\sigma_u(2)$,$3b_2/\delta_u(2)$]	7287
		18% [$4a_1/p^{(O)}(1)$,$5a_1/\Phi_u(\bar{1})$,$1b_1/\Phi_u(1)$,$1b_2/p^{(O)}(2)$,$2b_2/\sigma_u(2)$,$3b_2/\delta_u(1)$]	
		17% [$4a_1/p^{(O)}(2)$,$1b_1/\Phi_u(1)$,$1b_2/p^{(O)}(2)$,$2b_2/\sigma_u(2)$,$3b_2/\delta_u(1)$]	
	$^3B_1(2)$	31% [$4a_1/p^{(O)}(1)$,$5a_1/\Phi_u(\bar{1})$,$1b_2/p^{(O)}(2)$,$2b_2/\sigma_u(2)$,$3b_2/\delta_u(1)$,$1a_2/\delta_u(1)$]	8038
		11% [$4a_1/p^{(O)}(2)$,$5a_1/\Phi_u(1)$,$2b_1/\pi_u(1)$,$1b_2/p^{(O)}(\bar{1})$,$2b_2/\sigma_u(2)$,$3b_2/\delta_u(1)$]	
		10% [$4a_1/p^{(O)}(2)$,$1b_2/p^{(O)}(2)$,$2b_2/\sigma_u(2)$,$3b_2/\delta_u(1)$,$1a_2/\delta_u(1)$]	

Table B.3 – *Continued from previous page*

Term Symbol	Character : % [orbital(number of electron)]	E (cm^{-1})
	10% [$4a_1/p^{(O)}(2)$,$1b_1/\Phi_u(1)$,$2b_1/\pi_u(1)$,$1b_2/p^{(O)}(\overline{1})$,$2b_2/\sigma_u(2)$,$1a_2/\delta_u(1)$]	
$^5B_2(1)$	47% [$4a_1/p^{(O)}(2)$, $1b_1/\Phi_u(\overline{1})(1)$, $1b_2/p^{(O)}(2)$, $2b_2/\sigma_u(1)$, $3b_2/\delta_u(1)$, $1a_2/\delta_u(1)$]	8962
	41% [$4a_1/p^{(O)}(2)$, $5a_1/\Phi_u(1)$, $1b_1/\Phi_u(\overline{1})(1)$, $1b_2/p^{(O)}(1)$, $2b_2/\sigma_u(2)$, $1a_2/\delta_u(1)$]	
$^3A_1(1)$	39% [$4a_1/p^{(O)}(2)$, $1b_1/\Phi_u(\overline{1})(1)$, $2b_1/\pi_u(1)$, $1b_2/p^{(O)}(\overline{1})$, $2b_2/\sigma_u(2)$, $3b_2/\delta_u(1)$]	9645
	11% [4(2), $1b_1/\Phi_u(\overline{1})(1)$, 8(1), $1b_2/p^{(O)}(\overline{1})$, $2b_2/\sigma_u(2)$, $3b_2/\delta_u(1)$]	
$^3B_2(2)$	15% [$4a_1/p^{(O)}(2)$, $2b_1/\pi_u(1)$, $1b_2/p^{(O)}(2)$, $2b_2/\sigma_u(2)$, $1a_2/\delta_u(1)$]]	9731
	15% [$4a_1/p^{(O)}(1)$, $5a_1/\Phi_u(\overline{1})$, $2b_1/\pi_u(1)$, $1b_2/p^{(O)}(2)$, $2b_2/\sigma_u(2)$, $1a_2/\delta_u(1)$]	
	12% [$4a_1/p^{(O)}(2)$, $2b_1/\pi_u(1)$, $1b_2/p^{(O)}(\overline{1})$, $2b_2/\sigma_u(2)$, $3b_2/\delta_u(1)$, $1a_2/\delta_u(1)$]	
$^1A_2(1)$	26% [$4a_1/p^{(O)}(2)$, $5a_1/\Phi_u(1)$, $1b_2/p^{(O)}(1)$, $2b_2/\sigma_u(2)$, $11(\overline{1})$, $1a_2/\delta_u(\overline{1})$]	10293
	24% [$4a_1/p^{(O)}(2)$, $5a_1/\Phi_u(1)$, $1b_2/p^{(O)}(\overline{1})$, $2b_2/\sigma_u(2)$, $3b_2/\delta_u(1)$, $1a_2/\delta_u(\overline{1})$]	
	18% [$4a_1/p^{(O)}(2)$, $1b_1/\Phi_u(1)$, $1b_2/p^{(O)}(\overline{1})$, $2b_2/\sigma_u(2)$, $1a_2/\delta_u(2)$]	
	16% [$4a_1/p^{(O)}(2)$, $5a_1/\Phi_u(1)$, $1b_2/p^{(O)}(2)$, $2b_2/\sigma_u(2)$, $1a_2/\delta_u(\overline{1})$]	
$^1B_2(1)$	30% [$4a_1/p^{(O)}(2)$, $1b_1/\Phi_u(1)$, $1b_2/p^{(O)}(\overline{1})$, $2b_2/\sigma_u(2)$, $3b_2/\delta_u(1)$, $1a_2/\delta_u(\overline{1})$]	10604
	22% [$4a_1/p^{(O)}(2)$, $1b_1/\Phi_u(1)$, $1b_2/p^{(O)}(1)$, $2b_2/\sigma_u(2)$, $3b_2/\delta_u(\overline{1})$, $1a_2/\delta_u(\overline{1})$]	
	16% [$4a_1/p^{(O)}(2)$, $1b_1/\Phi_u(1)$, $1b_2/p^{(O)}(2)$, $2b_2/\sigma_u(2)$, $1a_2/\delta_u(\overline{1})$]	
	15% [$4a_1/p^{(O)}(2)$, $5a_1/\Phi_u(1)$, $1b_2/p^{(O)}(\overline{1})$, $2b_2/\sigma_u(2)$, $1a_2/\delta_u(2)$]	
$^5A_1(1)$	27% [$4a_1/p^{(O)}(2)$, $5a_1/\Phi_u(1)$, $1b_1/\Phi_u(1)$, $1b_2/p^{(O)}(2)$, $2b_2/\sigma_u(1)$, $1a_2/\delta_u(1)$]	10662
	15% [$4a_1/p^{(O)}(2)$, $2b_1/\pi_u^*(1)$, $1b_1/\Phi_u(1)$, $1b_2/p^{(O)}(2)$, $2b_2/\sigma_u(1)$, $1a_2/\delta_u(1)$]	
	12% [$4a_1/p^{(O)}(2)$, $5a_1/\Phi_u(1)$, $1b_1/\Phi_u(1)$, $1b_2/p^{(O)}(1)$, $2b_2/\sigma_u(2)$, $1a_2/\delta_u(1)$]	
$^3B_1(3)$	26% [$4a_1/p^{(O)}(2)$, $1b_1/\Phi_u(1)$, $2b_1/\pi_u(1)$, $1b_2/p^{(O)}(\overline{1})$, $2b_2/\sigma_u(2)$, $1a_2/\delta_u(1)$]	11567
	17% [$4a_1/p^{(O)}(1)$, $5a_1/\Phi_u(\overline{1})$, $1b_2/p^{(O)}(2)$, $2b_2/\sigma_u(2)$, $3b_2/\delta_u(1)$, $1a_2/\delta_u(1)$]	

Table B.3 – *Continued from previous page*

Term Symbol	Character : % [orbital(number of electron)]	E (cm^{-1})
$^1B_1(1)$	34% [$4a_1/p^{(O)}(2)$, $1b_2/p^{(O)}(1)$, $2b_2/\sigma_u(2)$, $3b_2/\delta_u(2)$, $1a_2/\delta_u(\bar{1})$]	11632
	18% [$4a_1/p^{(O)}(1)$, $5a_1/\Phi_u(\bar{1})$, $1b_2/p^{(O)}(2)$, $2b_2/\sigma_u(2)$, $3b_2/\delta_u(1)$, $1a_2/\delta_u(\bar{1})$]	
	17% [$4a_1/p^{(O)}(2)$, $1b_2/p^{(O)}(2)$, $2b_2/\sigma_u(2)$, $3b_2/\delta_u(1)$, $1a_2/\delta_u(\bar{1})$]	
$^5B_1(1)$	36% [$4a_1/p^{(O)}(2)$, $1b_1/\Phi_u(1)$, $2b_1/\pi_u(1)$, $1b_2/p^{(O)}(2)$, $2b_2/\sigma_u(1)$, $1a_2/\delta_u(1)$]	12017
	15% [$4a_1/p^{(O)}(2)$, $1b_1/\Phi_u(1)$, $2b_1/\pi_u(1)$, $1b_2/p^{(O)}(1)$, $2b_2/\sigma_u(2)$, $1a_2/\delta_u(1)$]	
$^5A_2(1)$	36% [$4a_1/p^{(O)}(2)$, $1b_1/\Phi_u(1)$, $2b_1/\pi_u(1)$, $1b_2/p^{(O)}(2)$, $2b_2/\sigma_u(1)$, $1a_2/\delta_u(1)$]	12017
	15% [$4a_1/p^{(O)}(2)$, $1b_1/\Phi_u(1)$, $2b_1/\pi_u(1)$, $1b_2/p^{(O)}(1)$, $2b_2/\sigma_u(2)$, $1a_2/\delta_u(1)$]	
$^3B_2(3)$	24% [$4a_1/p^{(O)}(2)$, $1b_1/\Phi_u(1)$, $1b_2/p^{(O)}(1)$, $2b_2/\sigma_u(2)$, $3b_2/\delta_u(1)$, $1a_2/\delta_u(\bar{1})$]	12023
	11% [$4a_1/p^{(O)}(2)$, $5a_1/\Phi_u(1)$, $1b_2/p^{(O)}(1)$, $2b_2/\sigma_u(2)$, $3b_2/\delta_u(2)$]	
$^3A_2(3)$	17% [$4a_1/p^{(O)}(2)$, $1b_1/\Phi_u(1)$, $1b_2/p^{(O)}(1)$, $2b_2/\sigma_u(2)$, $1a_2/\delta_u(2)$]	12940
	15% [$4a_1/p^{(O)}(2)$, $5a_1/\Phi_u(1)$, $1b_2/p^{(O)}(1)$, $2b_2/\sigma_u(2)$, $3b_2/\delta_u(1)$, $1a_2/\delta_u(\bar{1})$]	
$^1A_1(2)$	21% [$4a_1/p^{(O)}(2)$, $5a_1/\Phi_u(2)$, $1b_2/p^{(O)}(1)$, $2b_2/\sigma_u(2)$, $3b_2/\delta_u(\bar{1})$]	13213
	10% [$4a_1/p^{(O)}(1)$, $5a_1/\Phi_u(\bar{1})$, $1b_2/p^{(O)}(2)$, $2b_2/\sigma_u(2)$, $3b_2/\delta_u(2)$]	
	10% [$4a_1/p^{(O)}(2)$, $5a_1/\Phi_u(2)$, $1b_2/p^{(O)}(2)$, $2b_2/\sigma_u(2)$]	
$^3A_1(2)$	44% [$4a_1/p^{(O)}(2)$, $5a_1/\Phi_u(1)$, $1b_1/\Phi_u(1)$, $1b_2/p^{(O)}(\bar{1})$, $2b_2/\sigma_u(2)$, $1a_2/\delta_u(1)$]	13421
	29% [$4a_1/p^{(O)}(2)$, $5a_1/\Phi_u(1)$, $2b_1/\pi_u(1)$, $1b_2/p^{(O)}(\bar{1})$, $2b_2/\sigma_u(2)$, $1a_2/\delta_u(1)$]	
$^3B_1(4)$	29% [$4a_1/p^{(O)}(2)$, $2b_1/\pi_u^*(1)$, $1b_1/\Phi_u(1)$, $1b_2/p^{(O)}(\bar{1})$, $2b_2/\sigma_u(2)$, $3b_2/\delta_u(1)$]	13518
	15% [$4a_1/p^{(O)}(2)$, $5a_1/\Phi_u(1)$, $2b_1/\pi_u(1)$, $1b_2/p^{(O)}(\bar{1})$, $2b_2/\sigma_u(2)$, $3b_2/\delta_u(1)$]	
	13% [$4a_1/p^{(O)}(2)$, $2b_1/\pi_u^*(1)$, $1b_1/\Phi_u(1)$, $1b_2/p^{(O)}(2)$, $2b_2/\sigma_u(2)$]	
	11% [$4a_1/p^{(O)}(2)$, $5a_1/\Phi_u(1)$, $2b_1/\pi_u^*(1)$, $1b_2/p^{(O)}(\bar{1})$, $2b_2/\sigma_u(2)$, $1a_2/\delta_u(1)$]	
$^5A_1(2)$	29% [$4a_1/p^{(O)}(2)$, $1b_1/\Phi_u(1)$, $2b_1/\pi_u(1)$, $1b_2/p^{(O)}(2)$, $2b_2/\sigma_u(1)$, $3b_2/\delta_u(1)$]	13575

Table B.3 – *Continued from previous page*

Term Symbol	Character : % [orbital(number of electron)]	E (cm^{-1})
	14% [$4a_1/p^{(O)}(2)$, $5a_1/\Phi_u(1)$, $1b_1/\Phi_u(1)$, $1b_2/p^{(O)}(2)$, $2b_2/\sigma_u(1)$, $1a_2/\delta_u(1)$]	
	13% [$4a_1/p^{(O)}(2)$, $1b_1/\Phi_u(1)$, $2b_1/\pi_u(1)$, $1b_2/p^{(O)}(1)$, $2b_2/\sigma_u(2)$, $3b_2/\delta_u(1)$]	
	12% [$4a_1/p^{(O)}(2)$, $5a_1/\Phi_u(1)$, $2b_1/\pi_u(1)$, $1b_2/p^{(O)}(2)$, $2b_2/\sigma_u(1)$, $1a_2/\delta_u(1)$]	
$^5B_1(2)$	30% [$4a_1/p^{(O)}(2)$, $5a_1/\Phi_u(1)$, $1b_1/\Phi_u(1)$, $1b_2/p^{(O)}(2)$, $2b_2/\sigma_u(1)$, $3b_2/\delta_u(1)$]	13970
	20% [$4a_1/p^{(O)}(2)$, $5a_1/\Phi_u(1)$, $1b_1/\Phi_u(1)$, $1b_2/p^{(O)}(1)$, $2b_2/\sigma_u(2)$, $3b_2/\delta_u(1)$]	
	16% [$4a_1/p^{(O)}(2)$, $5a_1/\Phi_u(1)$, $2b_1/\pi_u(1)$, $1b_2/p^{(O)}(2)$, $2b_2/\sigma_u(1)$, $3b_2/\delta_u(1)$]	
	10 % [$4a_1/p^{(O)}(2)$, $5a_1/\Phi_u(1)$, $2b_1/\pi_u(1)$, $1b_2/p^{(O)}(1)$, $2b_2/\sigma_u(2)$, $3b_2/\delta_u(1)$]	
$^5A_2(2)$	30% [$4a_1/p^{(O)}(2)$, $5a_1/\Phi_u(1)$, $1b_1/\Phi_u(1)$, $1b_2/p^{(O)}(2)$, $2b_2/\sigma_u(1)$, $3b_2/\delta_u(1)$]	13971
	20% [$4a_1/p^{(O)}(2)$, $5a_1/\Phi_u(1)$, $1b_1/\Phi_u(1)$, $1b_2/p^{(O)}(1)$, $2b_2/\sigma_u(2)$, $3b_2/\delta_u(1)$]	
	16% [$4a_1/p^{(O)}(2)$, $5a_1/\Phi_u(1)$, $2b_1/\pi_u(1)$, $1b_2/p^{(O)}(2)$, $2b_2/\sigma_u(1)$, $3b_2/\delta_u(1)$]	
	10% [$4a_1/p^{(O)}(2)$, $5a_1/\Phi_u(1)$, $2b_1/\pi_u(1)$, $1b_2/p^{(O)}(1)$, $2b_2/\sigma_u(2)$, $3b_2/\delta_u(1)$]	
$^5B_1(3)$	86% [$4a_1/p^{(O)}(1)$, $5a_1/\Phi_u(1)$, $1b_2/p^{(O)}(2)$, $2b_2/\sigma_u(2)$, $3b_2/\delta_u(1)$, $1a_2/\delta_u(1)$]	14055
$^5A_2(3)$	86% [$4a_1/p^{(O)}(1)$, $5a_1/\Phi_u(1)$, $1b_2/p^{(O)}(2)$, $2b_2/\sigma_u(2)$, $3b_2/\delta_u(1)$, $1a_2/\delta_u(1)$]	14056
$^5A_1(3)$	80% [$4a_1/p^{(O)}(1)$, $1b_1/\Phi_u(1)$, $1b_2/p^{(O)}(2)$, $2b_2/\sigma_u(2)$, $3b_2/\delta_u(1)$, $1a_2/\delta_u(1)$]	14139
$^3A_1(3)$	58% [$4a_1/p^{(O)}(1)$, $1b_1/\Phi_u(\bar{1})$, $1b_2/p^{(O)}(2)$, $2b_2/\sigma_u(2)$, $3b_2/\delta_u(1)$, $1a_2/\delta_u(1)$]	14236
	20% [$4a_1/p^{(O)}(1)$, $1b_1/\Phi_u(1)$, $1b_2/p^{(O)}(2)$, $2b_2/\sigma_u(2)$, $3b_2/\delta_u(\bar{1})$, $1a_2/\delta_u(1)$]	
	10% [$4a_1/p^{(O)}(1)$, $1b_1/\Phi_u(1)$, $1b_2/p^{(O)}(2)$, $2b_2/\sigma_u(2)$, $3b_2/\delta_u(1)$, $1a_2/\delta_u(\bar{1})$]	
$^3B_2(4)$	19% [$4a_1/p^{(O)}(1)$, $5a_1/\Phi_u(\bar{1})$, $1b_1/\Phi_u(1)$, $1b_2/p^{(O)}(2)$, $2b_2/\sigma_u(2)$, $1a_2/\delta_u(1)$]	14843
	18% [$4a_1/p^{(O)}(2)$, $5a_1/\Phi_u(1)$, $1b_2/p^{(O)}(1)$, $2b_2/\sigma_u(2)$, $3b_2/\delta_u(2)$]	
$^1A_1(3)$	27% [$4a_1/p^{(O)}(2)$, $1b_1/\Phi_u(2)$, $1b_2/p^{(O)}(1)$, $2b_2/\sigma_u(2)$, $3b_2/\delta_u(\bar{1})$]	14889
	13% [$4a_1/p^{(O)}(2)$, $1b_1/\Phi_u(2)$, $1b_2/p^{(O)}(2)$, $2b_2/\sigma_u(2)$]	

Table B.3 – *Continued from previous page*

	Term Symbol	Character : % [orbital(number of electron)]	E (cm^{-1})
	$^1A_2(2)$	47% [$4a_1/p^{(O)}(2)$, $1b_1/\Phi_u(1)$, $1b_2/p^{(O)}(\bar{1})$, $2b_2/\sigma_u(2)$, $3b_2/\delta_u(2)$]	14984
		10% [$4a_1/p^{(O)}(2)$, $5a_1/\Phi_u(1)$, $1b_2/p^{(O)}(\bar{1})$, $2b_2/\sigma_u(2)$, $3b_2/\delta_u(1)$, $1a_2/\delta_u(\bar{1})$]	
		9% [$4a_1/p^{(O)}(2)$, $5a_1/\Phi_u(1)$, $1b_2/p^{(O)}(1)$, $2b_2/\sigma_u(2)$, $3b_2/\delta_u(\bar{1})$, $1a_2/\delta_u(\bar{1})$]	
	$^5B_2(2)$	64% [$4a_1/p^{(O)}(1)$, $5a_1/\Phi_u(1)$, $1b_1/\Phi_u(1)$, $1b_2/p^{(O)}(2)$, $2b_2/\sigma_u(2)$, $1a_2/\delta_u(1)$]	15035
		10% [$4a_1/p^{(O)}(1)$, 6(1), $1b_1/\Phi_u(1)$, $1b_2/p^{(O)}(2)$, $2b_2/\sigma_u(2)$, $1a_2/\delta_u(1)$]	
	$^1B_1(2)$	33% [$4a_1/p^{(O)}(2)$, $5a_1/\Phi_u(1)$,$1b_1/\Phi_u(\bar{1})$, $1b_2/p^{(O)}(1)$, $2b_2/\sigma_u(2)$, $3b_2/\delta_u(\bar{1})$]	15593
		13% [$4a_1/p^{(O)}(2)$, $5a_1/\Phi_u(1)$,$1b_1/\Phi_u(\bar{1})$, $1b_2/p^{(O)}(2)$, $2b_2/\sigma_u(2)$,]	
		12% [$4a_1/p^{(O)}(2)$, $1b_2/p^{(O)}(1)$, $2b_2/\sigma_u(2)$, $3b_2/\delta_u(2)$, $1a_2/\delta_u(\bar{1})$]	
		11% [$4a_1/p^{(O)}(2)$, $5a_1/\Phi_u(2)$, $1b_2/p^{(O)}(1)$, $2b_2/\sigma_u(2)$, $1a_2/\delta_u(\bar{1})$]	
SO	X	47.15% $^3B_2(1)$, 24.15% $^3A_2(1)$, 14.14% $^3B_1(1)$	0
	a	58.72% $^3B_2(1)$, 24.89% $^3A_2(1)$	1235
	b	73.37% $^3B_2(1)$	1783
	c	51.22% $^3A_2(1)$	3777
	d	23.54% $^3B_1(1)$, 18.35% $^1A_1(1)$, 16.73% $^3A_2(2)$, 10.23% $^3B_1(2)$	5660
	e	49.43% $^3B_1(1)$, 22.12% $^3A_1(1)$	6658
	f	43.87% $^3B_1(1)$, 19.21% $^3A_1(1)$, 11.3% $^3B_1(2)$	7062
	g	23.47% $^3B_2(1)$, 17.68% $^3A_2(1)$, 17.17% $^3B_1(2)$	7929
	h	26.14% $^3A_2(1)$, 21.08% $^5B_2(1)$, 18.73% $^3A_2(2)$	7973
	i	32.2% $^3A_2(2)$, 24.4% $^3A_2(1)$, 15% $^5B_2(1)$	8675
	j	28.2% $^3A_2(1)$, 22.38% $^3B_1(1)$, 11.46% $^5B_2(1)$	9096

Table B.3 – *Continued from previous page*

Term Symbol	Character : % [orbital(number of electron)]	E (cm^{-1})
k	28.45% $^3A_2(1)$, 26.41% $^3B_2(1)$	9345
l	30.77% $^3B_1(2)$, 19% $^3B_1(1)$	9399
m	16.69% $^3B_2(1)$, 14.81% $^5B_2(1)$	9690
n	28.51% $^3B_1(2)$, 11.78% $^3A_1(2)$, 10.3% $^3B_1(1)$	9879
o	24.08% $^3A_2(2)$, 15.86% $^5B_1(1)$, 13.35% $^3B_2(2)$	10224
p	25.31% $^3A_2(2)$, 14.83% $^3B_2(2)$, 9.57% $^5B_1(1)$	10235
q	23.29% $^5B_2(1)$, 13.35% $^5B_1(3)$	10342
r	29.37% $^5B_1(1)$, 24.74% $^5A_1(1)$, 10.19% $^5B_2(1)$, 10.05% $^5A_1(2)$	10686
s	23.12% $^3B_2(2)$, 20.68% $^3B_1(3)$, 15.13% $^3B_1(2)$	10749
t	25.96% $^5B_1(1)$, 20.75% $^5A_1(1)$, 15.44% $^5B_2(1)$	10768
u	23.74% $^5B_2(1)$, 11.62% $^3B_1(3)$, 10.37% $^5A_1(1)$	11022
v	24.63% $^5B_2(1)$, 21.07% $^5A_1(1)$, 12.44% $^3B_1(1)$	11207
w	14.48% $^3A_1(1)$, 10.17% $^3A_1(2)$	11616
x	36.43% $^5A_1(1)$, 12.09% $^3B_1(2)$	12429
y	20.5% $^3A_2(2)$	12567
z	11.52% $^1A_1(1)$, 10.25% $^3B_1(3)$, 10.04% $^3B_2(3)$	12693
aa	14.11% $^1A_2(1)$	12794
ab	29.09% $^3B_2(2)$, 24.21% $^3A_2(3)$	12873
ac	16.43% $^3A_1(3)$, 15.09% $^5B_1(2)$, 14.7% $^3A_1(1)$, 10.89% $^5B_1(1)$	13058
ad	30.37% $^3A_2(3)$, 13.89% $^1A_1(1)$,	13309
ae	20.38% $^5B_1(2)$, 13.23% $^5A_1(3)$, 9.98% $^5B_2(2)$	13341

Table B.3 – *Continued from previous page*

Term Symbol	Character : % [orbital(number of electron)]	E (cm^{-1})
af	34.08% $^3B_2(3)$, 16.97% $^1A_2(1)$, 11.74% $^1A_2(2)$	13488
ag	24.73% $^3A_1(1)$, 12.48% $^5B_1(2)$, 11.36% $^5B_1(1)$	13582
ah	18.48% $^5B_1(2)$, 15.12% $^5A_1(3)$	13814
ai	27.31% $^5B_2(1)$, 14.88% $^1B_2(1)$, 12.3% $^3A_1(1)$	13936
aj	28.12% $^5B_2(1)$, 19.38% $^5A_1(1)$, 10% $^5B_1(2)$	13996
ak	17.59% $^5B_1(2)$, 14.15% $^5B_1(3)$, 11.94% $^5A_1(2)$, 11.41% $^5A_1(1)$	14024
al	53.19% $^1B_1(1)$, 12.49% $^3A_2(3)$	14216
am	22.79% $^5A_1(2)$, 12.86% $^5B_1(3)$, 10.57% $^3B_1(3)$	14257
an	31.62% $^5B_2(1)$, 10.41% $^3A_1(2)$	14680
ao	19.07% $^5B_1(1)$, 17.32% $^5B_1(2)$, 16.76% $^5A_1(3)$	14724
ap	21.09% $^5A_1(1)$, 10.26% $^5A_1(2)$, 10% $^5B_1(3)$	14750
aq	16.59% $^5B_1(3)$, 13.06% $^5B_1(2)$, 9.69% $^5A_1(2)$	14874
ar	16.33% $^5B_1(1)$	15129
as	20.39% $^5A_1(2)$, 20.07% $^5B_1(1)$, 12.66% $^5B_1(3)$, 10.85% $^3B_1(3)$, 9.82% $^5A_1(1)$	15141
at	28.7% $^3B_2(2)$, 12.63% $^5B_2(1)$	15375
au	15.53% $^3A_1(2)$, 12.26% $^5B_1(3)$, 10.67% $^5B_1(1)$, 9.55% $^3B_2(2)$	15439
av	25.7% $^3B_2(3)$, 10.77% $^3B_2(2)$, 10.04% $^5A_1(2)$	15494
aw	23.7% $^5B_1(3)$, 12.34% $^3A_1(2)$, 11.09% $^3B_1(3)$	15616
ay	12.56% $^5A_1(3)$, 11.67% $^3B_1(2)$, 10.58% $^3A_1(3)$, 10.25% $^3A_2(3)$	15708
az	15.14% $^5B_1(3)$, 10.79% $^3B_1(3)$	15906
ba	18.56% $^3B_2(3)$, 16.95% $^5B_1(3)$	15948

TABLE B.4: Vertical transitions in cm^{-1} of the low-energy ($E < 16\,000\,cm^{-1}$) electronic states of PuO_3 at SF-CASPT2 and SO-CASPT2 levels obtained with the ANO-RCC-TZVP. Orbitals $1a_1$, $2a_1/\pi_u$, $3a_1$ always doubly occupied and do not appear in the following table.

	Term Symbol	Character : % [orbital(number of electron)]	E (cm^{-1})
SF	$^5A_g(1)$	84% [$1a_u/\delta_u(1)$, $2b_{2u}/\Phi_u(1)$, $2b_{1u}/\delta_u(1)$, $2b_{3u}/\Phi_u(1)$]	0
	$^5A_g(2)$	45% [$1a_u/\delta_u(1)$, $3b_{2u}/\pi_u(1)$, $2b_{1u}/\delta_u(1)$, $2b_{3u}/\Phi_u(1)$]	4798
		45% [$1a_u/\delta_u(1)$, $2b_{2u}/\Phi_u(1)$, $2b_{1u}/\delta_u 3(1)$, $3b_{3u}/\pi_u(1)$]	
	$^5B_{3u}(1)$	85% [$3a_g(1)$, $1a_u/\delta_u(1)$, $2b_{1u}/\delta_u(1)$, $2b_{3u}/\Phi_u(1)$]	5421
	$^5B_{2u?}(1)$	85% [$3a_g(1)$, $1a_u/\delta_u(1)$, $2b_{1u}/\delta_u(1)$, $2b_{3u}/\Phi_u(1)$]	5421
	$^5B_{3g}(1)$	44% [$2b_{2u}/\Phi_u(1)$, $3b_{2u}/\pi_u 1(1)$, $2b_{1u}/\delta_u(1)$, $2b_{3u}/\Phi_u(1)$]	6019
		44% [$1a_u/\delta_u(1)$, $2b_{2u}/\Phi_u(1)$, $2b_{3u}/\Phi_u(1)$, $3b_{3u}/\pi_u(1)$]	
	$^5B_{2g}(1)$	44% [$2b_{2u}/\Phi_u(1)$, $3b_{2u}/\pi_u(1)$, $2b_{1u}/\delta_u(1)$, $2b_{3u}/\Phi_u(1)$]	6019
		44% [$1a_u/\delta_u(1)$, $2b_{2u}/\Phi_u(1)$, $2b_{3u}/\Phi_u(1)$, $3b_{3u}/\pi_u(1)$]	
	$^5A_g(3)$	45% [$1a_u/\delta_u(1)$, $3b_{2u}/\pi_u(1)$, $2b_{1u}/\delta_u(1)$, $2b_{3u}/\Phi_u(1)$]	6067
		45% [$1a_u/\delta_u(1)$, $2b_{2u}/\Phi_u(1)$, $2b_{1u}/\delta_u(1)$, $3b_{3u}/\pi_u(1)$]	
	$^5B_{1g}(1)$	44% [$1a_u/\delta_u(1)$, $2b_{2u}/\Phi_u(1)$, $3b_{2u}/\pi_u(1)$, $2b_{1u}/\delta_u(1)$]	6158
		44% [$1a_u/\delta_u(1)$, $2b_{1u}/\delta_u(1)$, $2b_{3u}/\Phi_u(1)$, $3b_{3u}/\pi_u(1)$]	
	$^3B_{3u}(1)$	59% [$3a_g(1)$,$1a_u/\delta_u(\overline{1})$, $2b_{2u}/\Phi_u(1)$, $2b_{1u}/\delta_u(1)$]	6855
		19% [$3a_g(1)$,$1a_u/\delta_u(1)$, $2b_{2u}/\Phi_u(\overline{1})$, $2b_{1u}/\delta_u(1)$]	
		10% [$3a_g(1)$,$1a_u/\delta_u(1)$, $2b_{2u}/\Phi_u(1)$, $2b_{1u}/\delta_u(\overline{1})$]	
	$^3B_{2u}(1)$	59% [$3a_g(1)$, $1a_u/\delta_u(\overline{1})$, $2b_{1u}/\delta_u(1)$, $2b_{3u}/\Phi_u(1)$]	6855
		20% [$3a_g(1)$, $1a_u/\delta_u(1)$, $2b_{1u}/\delta_u(\overline{1})$, $2b_{3u}/\Phi_u(1)$]	

Table B.4 – *Continued from previous page*

Term Symbol	Character : % [orbital(number of electron)]	E (cm^{-1})
$^5B_{1g}(2)$	44% [$1a_u/\delta_u(1)$, $2b_{1u}/\delta_u(1)$, $2b_{3u}/\Phi_u(1)$, $3b_{3u}/\pi_u(1)$]	7293
	44% [$1a_u/\delta_u(1)$, $2b_{2u}/\Phi_u(1)$, $3b_{2u}/\pi_u(1)$, $2b_{1u}/\delta_u(1)$]	
$^5A_u(1)$	79% [$3a_g(1)$, $2b_{2u}/\Phi_u(1)$, $2b_{1u}/\delta_u(1)$, $2b_{3u}/\Phi_u(1)$]	7452
$^5B_{1u}(1)$	80% [$3a_g(1)$, $1a_u/\delta_u(1)$, $2b_{2u}/\Phi_u0(1)$, $2b_{3u}/\Phi_u(1)$]	7462
$^5B_{3g}(2)$	37% [$1a_u/\delta_u(1)$, $2b_{2u}/\Phi_u(1)$, $2b_{3u}/\Phi_u(1)$, $3b_{3u}/\pi_u(1)$]	7637
	33%[$2b_{2u}/\Phi_u(1)$, $3b_{2u}/\pi_u(1)$, $2b_{1u}/\delta_u3(1)$, $2b_{3u}/\Phi_u(1)$]	
	12% [$2b_{2u}/\Phi_u(1)$, $3b_{2u}/\pi_u(1)$, $2b_{1u}/\delta_u(1)$, $3b_{3u}/\pi_u(1)$]	
$^5B_{2g}(2)$	37% [$1a_u/\delta_u(1)$, $2b_{2u}/\Phi_u(1)$, $2b_{3u}/\Phi_u6(1)$, $3b_{3u}/\pi_u(1)$]	7637
	33%[$2b_{2u}/\Phi_u(1)$, $3b_{2u}/\pi_u(1)$, $2b_{1u}/\delta_u(1)$, $2b_{3u}/\Phi_u(1)$]	
	12% [$2b_{2u}/\Phi_u(1)$, $3b_{2u}/\pi_u(1)$, $2b_{1u}/\delta_u(1)$, $3b_{3u}/\pi_u(1)$]	
$^3B_{1u}(1)$	51%[$3a_g(1)$, $1a_u/\delta_u(1)$, $2b_{2u}/\Phi_u(\bar{1})$, $2b_{3u}/\Phi_u(1)$]	9586
	68%[$3a_g(1)$, $1a_u/\delta_u(1)$, $2b_{2u}/\Phi_u(\bar{1})$, $2b_{3u}/\Phi_u(1)$]	
$^3A_u(1)$	51% [$3a_g(1)$, $2b_{2u}/\Phi_u(\bar{1})$, $2b_{1u}/\delta_u(1)$, $2b_{3u}/\Phi_u(1)$]	9614
	17% [$3a_g(1)$, $2b_{2u}/\Phi_u(1)$, $2b_{1u}/\delta_u(\bar{1})$, $2b_{3u}/\Phi_u(1)$]	
$^3B_{3g}(1)$	38% [$1a_u/\delta_u(1)$, $2b_{2u}/\Phi_u(1)$, $2b_{1u}/\delta_u(2)$]	10101
	36% [$1a_u/\delta_u(2)$, $2b_{1u}/\delta_u(1)$, $2b_{3u}/\Phi_u(1)$]	
$^3B_{2g}(1)$	38% [$1a_u/\delta_u(1)$, $2b_{2u}/\Phi_u(1)$, $2b_{1u}/\delta_u(2)$]	10101
	36% [$1a_u/\delta_u(2)$, $2b_{1u}/\delta_u(1)$, $2b_{3u}/\Phi_u(1)$]	
$^3B_{1g}(1)$	24% [$1a_u/\delta_u(1)$, $2b_{2u}/\Phi_u(2)$, $2b_{1u}/\delta_u(1)$]	10308
	24% [$1a_u/\delta_u(1)$, $2b_{1u}/\delta_u(1)$, $2b_{3u}/\Phi_u(2)$]	
	19% [$2b_{2u}/\Phi_u(1)$, $2b_{1u}/\delta_u(2)$, $2b_{3u}/\Phi_u(1)$]	

Table B.4 – *Continued from previous page*

Term Symbol	Character : % [orbital(number of electron)]	E (cm^{-1})
	16% [$1a_u/\delta_u(1)$, $2b_{2u}/\Phi_u(1)$, $2b_{3u}/\Phi_u(1)$]	
$^5A_u(2)$	23% [$3a_g(1)$, $1a_u/\delta_u(1)$, $2b_{2u}/\Phi_u(1)$, $3b_{2u}/\pi_u(1)$]	11344
	23% [$3a_g(1)$, $1a_u/\delta_u(1)$, $2b_{3u}/\Phi_u(1)$, $3b_{3u}/\pi_u(1)$]	
	20% [$3a_g(1)$, $3b_{2u}/\pi_u(1)$, $2b_{1u}/\delta_u(1)$, $2b_{3u}/\Phi_u(1)$]	
	20% [$3a_g(1)$, $2b_{2u}/\Phi_u(1)$, $2b_{1u}/\delta_u(1)$, $3b_{3u}/\pi_u(1)$]	
$^5B_{1u}(2)$	23% [$3a_g(1)$, $2b_{1u}/\delta_u(1)$, $2b_{3u}/\Phi_u(1)$, $3b_{3u}/\pi_u(1)$]	11347
	23% [$3a_g(1)$, $2b_{2u}/\Phi_u(1)$, $3b_{2u}/\pi_u(1)$, $2b_{1u}/\delta_u(1)$]	
	19% [$3a_g(1)$, $1a_u/\delta_u(1)$, $2b_{2u}/\Phi_u(1)$, $3b_{3u}/\pi_u(1)$]	
	19% [$3a_g(1)$, $1a_u/\delta_u(1)$, 11(1), $2b_{3u}/\Phi_u(1)$]	
$^3B_{3g}(2)$	35%[$1a_u/\delta_u(2)$, $2b_{1u}/\delta_u(1)$, $2b_{3u}/\Phi_u(1)$]	11467
	33% [$1a_u/\delta_u(1)$, $3b_{2u}/\pi_u(1)$, $2b_{1u}/\delta_u(2)$]	
$^3B_{2g}(2)$	35%[$1a_u/\delta_u(2)$, $2b_{1u}/\delta_u(1)$, $2b_{3u}/\Phi_u(1)$]	11467
	33% [$1a_u/\delta_u(1)$, $3b_{2u}/\pi_u(1)$, $2b_{1u}/\delta_u(2)$]	
$^3B_{1g}(2)$	34% [$1a_u/\delta_u(2)$, $3b_{2u}/\pi_u(1)$, $2b_{3u}/\Phi_u(1)$]	12812
	33% [$3b_{2u}/\pi_u(1)$, $2b_{1u}/\delta_u(2)$, $2b_{3u}/\Phi_u(1)$]	
$^3A_g(1)$	51% [$1a_u/\delta_u(1)$, $2b_{2u}/\Phi_u(1)$, $2b_{1u}/\delta_u(\bar{1})$, $2b_{3u}/\Phi_u(1)$]	12815
	17% [$1a_u/\delta_u(1)$, $2b_{2u}/\Phi_u(\bar{1})$, $2b_{1u}/\delta_u(1)$, $2b_{3u}/\Phi_u(1)$]	
$^3B_{1u}(2)$	20%[$3a_g(1)$, $2b_{2u}/\Phi_u(\bar{1})$, $3b_{2u}/\pi_u(1)$, $2b_{1u}/\delta_u(1)$]	13398
	20%[$3a_g(1)$, $2b_{1u}/\delta_u(\bar{1})$, $2b_{3u}/\Phi_u(1)$, $3b_{3u}/\pi_u(1)$]	
	15%[$3a_g(1)$, $1a_u/\delta_u(\bar{1})$, $3b_{2u}/\pi_u(1)$, $2b_{3u}/\Phi_u(1)$]	
	15%[$3a_g(1)$, $1a_u/\delta_u(\bar{1})$, $2b_{2u}/\Phi_u(1)$, $3b_{3u}/\pi_u(1)$]	

Table B.4 – *Continued from previous page*

Term Symbol	Character : % [orbital(number of electron)]	E (cm^{-1})
${}^3A_u(2)$	15% [$3a_g(1)$, $1a_u/\delta_u(\bar{1})$, $2b_{2u}/\Phi_u(1)$, $3b_{2u}/\pi_u(1)$]	13402
	15% [$3a_g(1)$, $1a_u/\delta_u(\bar{1})$, $2b_{3u}/\Phi_u(1)$, $3b_{3u}/\pi_u(1)$]	
	14% [$3a_g(1)$, $3b_{2u}/\pi_u(\bar{1})$, $2b_{1u}/\delta_u(1)$, $2b_{3u}/\Phi_u(1)$]	
	14% [$3a_g(1)$, $2b_{2u}/\pi_u(\bar{1})$, $2b_{1u}/\delta_u(1)$, $3b_{3u}/\pi_u(1)$]	
${}^5B_{3g}(3)$	46% [$2b_{2u}/\Phi_u(1)$, $3b_{2u}/\pi_u(1)$, $2b_{1u}/\delta_u(1)$, $3b_{3u}/\pi_u(1)$]	13460
	45% [$1a_u/\delta_u(1)$, $3b_{2u}/\pi_u(1)$, $2b_{3u}/\Phi_u(1)$, $3b_{3u}/\pi_u(1)$]	
${}^5B_{2g}(3)$	46% [$2b_{2u}/\Phi_u(1)$, $3b_{2u}/\pi_u(1)$, $2b_{1u}/\delta_u(1)$, $3b_{3u}/\pi_u(1)$]	13460
	45% [$1a_u/\delta_u(1)$, $3b_{2u}/\pi_u(1)$, $2b_{3u}/\Phi_u(1)$, $3b_{3u}/\pi_u(1)$]	
${}^3B_{1g}(3)$	34% [$1a_u/\delta_u(1)$, $2b_{1u}/\delta_u(1)$, $2b_{3u}/\Phi_u(2)$]	13638
	34% [$1a_u/\delta_u(1)$, $3b_{2u}/\pi_u(2)$, $2b_{1u}/\delta_u(1)$]	
${}^3A_g(2)$	47% [$1a_u/\delta_u(1)$, $2b_{2u}/\Phi_u(1)$, $2b_{1u}/\delta_u(1)$, $2b_{3u}/\Phi_u(\bar{1})$]	13659
	17% [$1a_u/\delta_u(1)$, $2b_{2u}/\Phi_u(\bar{1})$, $2b_{1u}/\delta_u(1)$, $2b_{3u}/\Phi_u(1)$]	
${}^5B_{3u}(2)$	45% [$2a_g/\delta_u(1)$, $1a_u/\delta_u(1)$, $2b_{1u}/\delta_u(1)$, $2b_{3u}/\Phi_u6(1)$]	14688
	42% [$1b_{1g}/\delta_u(1)$, $1a_u/\delta_u(1)$, $2b_{2u}/\Phi_u0(1)$, $2b_{1u}/\delta_u(1)$]	
${}^5B_{2u}(2)$	45% [$2a_g/\delta_u(1)$, $1a_u/\delta_u(1)$, $2b_{1u}/\delta_u(1)$, $2b_{3u}/\Phi_u(1)$]	14688
	42% [$1b_{1g}/\delta_u(1)$, $1a_u/\delta_u(1)$, $2b_{2u}/\Phi_u(1)$, $2b_{1u}/\delta_u(1)$]	
${}^3B_{3u}(2)$	30% [$3a_g(1)$, $1a_u/\delta_u(1)$, $2b_{2u}/\Phi_u(1)$, $2b_{1u}/\delta_u(\bar{1})$]	15060
	22% [$3a_g(1)$, $1a_u/\delta_u(2)$, $2b_{3u}/\Phi_u(1)$]	
	22% [$3a_g(1)$, $2b_{1u}/\delta_u(2)$, $2b_{3u}/\Phi_u(1)$]	
	11% [$3a_g(1)$, $1a_u/\delta_u(\bar{1})$, $2b_{2u}/\Phi_u(1)$, $2b_{1u}/\delta_u(1)$]	
${}^3B_{2u}(2)$	34% [$3a_g(1)$, $1a_u/\delta_u(1)$, $2b_{1u}/\delta_u(\bar{1})$, $2b_{3u}/\Phi_u(1)$]	15062

Table B.4 – *Continued from previous page*

Term Symbol	Character : % [orbital(number of electron)]	E (cm^{-1})
	22% [$3a_g(1)$, $1a_u/\delta_u(2)$, $2b_{2u}/\Phi_u(1)$]	
	22% [$3a_g(1)$, $2b_{2u}/\Phi_u(1)$, $2b_{1u}/\delta_u(3)$]	
	11% [$3a_g(1)$, $1a_u/\delta_u(\bar{1})$, $2b_{1u}/\delta_u(1)$, $2b_{3u}/\Phi_u(1)$]	
$^1B_{3u}(1)$	32% [$3a_g(1)$, $1a_u/\delta_u(1)$, $2b_{1u}/\delta_u(1)$, $2b_{3u}/\Phi_u(1)$]	15336
	21% [$3a_g(1)$, $3b_{2u}/\pi_u(1)$, $2b_{1u}/\delta_u(2)$]	
	21% [$3a_g(1)$, $1a_u/\delta_u(2)$, $3b_{2u}/\pi_u(1)$]	
$^1B_{2u}(1)$	32% [$3a_g(1)$, $1a_u/\delta_u(1)$, $2b_{1u}/\delta_u(1)$, $2b_{3u}/\Phi_u(1)$]	15336
	21% [$3a_g(1)$, $3b_{2u}/\pi_u(1)$, $2b_{1u}/\delta_u(2)$]	
	21% [$3a_g(1)$, $1a_u/\delta_u(2)$, $3b_{2u}/\pi_u(1)$]	
$^3B_{3u}(3)$	29% [$3a_g(1)$, $1a_u/\delta_u(1)$, $2b_{2u}/\Phi_u(\bar{1})$, $2b_{1u}/\delta_u(1)$]	15370
	24% [$3a_g(1)$, $2b_{1u}/\delta_u(2)$, $2b_{3u}/\Phi_u(1)$]	
	23% [$3a_g(1)$, $1a_u/\delta_u(2)$, $2b_{3u}/\Phi_u(1)$]	
$^3B_{2u}(3)$	37% [$3a_g(1)$, $1a_u/\delta_u(1)$, $2b_{1u}/\delta_u(1)$, $2b_{3u}/\Phi_u(\bar{1})$]	15382
	24% [$3a_g(1)$, $2b_{2u}/\Phi_u(1)$, $2b_{1u}/\delta_u(3)$]	
	23% [$3a_g(1)$, $1a_u/\delta_u(2)$, $2b_{2u}/\Phi_u(1)$]	
$^5A_g(4)$	64% [$2b_{2u}/\Phi_u(1)$, $3b_{2u}/\pi_u(1)$, $2b_{3u}/\Phi_u(1)$, $3b_{3u}/\pi_u(1)$]	15800
	20% [$2b_{2u}/\Phi_u(1)$, $3b_{2u}/\pi_u(1)$, $2b_{1u}/\delta_u(1)$, $2b_{3u}/\Phi_u(1)$]	
	23% [$1a_u/\delta_u(1)$, $3b_{2u}/\pi_u(1)$, $2b_{1u}/\delta_u(1)$, $3b_{3u}/\pi_u(1)$]	
	14% [$2b_{2u}/\Phi_u(2)$, $2b_{1u}/\delta_u(1)$, $3b_{3u}/\pi_u(1)$]	
	10% [$2b_{1u}/\delta_u(1)$, $2b_{3u}/\Phi_u(2)$, $3b_{3u}/\pi_u(1)$]	
$^1B_{3u}(2)$	41% [$3a_g(1)$, $1a_u/\delta_u(1)$, 13(1), $2b_{3u}/\Phi_u(1)$]	15850

Table B.4 – *Continued from previous page*

	Term Symbol	Character : % [orbital(number of electron)]	E (cm^{-1})
		23% [$3a_g(1)$, $2b_{2u}/\Phi_u(1)$, $2b_{1u}/\delta_u(2)$]	
		23% [$3a_g(1)$, $1a_u/\delta_u(2)$, $2b_{2u}/\Phi_u(1)$]	
	$^1B_{2u}(2)$	41% [$3a_g(1)$, $1a_u/\delta_u(1)$, $2b_{1u}/\delta_u(1)$, $2b_{3u}/\Phi_u(1)$]	15850
		23% [$3a_g(1)$, $2b_{2u}/\Phi_u(1)$, $2b_{1u}/\delta_u(2)$]	
		23% [$3a_g(1)$, $1a_u/\delta_u(2)$, $2b_{2u}/\Phi_u(1)$]	
SO	0_g^-	48% $^5A_g(1)$, 22.45% $^3B_{1g}(1)$	0
	1_g	67% $^5A_g(1)$, 14.59% $^3B_{1g}(1)$	2462
	1_u	27% $^5B_{2u}(1)$, 26.81% $^5B_{3u}(1)$, 13.24% $^5A_u(1)$, 12.77% $^5B_{1u}(1)$	5851
	2_g	85.58% $^5A_g(1)$	5904
	2_u	24.14% $^5A_u(1)$, 21.34% $^5B_{2u}(1)$, 21.31% $^5B_{3u}(1)$	6266
	3_u	38.85% $^5B_{3u}(1)$, 24.97% $^3B_{2u}(1)$	7197
	a_g	49.54% $^5A_g(2)$, 36.86% $^5B_{1g}(1)$	7240
	b_g	31.53% $^5A_g(3)$, 23.96% $^5B_{1g}(2)$, 18.11% $^3B_{3g}(2)$, 18.11% $^3B_{2g}(2)$	7595
	c_u	22.24% $^3B_{2u}(1)$, 21.61% $^3B_{3u}(1)$, 12.23% $^3A_u(1)$, 10.77% $^5B_{2u}(1)$, 10.68% $^5B_{3u}(1)$	7911
	d_g	47.71% $^5A_g(2)$, 28.33% $^5B_{1g}(1)$, 15.29% $^5B_{2g}(1)$	8738
	e_g	32.7% $^5A_g(3)$, 23.46% $^5B_{1g}(2)$, 18.02% $^5A_g(1)$, 12.56% $^3B_{2g}(2)$, 12.56% $^3B_{3g}(2)$	8971
	f_g	49.36% $^5B_{2g}(1)$, 49.3% $^5B_{3g}(1)$	9610
	g_g	72.76% $^5A_g(2)$	10193
	h_g	44.58% $^5A_g(3)$, 22.96% $^5B_{1g}(2)$, 17.34% $^5B_{3g}(2)$	10763
	i_g	63.19% $^5B_{1g}(1)$, 10.62% $^5B_{2g}(1)$, 10.62% $^5B_{3g}(1)$	11038
	j_u	44.22% $^5A_u(2)$, 43.57% $^5B_{1u}(2)$	11105

Table B.4 – *Continued from previous page*

Term Symbol	Character : % [orbital(number of electron)]	E (cm^{-1})
k_u	48.86% $^5A_u(1)$, 43.03% $^5B_{1u}(1)$	11239
l_u	29.76% $^5B_{3u}(1)$, 29.64% $^5B_{2u}(1)$	11362
m_u	21.94% $^5A_u(1)$, 21.78% $^5B_{1u}(1)$, 18.43% $^5B_{3u}(1)$, 18.4% $^5B_{2u}(1)$	11700
n_g	19.12% $^5B_{2g}(2)$, 19.07% $^5B_{3g}(2)$, 17.44% $^3B_{1g}(1)$, 14.82% $^1A_g(1)$	11817
o_u	42.88% $^3B_{2u}(1)$, 31.88% $^5B_{3u}(1)$	11850
p_g	36.81% $^5B_{2g}(1)$, 36.81% $^5B_{3g}(1)$, 9.67% $^5A_g(3)$	12253
q_g	30.81% $^5B_{1g}(1)$, 23.75% $^5A_g(2)$, 17.24% $^3B_{2g}(1)$, 10.5% $^5B_{3g}(1)$	12345
r_u	36.84% $^5B_{1u}(1)$, 14.5% $^3B_{3u}(1)$, 14.32% $^3B_{2u}(1)$, 9.93% $^3A_u(3)$	12539
s_u	26.69% $^3A_u(2)$, 26.67% $^3B_{1u}(2)$, 21.97% $^5A_u(2)$, 21.84% $^5B_{1u}(2)$	12545
t_g	53.19% $^5B_{1g}(2)$, 14.79% $^5B_{2g}(2)$, 14.79% $^5B_{3g}(2)$	12687
u_u	25.54% $^5A_u(1)$, 19.8% $^3B_{1u}(1)$, 19.02% $^5B_{1u}(1)$	13216
v_u	43.47% $^3A_u(1)$, 24.48% $^3B_{1u}(1)$	13241
w_g	28.83% $^5B_{1g}(2)$, 20.15% $^5B_{2g}(2)$, 19.79% $^5A_g(3)$, 12.91% $^5B_{3g}(2)$, 12.71% $^5B_{2g}(1)$	13394
x_g	58.26% $^5B_{2g}(1)$	13728
y_g	34.24% $^5B_{1g}(1)$, 21.57% $^3B_{3g}(1)$, 21.56% $^3B_{2g}(1)$, 20.21% $^5A_g(2)$	14074
z_g	45.19% $^5B_{3g}(2)$, 38.99% $^5B_{2g}(2)$	14162
aa_u	47.44% $^3B_{1u}(1)$, 14.08% $^1A_u(1)$, 12.08% $^5A_u(1)$	14253
ab_g	32.6% $^5B_{3g}(1)$, 32.6% $^5B_{2g}(1)$, 17.93% $^3B_{1g}(2)$, 10.46% $^5A_g(2)$	14698
ac_g	35.2% $^5B_{3g}(2)$, 35.19% $^5B_{2g}(2)$, 11.61% $^3B_{3g}(2)$, 11.61% $^3B_{2g}(2)$	14747
ad_g	27.69% $^5B_{3g}(1)$, 27.69% $^5B_{2g}(1)$, 16.03% $^3A_g(1)$, 13.05% $^5B_{1g}(1)$	14862
ae_u	48.62% $^5A_u(3)$, 48.07% $^5B_{1u}(3)$	14968

Table B.4 – *Continued from previous page*

Term Symbol	Character : % [orbital(number of electron)]	E (cm^{-1})
af_g	24.6% $^5B_{2g}(1)$, 24.55% $^5B_{3g}(1)$, 14.87% $^3B_{1g}(2)$, 12.76% $^3A_g(1)$	15217
ag_g	57.87% $^5B_{3g}(2)$, 12.24% $^3B_{2g}(2)$	15786
ah_u	32.7% $^5B_{3u}(2)$, 32.65% $^5B_{2u}(2)$, 15.35% $^5B_{3u}(1)$, 14.96% $^5B_{2u}(1)$	15843
ai_g	35.75% $^5B_{2g}(3)$, 35.52% $^5B_{3g}(3)$, 12.29% $^5B_{1g}(1)$	15851

Appendix C

Additional ETS-NOCV Results

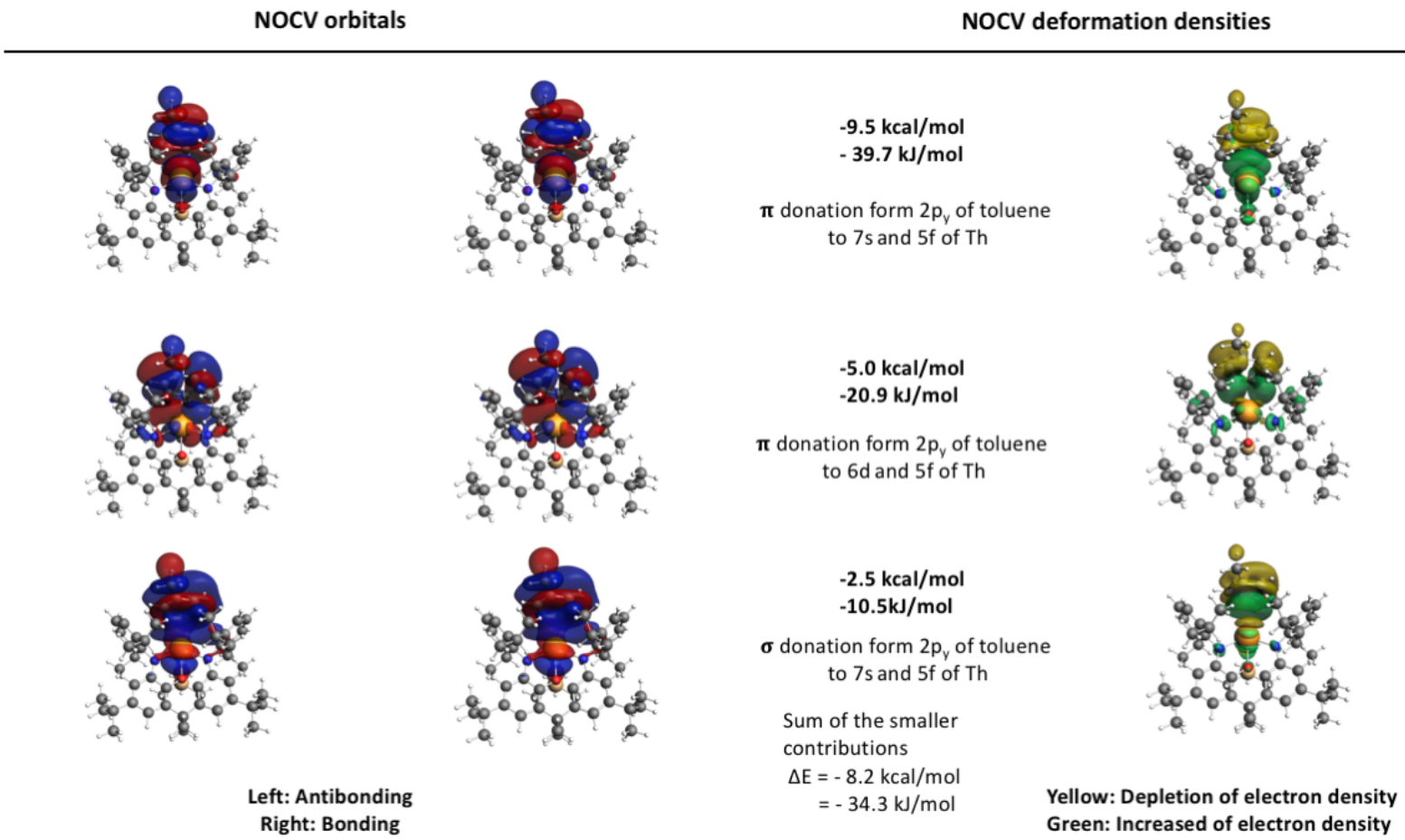

FIGURE C.1: On the left hand side: the NOCV Orbitals (with isosurfaces set to 0.01) and on the right hand side ETS-NOCV deformation density contributions, Increased (green) and decreased (yellow) electron density is presented relative to that in the isolated fragments (isosurfaces are set to 0.0001) for the molecule η^6**-3-Th-down**.

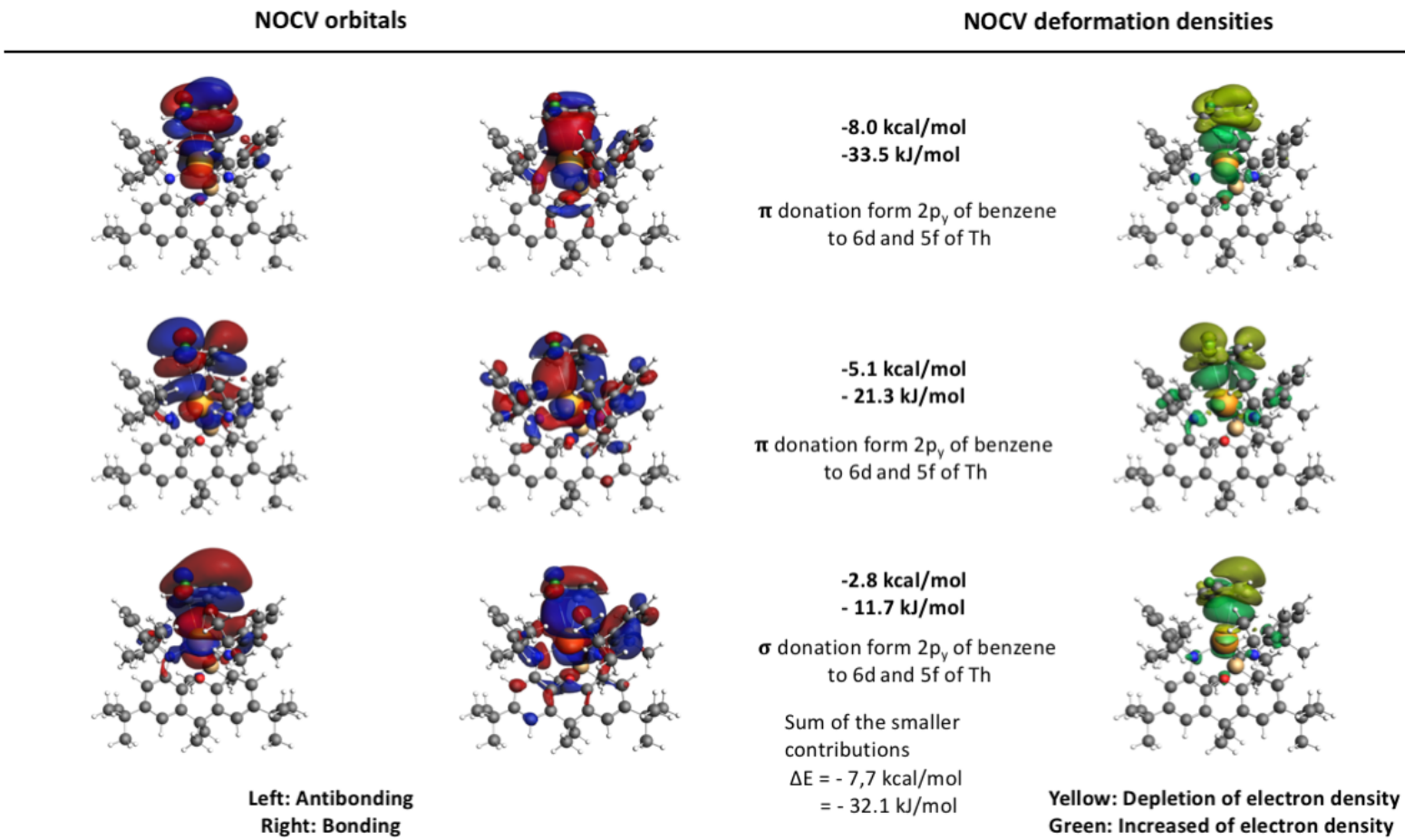

FIGURE C.2: On the left hand side: the NOCV Orbitals (with isosurfaces set to 0.01) and on the right hand side ETS-NOCV deformation density contributions, Increased (green) and decreased (yellow) electron density is presented relative to that in the isolated fragments (isosurfaces are set to 0.0001) for the molecule η^6**-5-Th-endo**.

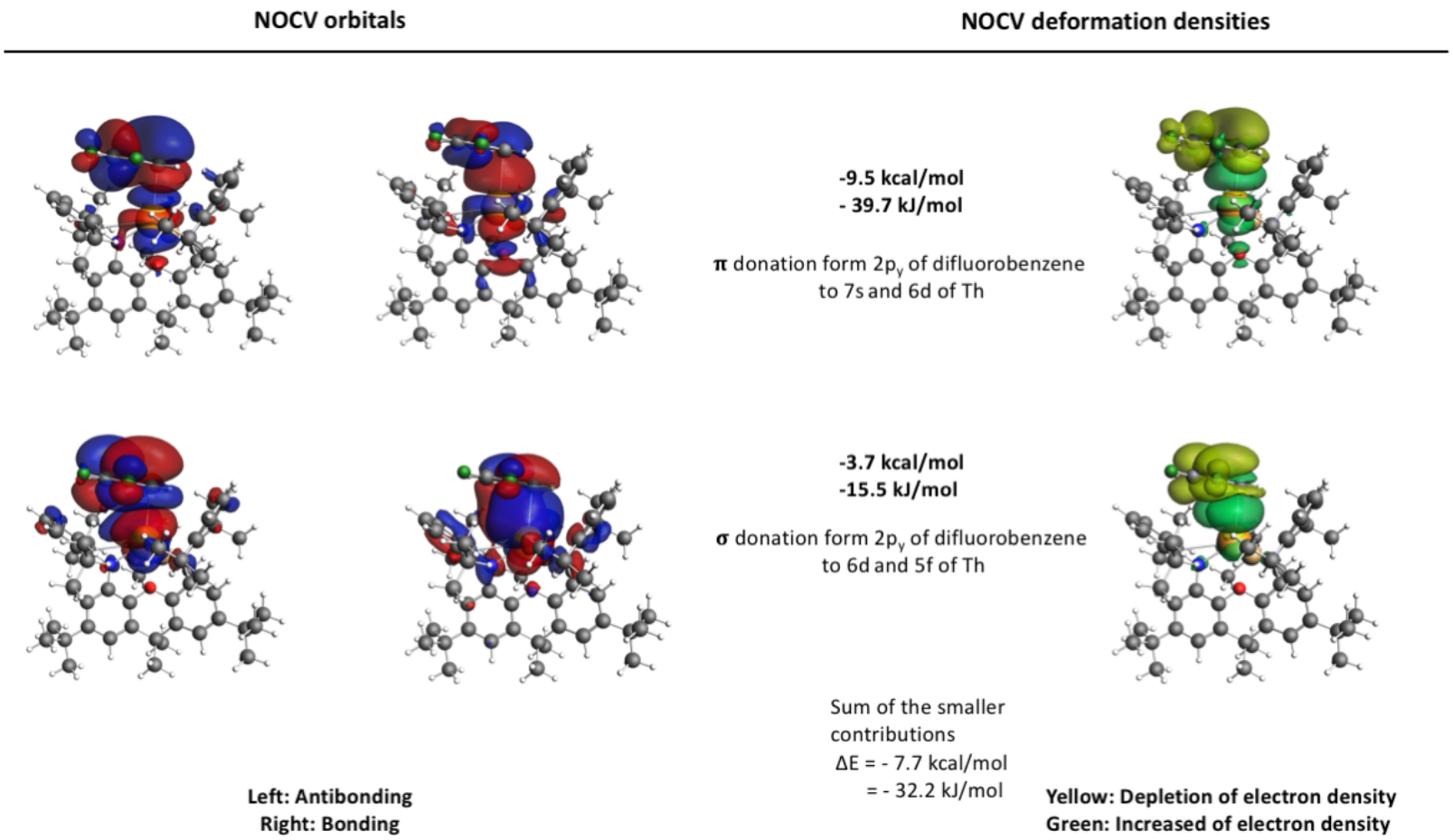

FIGURE C.3: On the left hand side: the NOCV Orbitals (with isosurfaces set to 0.01) and on the right hand side ETS-NOCV deformation density contributions, Increased (green) and decreased (yellow) electron density is presented relative to that in the isolated fragments (isosurfaces are set to 0.0001) for the molecule η^6**-6-Th-exo**

.

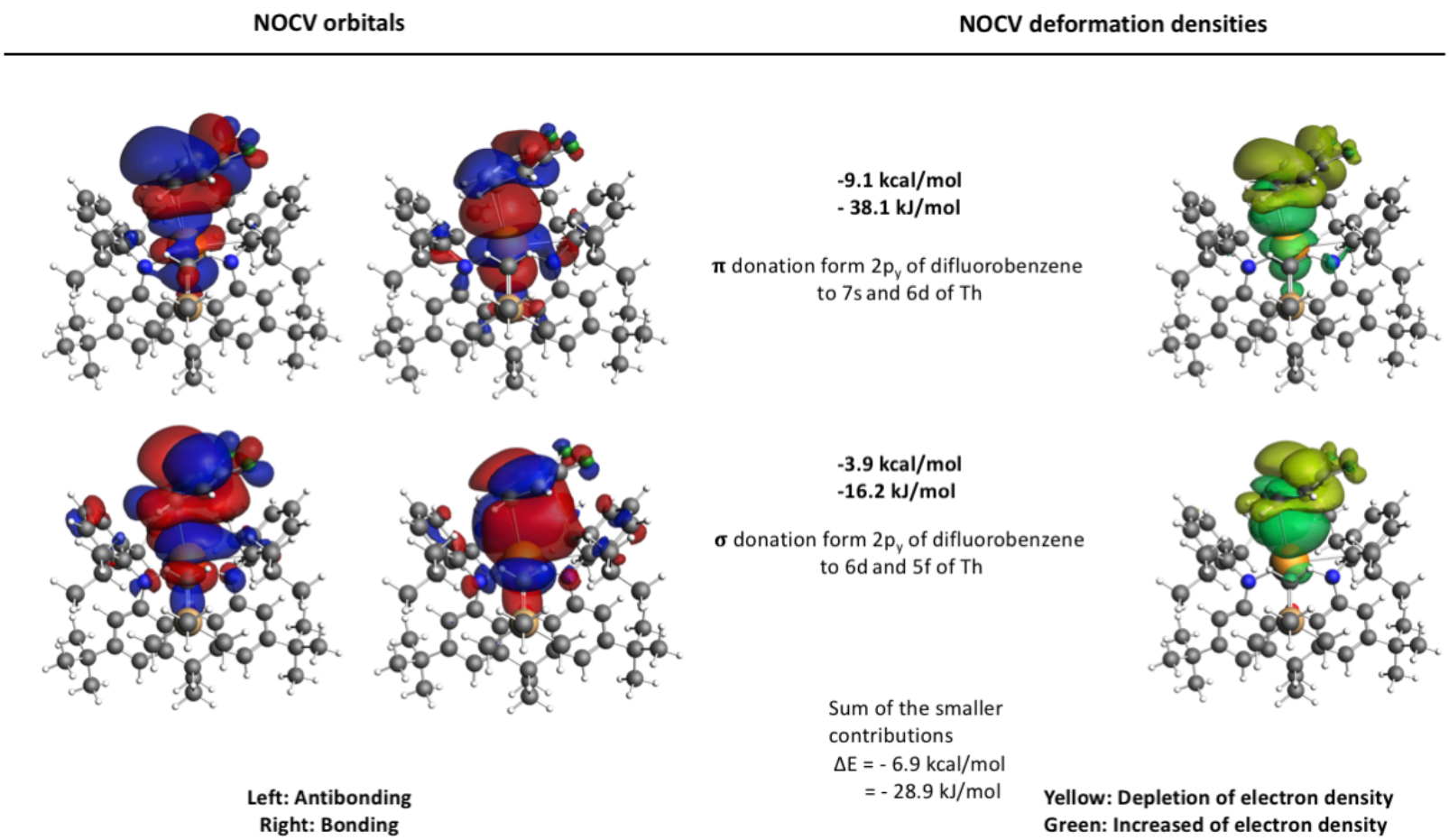

FIGURE C.4: On the left hand side: the NOCV Orbitals (with isosurfaces set to 0.01) and on the right hand side ETS-NOCV deformation density contributions, Increased (green) and decreased (yellow) electron density is presented relative to that in the isolated fragments (isosurfaces are set to 0.0001) for the molecule η^6**-6-Th-side**.

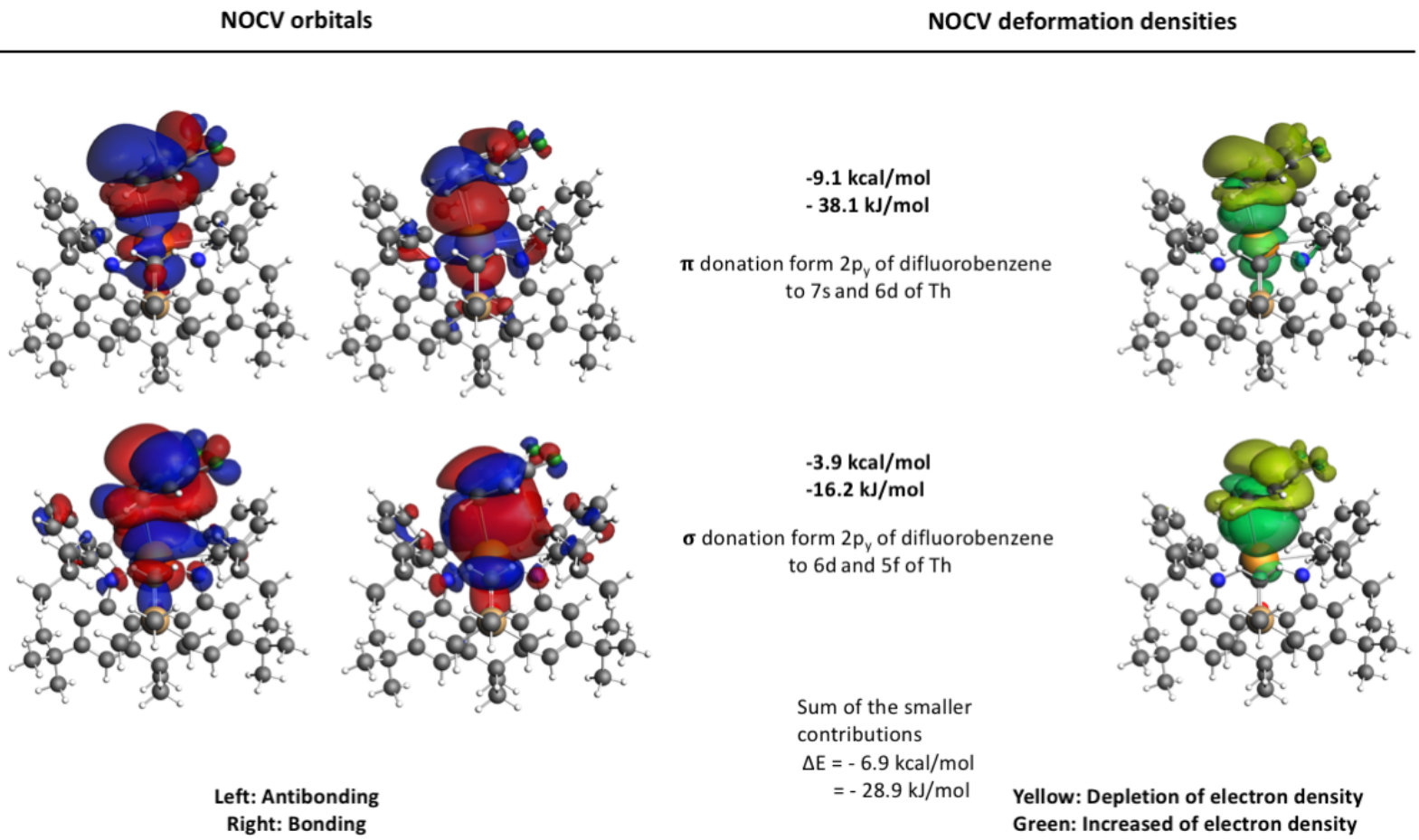

FIGURE C.5: On the left hand side: the NOCV Orbitals (with isosurfaces set to 0.01) and on the right hand side ETS-NOCV deformation density contributions, Increased (green) and decreased (yellow) electron density is presented relative to that in the isolated fragments (isosurfaces are set to 0.0001) for the molecule η^6**-6-Th-endo**.

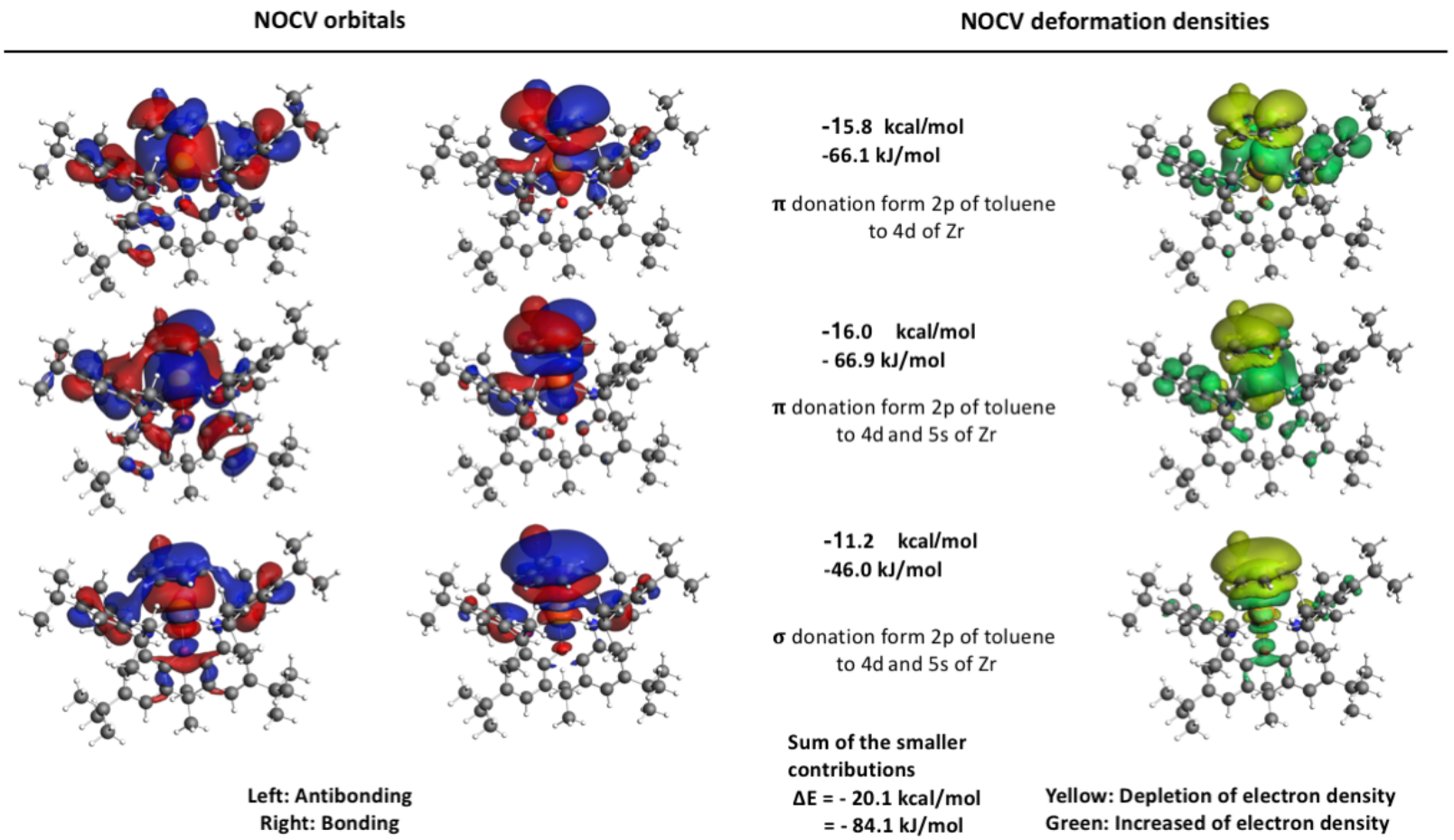

FIGURE C.6: On the left hand side: the NOCV Orbitals (with isosurfaces set to 0.01) and on the right hand side ETS-NOCV deformation density contributions, Increased (green) and decreased (yellow) electron density is presented relative to that in the isolated fragments (isosurfaces are set to 0.0001) for the molecule η^2-**E′-Zr**.

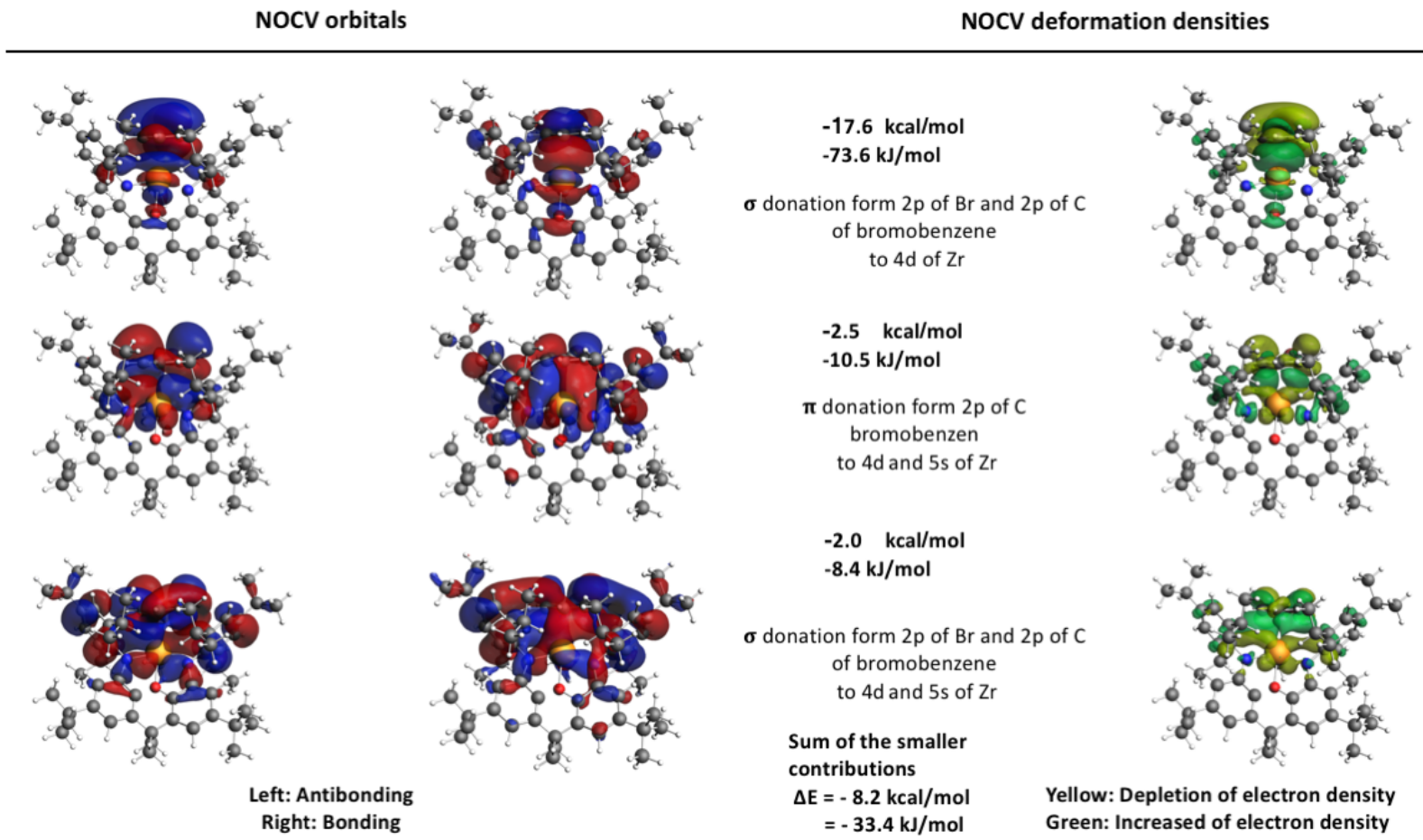

FIGURE C.7: On the left hand side: the NOCV Orbitals (with isosurfaces set to 0.01) and on the right hand side ETS-NOCV deformation density contributions, Increased (green) and decreased (yellow) electron density is presented relative to that in the isolated fragments (isosurfaces are set to 0.0001) for the molecule η^6**-4′-Zr-exo**.

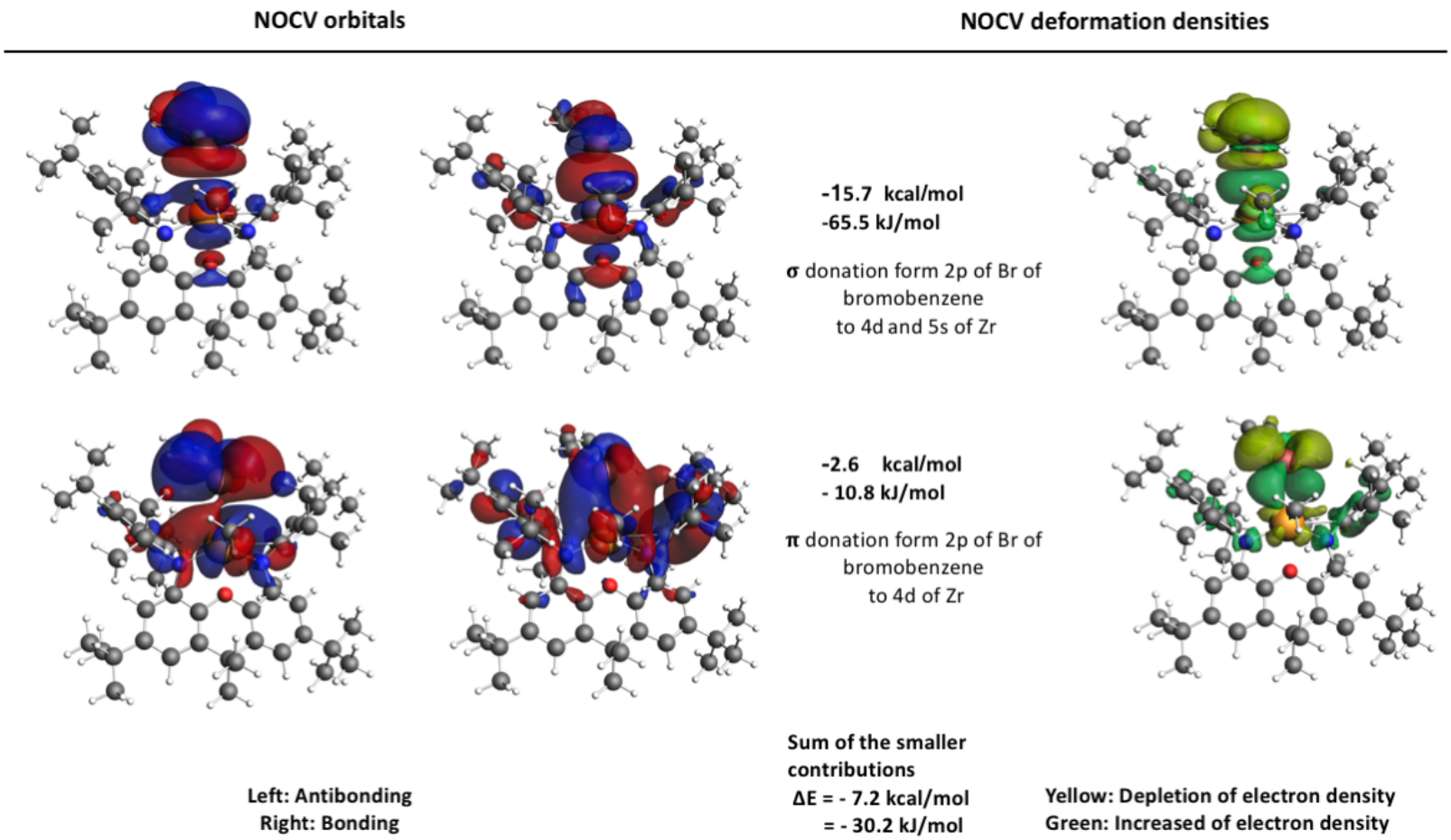

FIGURE C.8: On the left hand side: the NOCV Orbitals (with isosurfaces set to 0.01) and on the right hand side ETS-NOCV deformation density contributions, Increased (green) and decreased (yellow) electron density is presented relative to that in the isolated fragments (isosurfaces are set to 0.0001) for the molecule η^6**-4′-Zr-exo**.

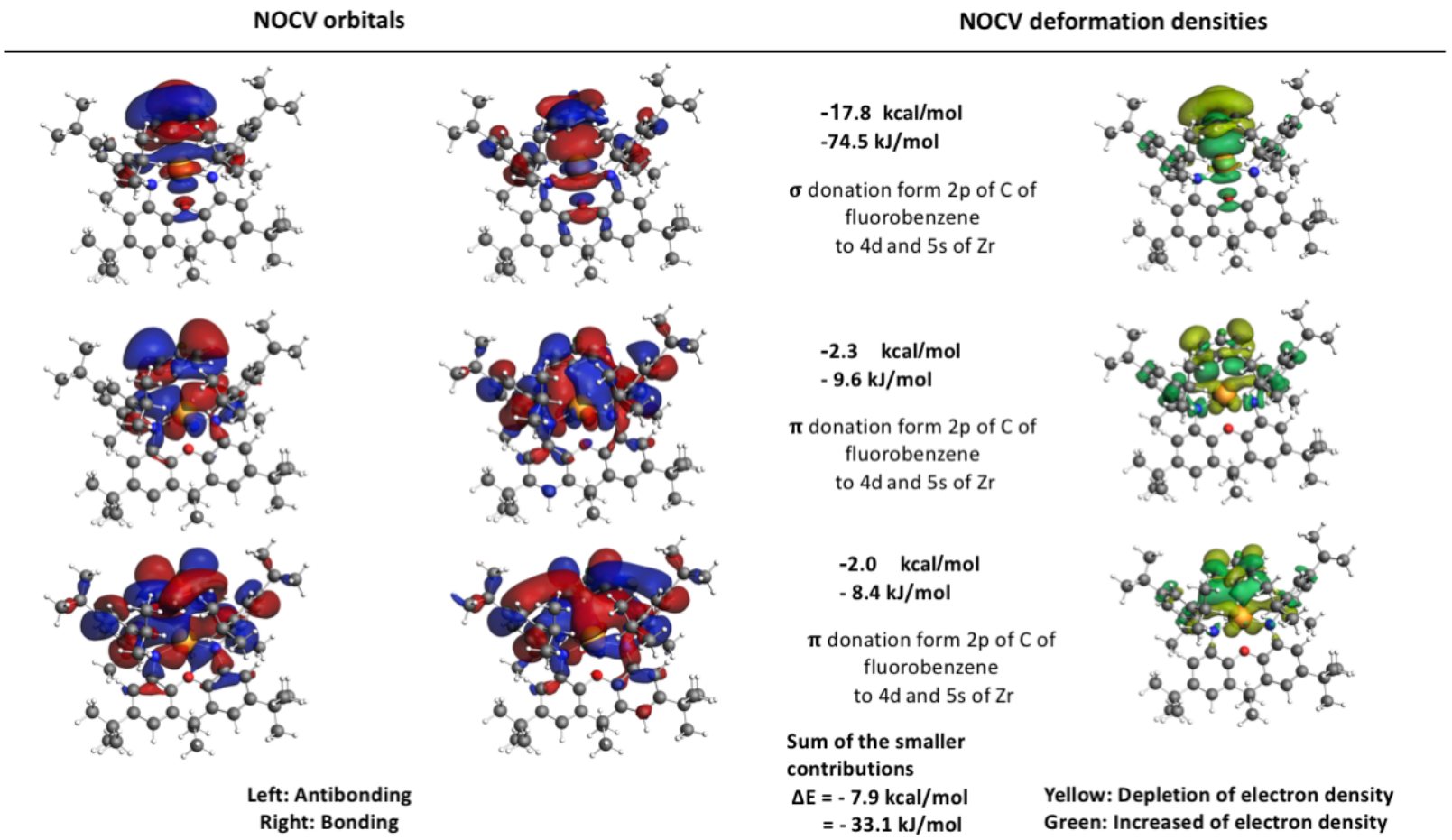

FIGURE C.9: On the left hand side: the NOCV Orbitals (with isosurfaces set to 0.01) and on the right hand side ETS-NOCV deformation density contributions, Increased (green) and decreased (yellow) electron density is presented relative to that in the isolated fragments (isosurfaces are set to 0.0001) for the molecule η^6**-5′-Zr-exo**.

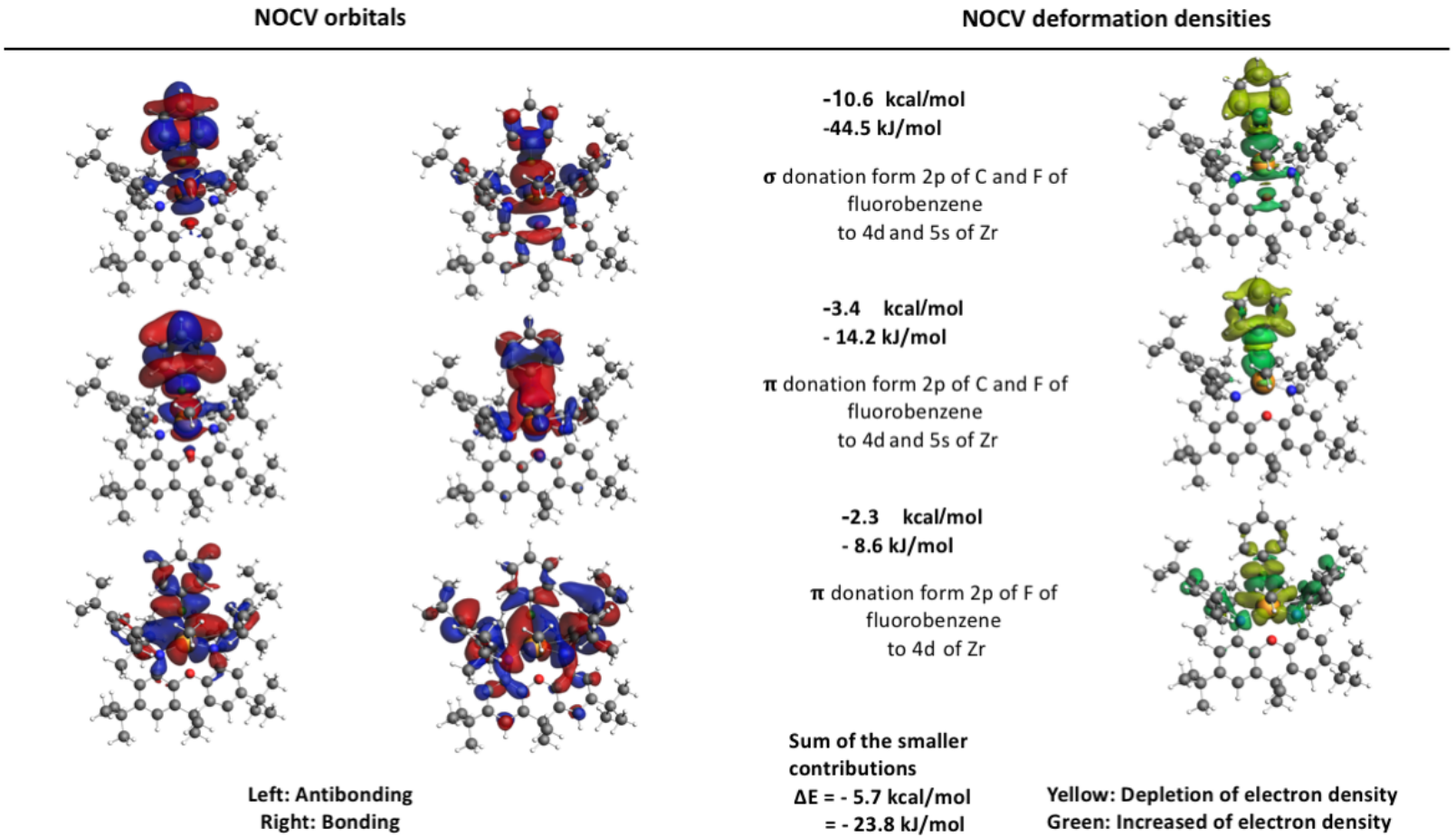

FIGURE C.10: On the left hand side: the NOCV Orbitals (with isosurfaces set to 0.01) and on the right hand side ETS-NOCV deformation density contributions, Increased (green) and decreased (yellow) electron density is presented relative to that in the isolated fragments (isosurfaces are set to 0.0001) for the molecule η^1**-5′-Zr-horizontal**.

Bibliography

[1] Bernd F. Straub. Organotransition Metal Chemistry. From Bonding to Catalysis. Edited by Vol. 49. 42. WILEY-VCH Verlag, 2010, pp. 7622–7622. DOI: 10.1002/anie.201004890.

[2] Ataf Ali Altaf et al. "Zirconium complexes in homogeneous ethylene polymerization". In: Journal of Coordination Chemistry 64.10 (2011), pp. 1815–1836. DOI: 10.1080/00958972.2011.568616.

[3] Andrew J. Peacock and Allison Calhoun. "Polymer Chemistry". In: Polymer Chemistry. Carl Hanser Verlag GmbH & Co. KG, 2006, pp. I–XIX. ISBN: 978-3-446-22283-0. DOI: doi:10.3139/9783446433434.fm.

[4] M Salvatores. "Physics and Safety of transmutation Systems". In: NEA Nuclear Science Rep 6090 (2006).

[5] R. P. Feynman. Quantum Electrodynamics. New York: WA. Benjamin, 1961.

[6] Attila Szabo and Neil S. Ostlund. Modern Quantum Chemistry: Introduction to Advanced First. Mineola: Dover Publications, Inc., 1996.

[7] Lev Davidovich Landau and Evgenii Mikhailovich Lifshitz. Quantum Mechanics: Non-Rel Vol. 3. Elsevier, 2013.

[8] W. Pauli. "Uber den Zusammenhang des Abschlusses der Elektronengruppen im Atom mit der Komplexstruktur der Spektren". In: Zeitschrift fur Physik 31.1 (1925), pp. 765–783. DOI: 10.1007/BF02980631.

[9] J. C. Slater. "A Simplification of the Hartree-Fock Method". In: Phys. Rev. 81 (3 1951), pp. 385–390. DOI: 10.1103/PhysRev.81.385.

[10] Frank Jensen. Introduction to Computational Chemistry. John Wiley & Sons, 2006. ISBN: 0470011874.

[11] Per-Olov L
owdin. "Quantum Theory of Many-Particle Systems. III. Extension of the Hartree-Fock Scheme to Include Degenerate Systems and Correlation Effects". In: Phys. Rev. 97 (6 1955), pp. 1509–1520. DOI: 10.1103/PhysRev.97.1509.

[12] L. González, D. Escudero, and L. Serrano-Andrés. "Progress and Challenges in the Calculation of Electronic Excited States". In: ChemPhysChem 13 (2012), pp. 28–51. ISSN: 1439-7641. DOI: 10.1002/cphc.201100200.

[13] Chr. Møller and M. S. Plesset. "Note on an Approximation Treatment for Many-Electron Systems". In: Phys. Rev. 46 (7 1934), pp. 618–622. DOI: 10.1103/PhysRev.46.618.

[14] Bernard Levy and Gaston Berthier. "Generalized brillouin theorem for multiconfigurational SCF theories". In: International Journal of Quantum Chemistr 2.2 (), pp. 307–319. DOI: 10.1002/qua.560020210.

[15] T Koopmans. "Über die Zuordnung von Wellenfunktionen und Eigenwerten zu den Einzelnen Elektronen Eines Atoms". In: Physica 1.1 (1934), pp. 104 –113. DOI: https://doi.org/10.1016/S0031-8914(34)90011-2.

[16] R J Bartlett. "Many-Body Perturbation Theory and Coupled Cluster Theory for Electron Correlation in Molecules". In: Annual Review of Physical Chemist 32.1 (1981), pp. 359–401. DOI: 10.1146/annurev.pc.32.100181.002043.

[17] A. Szabo and N. S. Ostlund. Modern Quantum Chemistry: Introduction to Advanced I New York: McGraw-Hill, 1989.

[18] Jiří Čížek. In: The Journal of Chemical Physics 45.11 (1966), pp. 4256–4266. DOI: 10.1063/1.1727484.

[19] Čižek J. and Paldus J. In: International Journal of Quantum Chemistry 5.4 (), pp. 359–379. DOI: 10.1002/qua.560050402.

[20] "Coupled cluster theory for high spin, open shell reference wave functions". In: The Journal of Chemical Physics 99.7 (1993), pp. 5219–5227. DOI: 10.1063/1.465990.

[21] Peter J. Knowles, Claudia Hampel, and Hans-Joachim Werner. "Erratum: "Coupled cluster theory for high spin, open shell reference wave functions" [J. Chem. Phys. 99, 5219 (1993)]". In: The Journal of Chemical Physics 112.6 (2000), pp. 3106–3107. DOI: 10.1063/1.480886.

[22] R. J. Bartlett and M. Musiał. "Coupled-Cluster Theory In Quantum Chemistry". In: Reviews of Modern Physics 79 (2007), pp. 291–350.

[23] George D. Purvis and Rodney J. Bartlett. In: The Journal of Chemical Physics 76.4 (1982), pp. 1910–1918. DOI: 10.1063/1.443164.

[24] Watts John D. and Bartlett Rodney J. In: International Journal of Quantum Chemistry 48.27 (), pp. 51–66. DOI: 10.1002/qua.560480809.

[25] Krishnan Raghavachari et al. "A fifth-order perturbation comparison of electron correlation theories". In: Chemical Physics Letters 157.6 (1989), pp. 479 –483. ISSN: 0009-2614. DOI: https://doi.org/10.1016/S0009-2614(89)87395-6.

[26] Miles J.O. Deegan and Peter J. Knowles. "Perturbative corrections to account for triple excitations in closed and open shell coupled cluster theories". In: Chemical Physics Letters 227.3 (1994), pp. 321 –326. ISSN: 0009-2614. DOI: https://doi.org/10.1016/0009-2614(94)00815-9.

[27] Rodney J. Bartlett. "Coupled-cluster approach to molecular structure and spectra: a step toward predictive quantum chemistry". In: The Journal of Physical Che 93.5 (1989), pp. 1697–1708. DOI: 10.1021/j100342a008.

[28] Peter M. W. Gill et al. In: The Journal of Chemical Physics 89.12 (1988), pp. 7307–7314. DOI: 10.1063/1.455312.

[29] Martin Rosenberg et al. "Excited State Aromaticity and Antiaromaticity: Opportunities for Photophysical and Photochemical Rationalizations". In: Chemical Reviews 114.10 (2014), pp. 5379–5425. DOI: 10.1021/cr300471v.

[30] Gustavo E. Scuseria. "The open-shell restricted Hartree—Fock singles and doubles coupled-cluster method including triple excitations CCSD (T): application to C+3". In: Chemical Physics Letters 176.1 (1991), pp. 27 –35. ISSN: 0009-2614. DOI: https://doi.org/10.1016/0009-2614(91)90005-T.

[31] Lee Timothy J. and Taylor Peter R. In: International Journal of Quantum Chemistry 36.S23 (), pp. 199–207. DOI: 10.1002/qua.560360824.

[32] Timothy J. Lee. "Comparison of the T1 and D1 diagnostics for electronic structure theory: a new definition for the open-shell D1 diagnostic". In: Chemical Physics Letters 372 (2003), pp. 362–367.

[33] Curtis L Janssen and Ida M B Nielsen. "New diagnostics for coupled-cluster and Møller-Plesset perturbation theory". In: Chem. Phys. Lett. 290 (1998), pp. 423–430.

[34] Timothy J Lee. "Comparison of the T1 and D1 diagnostics for electronic structure theory: a new definition for the open-shell D1 diagnostic". In: Chemical Physics Letters 372.3 (2003), pp. 362 –367. ISSN: 0009-2614. DOI: https://doi.org/10.1016/S0009-2614(03)00435-4.

[35] Matthew L. Leininger et al. "A new diagnostic for open-shell coupled-cluster theory". In: Chemical Physics Letters 328.4 (2000), pp. 431 – 436. ISSN: 0009-2614. DOI: https://doi.org/10.1016/S0009-2614(00)00966-0.

[36] Wanyi Jiang, Nathan J. DeYonker, and Angela K. Wilson. "Multireference Character for 3d Transition-Metal-Containing Molecules". In: J. Chem. Theory Comput. 8 (2012), pp. 460–468.

[37] P. Tecmer et al. "Electronic spectroscopy of UO_2^{2+}, NUO^+ and NUN: An Evaluation of Time-Dependent Density Functional Theory for Actinides". In: Phys. Chem. Chem. Phys. 13 (2011), pp. 6249–6259.

[38] P. Hohenberg and W. Kohn. "Inhomogeneous Electron Gas". In: Phys. Rev. 136 (1964), B864–B871. DOI: 10.1103/PhysRev.136.B864.

[39] W. Kohn and L. J. Sham. In: Phys. Rev. 140 (1965), A1133–A1138.

[40] J. P. Perdew and Y. Wang. "Accurate and simple analytic representation of the electron-gas correlation energy". In: Phys. Rev. B 45 (1992), pp. 13244–13249. DOI: 10.1103/PhysRevB.45.13244.

[41] S. H. Vosko, L. Wilk, and M. Nusair. "Accurate spin-dependent electron liquid correlation energies for local spin-density calculations - A critical analysis". In: Can. J. Phys. 58 (1980), pp. 1200–1211. DOI: 10.1139/p80-159.

[42] J. P. Perdew et al. "Atoms, molecules, solids, and surfaces: Applications of the generalized gradient approximation for exchange and correlation". In: Phys. Rev. B 46 (1992), pp. 6671–6687. DOI: 10.1103/PhysRevB.46.6671.

[43] J. P. Perdew, K. Burke, and M. Ernzerhof. "Generalized gradient approximation made simple". In: Phys. Rev. Lett. 77 (1996), pp. 3865–3868.

[44] P. J. Stephens et al. "Ab Initio Calculation of Vibrational Absorption and Circular Dichroism Spectra Using Density Functional Force Fields". In: The Journal of Physical Chemistry 98.45 (1994), pp. 11623–11627. DOI: 10.1021/j100096a001.

[45] Carlo Adamo and Vincenzo Barone. "Toward reliable density functional methods without adjustable parameters: The PBE0 model". In: The Journal of Chemical Physics 110.13 (1999), pp. 6158–6170. DOI: 10.1063/1.478522.

[46] John P. Perdew, Matthias Ernzerhof, and Kieron Burke. "Rationale for mixing exact exchange with density functional approximations". In: The Journal of Chemical Physics 105.22 (1996), pp. 9982–9985. DOI: 10.1063/1.472933.

[47] Christos P. Constantinides, Panayiotis A. Koutentis, and Jürgen Schatz. "A DFT Study of the Ground State Multiplicities of Linear vs Angular Polyheteroacenes". In: Journal of the American Chemical Society 126.49 (2004), pp. 16232–16241. DOI: 10.1021/ja045006t.

[48] Marcel Swart et al. "Validation of Exchange-Correlation Functionals for Spin States of Iron Complexes". In: The Journal of Physical Chemistry A 108.25 (2004), pp. 5479–5483. DOI: 10.1021/jp049043i.

[49] Stefan Grimme. "Semiempirical GGA-type density functional constructed with a long-range dispersion correction". In: Journal of Computational Chemistry 27.15 (), pp. 1787–1799. DOI: 10.1002/jcc.20495.

[50] Stefan Grimme et al. "A consistent and accurate ab initio parametrization of density functional dispersion correction (DFT-D) for the 94 elements H-Pu". In: The Journal of Chemical Physics 132.15 (2010), p. 154104. DOI: 10.1063/1.3382344.

[51] Stefan Grimme. "Accurate description of van der Waals complexes by density functional theory including empirical corrections". In: Journal of Computational C 25.12 (), pp. 1463–1473. DOI: 10.1002/jcc.20078.

[52] Pekka Pyykkö. "Relativistic effects in structural chemistry". EN. In: Chem. Rev. 88.3 (1988), pp. 563–594. ISSN: 0009-2665. DOI: 10.1021/cr00085a006.

[53] Albert A Michelson and Edward W Morley. In: Am. J. Sci. 134 (1887), p. 33.

[54] P. A. M. Dirac. "The quantum theory of the electron". In: Proc. R. Soc. London 117 (1928), p. 610.

[55] "A theory of electrons and protons". In: Proceedings of the Royal Society of London A: Ma 126.801 (1930), pp. 360–365. ISSN: 0950-1207. DOI: 10.1098/rspa.1930.0013. eprint: http://rspa.royalsocietypublishing.org/content/126/801/360.full.pdf.

[56] "IV. The triplets of helium". In: Philosophical Transactions of the Royal Society of London 228.659-669 (1929), pp. 151–196. ISSN: 0264-3952. DOI: 10.1098/rsta.1929.0004. eprint: http://rsta.royalsocietypublishing.org/content/228/659-669/151.full.pdf.

[57] G. Breit. "The Effect of Retardation on the Interaction of Two Electrons". In: Phys. Rev. 34 (4 1929), pp. 553–573. DOI: 10.1103/PhysRev.34.553.

[58] H. B. G. Casimir and D. Polder. "The Influence of Retardation on the London-van der Waals Forces". In: Phys. Rev. 73 (4 1948), pp. 360–372. DOI: 10.1103/PhysRev.73.360.

[59] Kenneth G Dyall and Knut Faegri Jr. Introduction to relativistic quantum chemistry. Oxford University Press, 2007.

[60] Markus Reiher and Alexander Wolf. Relativistic quantum chemistry: the fundamental John Wiley Sons, 2014.

[61] Christoph van Wüllen. "Molecular density functional calculations in the regular relativistic approximation: Method, application to coinage metal diatomics, hydrides, fluorides and chlorides, and comparison with first-order relativistic calculations". In: The Journal of Chemical Physics 109.2 (1998), pp. 392–399. DOI: 10.1063/1.476576.

[62] Alexander Wolf, Markus Reiher, and Bernd Artur Hess. "The generalized Douglas–Kroll transformation". In: The Journal of Chemical Physics 117.20 (2002), pp. 9215–9226. DOI: 10.1063/1.1515314.

[63] Markus Reiher and Alexander Wolf. "Exact decoupling of the Dirac Hamiltonian. II. The generalized Douglas–Kroll–Hess transformation up to arbitrary order". In: The Journal of Chemical Physics 121.22 (2004), pp. 10945–10956. DOI: 10.1063/1.1818681.

[64] L. L. Foldy and S. A. Wouthuysen. "On the Dirac Theory of Spin 1/2 Particles and Its Non-Relativistic Limit". In: Physical Review 78 (1950), p. 29.

[65] Bernd Artur Hess et al. "A mean-field spin-orbit method applicable to correlated wavefunctions". In: Chem. Phys. Lett. 251 (1996), pp. 365–371.

[66] M Krauss and W J Stevens. "Effective potentials in molecular quantum chemistry". In: Annual Review of Physical Chemistry 35.1 (1984), pp. 357–385.

[67] M. Dolg and X. Cao. "Relativistic Pseudopotentials: Their Development And Scope Of Applications". In: Chem. Rev. 112 (2012), pp. 403–480.

[68] Helmut Eschrig. Optimized LCAO Method and Electronic Structure of Extended Syst Jan. 1989.

[69] J. C. Slater. "Atomic Shielding Constants". In: Phys. Rev. 36 (1 1930), pp. 57–64. DOI: 10.1103/PhysRev.36.57.

[70] "Electronic wave functions - I. A general method of calculation for the stationary states of any molecular system". In: Proceedings of the Royal Society of London 200.1063 (1950), pp. 542–554. DOI: 10.1098/rspa.1950.0036.

[71] T. H. Dunning Jr. "Gaussian basis sets for use in correlated molecular calculations. I. The atoms boron through neon and hydrogen". In: J. Chem. Phys. 90 (1989), pp. 1007–1023. DOI: 10.1063/1.456153.

[72] J. M. L. Martin and A. Sundermann. "Correlation consistent valence basis sets for use with the Stuttgart-Dresden-Bonn relativistic effective core potentials: The atoms Ga-Kr and In-Xe". In: J. Chem. Phys. 114 (2001), pp. 3408–3420. DOI: 10.1063/1.1337864.

[73] Florian Weigend and Reinhart Ahlrichs. "Balanced basis sets of split valence, triple zeta valence and quadruple zeta valence quality for H to Rn: Design and assessment of accuracy". In: Phys. Chem. Chem. Phys. 7 (18 2005), pp. 3297–3305. DOI: 10.1039/B508541A.

[74] Florian Weigend. "Accurate Coulomb-fitting basis sets for H to Rn". In: Phys. Chem. Chem. Phys. 8 (9 2006), pp. 1057–1065. DOI: 10.1039/B515623H.

[75] Per-Olof Widmark, B. Joakim Persson, and Björn O. Roos. "Density matrix averaged atomic natural orbital (ANO) basis sets for correlated molecular wave functions". In: Theoretica chimica acta 79.6 (1991), pp. 419–432. ISSN: 1432-2234. DOI: 10.1007/BF01112569.

[76] Jan Almlöf and Peter R Taylor. "Atomic natural orbital (ANO) basis sets for quantum chemical calculations". In: Advances in Quantum Chemistry 22 (1991), pp. 301–373. DOI: 10.1016/S0065-3276(08)60366-4.

[77] B. O. Roos et al. "Main group atoms and dimers studied with a new relativistic ANO basis set". In: J. Phys. Chem. A 108 (2004), pp. 2851–2858. DOI: 10.1021/jp031064+.

[78] B. O. Roos et al. "New relativistic ANO basis sets for actinide atoms". In: Chem. Phys. Lett. 409 (2005), pp. 295–299. DOI: 10.1016/j.cplett.2005.05.011.

[79] M. Gutowski et al. "The basis set superposition error in correlated electronic structure calculations". In: Chemical Physics Letters 124.4 (1986), pp. 370 –375. ISSN: 0009-2614. DOI: https://doi.org/10.1016/0009-2614(86)85036-9.

[80] T. Helgaker, P. Jørgensen, and J. Olsen. Molecular Electronic-Structure Theory. New York: Wiley, 2000.

[81] David H. Bross and Kirk A. Peterson. "Theoretical spectroscopy study of the low-lying electronic states of UX and UX+, X = F and Cl". In: The Journal of Chemical Physics 143.18 (2015), p. 184313. DOI: 10.1063/1.4935492.

[82] Hans H. Brintzinger et al. "Stereospecific Olefin Polymerization with Chiral Metallocene Catalysts". In: Angewandte Chemie International Edition in Englis 34.11 (), pp. 1143–1170. DOI: 10.1002/anie.199511431.

[83] Raymond J. Butcher et al. In: Organometallics 15.5 (1996), pp. 1488–1496. DOI: 10.1021/om9508694.

[84] Li Jia et al. "Cationic d0/f0 metallocene catalysts. properties of binuclear organoborane Lewis acid cocatalysts and weakly coordinating counteranions derived therefrom". In: Organometallics 13.10 (1994), pp. 3755–3757. DOI: 10.1021/om00022a003.

[85] Xinmin. Yang, Charlotte. Stern, and Tobin J. Marks. "Models for organometallic molecule-support complexes. Very large counterion modulation of cationic actinide alkyl reactivity". In: Organometallics 10.4 (1991), pp. 840–842. DOI: 10.1021/om00050a008.

[86] Zerong Lin et al. "Models for organometallic molecule-support complexes. Synthesis and properties of cationic organoactinides". In: Journal of the Americ 109.13 (1987), pp. 4127–4129. DOI: 10.1021/ja00247a056.

[87] Ming Yuan He et al. "Supported organoactinides. Surface chemistry and catalytic properties of alumina-bound cyclopentadienyl and pentamethylcyclopentadienyl thorium and uranium hydrocarbyls and hydrides". In: Journal of the American Chemical Society 107.3 (1985), pp. 641–652. DOI: 10.1021/ja00289a016.

[88] Paul J. Toscano and Tobin J. Marks. "Supported organoactinides. High-resolution solid-state carbon-13 NMR studies of catalytically active, alumina-bound pentamethylcyclopentadienyl)thorium methyl and hydride complexes". In: Journal of the American Chemical Society 107.3 (1985), pp. 653–659. DOI: 10.1021/ja00289a017.

[89] William C. Finch et al. "Organometallic molecule-inorganic surface coordination and catalytic chemistry. In situ CPMAS NMR delineation of organoactinide adsorbate structure, dynamics, and reactivity". In:

Journal of the American Chemical Society 112.17 (1990), pp. 6221–6232. DOI: 10.1021/ja00173a009.

[90] David. Hedden and Tobin J. Marks. "[(CH3)5C5]2Th(CH3)2 surface chemistry and catalysis. Direct NMR spectroscopic observation of surface alkylation and ethylene insertion/polymerization on MgCl2". In: Journal of the American Chemical Society 110.5 (1988), pp. 1647–1649. DOI: 10.1021/ja00213a061.

[91] Tobin J. Marks. "Surface-bound metal hydrocarbyls. Organometallic connections between heterogeneous and homogeneous catalysis". In: Accounts of Chemical Research 25.2 (1992), pp. 57–65. DOI: 10.1021/ar00014a001.

[92] Li Jia et al. "Cationic Metallocene Polymerization Catalysts Based on Tetrakis(pentafluorophenyl)borate and Its Derivatives. Probing the Limits of Anion "Noncoordination" via a Synthetic, Solution Dynamic, Structural, and Catalytic Olefin Polymerization Study". In: Organometallics 16.5 (1997), pp. 842–857. DOI: 10.1021/om960880j.

[93] Jayachandran Jayakumar et al. "One-Pot Synthesis of Highly Substituted Polyheteroaromatic Compounds by Rhodium(III)-Catalyzed Multiple C-H Activation and Annulation". In: Angewandte Chemie International Edition 53.37 (), pp. 9889–9892. DOI: 10.1002/anie.201405183.

[94] Dennis B Malpass. Introduction to industrial polyethylene: properties, catalysts, and proce Vol. 45. John Wiley & Sons, 2010.

[95] Paul G. Hayes, Warren E. Piers, and Masood Parvez. In: Journal of the American Chemical 125.19 (2003). PMID: 12733887, pp. 5622–5623. DOI: 10.1021/ja034680s.

[96] Paul G. Hayes, Warren E. Piers, and Masood Parvez. "Arene Complexes of Diketiminato Supported Organoscandium Cations: Mechanism of Arene Exchange and Alkyne Insertion in Solvent Separated Ion Pairs". In: Chemistry – A European Journal 13.9 (2007), pp. 2632–2640. DOI: 10.1002/chem.200601087.

[97] Renato P. Orenha et al. "Nature of the Ru-àíNO Coordination Bond: Kohn–Sham Molecular Orbital and Energy Decomposition Analysis". In: ChemistryOpen 6.3 (), pp. 410–416. DOI: 10.1002/open.201700028.

[98] R. D. Shannon. "Revised effective ionic radii and systematic studies of interatomic distances in halides and chalcogenides". In: Acta Crystallographica Section A 32.5 (1976), pp. 751–767. DOI: 10.1107/S0567739476001551.

[99] Carlos A. Cruz et al. "Extremely Stable Thorium(IV) Dialkyl Complexes Supported by Rigid Tridentate 4,5-Bis(anilido)xanthene and 2,6-Bis(anilidomethyl)pyridine Ligands". In: Organometallics 26.3 (2007), pp. 692–701. DOI: 10.1021/om060914f.

[100] Carlos A. Cruz et al. In: Organometallics 28.6 (2009), pp. 1891–1899. DOI: 10.1021/om800624t.

[101] Carlos A. Cruz et al. "Single and Double Alkyl Abstraction from a Bis(anilido)xanthene Thorium(IV) Dibenzyl Complex: Isolation of an Organothorium Cation and a Thorium Dication". In: Organometallics 27.1 (2008), pp. 15–17. DOI: 10.1021/om7011503.

[102] Cassandra E. Hayes and Daniel B. Leznoff. "Diamido-Ether Uranium(IV) Alkyl Complexes as Single-Component Ethylene Polymerization Catalysts". In: Organometallics 29.4 (2010), pp. 767–774. DOI: 10.1021/om900546p.

[103] Paul J. Fagan et al. "Synthesis and properties of bis(pentamethylcyclopentadienyl) actinide hydrocarbyls and hydrides. A new class of highly reactive f-element organometallic compounds". In: Journal of the American Chemical Society 103.22 (1981), pp. 6650–6667. DOI: 10.1021/ja00412a021.

[104] Tobin J. Marks and William A. Wachter. "Tris(.eta.5-cyclopentadienyl)alkyl and -alkenyl compounds of thorium(IV)". In: Journal of the American Chemical Societ 98.3 (1976), pp. 703–710. DOI: 10.1021/ja00419a011.

[105] Andrew Streitwieser and Norio Yoshida. "Di-.pi.-cyclooctatetraenethorium". In: Journal of the American Chemical Society 91.26 (1969), pp. 7528–7528. DOI: 10.1021/ja01054a061.

[106] Andrew Streitwieser and Ulrich Mueller-Westerhoff. "Bis(cyclooctatetraenyl)uranium (uranocene). A new class of sandwich complexes that utilize atomic f orbitals". In: Journal of the American Chemical Society 90.26 (1968), pp. 7364–7364. DOI: 10.1021/ja01028a044.

[107] F.T. Edelmann and W.A. Herrmann. Synthetic Methods of Organometallic and Inorgan Thieme, 2014. ISBN: 9783131792211.

[108] Nicholas R. Andreychuk. "NON-DONOR LIGANDS IN ORGANOACTINIDE CHEMISTRY". PhD thesis. McMaster Univerity, 2017.

[109] Kelly S. A. Motolko et al. "Zirconium Complexes of a Rigid, Dianionic Pincer Ligand: Alkyl Cations, Arene Coordination, and Ethylene Polymerization". In: Organometallics 36.16 (2017), pp. 3084–3093. DOI: 10.1021/acs.organomet.7b00424.

[110] Benedict M. Gardner et al. "The role of 5f-orbital participation in unexpected inversion of the [sigma]-bond metathesis reactivity trend of triamidoamine thorium(iv) and uranium(iv) alkyls". In: Chem. Sci. 5 (6 2014), pp. 2489–2497. DOI: 10.1039/C4SC00182F.

[111] Elena Domeshek et al. "Organoactinides in the polymerization of ethylene: is TIBA a better cocatalyst than MAO?" In: Dalton Trans. 42 (25 2013), pp. 9069–9078. DOI: 10.1039/C3DT00032J. URL: http://dx.doi.org/10.1039/C3DT00032J.

[112] Tobin J. Marks and Victor W. Day. "Actinide Hydrocarbyl and Hydride Chemistry". In: Fundamental and Technological Aspects of Organo-f-Element Chem Ed. by Tobin J. Marks and Ignazio L. Fragalà. Dordrecht: Springer Netherlands, 1985, pp. 115–157. ISBN: 978-94-009-5406-9. DOI: 10.1007/978-94-009-5406-9_4.

[113] Axel D. Becke. In: The Journal of Chemical Physics 98.7 (1993), pp. 5648–5652. DOI: 10.1063/1.464913.

[114] John P. Perdew, Kieron Burke, and Matthias Ernzerhof. "Generalized Gradient Approximation Made Simple". In: Phys. Rev. Lett. 77 (18 1996), pp. 3865–3868. DOI: 10.1103/PhysRevLett.77.3865.

[115] Xiaoyan Cao, Michael Dolg, and Hermann Stoll. "Valence basis sets for relativistic energy-consistent small-core actinide pseudopotentials". In: The Journal of Chemical Physics 118.2 (2003), pp. 487–496. DOI: 10.1063/1.1521431.

[116] Xiaoyan Cao and Michael Dolg. "Segmented contraction scheme for small-core actinide pseudopotential basis sets". In: Journal of Molecular Structure: THEOC 673.1 (2004), pp. 203 –209. ISSN: 0166-1280. DOI: https://doi.org/10.1016/j.theochem.2003.12.015.

[117] Paula L. Diaconescu et al. In: Journal of the American Chemical Society 122.25 (2000), pp. 6108–6109. DOI: 10.1021/ja994484e.

[118] "Applications of the ETS-NOCV method in descriptions of chemical reactions". In: Journal of Molecular Modeling 17.9 (2011), p. 2337. ISSN: 0948-5023. DOI: 10.1007/s00894-011-1023-6.

[119] Mariusz P. Mitoraj, Artur Michalak, and Tom Ziegler. "On the Nature of the Agostic Bond between Metal Centers and Hydrogen Atoms in Alkyl Complexes. An Analysis Based on the Extended Transition State Method and the Natural Orbitals for Chemical Valence Scheme

(ETS-NOCV)". In: Organometallics 28.13 (2009), pp. 3727–3733. DOI: 10.1021/om900203m.

[120] Sung-Kwan Kim et al. In: Journal of the American Chemical Society 132.29 (2010). PMID: 20597488, pp. 9954–9955. DOI: 10.1021/ja101685u.

[121] E. Broclawik et al. "Formaldehyde activation by Cu(I) and Ag(I) sites in ZSM-5: ETS-NOCV analysis of charge transfer processes". In: Catalysis Today 169.1 (2011), pp. 45 –51. ISSN: 0920-5861. DOI: https://doi.org/10.1016/j.cattod.2010.08.020.

[122] Sylvester Ndambuki and Tom Ziegler. In: Inorganic Chemistry 51.14 (2012). PMID: 22731692, pp. 7794–7800. DOI: 10.1021/ic300824u.

[123] Mariusz P. Mitoraj and Artur Michalak. "On the asymmetry in molybdenum–oxygen bonding in the MoO3 structure: ETS–NOCV analysis". In: Structural Chemistry 23.5 (2012), pp. 1369–1375. ISSN: 1572-9001. DOI: 10.1007/s11224-012-0056-5.

[124] Holger Braunschweig et al. "Bond-strengthening backdonation in a transition-metal diborene complex". In: Nature Chemistry 5 (Dec. 2012), 115 EP –.

[125] Paul G. Hayes et al. "The Osmium–Silicon Triple Bond: Synthesis, Characterization, and Reactivity of an Osmium Silylyne Complex". In: Journal of the American Chemical Society 135.32 (2013), pp. 11780–11783. DOI: 10.1021/ja406799y.

[126] Ignacy Cukrowski, Jurgens H. de Lange, and Mariusz Mitoraj. In: The Journal of Physical Chemistry A 118.3 (2014), pp. 623–637. DOI: 10.1021/jp410744x.

[127] Estefania Fernandez Villanueva, Otilia Mo, and Manuel Yanez. "On the existence and characteristics of [small pi]-beryllium bonds". In: Phys. Chem. Chem. Phys. 16 (33 2014), pp. 17531–17536. DOI: 10.1039/C4CP01992J.

[128] Wan-Lu Li et al. "Electronic Structure and Bonding Situation in M2O2 (M = Be, Mg, Ca) Rhombic Clusters". In: The Journal of Physical Chemistry A 122.10 (2018), pp. 2816–2822. DOI: 10.1021/acs.jpca.8b01335.

[129] Ndambuki Sylvester and Ziegler Tom. "An analysis of unsupported triple and quadruple metal–metal bonds between two homonuclear group 6 transition elements based on the combined natural orbitals for chemical valence and extended transition state method". In: International Journal o 113.6 (), pp. 753–761. DOI: 10.1002/qua.24068.

[130] TURBOMOLE V5.10 2008, a development of University of Karlsruhe and Forschungszent

[131] K. Eichkorn et al. "Auxiliary basis sets for main row atoms and transition metals and their use to approximate Coulomb potentials". In: Theoretical Chemistry Accounts 97 (1997), p. 119.

[132] Martin ulka, L. Cantrel, and V. Vallet. "Theoretical Study of Plutonium(IV) Complexes Formed within the PUREX Process: A Proposal of a Plutonium Surrogate in Fire Conditions". In: J. Phys. Chem. A 118 (2014), pp. 10073–10080.

[133] Tom Ziegler and Arvi Rauk. "On the calculation of bonding energies by the Hartree Fock Slater method". In: Theoretica chimica acta 46.1 (1977), pp. 1–10. DOI: 10.1007/BF02401406.

[134] RF Nalewajski, AM Köster, and K Jug. "Chemical valence from the two-particle density matrix". In: Theoretica chimica acta 85.6 (1993), pp. 463–484.

[135] Roman F. Nalewajski and Janusz Mrozek. "Modified valence indices from the two-particle density matrix". In: International Journal of Quantum Chemistry 51.4 (1994), pp. 187–200. DOI: 10.1002/qua.560510403.

[136] Slawomir M. Cybulski and Marion L. Lytle. "The origin of deficiency of the supermolecule second-order Møller-Plesset approach for evaluating interaction energies". In: The Journal of Chemical Physics 127.14 (2007), p. 141102. DOI: 10.1063/1.2795693.

[137] C. David Sherrill, Tait Takatani, and Edward G. Hohenstein. "An Assessment of Theoretical Methods for Nonbonded Interactions: Comparison to Complete Basis Set Limit Coupled-Cluster Potential Energy Curves for the Benzene Dimer, the Methane Dimer, Benzene-àíMethane, and Benzene-àíH2S". In: The Journal of Physical Chemistry A 113.38 (2009), pp. 10146–10159. DOI: 10.1021/jp9034375.

[138] P. Gotcu-Freis et al. "Mass spectrometric studies of the vapour phase in the (Pu+O) system". In: The Journal of Chemical Thermodynamics 43.8 (2011), pp. 1164 –1173. ISSN: 0021-9614. DOI: https://doi.org/10.1016/j.jct.2011.02.024.

[139] V.P. Glushko et al. Thermodynamic Properties of Individual Substances. Ed. by V.P. Glushko (Ed.) Vol. 1-4. Nauka, Moscow, 1978-1982.

[140] E. H. P. Cordfunke and R. J. M. Konings. "Thermochemical data for reactor materials and fission products: The ECN database". In: Journal of Phase Equilibria 14.4 (1993), pp. 457–464. ISSN: 1054-9714. DOI: 10.1007/BF02671964.

[141] Rudy J. M. Konings et al. "The Thermodynamic Properties of the f-Elements and their Compounds. Part 2. The Lanthanide and Actinide Oxides". In: Journal of Physical and Chemical Reference Data 43.1 (2014), p. 013101. DOI: 10.1063/1.4825256.

[142] R. J. Ackermann, R. L. Faircloth, and M. H. Rand. "A Thermodynamic Study of the Vaporization Behavior of the Substoichiometric Plutonium Dioxide Phase1". In: The Journal of Physical Chemistry 70.11 (1966), pp. 3698–3706. DOI: 10.1021/j100883a055.

[143] PARDUE WILLIAM M. and KELLER DONALD L. "Volatility of PuO2 in Nonreducing Atmospheres". In: Journal of the American Ceramic Society 47.12 (), pp. 610–614. DOI: 10.1111/j.1151-2916.1964.tb13116.x.

[144] D. R. Messier. "Evaporation of Hypostoichiometric Plutonium Dioxide from 2070 ° to 2380 °K". In: Journal of the American Ceramic Society 51.12 (), pp. 710–713. DOI: 10.1111/j.1151-2916.1968.tb15933.x.

[145] C Ronchi et al. "Volatile molecule PuO3 observed from subliming plutonium dioxide". In: J. Nucl. Mat. 280.1 (2000), pp. 111–115. ISSN: 0022-3115. DOI: 10.1016/S0022-3115(00)00058-1.

[146] Oscar H. Krikorian et al. "Transpiration studies on the volatilities of PuO3(g) and PuO2(OH)2(g) from PuO2(s) in the presence of steam and oxygen and application to plutonium volatility in mixed-waste thermal oxidation processors". In: Journal of Nuclear Materials 247 (1997). Thermodynamics of Nuclear Materials, pp. 161 –171. ISSN: 0022-3115. DOI: https://doi.org/10.1016/S0022-3115(97)00043-3.

[147] Katharina Boguslawski et al. "On the multi-reference nature of plutonium oxides: PuO22+, PuO2, PuO3 and PuO2(OH)2". In: Phys. Chem. Chem. Phys. 19 (6 2017), pp. 4317–4329. DOI: 10.1039/C6CP05429C.

[148] Attila Kovács. "Relativistic Multireference Quantum Chemical Study of the Electronic Structure of Actinide Trioxide Molecules". In: J. Phys. Chem. A, 121.12 (2017), pp. 2523–2530. DOI: 10.1021/acs.jpca.7b01344.

[149] Meng Sheng Liao, Tapas Kar, and Steve Scheiner. In: The Journal of Physical Chemistry 108.15 (2004), pp. 3056–3063. DOI: 10.1021/jp036927d.

[150] E. F. Archibong and A. K. Ray. "An ab initio study of PuO_2 and of PuN_2". In: J. Mol. Struct. (THEOCHEM) 530 (2000), pp. 165–170. DOI: 10.1016/S0166-1280(00)00332-8.

[151] G. La Macchia et al. "A theoretical study of the ground state and lowest excited states of $PuO^{0/+/+2}$ and $PuO_2^{0/+/+2}$". In: Phys. Chem. Chem. Phys. 48 (2008), pp. 7278–7283.

[152] Lyudmila V. Moskaleva et al. "The heat of formation of gaseous PuO22+ from relativistic density functional calculations". In: Phys. Chem. Chem. Phys. 8 (32 2006), pp. 3767–3773. DOI: 10.1039/B607292E.

[153] Arie Landau et al. "Intermediate Hamiltonian Fock-space coupled-cluster method: Excitation energies of barium and radium". In: The Journal of Chemical Ph 113.22 (2000), pp. 9905–9910. DOI: 10.1063/1.1323258.

[154] Lucas Visscher, Ephraim Eliav, and Uzi Kaldor. "Formulation and implementation of the relativistic Fock-space coupled cluster method for molecules". In: The Journal of Chemical Physics 115.21 (2001), pp. 9720–9726. DOI: 10.1063/1.1415746.

[155] Arie Landau et al. "Intermediate Hamiltonian Fock-space coupled cluster method in the one-hole one-particle sector: Excitation energies of xenon and radon". In: The Journal of Chemical Physics 115.15 (2001), pp. 6862–6865. DOI: 10.1063/1.1405005.

[156] H.-J. Werner et al. MOLPRO, Version 2015.1, A Package Of Ab Initio Programs. 2015.

[157] Veryazov Valera, Malmqvist Per Åke, and Roos Björn O. "How to select active space for multiconfigurational quantum chemistry?" In: International Journal of Quantum Chemistry 111.13 (), pp. 3329–3338. DOI: 10.1002/qua.23068.

[158] Kerstin. Andersson et al. "Second-order perturbation theory with a CASSCF reference function". In: The Journal of Physical Chemistry 94.14 (1990), pp. 5483–5488. DOI: 10.1021/j100377a012.

[159] N. Forsberg and P.-Å. Malmqvist. "Multiconfiguration perturbation theory with imaginary level shift". In: Chem. Phys. Lett. 274 (1997), p. 196.

[160] J. Patrick Zobel, Juan J. Nogueira, and Leticia González. "The IPEA dilemma in CASPT2". In: Chem. Sci. 8 (2 2017), pp. 1482–1499. DOI: 10.1039/C6SC03759C.

[161] C. Angeli et al. "Introduction Of N-Electron Valence States For Multireference Perturbation Theory". In: J. Chem. Phys. 114 (2001), pp. 10252–10264.

[162] Kenneth G. Dyall. In: The Journal of Chemical Physics 102.12 (1995), pp. 4909–4918. DOI: 10.1063/1.469539.

[163] Per Åke Malmqvist, Björn O. Roos, and Bernd Schimmelpfennig. "The restricted active space (RAS) state interaction approach with spin–orbit coupling". In: Chemical Physics Letters 357.3 (2002), pp. 230 – 240. ISSN: 0009-2614. DOI: https://doi.org/10.1016/S0009-2614(02)00498-0.

[164] Branko Ruscic et al. In: The Journal of Physical Chemistry A 110.21 (2006), pp. 6592–6601. DOI: 10.1021/jp056311j.

[165] J D Cox, Donald D Wagman, and V A Medvedev. CODATA key values for thermodyna New York: Hemisphere Pub. Corp., 1989.

[166] R.J. Lemire, NEA Data Bank, and OECD Nuclear Energy Agency. Chemical Thermodynamics of Neptunium and Plutonium. Chemical thermodynamics. Elsevier, 2001. ISBN: 9780444503794.

[167] National Institute of Standards and Technology data base, http://www.nist.gov/chem (accessed on March 13, 2014).

[168] A. D. Becke. "Density-functional thermochemistry. III. The role of exact exchange". In: J. Chem. Phys. 98 (1993), pp. 5648–5653.

[169] P. J. Stephens et al. "Ab Initio Calculation of Vibrational Absorption and Circular Dichroism Spectra Using Density Functional Force Fields". In: J. Chem. Phys. 98 (1994), pp. 11623–11627.

[170] M. J. Frisch et al. Gaussian 09, Revision C.02. Gaussian, Inc., Wallingford, CT, 2004.

[171] Xiaoyan Cao, Michael Dolg, and Hermann Stoll. "Valence basis sets for relativistic energy-consistent small-core actinide pseudopotentials". In: J. Chem. Phys. 118.2 (2003), pp. 487–496.

[172] B. O. Roos et al. "Main group atoms and dimers studied with a new relativistic ANO basis set". In: J. Phys. Chem. A 108 (2004), pp. 2851–2858. DOI: 10.1021/jp031064+.

[173] Björn O. Roos et al. "New Relativistic ANO Basis Sets for Actinide Atoms". In: Chem. Phys. Lett. 409 (2005), pp. 295–299.

[174] E. F. Archibong and A. K. Ray. "An ab initio study of PuO_2 and of PuN_2". In: J. Mol. Struct. (THEOCHEM) 530 (2000), pp. 165–170. DOI: 10.1016/S0166-1280(00)00332-8.

[175] "The molecular mean-field approach for correlated relativistic calculations." In: J. Chem. Phys. 131.12 (Sept. 2009), p. 124116. ISSN: 1089-7690. DOI: 10.1063/1.3239505.

[176] L. Visscher, T. J. Lee, and K. G. Dyall. "Formulation and implementation of a relativistic unrestricted coupled-cluster method including noniterative connected triples". In: J. Chem. Phys. 105.19 (1996), pp. 8769–8776. DOI: 10.1063/1.472655.

[177] L. Visscher, E. Eliav, and U. Kaldor. "Formulation and implementation of the relativistic Fock-space coupled cluster method for molecules". In: J. Chem. Phys. 115 (2001), pp. 9720–9726. DOI: 10.1063/1.1415746.

[178] DIRAC, a relativistic ab initio electronic structure program, Release DIRAC16 (2016), written by H. J. Aa. Jensen, R. Bast, T. Saue, and L. Visscher, with contributions from V. Bakken, K. G. Dyall, S. Dubillard, U. Ekström, E. Eliav, T. Enevoldsen, E. Faßhauer, T. Fleig, O. Fossgaard, A. S. P. Gomes, T. Helgaker, J. Henriksson, M. Iliaš, Ch. R. Jacob, S. Knecht, S. Komorovský, O. Kullie, J. K. Lærdahl, C. V. Larsen, Y. S. Lee, H. S. Nataraj, M. K. Nayak, P. Norman, G. Olejniczak, J. Olsen, Y. C. Park, J. K. Pedersen, M. Pernpointner, R. di Remigio, K. Ruud, P. Sałek, B. Schimmelpfennig, J. Sikkema, A. J. Thorvaldsen, J. Thyssen, J. van Stralen, S. Villaume, O. Visser, T. Winther, and S. Yamamoto (see http://www.diracprogram.org).

[179] K. G. Dyall. "Relativistic double-zeta, triple-zeta, and quadruple-zeta basis sets for the 7*p* elements, with atomic and molecular applications". In: Theor. Chem. Acc. 131 (2012), pp. 1172–4. DOI: 10.1007/s00214-012-1172-4.

[180] K. G. Dyall. "Relativistic double-zeta, triple-zeta, and quadruple-zeta basis sets for the actinides Ac Lr". In: Theor. Chem. Acc. 117 (2007), pp. 491–500. DOI: 10.1007/s00214-006-0175-4.

[181] R. A. Kendall, T. H. Dunning Jr., and R. J. Harrison. "Electron affinities of the first-row atoms revisited. Systematic basis sets and wave functions". In: J. Chem. Phys. 96 (1992), pp. 6796–6806. DOI: 10.1063/1.462569.

[182] L. Visscher. "Approximate molecular relativistic Dirac-Coulomb calculations using a simple Coulombic correction". In: Theor. Chem. Acc. 98 (1997), pp. 68–70. DOI: 10.1007/s002140050280.

[183] J. D. Watts, J. Gauss, and R. J. Bartlett. "Coupled-cluster methods with noniterative triple excitations for restricted open-shell Hartree-Fock and other general single determinant reference functions. Energies and analytical gradients". In: J. Chem. Phys. 98 (1993), pp. 8718–8733.

[184] David H. Bross and Kirk A. Peterson. "Composite thermochemistry of gas phase U(VI)-containing molecules". In: J. Chem. Phys. 141.24 (2014), p. 244308. DOI: http://dx.doi.org/10.1063/1.4904721.

[185] A Shee et al. "Equation-of-Motion Coupled -Cluster Theory based on the 4-component Dirac–Coulomb(–Gaunt) Hamiltonian. Energies for single electron detachment, attachment and electronically excited states". In: The Journal of Chemical Physics (2018).

[186] Aquilante Francesco et al. "Molcas 8: New capabilities for multiconfigurational quantum chemical calculations across the periodic table". In: J. Comput. Chem. 37.5 (), pp. 506–541. DOI: 10.1002/jcc.24221.

[187] R. G. Denning and I. D. Morrison. "The electronic structure of actinyl ions: the excited-state absorption spectrum of $Cs_2UO_2Cl_4$". In: Chem. Phys. Lett. 180 (1991), p. 101.

[188] L. Bovey and S. Gerstenkorn. "Ground State of the First Spectrum of Plutonium (Pu i), from an Analysis of Its Atomic Spectrum". In: J. Opt. Soc. Am. 51.5 (1961), pp. 522–525. DOI: 10.1364/JOSA.51.000522.

[189] J. Blaise et al. In: C.R. Acad. Sci., Fr. 255 (1962), pp. 2403–2405.

[190] J. Blaise et al. In: Physica Scripta 22 (1980), pp. 224–230.

[191] Attila Kovács. "Relativistic Multireference Quantum Chemical Study of the Electronic Structure of Actinide Trioxide Molecules". In: J. Phys. Chem. A 121 (2017), pp. 2523–2530. ISSN: 1520-5215. DOI: 10.1021/acs.jpca.7b01344.

[192] G. La Macchia et al. "A theoretical study of the ground state and lowest excited states of $PuO^{0/+/+2}$ and $PuO_2^{0/+/+2}$". In: Phys. Chem. Chem. Phys. 48 (2008), pp. 7278–7283.

[193] E. G. Rauh and R. J. Ackermann. "First ionization potentials of some refractory oxide vapors". In: The Journal of Chemical Physics 60.4 (1974), pp. 1396–1400. DOI: 10.1063/1.1681210.

[194] F. Capone et al. "Mass Spectrometric Measurement Of the Ionization Energies and Cross Sections Of Uranium and Plutonium Oxide Vapors". In: The Journal of Physical Chemistry A 103.50 (1999), pp. 10899–10906. DOI: 10.1021/jp992405f.

[195] Marta Santos et al. "Gas-Phase Oxidation Reactions of Neptunium and Plutonium Ions Investigated via Fourier Transform Ion Cyclotron Resonance Mass Spectrometry". In: The Journal of Physical Chemistry A 106.31 (2002), pp. 7190–7194. DOI: 10.1021/jp025733f.

[196] F. Capone et al. "Controversy on the First Ionization Potential of PuO2 (Nearly) Settled by New Experimental Evidence". In: The Journal of Physical Chemistry A 109.51 (2005), pp. 12054–12058. DOI: 10.1021/jp055452i.

[197] E. R. Batista et al. "Density functional investigations of the properties and thermochemistry of UF_6 and UF_5 using valence-electron and all-electron approaches". In: J. Chem. Phys. 121 (2004), pp. 2144–2150. DOI: 10.1063/1.1768518.

[198] E. H. P. Cordfunke and R. J. M. Konings. "Thermochemical data for reactor materials and fission products: The ECN database". In: Journal of Phase Equilibria 14.4 (1993), pp. 457–464. ISSN: 1054-9714. DOI: 10.1007/BF02671964.

[199] Oscar H. Krikorian et al. "Transpiration studies on the volatilities of PuO3(g) and PuO2(OH)2(g) from PuO2(s) in the presence of steam and oxygen and application to plutonium volatility in mixed-waste thermal oxidation processors". In: Journal of Nuclear Materials 247 (1997). Thermodynamics of Nuclear Materials, pp. 161 –171. ISSN: 0022-3115. DOI: https://doi.org/10.1016/S0022-3115(97)00043-3.

[200] Attila Kovács et al. "Quantum Chemical Calculations and Experimental Investigations of Molecular Actinide Oxides". In: Chem. Rev. 115.4 (2015), pp. 1725–1759. DOI: 10.1021/cr500426s.

[201] Faoulat Miradji et al. "Thermodynamic Properties of Gaseous Ruthenium Species". In: J. Phys. Chem. A 119.20 (2015), pp. 4961–4971. DOI: 10.1021/acs.jpca.5b01645.

[202] Wanyi Jiang et al. "Comparative Study of Single and Double Hybrid Density Functionals for the Prediction of 3d Transition Metal Thermochemistry". In: Journal of Chemical Theory and Computation 8.11 (2012), pp. 4102–4111. DOI: 10.1021/ct300455e.

[203] Lars Goerigk and Stefan Grimme. "Efficient and Accurate Double-Hybrid-Meta-GGA Density Functionals—Evaluation with the Extended

GMTKN30 Database for General Main Group Thermochemistry, Kinetics, and Noncovalent Interactions". In: Journal of Chemical Theory and Computatio 7.2 (2011), pp. 291–309. DOI: 10.1021/ct100466k.

[204] Stefan Grimme. "Semiempirical hybrid density functional with perturbative second-order correlation". In: The Journal of Chemical Physics 124.3 (2006), p. 034108. DOI: 10.1063/1.2148954.

[205] Emmanuel Fromager. "Rigorous formulation of two-parameter double-hybrid density-functionals". In: The Journal of Chemical Physics 135.24 (2011), p. 244106. DOI: 10.1063/1.3671384.

[206] Julien Toulouse et al. "Communication: Rationale for a new class of double-hybrid approximations in density-functional theory". In: The Journal of Chemi 135.10 (2011), p. 101102. DOI: 10.1063/1.3640019.

[207] Kamal Sharkas, Julien Toulouse, and Andreas Savin. "Double-hybrid density-functional theory made rigorous". In: The Journal of Chemical Physics 134.6 (2011), p. 064113. DOI: 10.1063/1.3544215.

[208] Tobias Schwabe and Lars Goerigk. "Time-Dependent Double-Hybrid Density Functionals with Spin-Component and Spin-Opposite Scaling". In: Journal of Chemical Theory and Computation 13.9 (2017), pp. 4307–4323. DOI: 10.1021/acs.jctc.7b00386.

[209] Stefan Grimme and Frank Neese. "Double-hybrid density functional theory for excited electronic states of molecules". In: The Journal of Chemical Physics 127.15 (2007), p. 154116. DOI: 10.1063/1.2772854.

[210] Tobias Schwabe and Stefan Grimme. "Double-hybrid density functionals with long-range dispersion corrections: higher accuracy and extended applicability". In: Phys. Chem. Chem. Phys. 9 (26 2007), pp. 3397–3406. DOI: 10.1039/B704725H.

[211] Juan Aragó, Enrique Ortí, and Juan C. Sancho-García. "Nonlocal van der Waals Approach Merged with Double-Hybrid Density Functionals: Toward the Accurate Treatment of Noncovalent Interactions". In: Journal of Chemical Theory and Computation 9.8 (2013), pp. 3437–3443. DOI: 10.1021/ct4003527.

[212] Tobias Benighaus et al. "Semiempirical Double-Hybrid Density Functional with Improved Description of Long-Range Correlation". In: The Journal of Phys 112.12 (2008), pp. 2702–2712. DOI: 10.1021/jp710439w.

[213] Eric Brémond and Carlo Adamo. "Seeking for parameter-free double-hybrid functionals: The PBE0-DH model". In: The Journal of Chemical Physics 135.2 (2011), p. 024106. DOI: 10.1063/1.3604569.

[214] Jeng-Da Chai and Shan-Ping Mao. "Seeking for reliable double-hybrid density functionals without fitting parameters: The PBE0-2 functional". In: Chemical Physics Letters 538 (2012), pp. 121 –125. ISSN: 0009-2614. DOI: https://doi.org/10.1016/j.cplett.2012.04.045.

[215] Jeng-Da Chai and Martin Head-Gordon. "Long-range corrected hybrid density functionals with damped atom–atom dispersion corrections". In: Phys. Chem. Chem. Phys. 10 (44 2008), pp. 6615–6620. DOI: 10.1039/B810189B.

[216] Bun Chan and Leo Radom. "Obtaining Good Performance With Triple-Type Basis Sets in Double-Hybrid Density Functional Theory Procedures". In: Journal of Chemical Theory and Computation 7.9 (2011), pp. 2852–2863. DOI: 10.1021/ct200396x.

[217] Lars Goerigk and Stefan Grimme. "A thorough benchmark of density functional methods for general main group thermochemistry, kinetics, and noncovalent interactions". In: Phys. Chem. Chem. Phys. 13 (14 2011), pp. 6670–6688. DOI: 10.1039/C0CP02984J.

[218] David C. Graham et al. "Optimization and Basis-Set Dependence of a Restricted-Open-Shell Form of B2-PLYP Double-Hybrid Density Functional Theory". In: The Journal of Physical Chemistry A 113.36 (2009). PMID: 19645437, pp. 9861–9873. DOI: 10.1021/jp9042864.

[219] Amir Karton et al. "Highly Accurate First-Principles Benchmark Data Sets for the Parametrization and Validation of Density Functional and Other Approximate Methods. Derivation of a Robust, Generally Applicable, Double-Hybrid Functional for Thermochemistry and Thermochemical Kinetics". In: The Journal of Physical Chemistry A 112.50 (2008), pp. 12868–12886. DOI: 10.1021/jp801805p.

[220] Sebastian Kozuch and Jan M. L. Martin. "Spin-component-scaled double hybrids: An extensive search for the best fifth-rung functionals blending DFT and perturbation theory". In: Journal of Computational Chemistry 34.27 (), pp. 2327–2344. DOI: 10.1002/jcc.23391.

[221] Sebastian Kozuch, David Gruzman, and Jan M. L. Martin. "DSD-BLYP: A General Purpose Double Hybrid Density Functional Including Spin

Component Scaling and Dispersion Correction". In: The Journal of Physical Chemistry 114.48 (2010), pp. 20801–20808. DOI: 10.1021/jp1070852.

[222] Sebastian Kozuch and Jan M. L. Martin. "DSD-PBEP86: in search of the best double-hybrid DFT with spin-component scaled MP2 and dispersion corrections". In: Phys. Chem. Chem. Phys. 13 (45 2011), pp. 20104–20107. DOI: 10.1039/C1CP22592H.

[223] Afshan Mohajeri and Mojtaba Alipour. "B2-PPW91: A promising double-hybrid density functional for the electric response properties". In: The Journal of Chem 136.12 (2012), p. 124111. DOI: 10.1063/1.3698284.

[224] Roberto Peverati and Martin Head-Gordon. "Orbital optimized double-hybrid density functionals". In: The Journal of Chemical Physics 139.2 (2013), p. 024110. DOI: 10.1063/1.4812689.

[225] J. C. Sancho-García and A. J. Pérez-Jiménez. "Assessment of double-hybrid energy functionals for conjugated systems". In: The Journal of Chemical Physic 131.8 (2009), p. 084108. DOI: 10.1063/1.3212881.

[226] Tobias Schwabe and Stefan Grimme. "Towards chemical accuracy for the thermodynamics of large molecules: new hybrid density functionals including non-local correlation effects". In: Phys. Chem. Chem. Phys. 8 (38 2006), pp. 4398–4401. DOI: 10.1039/B608478H.

[227] Sidi M. O. Souvi, Kamal Sharkas, and Julien Toulouse. "Double-hybrid density-functional theory with meta-generalized-gradient approximations". In: The Journal of Chemical Physics 140.8 (2014), p. 084107. DOI: 10.1063/1.4865963.

[228] Alex Tarnopolsky et al. "Double-Hybrid Functionals for Thermochemical Kinetics". In: The Journal of Physical Chemistry A 112.1 (2008), pp. 3–8. DOI: 10.1021/jp710179r.

[229] Julien Toulouse et al. "Communication: Rationale for a new class of double-hybrid approximations in density-functional theory". In: The Journal of Chemi 135.10 (2011), p. 101102. DOI: 10.1063/1.3640019.

[230] Igor Ying Zhang et al. "Doubly hybrid density functional xDH-PBE0 from a parameter-free global hybrid model PBE0". In: The Journal of Chemical Physics 136.17 (2012), p. 174103. DOI: 10.1063/1.3703893.

[231] Igor Ying Zhang and Xin Xu. "Reaching a Uniform Accuracy for Complex Molecular Systems: Long-Range-Corrected XYG3 Doubly Hybrid Density Functional". In: The Journal of Physical Chemistry Letters 4.10 (2013), pp. 1669–1675. DOI: 10.1021/jz400695u.

[232] Ying Zhang, Xin Xu, and William A. Goddard. "Doubly hybrid density functional for accurate descriptions of nonbond interactions, thermochemistry, and thermochemical kinetics". In: Proceedings of the National Academy of S (2009). ISSN: 0027-8424. DOI: 10.1073/pnas.0901093106.

[233] Igor Ying Zhang et al. "A fast doubly hybrid density functional method close to chemical accuracy using a local opposite spin ansatz". In: Proceedings of the National Academy of Sciences 108.50 (2011), pp. 19896–19900. DOI: 10.1073/pnas.1115123108.

[234] Lars Goerigk and Stefan Grimme. "Double-hybrid density functionals". In: Wiley Interdisciplinary Reviews: Computational Molecular Science 4.6 (), pp. 576–600. DOI: 10.1002/wcms.1193.

[235] Liam Wilbraham, Carlo Adamo, and Ilaria Ciofini. "Communication: Evaluating non-empirical double hybrid functionals for spin-state energetics in transition-metal complexes". In: The Journal of Chemical Physics 148.4 (2018), p. 041103. DOI: 10.1063/1.5019641.

[236] Miho Isegawa, Frank Neese, and Dimitrios A. Pantazis. "Ionization Energies and Aqueous Redox Potentials of Organic Molecules: Comparison of DFT, Correlated ab Initio Theory and Pair Natural Orbital Approaches". In: Journal of Chemical Theory and Computation 12.5 (2016), pp. 2272–2284. DOI: 10.1021/acs.jctc.6b00252.

[237] Tomasz Seidler, Katarzyna Stadnicka, and Benoît Champagne. "Evaluation of the Linear and Second-Order NLO Properties of Molecular Crystals within the Local Field Theory: Electron Correlation Effects, Choice of XC Functional, ZPVA Contributions, and Impact of the Geometry in the Case of 2-Methyl-4-nitroaniline". In: Journal of Chemical Theory and Compu 10.5 (2014), pp. 2114–2124. DOI: 10.1021/ct5001654.

[238] Kirk A. Peterson. "Correlation consistent basis sets for actinides. I. The Th and U atoms". In: The Journal of Chemical Physics 142.7 (2015), p. 074105. DOI: 10.1063/1.4907596.

[239] Timofei Privalov et al. "Structure and Thermodynamics of Uranium(VI) Complexes in the Gas Phase: A Comparison of Experimental and ab Initio Data". In: The Journal of Physical Chemistry A 106.46 (2002), pp. 11277–11282. DOI: 10.1021/jp0260402.

[240] M. Dolg, H. Stoll, and H. Preuss. "Energy Aadjusted ab initio pseudopotentials for the rare earth elements". In: The Journal of Chemical Physics 90.3 (1989), pp. 1730–1734. DOI: 10.1063/1.456066.

[241] G. V. Girichev et al. “Molecular structure and vibrational characteristics of thorium tetrafluoride”. In: Journal of Structural Chemistry 40.2 (1999), p. 207.

[242] Yu Gong et al. “Infrared Spectroscopic and Theoretical Investigations of the OUF2 and OThF2 Molecules with Triple Oxo Bond Character”. In: Inorganic Chemistry 51.12 (2012), pp. 6983–6991. DOI: 10.1021/ic3009128.

[243] Monica Vasiliu et al. “Reliable Potential Energy Surfaces for the Reactions of H2O with ThO2, PaO2(+), UO2(2+), and UO2(.)” In: J. Phys. Chem. A 119.46 (2015), pp. 11422–11431. DOI: 10.1021/acs.jpca.5b08618.

[244] Georg Schreckenbach, P. Jeffrey Hay, and Richard L. Martin. “Density functional calculations on actinide compounds: Survey of recent progress and application to [UO2X4]2-(X=F, Cl, OH) and AnF6 (An=U, Np, Pu)”. In: Journal of Computational Chemistry 20.1 (), pp. 70–90. DOI: 10.1002/(SICI)1096-987X(19990115)20:1<70::AID-JCC9>3.0.CO;2-F.

[245] R. D. Wesley and C. W. DeKock. “Geometry and Infrared Spectra of Matrix-Isolated Rare-Earth Halides. I. LaF3, CeF3, PrF3, NdF3, SmF3, and EuF3”. In: The Journal of Chemical Physics 55.8 (1971), pp. 3866–3877. DOI: 10.1063/1.1676673.

[246] Roger L. De Kock et al. “A theoretical study of the linear versus bent geometry for several MX2 molecules: MgF2, CaH2, CaF2, CeO2 and YbCl2”. In: Polyhedron 9.15 (1990), pp. 1919 –1934. DOI: https://doi.org/10.1016/S0277-5387(00)84004-8.

[247] V. G. Solomonik, A. Yu. Yachmenev, and A. N. Smirnov. “Structure, force fields, and vibrational spectra of cerium tetrahalides”. In: Journal of Structural Ch 49.4 (2008), pp. 613–620. DOI: 10.1007/s10947-008-0085-5.

[248] Tanya Mikulas et al. “Reactions of Lanthanide Atoms with Oxygen Difluoride and the Role of the Ln Oxidation State”. In: Inorganic Chemistry 53.1 (2014), pp. 446–456. DOI: 10.1021/ic402422h.

[249] V. Yu. Buz’ko, G. Yu. Chuiko, and Kh. B. Kushkhov. “Ab initio study of the structure and stability of AcF n (3 -àí n)+ of complexes (n = 1-àí7)”. In: Russian Journal of Inorganic Chemistry 57.6 (2012), pp. 838–842.